University of Southampton Research Repository

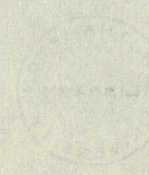THE STRUCTURE OF TURBULENT SHEAR FLOW

by

Philip John Morris, B.Sc.(Hons.)Eng., M.Sc.

A Thesis submitted for the degree of

Doctor of Philosophy in the Faculty of

Engineering.

Department of Aeronautics and Astronautics

University of Southampton

August, 1971.

CORRIGENDA

p. 17   line 1   '(1.30)'   becomes   '(1.20)'

p. 17   line 3   '(1.31)'   becomes   '(1.21)'

p. 28   line 18   insert   '(2.21)'   after equation

p. 82   line 10   '(v)$_{\delta_0}$ becomes   '(v)$_{S_0}$'

p. 82   line 11   'A$_z$'   becomes   'A$_2$'

p. 85   line 16   insert 'number' after Reynolds

p. 87   line 19   delete 'this manner'.   Insert 'Schubauer and Skramstads manner

p. 90   Line 8   '$R_\theta = \dfrac{U_\alpha \theta}{\upsilon}$ becomes   '$R_\theta = \dfrac{U_d \theta}{\upsilon}$'

p.105   line 13   '$\ell = \left(\dfrac{\upsilon x}{U_d}\right)^{\frac{1}{2}}$'   becomes   '$\ell = \left(\dfrac{\upsilon x}{U_d}\right)^{\frac{1}{2}}$'

p.130   line 7   '$+\dfrac{1}{k_1}\displaystyle\int_{-\infty}^{\infty}\int_{-\infty}^{\infty}\kappa_1\hat{\psi}(\kappa_1,w)\ldots$'   becomes   '$+\dfrac{1}{k_1}\displaystyle\int_{-\infty}^{\infty}\int_{-\infty}^{\infty}\kappa_1\hat{\psi}'(\kappa_1,w)\ldots$'

p.132   line 11   '$-\left(\dfrac{\partial u_1\omega_3}{\partial x_1}+\dfrac{\partial u_2\omega_3}{\partial x_2}\right)$'   becomes   '$-\left(\dfrac{\overline{\partial u_1\omega_3}}{\partial x_1}+\dfrac{\partial u_2\omega_3}{\partial x_2}\right)$'

p. 150.   line 1   delete   sentence beginning 'The experimental results...'

insert   'The theoretical results are plotted such that

their maximum value coincides with the maximum experimental value'.

p.169   line 6   'equation (7.30)'   becomes   'equation (7.31)'

ABSTRACT

FACULTY OF ENGINEERING

AERONAUTICS AND ASTRONAUTICS

Doctor of Philosophy

THE STRUCTURE OF TURBULENT SHEAR FLOW

by Philip John Morris.

A theoretical investigation is made of the mixing layer between two streams. The work is divided into four sections. The first involves the solution of the mean problem of laminar and turbulent mixing. The equations of motion are written in terms of a similarity variable. An eddy viscosity hypothesis is made to describe the shear stresses. The similarity equations for both laminar and turbulent problems are solved numerically by an iterative scheme.

The second section examines the stability of the mixing layer. The Orr-Sommerfeld equation of hydrodynamic stability is solved numerically. Both cases of spatial and temporal amplification are examined. The shear layer is shown to be unstable to both spatially and temporally growing disturbances at all Reynolds numbers. A correction is made for the divergence of the mean flow and leads to a value of critical Reynolds number of 12.3.

The third section presents a model for the turbulent mixing layer. A set of partial differential equations describing the flow are obtained. A Fourier transform technique is employed

to reduce this set to an ordinary differential equation for the fluctuating flow field. The homogeneous form of this equation is solved numerically. The resulting predictions of fluctuating velocity, pressure and their correlations are compared with measured values. The agreement is good in certain cases and this serves as a guide to components of the flow governed by non-linear processes.

The final section examines the non-linear growth of the mixing layer through transition from laminar to turbulent flow. A set of integral momentum and energy equations are written in terms of a number of shape parameters of mean and fluctuating flow. The amplitude of disturbances is shown to grow rapidly and reach a limiting value. A sudden growth of the mixing layer thickness through transition is also predicted. Comparison is made with experimental results.

Acknowledgements

The work was performed at the University of Southampton in the Department of Aeronautics and Astronautics and the Institute of Sound and Vibration Research.

The author wishes to thank the Science Research Council and the Ministry of Technology for their financial support in this project.

The author gratefully acknowledges the help and encouragement of Professor G.M.Lilley in his supervision of this work.

The author also wishes to thank members of the Computing Service at Southampton University and the Atlas Computing Laboratory, Chilton for their help. Thanks are also due to the many members of staff and friends at Southampton for their helpful discussions and ideas. The author is also grateful to Mrs. L.Tudor Pole for typing this thesis so quickly.

Finally the author wishes to thank his wife for her patience during many hours as a computer widow and her extra financial assistance.

Contents

CHAPTER 1

Introduction

The motion of a fluid may be conveniently classified under three separate headings: steady laminar flow, unsteady laminar flow and turbulent flow. These classes of motion are best described by reference to a series of identical experiments. If a property of the fluid, such as velocity or pressure, is measured in all the experiments then, in the case of steady laminar flow, it will not vary with time or from experiment to experiment. For the second type of motion, unsteady laminar flow, we would find that, although the measured property is a function of time, it will not vary from experiment to experiment. In both these cases the properties of the fluid are determinate. In turbulent flow however the property would be fluctuating in time and between experiments and would appear random in nature. So we can say that turbulent flow does not appear determinate in any simple sense. However, turbulent flows and their effects are commonly encountered in most cases of fluid motion. It is true to say that one is more likely to meet turbulent flow than laminar flow in most engineering situations. So it becomes important to know how turbulent flow behaves. At the same time it is necessary to know why they behave the way they do in order to formulate rules for practical use and, with a basic understanding of the phenomenon, to propose methods for its application and control.

Turbulence is three-dimensional, non-linear and diffusive.
Diffusion in turbulence accounts for the differing character-
istics of, for instance, mean velocity distributions and heat
transfer between laminar and turbulent flow. In the kinetic
theory of gases the diffusion of molecules is explained in
terms of the random motion of the molecules, where a molecule,
by a process of random walk, moves farther and farther from its
point of departure. Turbulent diffusion may also be likened
to a random walk but now the translations and collisions occur
between separate bodies of fluid.

The non-linear character of turbulence presents the hardest
problem in any attempts at its understanding. The Navier -
Stokes equations, which, it is generally accepted, adequately
describe the fluid motion in terms of mean and fluctuating
components, are non-linear. Although a complete solution of
these equations is possible on a high speed digital computer,
the process would take a long time and it is questionable
whether the information gathered would be worth the effort.
What part does non-linearity play in the phenomenon of tur-
bulence? One clear fact that emerges from experiments is that
the magnitude of the turbulent fluctuations is an order of
magnitude smaller than that of the mean flow. So it seems
reasonable to argue that there exists some process in the
flow that limits the amplitude of the fluctuations. However,
in order to maintain the turbulence, there must exist a
process for the generation and growth of the fluctuations. It

is the author's view that both these mechanisms are best assigned to non-linearity. However, there exists no widely accepted view on the role of the non-linear actions. If non-linear effects are entirely damping effects, what mechanism is there to prevent the turbulence being in a continual state of decay and, if that is the case, how can disturbances grow? So one might reasonably argue that small disturbances are amplified, by a linear or non-linear process, to some amplitude where non-linearity prevents their further growth.

The very nature of turbulence, its three-dimensionality and its randomness, has made experiments in this field highly complicated. At the same time the techniques developed to make these measurements have been ingenious and sophisticated. Turbulence occurs in very many flow situations but the number of flow configurations considered in experiments is relatively few. Because of this there has been a great deal of duplication of measurements. In many instances the apparently differing results from seemingly identical experiments has often initially led more to confusion than to enlightenment. However, the accuracy of experiments is continually increasing as the techniques become more sophisticated, and the results of these experiments are invaluable in any attempts to understand the mechanisms in turbulence.

The description of turbulent motion as a function of space and time is made nearly impossible by its complicated nature. However, it is possible to regard turbulence as a phenomenon in which the fluctuating quantities are to have

random variations with space and time. In this way it becomes possible to describe the turbulence in terms of a number of statistical properties. The statistical theory of turbulence was initiated by G.I. Taylor (1935). Subsequent studies of the structure of turbulent shear flow have been greatly influenced by the statistical theory as it presented the possibility of describing the turbulent motion analytically from the equation of motion without arbitrary assumptions. Much experimental work has thus been directed at measuring statistical properties of the turbulence such as velocity-velocity correlations and root mean squares of the flow properties. The measurement of these properties enables the researcher to gain a clearer understanding of the physical nature of the flow. Advanced measurement techniques have recently enabled workers to measure space and time correlations and power spectra of turbulent velocity components in many different shear flows. Notable contributions have been made by Favre, Gaviglio and Dumas (1958) for the turbulent boundary layer, Grant (1958) for boundary layers, wakes and grid turbulence, and Bradshaw, Ferriss and Johnson (1964), for a circular jet. The measurement of fluctuating pressures in turbulence presents more experimental problems than the measurement of velocity fluctuations; however, experiments have been carried out by Fuchs (1968) for a jet and in the boundary layer correlations between wall pressure fluctuations and velocity components have been made by Hodgson (1962) and Tu and Willmorth (1966).

Thus it can be seen that, with the introduction of more sophisticated techniques such as conditional sampling for the measurement of intermittancy, see Wygnanski and Fiedler (1970), experimental investigations have reached a very advanced state.

Theoretical investigations have not advanced as quickly as experimental work in describing the nature of turbulent motion. Much of the work has been applied to isotropic and homogeneous turbulence, most of which work is described by Batchelor (1953). The extension of this work to inhomogeneous turbulence has led to great difficulties and one is often forced to empirical hypotheses. Fundamental to the description of turbulence is the description of the mechanism by which the Reynolds shear stress is maintained. Many of the early theories of turbulent flow were of a phenomenological nature and described the shear stress in terms of a mixing length or an eddy viscosity. Assuming a similarity condition the equations of motion could then be solved for distribution of mean velocity. Only Reichardt pointed out that the comparison of the results of the various theories with experimental data, which usually contained a lot of scatter, would not allow a decision to be made in favour of any particular theory. He proposed an inductive theory, described by Abramovitch (1963), based on the results of experimental investigations of directly measurable quantities such as the mean square of the axial velocity fluctuations. The assumption of a constant eddy viscosity has led to a number of useful predictions, however it is clear that the shear stress is not a local property

of the flow but a function of the whole flow field.

The next major development, subsequent to the phenomeno-logical theories and statistical theories, was made by Townsend (1956) with the publication of his monograph, 'The Structure of Turbulent Shear Flow'. He presented an inductive account of the processes involved in turbulent shear flows. He proposed that the turbulence could be separated into various scales of eddy motion. The medium scale eddies would contain almost all of the turbulent energy. The large eddies would be responsible for the distortion of the turbulence front and would control the entrainment of irrotational fluid. They would also be responsible for the intermittent nature of the turbulence. In the same year another new development was proposed by Malkus (1956). Malkus studied the turbulent shear flow in a channel without any empirical assumptions. In his theory he assumed that the non-linear momentum transport had only a stabilising effect on the mean flow. His hypothesis may be stated that firstly, the mean flow will be stable if perturbations of the mean flow are marginally stable and satisfy the Orr-Sommerfeld equation, and secondly, that the scale of these marginally stable modes will be the smallest scale present in the momentum transport spectrum. These hypotheses mean that the mean profile will be marginally stable in an Orr-Sommerfeld sense and that the Reynolds shear stress is composed of scales larger than the smallest scale in the spectrum of momentum transport. The equation

of mean motion for channel flow may be written

$$\frac{\partial}{\partial y} \, \overline{uv} \; = \; \frac{\tau_o}{d} + \nu \, \frac{\partial^2 U}{\partial y^2} \quad , \tag{1.1}$$

where $\tau_o = -\frac{d}{\rho} \, \frac{\partial P}{\partial x}$, where P is the wall pressure and d is

the separation of the walls.

We may write $\overline{uv}$ as a series of orthogonal functions where the

last term in the series corresponds to the smallest scale of

the fluctuations. Thus we write,

$$\overline{uv} \; = \; \sum_{n=1}^{n_o} A_n \, \sin \frac{2n\pi y}{d} \quad . \tag{1.2}$$

Substituting the series (1.2) into equation (1.1) leads to,

$$\frac{d^2 U}{dy^2} \; = \; \sum_{n=1}^{n_o} B_n \, \cos \; \frac{2n\pi y}{d} \; - \; \frac{\tau_o}{\nu d} \tag{1.3}$$

Assuming that $\frac{d^2 U}{dy^2}$ is positive definite we may guard against the

possibility of inflectional instability. Malkus then proposed

to find the mean profile which would make the rate of dissipation

of potential energy into heat a maximum. This condition would

then fix the value of n_o. The rate of dissipation of energy

by viscosity will equal the rate of mechanical work done by

shearing stresses. The total rate of dissipation per unit

mass is given by

$$D = \tau_o U_m \; , \tag{1.4}$$

where U_m is the y-averaged mean velocity which is the reference

velocity. We need to find the conditions for maximum D, which

will clearly occur for maximum τ_o, U_m being fixed. Thus we consider the maximum value of the non-dimensional quantity $\frac{R\tau_o}{U_m^2}$, where $R = \frac{U_m d}{\nu}$ is known. Alternatively, we may keep this quantity constant and find the minimum Reynolds number associated with the marginally stable solution of the Orr-Sommerfeld equation. This then fixes the value of n_o which gives the last term in the series for $\overline{uv}$. The subsequent determination of the mean velocity profile through optimisation of the dissipation rate involves much complicated analysis. However, the solution obtained by Malkus was in close agreement with the measurements of Laufer (1951) and is the only profile obtained on purely theoretical analysis.

The success of Malkus' theory has led a number of researchers to analyse his hypothesis. Townsend (1962) reviewed Malkus' work and discussed its physical implications. We may note that the total energy dissipation is determined by the velocity gradient at the walls. As the Reynolds number of the flow tends to infinity the velocity profile at the channel centre becomes flatter and approaches a constant value, thus maximum dissipation will occur for infinite Reynolds number. Townsend also noted that the modes considered by Malkus obtained their energy directly from the mean motion but the energy was lost to a background of isotropic eddies by a non-linear transfer process supporting the idea of the stabilising effects of non-linear phenomena.

More recently Reynolds and Tiederman (1967) contradict the

Malkus theory. As a result of extensive numerical calculations

they conclude that the experimental profiles were stable in

linear perturbation theory and the marginally stable ones

do not correspond with experiment. They could not find any

neutral stability curve in this case. However Eckhaus (1965)

points out that in the classical calculation of critical

curves it is considered that if other eigenvalues than the

ones considered exist, then they are all stabilising. He also

notes that unless there exists an infinite denumerable sequence

of eigenvalues in the case of Poiseville flow such that the

(n + 1)th eigenvalue is more stable than the n-th, then no

critical curve may exist. The number of eigenvalues of the

Orr-Sommerfeld equation was considered by Corcos and Sellars

(1959) for the case of Poiseuille flow in a circular pipe.

They concluded that, as for every fixed value of Reynolds

number and wavenumber the number of eigenvalues was finite,

the number of eigenvalues is finite. Eckhaus extends this

argument to state that as the Reynolds number tends to in-

finity the number of eigenvalues is finite for each fixed

value of R but increases without limit as $R \to \infty$. We will

now consider other lines of recent research on the problem

of turbulent shear flow.

We have previously noted that the description of the

Reynolds shear stress is fundamental to study of turbulent

shear flows. Phillips (1967) presented a hypothesis for

the gradient of Reynolds shear stress as a function of the

convected integral time scale. The generation of Reynolds shear stress is generated by the interaction of the fluctuations and mean velocity field. The interaction between uniform shear and a single Fourier component of the turbulent flow has been considered by, amongst others, Moffatt (1965). He concluded that, in an analysis which neglected the interaction between separate fluctuations, there existed no unique relationship between the local mean velocity gradient and the Reynolds stress. This supports the idea that the Reynolds stress is not a 'local' property of the turbulent field but a property of the whole field. We may simply show that the Boussinesq hypothesis of constant eddy viscosity is not valid. He hypothesised that the shear stresses would be proportional to the local velocity gradient. He wrote

$$-\overline{u_i u_j} = \nu_T \left(\frac{\partial U_i}{\partial x_j} + \frac{\partial U_j}{\partial x_i} \right), \tag{1.5}$$

where ν_T is the eddy viscosity and U_i and u_i are the mean and fluctuating components of velocity in the x_i-direction. If we consider the case of $i = j$ in (1.4) we see that for an incompressible fluid,

$$-\overline{u_i u_i} = 2\nu_T \frac{\partial U_i}{\partial x_i} = 0, \tag{1.6}$$

which implies no turbulence exists in incompressible flow. Phillips noted that experiments show that the energy containing turbulent components, which generate the Reynolds stress, have scales of the same order as the mean flow. He

pointed out that it is the variation of Reynolds stress that occurs in the momentum equation and he argued that one should consider the relation between variation in the Reynolds stress and variations in the mean velocity gradient. A similar association was found by Miles (1957) in the case of inviscid laminar air flow over water waves. He found that the stress difference across the critical layer, where the wave speed equals the wind speed, is proportional to the ratio of local mean velocity curvature to its slope. Phillips derived a similar expression for the contribution to the shear stress across the 'matched layer', where the mean velocity is equal to the wave speed. He wrote this as

$$\Delta\tau_p = A_m \rho \ \{\frac{-U''}{k \ U'} \ \overline{W^2}\}_{z_m} \ , \qquad (1.7)$$

where A_m is a numerical constant and the term in brackets is evaluated at the matched layer where $z = z_m$. $\overline{W^2}$ is the mean square periodic perturbation in the z-direction. He then considered the turbulent motion in a Fourier decomposition as the superposition of a large number of small travelling perturbations, periodic in space in the x-y plane. By considering the contribution from all the wavenumbers of the turbulence with their matched layers at z_m he derived the expression for the gradient of the Reynolds stress,

$$\frac{d\tau}{dz} = A \ \textcircled{H} \ \overline{W^2} \ \frac{d^2 U}{dz^2} \ , \qquad (1.8)$$

where A is a number, $\textcircled{H}$ is the convected integral time scale

of the W-velocity fluctuations and $U(z)$ is the mean velocity profile. Thus we may write the eddy viscosity

$$\nu_T(z) = A \; \textcircled{H} \; \overline{w^2} \qquad (1.9)$$

From equations (1.8) and (1.9) we see that the Reynolds stress is not a local property of the flow. Although the Reynolds stress gradient would appear to be a local function of the curvature of mean velocity and velocity fluctuations but the convected time integral scale involves a history of the turbulence. We also see the importance of the energy containing eddies in supporting the Reynolds stress as the eddy viscosity is proportional to kinetic energy density of the W-velocity fluctuations. The inclusion of the convected integral time scale shows that the longer the W-fluctuation remains coherent the greater their contribution to the shear stress. However, Hall (1968) has pointed out that if Phillips' expression is integrated across a jet or wake momentum will not be conserved which suggests that Phillips' hypothesis may not be useful in these cases.

Another formulation of the problem has been given by Lilley. He compared the turbulence terms in the vorticity equation with those in the equations of motion and derived an expression in two-dimensional flow which is given by,

$$-\overline{u_1 u_2} = \int \overline{\omega_3 u_2} \; dx_2, \qquad (1.10)$$

where ω_3 is fluctuating vorticity in two dimensions. In a

manner similar to Phillips we note that the Reynolds stress is

a global property of the flow and also that it obtains its

value from regions of high vorticity production. Lilley (1967)

observed that it would be possible to write,

$$\overline{\omega_3 u_2} \;=\; -\,A\,\ell^2\,\frac{\partial\Omega}{\partial x_2}\,(\overline{u_2^2})^{\frac{1}{2}}, \tag{1.11}$$

where A is an arbitrary constant, Ω is the mean vorticity and

ℓ is a mixing length. From equation (1.10) we see that,

$$-\overline{u_1 u_2} \;=\; \int A\,\ell^2\,\frac{\partial\Omega}{\partial x_2}\,(\overline{u_2^2})^{\frac{1}{2}}\,dx_2 \tag{1.12}$$

The right hand side may be integrated numerically with the

measurements of root mean square velocity fluctuations and the

mean velocity profile. We may note that in Phillips' formu-

lation of the problem the Reynolds stress is related to the

kinetic energy of the transverse velocity fluctuations and in

Lilley's formulation it is related to the fluctuating vorticity.

Towards the edge of the mixing layer, or the free edge of any

shear flow, the value of $\overline{u_1 u_2}$ falls rapidly to zero as does

the value of $\overline{\omega_3^2}$ whereas the kinetic energy of the fluctuations

remains small but finite. Thus a system connecting shear

stress to fluctuating vorticity is more reasonable. Sharma

(1968) noted that as well as not meeting the requirement of

conservation of momentum in the jet or wake, Phillips' expression

may not be useful in the logarithmic region of the boundary

layer as here the inverse of x_2 will appear on the right hand

side of his expression and will give very large values of $\overline{u_1 u_2}$

for small values of x_2. However, we see that both the

expressions of Lilley and Phillips are similar in nature and

in both cases empirical values have to be found for constants.

An entirely different formulation of the problem has been

suggested by Landahl (1967). He considered that the turbulent

motion in a shear flow may be examined as a wave-propagation

phenomenon. Making use of a Fourier transform technique he

derived an equation of the Orr-Sommerfeld type for the

turbulent fluctuations. His numerical solution of the linear-

ized equation showed that, for infinitessimal disturbances,

the turbulent boundary layer with zero pressure gradient is

stable. We will now briefly summarise his analysis. First

let us consider a wave-guide with stationary random disturb-

ances. If we call the random signal $p(x,t)$ and assume

homogeneity in x then we may introduce the Fourier transform

$\hat{p}(k,w)$ defined by

$$\hat{p}(k,\omega) = \int_{-\infty}^{\infty}\int_{-\infty}^{\infty} e^{-i(kx-\omega t)} p(x,t) \, dx dt, \qquad (1.13)$$

where ω is the frequency and k is the wave number. The wave-

number frequency spectrum, $\hat{S}_{pp}(k,\omega)$, being defined as the

Fourier transform of S_{pp}, the cross spectral density, may then

be written,

$$\hat{S}_{pp}(k,\omega) = \frac{\overline{\hat{p}(k,\omega) \, \hat{p}^*(k',\omega')}}{\delta(k-k', \omega-\omega')} \qquad (1.14)$$

where δ is the generalized Dirac delta function and the

star denotes the complex conjugation. The bar denotes an

ensemble average. The inverse Fourier transform of (1.14)

leads to the cross spectral density function such that,

$$S_{pp}(\xi,\omega) = \frac{1}{2\pi} \int_{-\infty}^{\infty} e^{ik\xi} \, \hat{S}_{pp}(k,\omega)dk \qquad (1.15)$$

The random disturbances will excite the wave modes in the wave-guide and thus the Fourier transform of $p(x,t)$ will contain terms of the form,

$$\frac{c^{(n)}}{k - \alpha^{(n)}} \qquad , \qquad (1.16)$$

where $\alpha^{(n)} = \alpha_R^{(n)} + i\,\alpha_I^{(n)}$ are the wave propagation constants. In order to ensure that the disturbance field is statistically homogeneous in x, it is assumed that all the waves are damped, and hence $\alpha_I^{(n)}$ is positive for waves travelling in the positive x-direction. This condition is essential in the linear model, however statistical homogeneity may be preserved for amplifying disturbances when non-linear amplitude limiting processes occur. For the case of lightly damped wave modes, which will correlate over the largest distance, where $|\alpha_I^{(n)}| \ll |\alpha_R^{(n)}|$ then the cross spectral density will be of the form,

$$S_{pp}(\xi,\omega) = \sum_n \frac{1}{2\alpha_I^{(n)}} \, \phi^{(n,n)}(\omega) \, \exp(i\alpha_R^{(n)}\xi - \alpha_I^{(n)}|\xi|), \quad (1.17)$$

where

$$\phi^{(n,n)} = \frac{G^{(n)}(\alpha^{(n)},\omega)\, G^{(n)*}(k',\omega')}{\delta(\alpha^{(n)} - k', \; \omega-\omega')} \qquad (1.18)$$

and the coefficients $G^{(n)}$ are related to the coefficients $c^{(n)}$ in equation (1.16) and are functions of wave number and frequency.

- 15 -

In order to evaluate the term $\phi^{(n,n)}$ in equation (1.18)

Landahl introduces infinitessimal disturbances into the equations

of motion and after employing a Fourier transform technique he

obtains the equation,

$$(U-c)(\phi'' - k^2\phi) - U''\phi + \frac{i}{\alpha R}(\phi^{iv} - 2k^2\phi'' + k^4\phi)$$

$$= \hat{q}/\alpha k, \tag{1.18}$$

where ϕ is the Fourier transform of the disturbance stream

function, U is the mean velocity, $k = (\alpha^2 + \beta^2)^{\frac{1}{2}}$, where α and β

are the non-dimensional wave numbers in the x- and z-directions

respectively. $\hat{q}$ is the Fourier transform of the non-linear

Reynolds stress terms and is regarded as known and will be

considered as a forcing function. The main contribution to the

cross spectral density is assumed to come from the least attenu-

ated mode and then $S_{pp}(\xi,\zeta,\omega)$, for three dimensional disturbances

may be written,

$$S_{pp}(\xi,\zeta,\omega) = \frac{1}{2\pi} \int_{-\infty}^{\infty} \frac{\Phi^{(o,o)}}{2\alpha_I^{(o)}} \exp(i\alpha_R^{(o)}\xi - \alpha_I^{(o)}|\xi|$$

$$+ i\beta\zeta)\,d\beta \tag{1.19}$$

Landahl then notes that the main contribution to the integral

in (1.19) will come from the $\Phi^{(o,o)}$ terms as the eigenvalues

are only slightly sensitive to the wave angle. He is then

able to express the cross spectral density in terms of

expressions which are independent functions of the longitudinal

and transverse separations and he writes this in the form,

$$S_{pp}(\xi,\zeta,\omega) = S(\omega) \exp\left(\frac{i\omega\xi}{U_c}\right) A\left(\frac{\omega\xi}{U_c}\right) B\left(\frac{\omega\zeta}{U_c}\right) , \qquad (1.30)$$

where U_c is the convection velocity given by,

$$U_c = \omega/\alpha_R . \qquad (1.31)$$

This expression (1.20) was proposed by Corcos (1964) on the basis of the experiments by Willmarth and Wooldridge (1962). Willmarth and Roos (1965) showed that there existed regions of separation and non-dimensional frequency where Corcos' similarity formulation does not hold. It is not valid for $\omega\delta^*/U_\infty > 3$, $|\zeta|/\delta^* < 0.7$ and for $\omega\delta^*/U_\infty < 1$, $|\zeta|/\delta^* > 1$.

In his calculations of convection velocity Landahl's equation (1.21) means he has equated convection velocity and phase velocity. This convection velocity was found to be too low by 30%. However, if a viscosity of a much higher value was assumed the convection velocities agreed with experiments. Landahl concluded that one should consider the propagation of a wave in a flow with pre-existing fluctuations, which may act like an eddy viscosity. However, the inclusion of an eddy viscosity means the problem must be reformed as, for instance, the mean velocity will be a function of the disturbed flow.

In Landahl's analysis we also see that the ratio α_I/α_R is taken as constant though it would appear that the variation of α_I with frequency is much greater than that of α_R. Landahl chooses a constant value of α_I/α_R as he notes

that the calculated decay rate has an uncertainty, the major

contribution to which coming from the uncertainty in the mean

velocity profile. This implies that an eddy will decay in a

distance proportional to its size. The calculations of

Sharma (1968) show that the ratio α_I/α_R is not constant and

the proportional rate of decay of small eddies is much greater

than that of the larger eddies. Landahl's results also indi-

cate that the wave number/frequency ratio is constant, which

implies that the system is non-dispersive.

The non-linear terms in Landahl's work are treated as a

forcing function needed to maintain an otherwise continuously

decaying disturbance field. It is clear that this assumption

will not hold when there exists an unstable mode in the flow.

It is likely that turbulent bursts in the boundary layer,

which Landahl associates with a non-linear process, are the

result of instabilities in the mean profile. Experiments

indicate that these bursts occur in the region where large

variations occur in the derivatives of the mean velocity

profile and it is this, as Landahl notes, which leads to

uncertainty in his calculations of the amplification factors.

Landahl also relies on there only being one dominant mode

in the flow which is not the case for instance in the jet,

where Lessen et al (1965) found more than one unstable

mode.

It would appear that the range of application of Landahl's

hypothesis is limited to flows where there exist no amplifying

disturbances. In these cases the assumption that non-linear

terms are forcing functions is more reasonable. This is only possible in certain cases in the light of a linear analysis. For the case of the boundary layer, Sharma (1968) found that there are amplifying modes. We may also recall that Malkus hypothesised that the non-linear terms have a stabilising influence on the flow.

In our present study of the turbulent mixing layer between two streams will we have need to call on the non-linear terms to act as both stabilising and destabilising influences. In order to present a complete study of the mixing layer the work will be divided into four sections. We will firstly consider the solution of the mean equations of motion for both cases of laminar and turbulent mixing. Secondly, we will examine the stability of a laminar mixing layer between two streams of finite velocity. We will then present a model for the structure of the turbulent mixing layer. Finally, the effects of finite amplitude disturbances in the mixing layer will be examined. A review of previous work on these various topics will be presented in the relevant sections.

In the next chapter we will derive the governing differential and integral equation of the mixing layer between two streams.

CHAPTER 2

Mathematical Derivation

In this chapter the equations that describe the turbulent shear flow problem will be described. These equations will be presented in a convenient form for the performance of numerical calculations.

2.1 Governing Differential Equations

For convenience we will derive the equation using tensor notation. Repeated suffices will imply summation over the values of the repeated suffix. A point in the flow is written as $\underset{\sim}{x}$ with co-ordinates x_i where, for rectangular cartesian co-ordinates, $i = 1,2,3$ and the velocity component of the flow in the x_i direction is given by u_i. In certain sections of the analysis the notation (x,y,z) and (u,v,w) will be used instead of x_i and u_i respectively.

It is initially assumed that the fluid is incompressible and that the fluid properties are independent of temperature. Thus fluctuations of fluid density due to pressure, entropy and vortical fluctuations are neglected. These assumptions are valid if the flow speed is low. When calculations of the acoustic radiation of the flow are to be made the compressible flow equations must be used. However, the incompressible flow problem will be solved as the starting point for dealing with the complete problem.

The equation of continuity for incompressible flow may be written,

$$\frac{\partial u_i}{\partial x_i} = 0 \qquad\qquad (2.1)$$

The Navier-Stokes equations will be assumed to describe the motions of both turbulent and laminar flow. They may be written for turbulent incompressible flow as,

$$\frac{\partial u_i}{\partial t} + u_j \frac{\partial u_i}{\partial x_j} = -\frac{1}{\rho} \frac{\partial p}{\partial x_i} + \nu \nabla^2 u_i \quad . \qquad (2.2)$$

Using the equation of continuity (2.1), equation (2.2) may be rewritten,

$$\frac{\partial u_i}{\partial t} + \frac{\partial u_i u_j}{\partial x_j} = -\frac{1}{\rho} \frac{\partial p}{\partial x_i} + \nu \nabla^2 u_i \quad , \qquad (2.3)$$

where $i,j = 1,2,3$, (x_1, x_2, x_3) are a set of orthogonal co-ordinates, $\nabla^2 = \frac{\partial^2}{\partial x_1^2} + \frac{\partial^2}{\partial x_2^2} + \frac{\partial^2}{\partial x_3^2}$, u_i is the instantaneous velocity component parallel to the x_i axis, ρ is the fluid density, p is the pressure and ν is the kinematic viscosity, u/ρ.

The instantaneous values of velocity and pressure may be written as,

$$u_i(x_i,t) = U_i(x_i) + u_i{}'(x_i,t) \qquad)$$
$$\qquad\qquad\qquad\qquad\qquad\qquad) \qquad (2.4)$$
$$\text{and} \quad p(x_i,t) = P(x_i) + p'(x_i,t) \qquad)$$

where $u_i{}'$ and p' are the turbulent fluctuations and U_i and P are the average values of velocity and pressure averaged according to,

$$U_i = \lim_{T \to \infty} \frac{1}{2T} \int_{-T}^{T} u_i \, dt, \text{ etc.}$$

By substitution of the relations (2.4) into (2.2) and (2.3) and averaging over a long period, we have,

$$\frac{\partial U_i}{\partial x_i} = 0,$$

and   (2.5)

$$\frac{\partial U_i U_j}{\partial x_j} + \frac{\partial \overline{u_i' u_j'}}{\partial x_j} = -\frac{1}{\rho}\frac{\partial P}{\partial x_i} + \nu \nabla^2(U_i)$$

When the equations for the mean flow (2.5) are subtracted from equations (2.1) and (2.3) we obtain the equations for the fluctuations,

$$\frac{\partial u_i'}{\partial x_i} = 0,$$
                                                                                       (2.6)

$$\frac{\partial u_i'}{\partial t} + \frac{\partial u_i' U_j}{\partial x_j} + \frac{\partial U_i u_j'}{\partial x_j} + \frac{\partial u_i' u_j'}{\partial x_j} - \frac{\partial \overline{u_i' u_j'}}{\partial x_j} = -\frac{1}{\rho}\frac{\partial p'}{\partial x_i} + \nu \nabla^2(u_i')$$

If it is argued that the disturbance motion is rotational it is convenient to rewrite the equations in terms of a fluctuating vorticity. Thus on making use of the alternating, third-order tensor, ε_{ijk},

where (i) $\varepsilon_{ijk} = 0$ if any two of the indices ijk are equal,

   (ii) $\varepsilon_{123} = \varepsilon_{231} = \varepsilon_{312} = 1$,

and (iii) $\varepsilon_{132} = \varepsilon_{321} = \varepsilon_{213} = -1$, equations (2.2) may be written in terms of the vorticity. Helmholtz's equations for the vorticity follow and are,

$$\frac{\partial \omega_i}{\partial t} + u_j \frac{\partial \omega_i}{\partial x_j} = \omega_j \frac{\partial u_i}{\partial x_j} + \nu \nabla^2 \omega_i,$$ (2.7)

where the vorticity, ω_k, is given by,

$$\omega_k = \frac{\partial u_i}{\partial x_j} \varepsilon_{ijk} \qquad .$$ (2.8)

Now since the divergence of the vorticity is zero, or in
tensor notation,

$$\frac{\partial \omega_i}{\partial x_i} = 0,$$

then equation (2.7) may be rewritten,

$$\frac{\partial \omega_i}{\partial t} + \frac{\partial \omega_i u_j}{\partial x_j} = \frac{\partial u_i \omega_j}{\partial x_j} + \nu \nabla^2 \omega_i \qquad (2.9)$$

If the instantaneous value of the vorticity is written as,

$$\omega_i(x_i, t) = \Omega_i(x_i) + \omega_i'(x_i, t),$$

then substitution of this relation into equation (2.9) and
averaging over a long time period yields the equation for the
mean vorticity,

$$\frac{\partial \Omega_i U_j}{\partial x_j} - \frac{\partial U_i \Omega_j}{\partial x_j} + \frac{\partial \overline{\omega_i' u_j'}}{\partial x_j} - \frac{\partial \overline{u_i' \omega_j'}}{\partial x_j} = \nu \; \nabla^2 (\Omega_i) \; . \qquad (2.10)$$

To obtain the equation for the vorticity fluctuations equation
(2.10) is subtracted from equation (2.7) to yield,

$$\frac{\partial \omega_i'}{\partial t} + \frac{\partial U_j \omega_i'}{\partial x_j} + \frac{\partial \Omega_i u_j'}{\partial x_j} - \frac{\partial \Omega_j u_i'}{\partial x_j} - \frac{\partial U_i \omega_j'}{\partial x_j} + \chi_i = \nu \; \nabla^2 (\omega_i')$$

$$\text{where } \chi_i = \frac{\partial (u_j' \omega_i' - u_i' \omega_j')}{\partial x_j} - \frac{\partial (\overline{u_j' \omega_i'} - \overline{u_i' \omega_j'})}{\partial x_j} \qquad (2.11)$$

Having derived the general differential equations which describe
the motion of a turbulent fluid, the next sections will con-
sider their application to the problem of the turbulent mixing
of two parallel streams. Firstly, the equations that describe

the stability of the flow will be derived. The integral

equations of the mean flow and the fluctuations will be derived

and the significance of the components in the equations will be

discussed.

2.2 Derivation of the Equations for the Stability of the Viscous Shear Layer

The study of hydrodynamic stability was initiated with the

work of Helmholtz, (1868). This contribution was followed by

the works of Reynolds (1883), Kelvin (1880) and Rayleigh (1878

onwards). The derivation of the equations which included the

effects of viscosity and enabled a critical Reynolds number to

be calculated, was arrived at independently by Orr (1907) and

Sommerfeld (1908). The Orr-Sommerfeld equation was derived by

considering two-dimensional wave-like disturbances superimposed

on the parallel mean flow. The equation remained unsolved for

a number of years until Tollmien (1929) obtained the first

critical Reynolds number. A review of methods of solution of

the Orr-Sommerfeld equation is presented later, however we will

be concerned here with its derivation for non-parallel flows

and three-dimensional disturbances.

2.2.1 The Stability of the Shear Layer to Three-dimensional Disturbances

In this section we will derive the stability equation for

a shear layer with two-dimensional mean flow. x_1 is measured

along the line of separation of the two parallel streams prior

to mixing, x_3 is measured in the transverse direction across

the plane of mixing and x_2 is measured normal to x_1 and x_3.

The origin of co-ordinates is taken as the point at which

mixing theoretically commences, see diagram below.
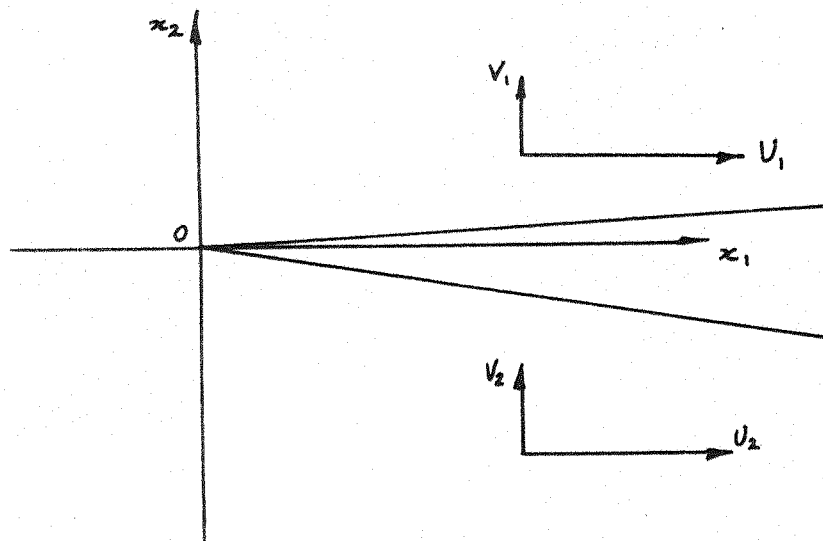
As a consequence of the assumption of a two-dimensional mean flow we have that the mean velocity is a function of x_1 and x_2. The assumption of a parallel mean flow will be considered at a later stage when the stability equations in their fuller form have been derived. Thus we may write,

$$
\begin{aligned}
u_1(x_i,t) &= U(x_1,x_2) + u_1'(x_i,t) \\
u_2(x_i,t) &= V(x_1,x_2) + u_2'(x_i,t) \\
u_3(x_i,t) &= \qquad\qquad u_3'(x_i,t) \\
\text{and}\quad p(x_i,t) &= P(x_1,x_2) + p'(x_i,t)
\end{aligned}
\tag{2.12}
$$

The corresponding relations for the vorticity components are written,

$$
\begin{aligned}
\omega_1(x_i,t) &= \qquad\qquad \omega_1'(x_i,t) \\
\omega_2(x_i,t) &= \qquad\qquad \omega_2'(x_i,t) \\
\text{and}\quad \omega_3(x_i,t) &= \Omega_3(x_1,x_2) + \omega_3'(x_i,t)
\end{aligned}
\tag{2.13}
$$

Substitution of these relations into equation (2.11) and the first of equation (2.6) yields;

- 24 -

$$\left\{\frac{\partial}{\partial t} + \frac{U\partial}{\partial x_1} + \frac{V\partial}{\partial x_2}\right\}\omega_1 - \Omega_3\frac{\partial u_1}{\partial x_3} - \omega_1\frac{\partial U}{\partial x_1} - \omega_2\frac{\partial U}{\partial x_2} + \chi_1 = \nu\,\nabla^2(\omega_1)$$

$$\left\{\frac{\partial}{\partial t} + \frac{U\partial}{\partial x_1} + \frac{V\partial}{\partial x_2}\right\}\omega_2 - \Omega_3\frac{\partial u_2}{\partial x_3} - \omega_1\frac{\partial V}{\partial x_1} - \omega_2\frac{\partial V}{\partial x_2} + \chi_2 = \nu\,\nabla^2(\omega_2) \qquad (2.14)$$

$$\left\{\frac{\partial}{\partial t} + \frac{U\partial}{\partial x_1} + \frac{V\partial}{\partial x_2}\right\}\omega_3 + u_1\frac{\partial\Omega_3}{\partial x_1} + u_2\frac{\partial\Omega_3}{\partial x_2} - \Omega_3\frac{\partial u_3}{\partial x_3} + \chi_3 = \nu\,\nabla^2(\omega_3)$$

and

$$\frac{\partial u_1}{\partial x_1} + \frac{\partial u_2}{\partial x_2} + \frac{\partial u_3}{\partial x_3} = 0$$

where

$$\chi_1 = \frac{\partial(u_2\omega_1 - u_1\omega_2)}{\partial x_2} + \frac{\partial(u_3\omega_1 - u_1\omega_3)}{\partial x_3} - \left\{(\overline{\quad}) + (\overline{\quad})\right\}$$

$$\chi_2 = \frac{\partial(u_1\omega_2 - u_2\omega_1)}{\partial x_1} + \frac{\partial(u_3\omega_2 - u_2\omega_3)}{\partial x_3} - \left\{(\overline{\quad}) + (\overline{\quad})\right\}$$

and

$$\chi_3 = \frac{\partial(u_1\omega_3 - u_3\omega_1)}{\partial x_1} + \frac{\partial(u_2\omega_3 - u_3\omega_2)}{\partial x_2} - \left\{(\overline{\quad}) + (\overline{\quad})\right\}$$

where the bracketted terms, $(\overline{\quad})$, represent the time averages

of the preceding fluctuating quantities. The primes denoting

fluctuating quantities have been omitted for convenience.

In linearised theory it is assumed that, as the fluctua-

tions are infinitesimal, products of fluctuations and their

derivatives, such as $\dfrac{\partial u_2\omega_1}{\partial x_2}$, may be neglected in comparison with

the other terms in the equations. In the subsequent analysis

we will discard the x_1 - momentum equation in (2.14) in favour

of the equation of continuity. We will further assume that

in equations (2.13) the mean vorticity component, Ω_3, is

dominated by the term $\dfrac{\partial U}{\partial x_2}$. Then the last three equations of

(2.14) become,

$$\left\{\frac{\partial}{\partial t} + \frac{U\partial}{\partial x_1} + \frac{V\partial}{\partial x_2} - \nu \nabla^2\right\}\omega_2 - \frac{\partial V}{\partial x_2}\omega_2 + \frac{\partial U}{\partial x_2}\frac{\partial u_2}{\partial x_3} = 0 \qquad)$$

$$\left\{\frac{\partial}{\partial t} + \frac{U\partial}{\partial x_1} + \frac{V\partial}{\partial x_2} - \nu \nabla^2\right\}\omega_3 + \frac{\partial U}{\partial x_2}\frac{\partial u_3}{\partial x_3} - u_2\frac{\partial^2 U}{\partial x_2^2} + u_1\frac{\partial^2 V}{\partial x_2^2} = 0 \quad) \quad (2.15)$$

$$\text{and} \quad \frac{\partial u_1}{\partial x_1} + \frac{\partial u_2}{\partial x_2} + \frac{\partial u_3}{\partial x_3} = 0 \qquad)$$

In these equations we have retained those terms in the mean flow
that are of order unity or greater according to the normal
boundary layer approximation.

In order to reduce these partial differential equations to
an ordinary differential equation we will make use of the Fourier
transform method. We will assume that the flow is statistically
stationary in the x_1-x_3 plane and that the boundary conditions
may be written in terms of the transverse distance x_2. We will
reduce the set of equations (2.15) to a set of ordinary differ-
ential equations by using the Fourier transform with respect to
x_1, x_3 and t. Thus we write,

$$\hat{q}(\underset{\sim}{k}, \omega, x_2) = \frac{1}{(2\pi)^3}\int\!\!\!\int\!\!\!\int_{-\infty}^{\infty}\exp\{-i(k_1 x_1 + k_3 x_3 - \omega t)\}$$

$$(2.16)$$

$$q(x_1, x_3, t, x_2)dx_1 dx_3 dt$$

where $q(x_1, x_3, t; x_2)$ is a generalised disturbance function de-
pendent on space and time, $\hat{q}(\underset{\sim}{k}, \omega; x_2)$ is its Fourier transform,
$\underset{\sim}{k} = (k_1, k_3)$ is the wave number vector of the fluctuation in the
x_1, x_3 plane and ω is the complex frequency. The Fourier trans-
form for the velocity fluctuation can be written,

$$\hat{u}_i(\underset{\sim}{k},\omega;x_2) = \frac{1}{(2\pi)^3} \int\!\!\!\int\!\!\!\int_{-\infty}^{\infty} \exp\{-i(k_1 x_1 + k_3 x_3 - \omega t)\}$$

$$u_i(x_1,x_3,t;x_2)dx_1 dx_3 dt.$$

(2.16a)

where $\hat{u}_i(\underset{\sim}{k},\omega;x_2)$ is the complex Fourier transform of the velocity fluctuation $u_i(\underset{\sim}{x},t)$. The limits of integration over x_1 would be better considered as $(\chi, -\chi)$ with $\chi \to \infty$ to guard against the possibility of divergence of the integral of $\underline{u}$ at infinity.

In equation (2.15) we note that the derivatives of the mean velocities are all with respect to x_2. In order to facilitate the transformation of the equations we will assume that U and V are functions of x_2 only bearing in mind the weak dependence of both on x_1.

Transformations of the form (2.16a) of the velocity fluctuations are used and equations (2.15) may be written, with the vorticity fluctuations replaced by their velocity components, as follows,

$$\{\Delta - \frac{\partial V}{\partial x_2}\}(i\beta \hat{u}_1 - i\alpha \hat{u}_3) + i\beta \frac{\partial U}{\partial x_2} \hat{u}_2 = 0,$$

$$\Delta(i\alpha \hat{u}_2 - \frac{\partial \hat{u}_1}{\partial x_2}) + i\beta \frac{\partial U}{\partial x_2} \hat{u}_3 - \frac{\partial^2 U}{\partial x_2^2} \hat{u}_2 + \frac{\partial^2 V}{\partial x_2^2} \hat{u}_1 = 0,$$

and $i\alpha \hat{u}_1 + \frac{\partial \hat{u}_2}{\partial x_2} + i\beta \hat{u}_3 = 0,$

where Δ is the operator $\left[i\alpha(U - \frac{\omega}{\alpha}) + \frac{V\partial}{\partial x_2} - \frac{1}{R}\{\frac{\partial^2}{\partial x_2^2} - (\alpha^2 + \beta^2)\}\right]$

All quantities have been non-dimensionalised with respect to a reference velocity U_0, and a reference length L. Also $\alpha = k_1 L$, $\beta = k_3 L$ and $R = \frac{U_0 L}{\nu}$.

We note that

$$\{\Delta \frac{\partial}{\partial x_2} - \frac{\partial}{\partial x_2} \Delta\} = -i\alpha \frac{\partial U}{\partial x_2} - \frac{\partial V}{\partial x_2} \frac{\partial}{\partial x_2} \quad . \tag{2.18}$$

Eliminating $\hat{u}_3$ between the second and third equations of (2.17) we obtain,

$$\left[\Delta \frac{\partial}{\partial x_2} + i\alpha \frac{\partial U}{\partial x_2} - \frac{\partial^2 V}{\partial x_2^2}\right] \hat{u}_1 - \left[i\alpha\Delta - \frac{\partial U}{\partial x_2} \frac{\partial}{\partial x_2} - \frac{\partial^2 U}{\partial x_2^2}\right] \hat{u}_2 = 0. \quad \text{Making}$$

use of relation (2.18) we may rewrite this in the form,

$$\left[\frac{\partial}{\partial x_2}(\Delta - \frac{\partial V}{\partial x_2})\right] \hat{u}_1 - \left[i\alpha\Delta - \frac{\partial U}{\partial x_2} \frac{\partial}{\partial x_2} - \frac{\partial^2 U}{\partial x_2^2}\right] \hat{u}_2 = 0. \tag{2.19}$$

We now eliminate $\hat{u}_3$ between the first and third of equation (2.17) to obtain,

$$\{(\alpha^2 + \beta^2)\left[\Delta - \frac{\partial V}{\partial x_2}\right]\} \hat{u}_1 + \{\beta^2 \frac{\partial U}{\partial x_2} - i\alpha\left[\Delta - \frac{\partial V}{\partial x_2}\right] \frac{\partial}{\partial x_2}\} \hat{u}_2 = 0.$$

If we differentiate this equation with respect to x_2 we obtain,

$$(\alpha^2 + \beta^2)\{\frac{\partial}{\partial x_2} (\Delta - \frac{\partial V}{\partial X_2})\} \hat{u}_1 + \{\beta^2 \frac{\partial^2 U}{\partial x_2^2} + \beta^2 \frac{\partial U}{\partial x_2} \frac{\partial}{\partial x_2}$$

$$-i\alpha\left[\frac{\partial}{\partial x_2} (\Delta - \frac{\partial V}{\partial x_2}) \frac{\partial}{\partial x_2}\right]\} \hat{u}_2 = 0 \tag{2.20}$$

Eliminating $\{\frac{\partial}{\partial x_2} (\Delta - \frac{\partial V}{\partial x_2})\}\hat{u}_1$ between equations (2.19) and (2.20) and replacing the operator Δ we obtain, after some rearrangement,

$$(U - \frac{\omega}{\alpha})\{\hat{u}_2'' - (\alpha^2 + \beta^2)\hat{u}_2\} - U''\hat{u}_2 + \frac{i}{\alpha R} \{\hat{u}_2^{iv} - 2(\alpha^2 + \beta^2)\hat{u}_2''$$

$$+ (\alpha^2 + \beta^2)^2 \hat{u}_2\}$$

$$= \frac{i}{\alpha}\{V\hat{u}_2''' - (V'' + (\alpha^2 + \beta^2)V)\hat{u}_2'\}$$

where primes denote differentiation with respect to x_2.

If the right hand side of equation (2.21) is set equal to zero then we obtain the Orr-Sommerfeld equation for three-dimensional disturbances,

$$(U - \frac{\omega}{\alpha})\{\hat{u}_2{}'' - (\alpha^2 + \beta^2)\hat{u}_2\} - U'' \hat{u}_2 + \frac{i}{\alpha R} \{\hat{u}_2^{iv} - 2(\alpha^2 + \beta^2)\hat{u}_2'' +$$
$$+ (\alpha^2 + \beta^2)^2\hat{u}_2\} = 0 \qquad (2.21a)$$

Equation (2.21a) would have resulted from the analysis if an assumption of parallel flow had been made. The coefficients of the terms on the right hand side of equation (2.21) are small compared with the coefficients of the Orr-Sommerfeld equation. It may be argued that the inclusion of these terms in the equation will not greatly affect its solution. However, the divergence of the flow is a necessary factor in the solution, as a parallel flow assumption fails to provide a critical Reynolds number. It will be argued that the effect of diverg-ence of the flow is accounted for best by modifying the eigen-values found for equation (2.21a). The corresponding eigen-functions of equation (2.21a) are known to change very slowly with change in eigenvalues and it may be argued that the eigen-functions corresponding to the modified eigenvalues will closely approximate to those of the unmodified values. We will argue that the flow divergence will affect the energy of the inter-action between the disturbances and the mean flow and we will modify the eigenvalues according to this argument.

2.3 The Integral Equations for the Flow

The integral equations of the mean flow are obtained by integrating over the transverse co-ordinate, x_2. The equations

may then be reduced to ordinary differential equations in x_1.

We will make use of the boundary layer type approximations, that is,

i) $V/U \ll 1$

ii) $\frac{\partial}{\partial x}/\frac{\partial}{\partial y} \ll 1$, or the growth of the layer is small.

The mean momentum equation may be obtained from the mean vorticity equation (2.10), which may be rewritten for a two dimensional mean flow as,

$$U\frac{\partial U}{\partial x} + V\frac{\partial U}{\partial y} + \frac{\partial \overline{uv}}{\partial y} + \frac{\partial}{\partial x}(\overline{u}^2 - \overline{v}^2) = \nu \frac{\partial^2 U}{\partial y^2} \qquad (2.22)$$

Let $\delta_1(x)$ be the edge of the mixing layer on the side with velocity U_1 and $-\delta_2(x)$ be the edge on the side with velocity U_2. Then integrating equation (2.22) between the edges of the layer we obtain,

$$\int_{-\delta_2}^{\delta_1} \frac{\partial}{\partial x}\left[(U - U_1)(U - U_2) + (\overline{u}^2 - \overline{v}^2)\right] dy + \left[V_2 U_1 - U_2 V_1\right] = 0. \qquad (2.23)$$

Here we have assumed that the disturbances have zero magnitude at the edges of the layer and we have introduced into the integrand the two zero terms, $-\frac{V\partial U_1 + U_2}{\partial y}$ and $\frac{\partial U_1 U_2}{\partial x}$. In this way the integrand is zero on both sides of the mixing layer. The equation for the differentiation of an integral may be written as,

$$\int_{\alpha(a)}^{\beta(a)} \frac{\partial}{\partial a}\left[f(b,a)\right] db = \frac{\partial}{\partial a}\int_{\alpha(a)}^{\beta(a)}\left[f(b,a)\right] db + f(\alpha,a)\frac{d\alpha}{da} - f(\beta,a)\frac{\partial\beta}{\partial a} \qquad (2.24)$$

Making use of this relation we may rewrite eq. (2.23) as

$$\frac{d}{dx} \int_{-\delta_2}^{\delta_1} [(U - U_1)(U - U_2) + (\overline{u^2} - \overline{v^2})] dy + [V_2 U_1 - U_2 V_1] = 0 \qquad (2.25)$$

The mechanical energy equation may be obtained most conveniently

for the mixing layer by multiplying equation (2.22) throughout

by $U - \dfrac{(U_1 + U_2)}{2}$, that is,

$$U^2 \frac{\partial U}{\partial x} + UV \frac{\partial U}{\partial y} - \frac{U(U_1 + U_2)}{2} \frac{\partial U}{\partial x} - \frac{V}{2} \frac{\partial (U_1 + U_2)U}{\partial y} + [U - \frac{(U_1 + U_2)}{2}]$$

$$\frac{\partial \overline{uv}}{\partial y} + [U - \frac{(U_1 + U_2)}{2}] \frac{\partial (\overline{u^2} - \overline{v^2})}{\partial x}$$

$$= \nu U \frac{\partial^2 U}{\partial y^2} - \frac{\nu}{2} (U_1 + U_2) \frac{\partial^2 U}{\partial y^2} \qquad (2.26)$$

Integrating equation (2.26) across the mixing layer we obtain,

$$\int_{-\delta_2}^{\delta_1} \frac{d}{dx} \{ \frac{1}{2} [U(U - U_1)(U - U_2)] + [U - \frac{(U_1 + U_2)}{2}] (\overline{u^2} - \overline{v^2}) \} dy$$

$$= \int_{-\delta_2}^{\delta_1} (\overline{u^2} - \overline{v^2}) \frac{\partial U}{\partial x} dy + \int_{-\delta_2}^{\delta_1} \overline{uv} \frac{\partial U}{\partial y} dy - \nu \int_{-\delta_2}^{\delta_1} (\frac{\partial U}{\partial y})^2 dy,$$

where we have introduced into the integrand the zero term,
$\dfrac{V}{2} \dfrac{\partial U_1 U_2}{\partial y}$. Making use of relation (2.24) the integral of the

mean mechanical energy equation may be written,

$$\frac{d}{dx} \int_{-\delta_2}^{\delta_1} \{ \frac{1}{2} [U(U - U_1)(U - U_2)] + [U - \frac{(U_1 + U_2)}{2}](\overline{u^2} - \overline{v^2}) \} dy$$

$$= \int_{-\delta_2}^{\delta_1} (\overline{u^2} - \overline{v^2}) \frac{\partial U}{\partial x} dy + \int_{-\delta_2}^{\delta_1} \overline{uv} \frac{\partial U}{\partial y} dy - \nu \int_{-\delta_2}^{\delta_1} (\frac{\partial U}{\partial y})^2 dy. \qquad (2.27)$$

The energy equation for the fluctuation may be obtained by multiplying the second equation of (2.6) throughout by u_i. We then obtain,

$$u_i \frac{\partial u_i}{\partial t} + \frac{u_i \partial u_i U_j}{\partial x_j} + \frac{u_i \partial U_i u_j}{\partial x_j} + \frac{u_i \partial u_i u_j}{\partial x_j} - \frac{u_i \partial \overline{u_i u_j}}{\partial x_j} =$$

$$= - \frac{1}{\rho} \frac{\partial p u_i}{\partial x_i} + \nu \, u_i \, \nabla^2 (u_i) \tag{2.28}$$

If we introduce the kinetic energy of the turbulence per unit mass, written as,

$$\frac{q^2}{2} = \frac{u_i u_i}{2} \quad ,$$

then equation (2.28) may be written as, having averaged over a long period,

$$\left[\frac{\partial}{\partial x_j} \left(U_j \frac{\overline{q^2}}{2} \right) \right] + \frac{\partial}{\partial x_j} \left[\overline{u_j \frac{q^2}{2}} + \frac{\overline{p u_j}}{\rho} \right] = \nu \, \nabla^2 \frac{\overline{q^2}}{2} - \nu \overline{\left(\frac{\partial u_i}{\partial x_j} \right)^2} -$$

$$- \overline{u_i u_j} \frac{\partial U_i}{\partial x_j} \tag{2.29}$$

We will assume that the motion is two-dimensional for mean quantities and time averaged fluctuations. Thus we will neglect $\overline{w^2}$ etc. and also assume that $\frac{\partial (\quad)}{\partial z} = 0$. It will be shown, in our later discussion on the stability of the mixing layer, that the most amplifying disturbances are two-dimensional. Experiments have also shown that in the transition region the disturbances are essentially two-dimensional. Thus, if we confine ourselves in our subsequent analysis to this region of the flow then we may treat the whole flow as two dimensional. If we integrate equation (2.29) over the transverse co-ordinate

y we obtain,

$$\frac{1}{2} \int_{-\delta_2}^{\delta_1} \frac{d}{dx} \left[U(\overline{u^2} + \overline{v^2}) + \overline{u^3} + \overline{uv^2} + \frac{2\overline{up}}{\rho} \right] dy$$

$$= - \int_{-\delta_2}^{\delta_1} (\overline{u^2} - \overline{v^2}) \frac{\partial U}{\partial x} \, dy - \int_{-\delta_2}^{\delta_1} \overline{uv} \left(\frac{\partial U}{\partial y} + \frac{\partial V}{\partial x} \right) dy \qquad (2.30)$$

$$+ \frac{\nu}{2} \int_{-\delta_2}^{\delta_1} \frac{d^2}{dx^2} (\overline{u^2} + \overline{v^2}) - \nu \int_{-\delta_2}^{\delta_1} \left[\overline{\left(\frac{\partial u}{\partial x}\right)^2} + \overline{\left(\frac{\partial u}{\partial y}\right)^2} + \overline{\left(\frac{\partial v}{\partial x}\right)^2} + \overline{\left(\frac{\partial v}{\partial y}\right)^2} \right] dy$$

Finally, making use of relationship (2.24), the integral of

the mean fluctuation energy equation may be written:

$$\frac{1}{2} \frac{d}{dx} \int_{-\delta_2}^{\delta_1} \left[U(\overline{u^2} + \overline{v^2}) + \overline{u^3} + \overline{uv^2} + \frac{2\overline{up}}{\rho} \right] dy$$

$$= - \int_{-\delta_2}^{\delta_1} (\overline{u^2} - \overline{v^2}) \frac{\partial U}{\partial x} \, dy - \int_{-\delta_2}^{\delta_1} \overline{uv} \, \frac{\partial U}{\partial y} - \nu \int_{-\delta_2}^{\delta} \left[\overline{\left(\frac{\partial u}{\partial x}\right)^2} + \overline{\left(\frac{\partial u}{\partial y}\right)^2} + \right.$$

$$\left. + \overline{\left(\frac{\partial v}{\partial x}\right)^2} + \overline{\left(\frac{\partial v}{\partial y}\right)^2} \right] dy \qquad (2.31)$$

Here we have neglected the terms $\frac{\partial V}{\partial x}$ and $\frac{d^2}{dx^2} \int (\overline{u^2} + \overline{v^2}) dy$

according to our boundary layer type assumptions.

It should be noted that in our derivation of equation

(2.31) the averaging of the fluctuations has been carried out

over a long time period assuming that the turbulent field is

stationary. In later analysis, where a single component of

frequency will be assumed to exist, the integration will be

performed over a single period.

It is interesting to note briefly the function of the various terms in the fluctuating energy equation. Let us consider equation (2.29). The first term in brackets on the left hand side of the equation represents the change in kinetic energy of the turbulent field. The second term represents the diffusion of the total turbulent energy by the turbulence itself. We may rewrite equation (2.29) as,

$$\left[\frac{\partial}{\partial x_j}\left(U_j\frac{\overline{q^2}}{2}\right)\right] + \frac{\partial}{\partial x_j}\left[\overline{u_j\frac{q^2}{2}} + \frac{\overline{pu_i}}{\rho}\right] = \nu\frac{\partial}{\partial x_i}\ \overline{u_j\left(\frac{\partial u_i}{\partial x_j} + \frac{\partial u_j}{\partial x_i}\right)}$$

$$- \nu\overline{\left(\frac{\partial u_i}{\partial x_j} + \frac{\partial u_j}{\partial x_i}\right)\frac{\partial u_j}{\partial x_i}} - \overline{u_i u_j}\frac{\partial U_i}{\partial x_j} \qquad (2.32)$$

The first term on the right hand side of equation (2.32) represents the work done per unit mass and time by the viscous shear stresses of the turbulence and the second viscous term represents the dissipation per unit mass by the turbulence. The final term describes the transfer of energy between the mean motion and the turbulent shear stresses.

A qualitative analysis of the behaviour of the flow field in a non-linear region may be obtained by considering equation (2.29). The difference between the two small quantities $\overline{u^2}$ and $\overline{v^2}$ may be assumed to be small. Then we see that when the fluctuations are very small the production term will be negligible compared with the viscous dissipation term and the solution of the equation will be that for a laminar mixing layer. As the fluctuation grows the Reynolds stress term becomes comparable in magnitude with the dissipation term and the mean flow will deviate from the laminar solution. As the fluctuation amplitude increases further the Reynolds stress

term dominates and the mean flow then satisfies the solution
of the turbulent mixing layer equations.

In the next chapter we will consider the solution of
the mean velocity equations for turbulent and laminar mixing
layers. These solutions are a required input for the sub-
sequent solution of the small disturbance and stability
equations.

CHAPTER 3

THE SOLUTION OF THE MEAN EQUATIONS FOR THE MIXING OF TWO STREAMS

3.1 Introduction

The mixing of two parallel streams can be usefully divided
into two types: laminar and turbulent. For both cases of mixing
it is possible to deduce that a similar solution will exist. In
the case of laminar mixing the rate of spread of the mixing layer
is a function of the square root of downstream distance and for
turbulent mixing the spread rate is constant. The differential
equations for the stream functions, defined in terms of a simi-
larity co-ordinate, may be derived for laminar flow without any
assumptions other than the boundary layer type assumptions. For
turbulent mixing, however, some hypothesis must be made regarding
the behaviour of the Reynolds stress. The inclusion of a stream
function in the equations of motion leads in both cases to a
third order differential equation. There are thus three boundary
conditions required for a unique solution. In this chapter we
will derive and solve the differential equations governing the
laminar and turbulent mixing of two streams.

3.2.1. The Laminar Mixing of Two Parallel Streams

The solution of the laminar boundary layer equations for
mixing of parallel streams was performed by Lessen (1950) in
his stability analysis of a laminar mixing layer. He derived
the differential equation for the streamfunction, having
assumed a similarity variable, using a general analysis with
both undisturbed streams having finite velocity. In order to

be able to expand a solution of a transformed form of the differential equation it was necessary to limit the boundary conditions such that one stream was at rest. The laminar mixing problem was tackled by Lock (1951) and solved for the case of the mixing of streams of different fluids for various velocity ratios. Lock assumed as a third boundary condition, to be discussed later, that $f(o) = 0$ where f is the stream function in terms of a similarity co-ordinate η. Lin (1953) solved the problem using a modification of Gortler's (1942) method for turbulent mixing. Crane (1957) extended this work to deal with the problem of the compressible mixing of two streams.

It is thought useful at this stage to consider the boundary conditions on the problem. There are two boundary conditions apparent in the problem, namely,

$$U \to U_1 \qquad \text{as} \qquad y \to \infty$$

and $\qquad\qquad\qquad\qquad\qquad\qquad\qquad\qquad\qquad\qquad$ (3.1)

$$U \to U_2 \qquad \text{as} \qquad y \to -\infty$$

The third boundary condition necessary for a unique solution of the third order differential equation of the streamfunction is not so clear. The simplest condition used by Lin (1953) and Gortler (1942) implied that the x-component of velocity along the interface was the mean of the two stream velocities. Lin noted that the choice of the third boundary condition was arbitrary up to a translation along the η-axis. Crane (1957) proposed that the third boundary condition should be of the form $\psi(\eta_o) = 0$ where η_o was to be determined by experiment or

some other means. Kuethe (1935) applied the boundary condition

proposed by von Karman based on the balancing of transverse

momentum. This was applied to the turbulent case which has

the same indeterminateness as the laminar problem. The boundary

condition was,

$$U_1 V_1 + U_2 V_2 = 0 \qquad\qquad (3.2)$$

where V_1 and V_2 are the mean transverse velocities above and

below the mixing layer. Ting (1959) derived the third boundary

condition for the zero order solution of the mixing region for

several cases of subsonic and supersonic streams. Ting intro-

duced a stretched co-ordinate Y where $Y = \dfrac{y}{\epsilon}$ and $\dfrac{1}{\epsilon}$ is of the

order of the square root of the Reynolds number. He then showed

that the pressure difference across the mixing layer is of

order ϵ^2. Thus orientating the velocity profile of the zero-

order solution such that the pressure difference is balanced

across the layer led him to the third boundary condition. He

concluded that the correct boundary condition for incompressible

flow was,

$$\rho_0 U_1 V^{(o)} \left(\frac{x}{L}, \infty\right) + \rho_0 U_2 V^{(o)}\left(\frac{x}{L}, -\infty\right) = 0, \qquad (3.3)$$

where $V^{(o)}\left(\frac{x}{L}, \frac{Y}{L}\right)$ is the zero order transverse velocity in an

expansion in terms of ϵ, which is equivalent to the condition

(3.2) proposed by von Karman. A detailed discussion of the

third boundary condition is given in Appendix I.

We will now derive the equations for the mean flow in

laminar or turbulent mixing. It will be seen that the form

of the resulting equations for the similarity stream functions

are very similar to each other in both cases of mixing.

3.2.2 Derivation of Equations

We will consider the steady flow of a viscous incompressible fluid. Two uniform streams of velocity U_1 and U_2 begin mixing at the point $x = 0$. We will assume that the mixing is two-dimensional. Introducing the normal boundary layer assumptions, described in the previous chapter, we may write the equations of continuity and momentum,

$$
\frac{\partial U}{\partial x} + \frac{\partial V}{\partial y} = 0,
$$

$$
U\frac{\partial U}{\partial x} + V\frac{\partial U}{\partial y} = -\frac{1}{\rho}\frac{\partial P}{\partial x} + \nu\frac{\partial^2 U}{\partial y^2}
$$

$$
\frac{\partial P}{\partial y} = 0
$$

$$(3.4)$$

The velocity in the x-direction is assumed to be constant outside the layer where one has $\frac{\partial U}{\partial x} = 0$. Thus we may write equations (3.4),

$$
\frac{\partial U}{\partial x} + \frac{\partial V}{\partial y} = 0 \tag{3.5}
$$

and

$$
U\frac{\partial U}{\partial x} + V\frac{\partial U}{\partial y} = \nu\frac{\partial^2 U}{\partial y^2} \tag{3.6}
$$

We will introduce a stream function, ψ, given by,

$$
\psi = U_s \sqrt{\frac{\nu x}{U_s}} \left\{ \frac{U_d}{U_s} f(\eta) + \eta \right\} , \tag{3.7}
$$

where $U_s = \dfrac{U_1 + U_2}{2}$, $U_d = \dfrac{U_1 - U_2}{2}$ and

η, the similarity variable is given by,

$$\eta = y \sqrt{\frac{U_s}{\nu x}}$$

U_s is used in the definition of η rather than U_d in order
that the square root will always be real for $x > 0$ independent
of the values of U_1 and U_2. (This assumes that one of the
streams is not flowing in the negative x-direction). The com-
ponents of velocity in the x- and y-directions may now be
written,

$$U = \frac{\partial \psi}{\partial y} = U_s + U_d \, f'(\eta), \text{ and} \tag{3.9}$$

$$V = \frac{-\partial \psi}{\partial x} = \frac{U_d}{2} \sqrt{\frac{\nu}{x U_s}} \{\eta \, f'(\eta) - f(\eta)\} \tag{3.10}$$

The boundary conditions are

$$U = U_1 \text{ as } y \to \infty$$
$$U = U_2 \text{ as } y \to -\infty$$

and $U_1 V_1 + U_2 V_2 = 0$.

In terms of the new similarity function the boundary conditions
are,

$$\left.
\begin{aligned}
&f'(\eta) \to 1 \text{ as } \eta \to \infty \\
&f'(\eta) \to -1 \text{ as } \eta \to -\infty \\
&\text{and } U_1 - U_2 = \lim_{\eta \to \infty} \{ \frac{U_1 f(\eta) + U_2 f(\eta)}{\eta} \}
\end{aligned}
\right\} \tag{3.11}$$

It can be seen that our choice of the form (3.7) for the
stream function leads to boundary conditions on the first
derivative, which determines the mean velocity in the x-
direction which are independent of U_1 and U_2.

Substituting equations (3.9) and (3.10) into equation

(3.6) leads to the differential equation for f,

$$2f'''(\eta) + f''(\eta)\left[\eta + f(\eta)\,\frac{U_d}{U_s}\right] = 0 \qquad\qquad (3.12)$$

We see from equation (3.12) that $f(\eta)$ is not a universal function of η for all values of U_d/U_s, thus we may write,

$$f(\eta) \equiv f(\eta;\,\frac{U_d}{U_s}).$$

Equation (3.12) may be solved numerically subject to the boundary conditions (3.11). As the method of solution is very similar to that used for the turbulent mixing problem we will deal with the numerical solutions for both cases after first deriving the appropriate equations for turbulent flow.

3.3.1 The Turbulent Mixing of Two Parallel Streams

In dealing with turbulent flow we may see that the effect of viscosity no longer controls the mean motion but affects the small scale motions involving dissipation and heat production. The essential difference, between laminar and turbulent flows, in the form of the momentum equations we use below, lies in the dominance of the Reynolds stress in comparison with the viscous terms. At present all solutions of the mean turbulent mixing problem require the use of an assumption for the nature of the shear stress. The two most widely used hypotheses, both introduced by Prandtl, are the mixing-length hypothesis, Prandtl (1925), and the constant exchange coefficient or constant eddy viscosity hypothesis, Prandtl (1942). Using the mixing length hypothesis, Tollmien (1926)

- 41 -

obtained a solution for the mean velocity profile of a mixing

layer with one stream at rest. An empirical constant related to

the rate of spread of the layer had to be provided. Kuethe

(1935) extended this analysis to the case of both streams having

finite velocity. In his analysis he used the third boundary

condition proposed by von Karman which we have earlier demon-

strated is the appropriate one for incompressible flow. Gortler

(1942) solved the same problem as Kuethe but used Prandtl's

second hypothesis. Mills (1968) also made use of the eddy

viscosity hypothesis in his numerical investigation of the

mixing layer. He transformed the momentum and energy equations

into equations for the shear stress and enthalpy with new in-

dependent variables x and U. The equations for compressible

flow were then solved by a method of successive approximation.

A numerical solution has also been obtained by Baker and

Weinstein (1968) for the problem of both homogeneous and heter-

ogeneous mixing. We will now derive the equation governing

the mean motion in a turbulent mixing layer.

3.3.2 Derivation of Equations

Let us assume that two non-turbulent, parallel streams

of velocity of U_1 and U_2 begin mixing at x = 0. As in the

case of laminar flow it is assumed that the flow is similar,

at all stations downstream of x = 0, for the mean flow in

the mixing region.

Assuming that to the zeroth order pressure is constant -

everywhere inside the mixing region then for two-dimensional,

incompressible flow the mean flow equations of continuity and

and momentum may be written,

$$\frac{\partial U}{\partial x} + \frac{\partial V}{\partial y} = 0, \tag{3.13}$$

and

$$U\frac{\partial U}{\partial x} + V\frac{\partial U}{\partial y} = \nu\frac{\partial^2 U}{\partial y^2} - \frac{\partial \overline{uv}}{\partial y} - \frac{\partial}{\partial x}(\overline{u^2} + \overline{v^2}) \; . \tag{3.14}$$

In the equations of motion of a turbulent fluid the viscous and normal stress terms are known to be small and they may be neglected. Then equation (3.14) becomes,

$$U\frac{\partial U}{\partial x} + V\frac{\partial U}{\partial y} = \frac{\partial \overline{uv}}{\partial y} \tag{3.15}$$

Let us introduce the stream function ψ, given by,

$$\psi = U_s L(x) \{\frac{U_d}{U_s} F(\xi) + \xi\}, \tag{3.16}$$

where U_s and U_d are defined as in the case of laminar mixing and ξ, the similarity variable is given by,

$$\xi = \frac{y}{L(x)}$$

where $L(x)$ is a measure of the mixing layer width to be defined more accurately later. We may now write the velocity components,

$$U = U_s + U_d F'(\xi) \tag{3.17}$$

and

$$V = U_d \frac{dL}{dx} \{\xi F'(\xi) - F(\xi)\} \; , \tag{3.18}$$

where primes denote differentiation with respect to ξ. Substituting equations (3.17) and (3.18) into equation (3.15) we obtain,

$$\frac{dL}{dx} \{\xi + \frac{U_d}{U_s} F(\xi)\} F''(\xi) = \frac{d}{d\xi} \left(\frac{\overline{uv}}{U_s U_d}\right) \qquad (3.19)$$

It will be shown in Appendix I that we may use the third boundary condition given above, (3.2), for both the laminar and turbulent problems. Then the boundary conditions on $F(\xi)$ are,

$$
\begin{aligned}
&F'(\xi) \to 1 && \text{as} && \xi \to +\infty \\
&F'(\xi) \to 1 && \text{as} && \xi \to -\infty \\
&\text{and} \quad U_1 - U_2 \quad \underset{\xi \to \infty}{\text{Lin}} \left\{\frac{U_1 F'(\xi) + U_2 F'(-\xi)}{\xi}\right\}
\end{aligned}
\qquad (3.20)
$$

The problem is to determine the mean fluctuating shear stress, $\overline{uv}$. The experiments of Wygnanski and Fiedler (1970) have shown that if measurements of the shear stress $\overline{uv}$, are made only when the measuring instrument is embedded in rotational flow, by means of conditional sampling, then the eddy viscosity, defined by $\nu_T = \left|\overline{uv}/\frac{\partial U}{\partial y}\right|$, is constant across the flow. Remembering that we have considered the flow to be rotational throughout, it seems reasonable to assume that the eddy viscosity is given by,

$\nu_T = \gamma \times$ constant, where γ is the intermittency function which is assumed to be a function of our similarity variable.

Let us therefore introduce an eddy viscosity defined by the relation,

$$-\overline{uv} = \nu_T \frac{\partial U}{\partial y} , \qquad (3.21)$$

the substitution of (3.21) into equation (3.14) with only the normal stress terms omitted yields,

- 44 -

$$L \frac{dL}{dx} \{U_s + U_d F(\xi)\} F''(\xi) + (\nu + \nu_T) F'''(\xi) +$$

$$\frac{\partial \nu_T}{\partial \xi} F''(\xi) = 0 \qquad (3.22)$$

Let $\nu_T = \nu_0 G(\xi)$ and $\sigma = \frac{\nu}{\nu_0}$, where ν_0 is the maximum value of ν_T, then equation (3.22) may be written,

$$\frac{U_d}{R_T \frac{dL}{dx}} \{\sigma F''' + \frac{d(G.F'')}{d\xi}\} + \{U_s \xi + U_d F\} F'' = 0, \qquad (3.23)$$

where R_T is the turbulent Reynolds number defined by,

$$R_T = \frac{|U_d| L}{\nu_0} \qquad (3.24)$$

The assumption of a constant eddy viscosity would lead to the equation,

$$\frac{U_d (1 + \sigma) F'''}{U_s R_T \frac{dL}{dx}} + \{\xi + \frac{U_d}{U_s} F\} F'' = 0, \qquad (3.24a)$$

which is the laminar flow equation (3.12) with a change of coefficient on the third derivative of F. This fact was noted by Lin (1953) who was able to make use of Gortler's calculations for the turbulent mixing layer in his own calculations of the laminar flow problem.

3.4.1 Solution of the Similarity Equations for Laminar and Turbulent Mixing Layers

Before describing the method of solution which is employed for both the laminar and turbulent cases we will evaluate the coefficients in the turbulent similarity equation (3.23). We

need to evaluate four factors,

i) the ratio of kinematic to eddy viscosities, σ,

ii) the distribution of eddy viscosity as a function

of ξ, $G(\xi)$,

iii) the variation of turbulent Reynolds number with

velocity ratio, $R_T(\frac{U_d}{U_s})$,

and

iv) the variation of spread rate with velocity ratio.

The magnitude of the ratio of kinematic to eddy viscosity is very small. We can see from equation (3.23) that the ratio will only affect the solution appreciably in regions where $G(\xi)$ tends to zero. We will see later that this occurs at the edges of the mixing layer. The experimental results of Yule (1970) showed that the maximum value of eddy viscosity is given by,

$$\frac{\nu_o}{x(U_1 - U_2)} = 7 \times 10^{-4}, \qquad (3.25)$$

which result we will use in our calculations.

Lessen, Harpavat and Zien (1969) note that in their solution, choosing $G(\xi) = 1$, the velocity profile is an error function and therefore,

$$\frac{dU}{d\xi} = c_1 \exp\left(-\frac{\xi^2}{2}\right) \qquad (3.26)$$

They argue that as, from mixing length theory, the eddy viscosity is proportional to the magnitude of $\frac{\partial U}{\partial y}$, then a plausible distribution of eddy viscosity may be of the form,

$$\nu_{\mathrm{T}} = \nu_{\mathrm{o}} \exp(-A\xi^2) \qquad (3.27)$$

where A is a constant with approximate value $\frac{1}{2}$. However, in our calculations the inflection point of the velocity profile does not occur at $\xi = 0$ and thus a better representation of the eddy viscosity distribution would be,

$$\nu_{\mathrm{T}} = \nu_{\mathrm{o}} \exp\left[-A(\xi - \xi_{\mathrm{F}})^2\right] \qquad (3.28)$$

In our calculations the value of ξ_{F} is taken to be the value of ξ for which $\frac{d^3F}{d\xi^3} = 0$. This was calculated from a constant eddy viscosity analysis. When $\frac{d^3F}{d\xi^3} = 0$ then $\frac{dU}{dy}$ is a maximum and from mixing-length arguments we may take this to be the position of the maximum in the eddy viscosity distribution. This may also be argued by considering single components of the fluctuating flow. Foote and Lin (1950) considered the distribution of Reynolds' stress based on solutions of the inviscid Orr-Sommerfeld equation. If u and v are given by,

$$u = \hat{u}(y)\, e^{i\alpha(x-ct)}$$

and

$$v = \hat{v}(y)\, e^{i\alpha(x-ct)}$$

where $\hat{u}$ and $\hat{v}$ are the complex y-distributions of u and v satisfying the inviscid stability equation

$$\hat{v}'' - \alpha^2 \hat{v} + \frac{U''}{(U - c)}\, \hat{v} = 0, \qquad (3.29)$$

then $\overline{uv}$ is given by,

$$\overline{uv} = \frac{1}{2\alpha}\,(v_i v_r' - v_i' v_r)e^{2\alpha c_i t}, \qquad (3.30)$$

- 47 -

where the subscripts i and r refer to the imaginary and real

parts respectively. Multiplying equation (3.29) by the complex

conjugate of $\hat{v}$ we obtain,

$$\hat{v}''\hat{v}* - \alpha^2\hat{v}\hat{v}* + \frac{U''}{(U-c)} \ \ vv* = 0 \tag{3.31}$$

The imaginary part of the equation is obtained by subtract-

ing the complex conjugate of equation (3.31) from itself,

$$\frac{d}{dy} (\hat{v}'\hat{v}* - \hat{v}'*\hat{v}) = \frac{-i|\hat{v}|^2 2c_i U''}{|U-c|^2} \tag{3.32}$$

Now $(\hat{v}_r\hat{v}_i' - \hat{v}_i\hat{v}_r') = - \frac{i}{2}(\hat{v}'\hat{v}* - \hat{v}*'\hat{v})$ and thus from equations

(3.32) and (3.30) we have $\frac{\partial \tau}{\partial y} = \frac{-\rho}{2\alpha} \cdot e^{2\alpha c_i t} \cdot c_i \cdot \frac{U''|\hat{v}|^2}{|U-c|^2}$, (3.33)

where $\tau = -\rho\overline{uv}$ is the Reynolds' stress.

From equation (3.33) we see that the gradient of the

Reynolds' stress is zero at the inflection point of the mean

velocity profile. This simple example, which disregards the

singularity U = c which occurs in inviscid theory and also

only considers temporal amplification theory (see Chapter 4),

is given as a justification for the choice of the value of

ξ_F being the value of ξ at which $\frac{d^3F}{d\xi^3}$ is zero. At a later

stage in this work we will discuss this form of representation

of the disturbances in turbulent flow by particular single

components of the disturbed flow. It will be seen that this

method provids a good representation of the turbulence.

In our calculations we will consider three eddy viscosity

distributions,

i)   constant eddy viscosity,

ii)   equation (3.27) and

iii)   equation (3.28) where the value of ξ_F is determined

       from the constant eddy viscosity analysis.

Lilley (1967) has suggested how the variation of turbulent

Reynolds number with velocity ratio may be obtained. Let us

write the width of the mixing layer L,

$$L = W \, x,$$

where $W = W(\dfrac{U_d}{U_s})$ is a function of the velocity ratio. Then

substituting into equation (3.19) we obtain,

$$\{\xi + \frac{U_d}{U_s} F(\xi)\} F''(\xi) = \frac{d}{d\xi} \{\frac{\overline{uv}}{U_s U_d W}\} \qquad (3.34)$$

We have previously noted that the similarity equation for

turbulent flow, equation (3.23), and that for laminar flow,

equation (3.12), are of a similar form for the simple case

of constant eddy viscosity. Ꮤe will also see that experi-

mental results show that when mean velocity profiles of

laminar and turbulent mixing regions are plotted against a

variable based on the width of the mixing layer then the

profiles coincide closely. Thus we could argue that for

equation (3.34) to have a similar form, as a function of the

velocity ratio, with the laminar case then $\overline{uv}$ has to be a

function of ξ and proportional to $U_s U_d W$.

Thus from our definition of eddy viscosity we see that

$$\frac{\tau}{W \rho U_d^2} = \frac{\nu_T F''}{W \, L \, U_d} \quad , \text{ where } \tau \text{ is the Reynolds' stress defined above}$$

- 49 -

i.e. $\quad \dfrac{\tau}{W \rho U_d{}^2} = \dfrac{F''}{R_T W}$, which may be written,

$$\frac{\tau}{W \, U_s U_d \rho} = \frac{U_d}{U_s W} \cdot \frac{F''}{R_T} \tag{3.35}$$

However, we require that $\dfrac{\tau}{\rho U_s U_d W}$ be independent of $\dfrac{U_d}{U_s}$ which implies from equation (3.35) that

$$R_T = \text{const} \times \frac{U_d}{U_s W} \tag{3.36}$$

Gartshore (1965) has proposed that the turbulent Reynolds number is of the form

$$\frac{1}{R_T} = \frac{1}{R_{T_o}} \left(1 + \lambda \left| \frac{B}{A} \right| \right) \tag{3.37}$$

where $A = \dfrac{\partial U}{\partial y}$, $\qquad B = \dfrac{\partial U}{\partial x}$,

and R_{T_o} is the value of the turbulent Reynolds number when $B = 0$ which, in our case, occurs along the line $\xi = \xi_o$. The value of λ is determined from experimental results. Newman (1967) obtains these constants and writes equation (3.37) in the form,

$$\frac{1}{R_T} = .077 \{ 1 - 9.1 \, |\xi_o| \, W \} \tag{3.38}$$

Substituting equation (3.36) into equation (3.38) we obtain,

$$\frac{c U_d}{U_s W} = \frac{1}{.077(1 - 9.1 \, |\xi_o| W)} \quad .$$

and rearranging to obtain an equation for W we have,

$$W = W(\frac{U_d}{U_s}) = \frac{(.077 \cdot \frac{U_d}{U_s})}{(1 + c_1 |\xi_0| \frac{U_d}{U_s})} \qquad (3.39)$$

Making use of this expression for W we obtain a relationship

for the turbulent Reynolds number as a function velocity ratio

parameter, $\frac{U_d}{U_s} = \frac{U_1 - U_2}{U_1 + U_2}$,

$$R_T(\frac{U_d}{U_s}) = R_T(1) \{\frac{1 + c_2 (\frac{U_d}{U_s})}{1 + c_2}\} \qquad (3.40)$$

From the numerical values given by Newman for R_T for a jet

with still surroundings and a small perturbation wake we may

write,

$$R_T(\frac{U_d}{U_s}) = 32.9\{\frac{1 + 1.5 (\frac{U_d}{U_s})}{2.5}\} \qquad (3.41)$$

It can be seen from equation (3.41) and our definition of

turbulent Reynolds number that the magnitude of the eddy

viscosity decreases as the velocities of the two streams

approach one another in order that there is a finite value

of R_T for this case.

Equation (3.39) gives the variation of spread rate with

velocity ratio. We will now define the width parameter $L(x)$

more accurately and then we will consider the analysis used

by Abramovitch (1963) which will be compared with our present

formulation.

We will define L for the mixing layer as the distance

between the points where the mean velocity differs from the

average velocity of the two streams by $\frac{U_d}{2}$. This is shown

in the diagram below
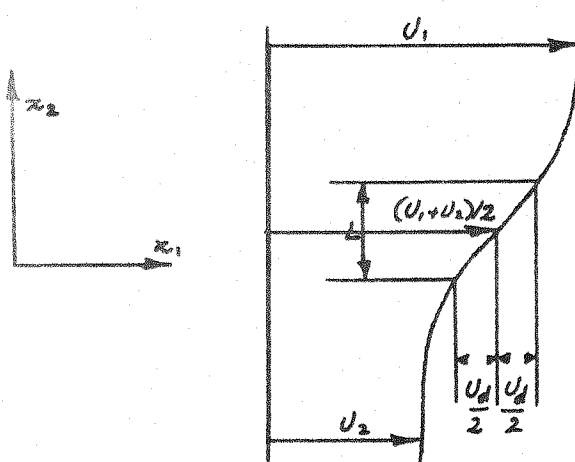
We will now consider the arguments used by Abramovitch (1963) to
describe the rate of spread of the mixing layer. He made use
of mixing length ideas to conclude that the rate of increase
in the layer thickness was proportional to the perturbation
component of the transverse velocity which was proportional to
the difference in velocities at the boundaries, i.e.

$$\frac{dL}{dt} \propto v' ,$$ (3.42)

and

$$v' \propto U_1 - U_2$$ (3.43)

Making use of equation (3.42) with $\frac{dx}{dt} = U$ we obtain

$$\frac{dL}{dx} \propto \frac{|U_1 - U_2|}{|U|}$$ (3.44)

We need to determine the value of the mean characteristic
velocity in the denominator of equation (3.44). Abramovitch
argues that for incompressible fluid this value is close to
the arithmetic mean of the boundary velocities. Thus we

may write,

$$\frac{dL}{dx} = \psi\left\{\frac{|U_1 - U_2|}{U_1 + U_2}\right\} \tag{3.45}$$

Newman (1967) expanded this as a polynomial,

$$\frac{dL}{dx} = A_o + A_1\frac{|U_1 - U_2|}{(U_1 + U_2)} + A_2\frac{|U_1 - U_2|^2}{(U_1 + U_2)^2} + \text{---} \tag{3.46}$$

If $U_1 - U_2 = 0$ then $\frac{dL}{dx} = 0$ and thus $A_o = 0$. Then taking the first term only in the expansion as chosen by Abramovitch we have,

$$\frac{dL}{dx} = c\frac{|U_1 - U_2|}{(U_1 + U_2)} \tag{3.47}$$

This result is the same as that obtained from our previous analysis for the turbulent Reynolds number. From equation (3.39) we have,

$$W = \frac{dL}{dx} = \frac{k_1\frac{|U_1 - U_2|}{(U_1 + U_2)}}{1 + k_2\frac{|U_1 - U_2|}{(U_1 + U_2)}}, \tag{3.48}$$

where $k_1 = 0.077$ and $k_2 = c_1|\xi_o|$. Expanding the denominator we obtain,

$$\frac{dL}{dx} = k_1\frac{|U_1 - U_2|}{(U_1 + U_2)}\left\{1 - k_2\frac{U_1 - U_2}{(U_1 + U_2)} + \frac{k_2^2}{2}\frac{|U_1 - U_2|^2}{(U_1 + U_2)^2} - \ldots\right\} \tag{3.49}$$

The first term in the expansion (3.49) is identical to the expression (3.47). It may be expected that this first term representation will be valid for $U_1 \gg U_2$. The variation

of rate of spread with velocity ratio is shown in Figure 1. The collected results of Abramovitch (1963) show good agreement with the form of equation (3.47) though their numerical value is determined by the choice of W when $U_2 = 0$. The results of Yule (1970) and Sabin (1965) suggest that the constant k_1 should have a value of approximately .10. The constant given by Newman (1967) is .104. From equations (3.39) and (3.38) we may see that the choice of $c = k_1 = .104$ leads to the result, $R_{T_0} = 9.6$. The values of R_T calculated from experiments is tabulated by Newman, part of this table is shown below.

Experimenter	Year	Range of $\left|\dfrac{U_{defect}}{U_1}\right|$	Type of Body	R_T
Reichardt	1951	.080 – .057	Circular Cylinder	10.4
Schlichting	1960	.061 – .025	"	13.0
Townsend	1956	.045 – .031	"	13.3
Gartshore	1965	.111 – .071	Square Cylinder	8.6
Silverstein et. al.	1939		Aerofoil NACA 0018	8.4

In his evaluation of the constants in equation (3.38), Newman uses experimental results and we may see from the above table that for the small perturbation wake R_T lies in the range 8.4 $\rightarrow$ 13.3. For the small perturbation wake, $\left|\dfrac{B}{A}\right| \rightarrow 0$ and thus $R_T \rightarrow R_{T_0}$. The average value of the experimental results above for R_{T_0} is 10.7 which agrees more closely with the results obtained from the calculations from the rate of spread analysis. In order to achieve consistency in our calculations and also make use of the more easily measurable results, we will choose the constant

$k_1 = .104$. Then equations (3.40) and (3.47) become,

$$R_T(\frac{U_d}{U_s}) = 32.9 \{\frac{1 + 1.43 (\frac{U_d}{U_s})}{2.43}\} \text{ and} \qquad (3.50)$$

$$\frac{dL}{dx} = .104\{\frac{|U_1 - U_2|}{(U_1 + U_2)}\} \qquad (3.51)$$

These equations are used in our calculations for the turbulent mixing layer.

3.4.2 Numerical Method of Solution

The same numerical procedure is used for the solution of both the laminar and turbulent problems. As the solution of the turbulent case, equation (3.23) is algebraically more complicated, we will examine it in detail and only give the corresponding equations for laminar flow when convenient.

Equation (3.23) may be written,

$$\{\xi + \frac{U_d}{U_s}(F + \frac{1}{R_T \frac{dL}{dx}} G')\} F'' + \frac{\frac{U_d}{U_s}}{R_T \frac{dL}{dx}} \{\sigma + G\} F''' = 0 \qquad (3.52)$$

Let us introduce a new function $P(\xi)$ defined by,

$$P(\xi) = \frac{dF(\xi)}{d\xi} , \qquad (3.53)$$

then equation (3.52) becomes,

$$\{\xi + \frac{U_d}{U_s} (F + \frac{1}{R_T \frac{dL}{dx}} G')\}P' + \{\frac{\frac{U_d}{U_s}}{R_T \frac{dL}{dx}} (\sigma + G) \}P'' = 0 \qquad (3.54)$$

The equivalent form of equation (3.12) for laminar flow is,

$$\{\eta + \frac{U_d}{U_s} f\}p' + 2p'' = 0, \qquad (3.55)$$

- 55 -

where $F(\eta) = \dfrac{df(\eta)}{d\eta}$ (3.56)

We will now write these equations in finite difference form.
Equation (3.53) may be written

$$(F_r - F_{r-1}) = \frac{1}{2} h (P_r + P_{r-1}) ,$$ (3.57)

where h is the step difference in ξ between stations 'r-1' and
'r'. Equation (3.54) may be written,

$$\{\frac{\frac{U_d}{U_s}}{R_T \frac{dL}{dx}} (\sigma + G_r) - \frac{h}{2} [\xi_r + \frac{U_d}{U_s} (F_r + \frac{G'_r}{R_T \frac{dL}{dx}})]\} P_{r-1} - \{\frac{\frac{U_d}{U_s} \cdot 2}{R_T \frac{dL}{dx}} (\sigma + G_r)\} P_r$$

(3.58)

$$+ \{\frac{\frac{U_d}{U_s}}{R_T \frac{dL}{dx}} (\sigma + G_r) + \frac{h}{2} [\xi_r + \frac{U_d}{U_s} (F_r + \frac{G'_r}{R_T \frac{dL}{dx}})]\} P_{r+1} = 0$$

The equivalent finite difference form of equation (3.55) is,

$$\{4 - h(\eta_r + \frac{U_d}{U_s} f_r)\} P_{r-1} - 8p_r + \{4 + h(\eta_r + \frac{U_d}{U_s} f_r)\} P_{r+1} = 0$$ (3.59)

Equations (3.58) and (3.59) are solved by an iterative procedure.
An initial assumption is made for the values of $F'(\xi)$. In our
calculations a sine form was chosen. The value of $F(\xi)$ is then
calculated using equation (3.57). The finite difference equation
(3.58) may be written in matrix form,

$$|A| \ \overline{P} = \overline{B}$$ (3.60)

where $|A|$ is a triple diagonal matrix and $\overline{P}$ and $\overline{B}$ are column
vectors, the first and last elements of $\overline{B}$ being determined by

the boundary conditions on $P(\xi)$ and the rest of its elements being zero. The system of linear algebraic equations (3.60) is solved using Gaussian elimination without pivots giving a new value for $P(\xi)$. The new value of $F(\xi)$ is calculated by evaluating the transverse velocity according to equation (3.18) and applying the third boundary condition (3.2). The iteration procedure is repeated until successive values of $P(\xi)$ differ by less than a chosen small quantity.

3.4.3 The Computer Program

The flow diagram of the program is shown in figure 2. The data to be read in are the velocities of the two streams, the ratio of kinematic to eddy viscosity, the step size and the numerical value of the desired accuracy of the iteration. Having evaluated U_d/U_s the subroutines SPREAD and RTURB are called which evaluate $\frac{dL}{dx}$ and R_T according to equations (3.50) and (3.51) respectively. The subroutine EDIVIS then calculates the distribution of eddy viscosity for either constant eddy viscosity or according to equations (3.27) or equation (3.28), where ϵ_F is previously determined from a calculation involving constant eddy viscosity. The initial guess at the values of $P(\xi)$ is calculated as a sine function and the values of $F(\xi)$ are calculated from equation (3.57). The set of linear algebraic equations are calculated and solved using Gaussian Elimination without pivots. The new value of $P(\xi)$ is then taken as the average value of P_I and P_{I+1}. If convergence is not achieved within ten iterations sets of four iterated values are used

to calculate the new value of $P(\xi)$ using linear interpolation. When the sum of the differences $P_{I+1} - P_I$ becomes less than the desired value, the program outputs the values of $F'(\xi)$, $V(\xi)$ and their derivatives.

3.5 Computation Results

The calculations were performed for values of U_2/U_1 of 0.61 and 0.0. The first value of velocity ratio was chosen so that comparison could be made with the measurements of Yule (1970). Results from the calculations using the second velocity ratio were required for our subsequent calculations of finite amplitude effects on the growth of the mixing layer.

The computed function $f'(\eta)$ for laminar flow and velocity ratio 0.61 is shown in Figure 3. The calculations are compared with those of Lin (1953) for a velocity ratio of 0.667. Lin's results have been recalculated for a change in definition of the similarity variable, η.

The convergence of the iteration scheme is shown in Figure 4. It was found that as the value of U_2 tended to zero so the convergence of the solution became slower. If a simple iteration scheme is used where $P_{I+1} = P_I$ as many as 800 iterations were required. The iterative scheme used in the calculations for figure 4 set $P_{I+1} = \dfrac{P_I + P_{I+1}}{2}$ for the first ten calculations and then sets of four iterated values of P_I were used in a linear interpolation for the new value of P.

The effect on the velocity distribution of the choice of eddy viscosity distribution is shown in figure 5. Here the

function $F'''(\xi)$ is presented, where

$$F'''(\xi) = \frac{1}{U_d} \frac{d^2 U}{d\xi^2}$$

It can be seen that if the physically incorrect assumption of a symmetric eddy viscosity distribution is considered then the maximum absolute magnitude of second derivative of velocity occurs towards the lower velocity edge of the shear layer. If the constant eddy viscosity assumption is made then the magnitude of the second derivative of velocity decreases and the solution tends towards the laminar result as can be seen from examination of equation (3.24a).

The effect of choice of the constant A in equation (3.27) is shown in Figure 6. The variation is most noticeable at the edges of the mixing layer. The experimental results of Yule (1970) are plotted for comparison. It was found that a value of A of 0.7 gave best agreement with these experimental results. We have previously noted that the distribution of eddy viscosity given by $G(\xi)$ should correspond to the intermittency of the flow. In figure 7 the experimental values of intermittency measured by Wygnanski and Fiedler (1970) are compared with $G(\xi)$ with A = 0.7. The agreement is very good, especially in the centre of the region. The experiments by Wygnanski and Fiedler do however suggest that the value of A in our definition of eddy viscosity should take two values, one for the high velocity side of the layer and another for the lower velocity side.

It is interesting to note that the shear stress is an integral function of the product of the z-component of the vorticity disturbance and the y-direction velocity fluctuation. This was noted by Lilley (1967) who put,

$$\frac{\partial \overline{uv}}{\partial y} = \overline{\omega_3 v} \tag{3.61}$$

Integrating equation (3.61) with respect to y we obtain

$$\overline{uv} = \int_{-\infty}^{y} \overline{v\omega_3} \, dy' \tag{3.62}$$

Making use of mixing length ideas we would expect the integrand in equation (3.62) to have a positive peak at $y = -y_1$ and a negative peak at $y = y_2$, where y_1 and y_2 lie close to the points of maximum value of $\frac{\partial^2 U}{\partial y^2}$. This is sketched below. The corresponding integral is also sketched and we see that we have predicted a constant shear stress across the flow between $-y_1$ and y_2.
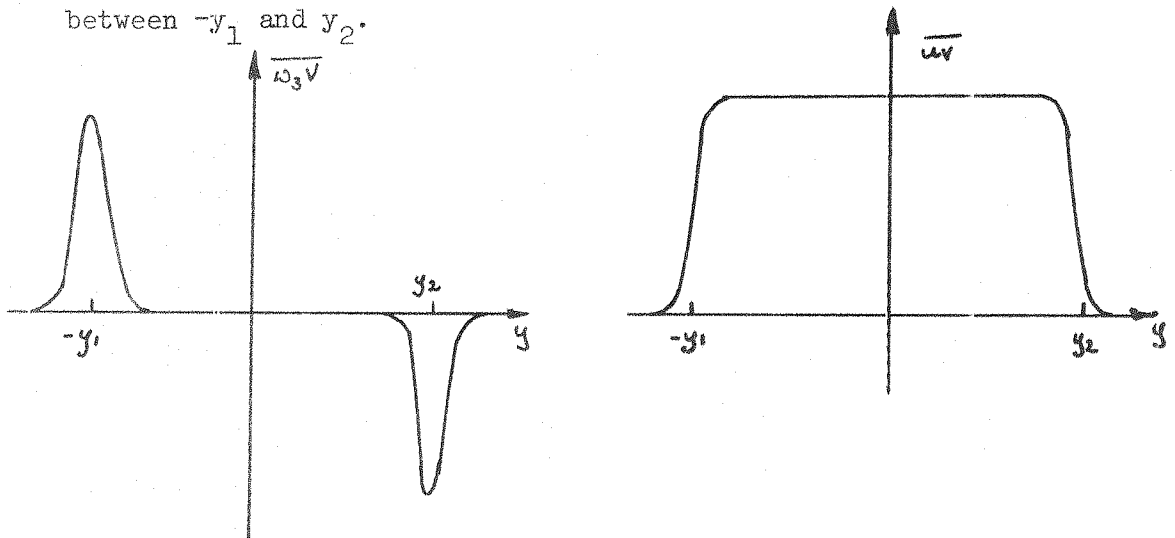
However, we have previously noted that we have assumed that

the flow is rotational throughout whereas the above analysis refers only to the turbulent fluid. Thus we would expect that taking account of intermittency would result in a rounding off of the $\overline{uv}$ distribution. From equation (3.21) we have that the eddy viscosity is given by, $\nu_T = -\overline{uv}/\frac{\partial U}{\partial y}$, and so we would expect that the distribution of eddy viscosity in equation (3.28) would be too large outside the values $y = -y_1$ and $y = y_2$. These two positions are shown on Figure 7 and we note that our prediction does appear to be too large outside these values.

The function $F'(\xi)$ for turbulent flow and velocity ratio 0.61 is shown in figure 8. The constants for the calculation were,

(i) $A = 0.7$

(ii) $\sigma = .0033$

and

(iii) $\xi_F = -.13123$.

The experimental results of Yule are plotted for comparison and the agreement is good over the whole mixing layer. The constant eddy viscosity calculation is also shown for comparison and it can be seen that the agreement between theory and experiment is poor at the edges of the mixing layer.

By considering the momentum integral equation (2.23) we may define the momentum thickness of the mixing layer between streams of velocity U_1 and U_2 as, (see Lin 1953),

$$\theta = \frac{1}{U_d^2} \int_{-\infty}^{\infty} (U_1 - U)(U - U_2) \, dy \qquad (3.63)$$

Then for the laminar flow case we may write,

$$\theta_L = \sqrt{\frac{\nu x}{U_s}} \int_{-\infty}^{\infty} (1 - f')(1 + f') \, d\eta, \tag{3.64}$$

and for the turbulent case,

$$\theta_T = L \int_{-\infty}^{\infty} (1 - F')(1 + F') \, d\xi \tag{3.65}$$

Thus the non-dimensional co-ordinate y/θ, is given, in the laminar case, by

$$y/\theta_L = \eta / \left[\int_{-\infty}^{\infty} (1 - f')(1 + f') \, d\eta \right], \tag{3.66}$$

and in the turbulent case by,

$$y/\theta_T = \xi / \left[\int_{-\infty}^{\infty} (1 - F')(1 + F') \, d\xi \right] \tag{3.67}$$

Making use of equations (3.66) and (3.67) the functions F' and f' are plotted as functions of $(\frac{y-b}{\theta})$ in figure 9, where b is the value of y at which $U = U_s$. As Sato(1956) points out, in his work on the transition of the mixing layer, the two curves show so slight a difference that it is difficult to tell the transition point from the mean profiles alone. The calculations in figure 9 are for a value of $U_2 = 0$. The results are compared in the laminar case with the calculations of Lin and in the turbulent case with the experiments of Liepmann and Laufer (1947). The agreement is good except for the turbulent case at the lowest velocity edge of the mixing region where measurements of the mean velocity are most difficult.

The measurements in this region are not reliable as the axial velocity is no longer large in comparison with the transverse velocity. Liepmann and Laufer note that their hot-wire measurements are accurate in the range $\infty > \theta > -0.8$. They compared their hot-wire measurements with the measurements using a total head tube and the results differed outside the range given above. In this region the hot-wire will produce an output which is crudely proportional to the square root of the sums of the squares of the axial and transverse velocities. Thus the recorded value of axial velocity will be greater than its true value, which agrees with our theoretical prediction.

At a later stage we will use this non-dimensional form of the mean velocity profile to represent the shape of the mean velocity profile through transition.

The calculated results for the two velocity ratios are tabulated in Tables I and II.

In the next chapter we will consider the analytic and numerical methods for the solution of the Orr-Sommerfeld Equation, which will be subsequently solved using the mean velocity profiles calculated in this chapter.

CHAPTER 4

Review of Methods of Solution of the Orr-Sommerfeld Equation

In Chapter 2 we derived the linear equation of hydro-
dynamic stability for parallel mean flow and three dimensional
disturbances. Before we go on to solve this equation for the
case of the stability of a laminar mixing layer, and at a later
stage solve a similar equation in our discussion of the
turbulent mixing layer, it is thought to be useful to review
previous analytic and numerical methods of solution of the
Orr-Sommerfeld equation.

The Orr-Sommerfeld equation is an ordinary linear differ-
ential equation of the fourth order. The methods of analysis
used in its solution have been variational methods (Lee and
Reynolds, 1964), expansion methods (Dolph and Lewis, 1958) and
asymptotic methods. Because of the magnitude of the Reynolds
number, the asymptotic methods have played the most important
role in analytical solutions. With the advent of the high speed
digital computer, numerical methods have recently proved very
successful. A collection of the various asymptotic methods is
presented by Lin (1955) and more recently accounts of develop-
ments in the methods of solution have been presented by Chandra-
rasekhar (1961) and Betchov and Criminale (1967).

The stability equation derived in Chapter 2, equation
(2.21a), is rewritten now for convenience,

$$(U - \frac{\omega}{\alpha})(\hat{v}'' - (\alpha^2 + \beta^2)\hat{v}) - U''\hat{v} + \frac{i}{\alpha R}(\hat{v}^{iv} - 2(\alpha^2 + \beta^2)\hat{v}'' +$$

$$(\alpha^2 + \beta^2)^2\hat{v}) = 0 \qquad\qquad (4.1)$$

We will now introduce a set of transformations, used by Squire (1933), that reduces equation (4.1) for the three-dimensional disturbance to an equivalent two-dimensional problem. Let us set,

$$v = \hat{v} , \quad c = \omega/\alpha , \quad \overline{\alpha}^2 = \alpha^2 + \beta^2 , \quad)$$
$$\left. \begin{array}{c} \\ \\ \end{array} \right\} \quad (4.2)$$
$$\overline{\alpha u} = \alpha \hat{u} + \beta \hat{w} \quad \text{and} \quad \overline{\alpha R} = \alpha R \quad)$$

Equation (4.1) then becomes,

$$(U - c)(v'' - \overline{\alpha}^2 v) - U''v + \frac{i}{\overline{\alpha R}} (v^{iv} - 2\overline{\alpha}^2 v'' + \overline{\alpha}^4 v) = 0 \quad (4.3)$$

Equation (4.3) is the Orr-Sommerfeld equation for a two-dimensional disturbance with wave-number $\overline{\alpha}$ in the x-direction and Reynolds number $\overline{R}$. It can be seen from (4.2) that $\overline{R} < R$. Thus we may confine our discussions of hydrodynamic stability to two-dimensional disturbances noting that results for a three-dimensional disturbance may be derived from the two-dimensional results.

4.1.1. <u>Analytical Methods</u>

The earliest analyses in hydrodynamic stability theory were concerned with the inviscid problem. As it is expected that instability in the mean flow profile will occur at high Reynolds number it is interesting to examine the inviscid form of equation (4.3) which is obtained as $\overline{R} \to \infty$,

$$(U - c)(v'' - \alpha^2 v) - U''v = 0, \quad (4.4)$$

where the bars denoting transformed terms have been dropped as we are confining ourselves to a discussion of two-dimensional disturbances. Equation (4.4) is known as the Inviscid Orr-

Sommerfeld or Rayleigh equation. Lord Rayleigh (1880) showed

that an inflection point in the mean velocity profile was a

necessary condition for flow to be unstable. This result may

be easily derived. Let us multiply equation (4.4) by v^*, the

complex conjugate of v, divide by (U - c) and integrate between

some limits y_1 and y_2. We then obtain,

$$\int_{y_1}^{y_2} \left[(v'v^*)' - v'v^{*'} - \alpha^2 vv^* \right] dy - \int_{y_1}^{y_2} \frac{U'' vv^*}{(U - c)} dy = 0 \qquad (4.5)$$

The first term may be integrated exactly as follows,

$$\int_{y_1}^{y_2} (v'v^*)' dy = \left[v'v^* \right]_{y_1}^{y_2} \qquad (4.6)$$

The limits y_1 and y_2 are either located at walls or at $\pm\infty$ and in

either case the integral term, equation (4.6), will vanish. It

then follows that we may write equation (4.5),

$$\int_{y_1}^{y_2} \frac{U'' vv^*}{(U - c)} dy = -k^2 \qquad (4.7)$$

where k is a real number and α is assumed real. For complex c

the imaginary part of equation (4.7) is

$$c_i \int_{y_1}^{y_2} \frac{U'' vv^*}{(U-c_r)^2 + c_i^2} dy = 0 \qquad (4.8)$$

On examining this equation we see that unless c_i is zero then

U'' must have at least one zero in the range of integration.

A further result derived by Høiland (1953) demonstrated

that an unstable oscillation can only exist if the mean

vorticity has an absolute maximum within the flow at the point

of inflection.

However, it must be noted that these results are for inviscid flow and thus it is possible for a mean velocity profile with no inflection point to be unstable if the viscous components of the Orr-Sommerfeld equation are retained.

The Orr-Sommerfeld equation will have four linearly independent solutions and we may write the solution,

$$v = \sum_{n=1}^{4} k_n V_n \quad , \tag{4.9}$$

where V_n are the independent solutions and k_n are four constants determined from the boundary conditions which may be written,

$$v_1 = v_1' = v_2 = v_2' = 0, \tag{4.10}$$

where the suffices 1,2 refer to the position of the boundary conditions. In the case of free shear flows the boundary conditions are applied at infinity and in bounded flows are applied at the walls. For a boundary layer one pair of conditions is applied at the wall, the other pair at infinity. For a non-trivial solution,

$$\begin{vmatrix} V_{11} & V_{21} & V_{31} & V_{41} \\ V_{12} & V_{22} & V_{32} & V_{42} \\ V_{11}' & V_{21}' & V_{31}' & V_{41}' \\ V_{12}' & V_{22}' & V_{32}' & V_{42}' \end{vmatrix} = 0 \tag{4.11}$$

This relationship may be written,

$$F(\alpha, R, c) = 0 . \tag{4.12}$$

Equation (4.12) is a secular equation formed from the eigenvalue problem posed by equations (4.3) and (4.10). We see from equation (4.12) that the parameters affecting the wave propagation are the Reynolds number R, the wavenumber α, which may be real or complex and $c = c_r + ic_i$. In the solution of the Orr-Sommerfeld equation two cases arise. The first will be referred to as temporal amplification and is characterized by the following properties,

α is real, $\omega = \alpha c$ is complex,

c_r is the phase velocity,

$c_i < 0$ corresponds to damped disturbances,

$c_i = 0$ corresponds to neutral disturbances and

$c_i > 0$ corresponds to amplified disturbances.

The second case will be referred to as spatial amplification and is similarly characterized by,

$\omega = \alpha c$ is real, α is complex

$\alpha_i < 0$ corresponds to amplified disturbances,

$\alpha_i = 0$ corresponds to neutral disturbances and

$\alpha_i > 0$ corresponds to damped disturbances.

Until recently only the temporal amplification was studied but experimental investigations and the works of Gaster (1963, 1965a, 1965b) have now focussed attention on the spatial problem. However the secular equation (4.12) applies to both cases.

We will now examine a number of analytical approaches to the solution of the Orr-Sommerfeld equation.

4.1.2 The Asymptotic Solutions of the Orr-Sommerfeld Equation

A description of various methods of solution is given by Reid (1965) and we will summarise his work here.

We will first examine solutions at large values of αR by an expansion of the solution in inverse powers of $i\alpha R$,

$$v(y) = v^{(0)}(y) + \frac{1}{(i\alpha R)} v^{(1)}(y) + \ldots, \qquad (4.13)$$

where the first term in the expansion, $v^{(0)}(y)$ satisfies the inviscid equation (4.4), which is singular at the point or points where $(U - c)$ is zero unless U'' also vanishes there. Tollmien (1929) obtained the two solutions as a power series in $y - y_c$, where y_c is the value of y at which $U = c$. In the neighbourhood of the singular point there exists the analytic solution,

$$v_A(y) = (y - y_c) \, P_A(y - y_c),$$

$$(4.14)$$

where

$$P_A(y - y_c) = 1 + \frac{U''_c}{2 \, U'_c} \, (y - y_c) + (U''_c + \alpha^2)(y - y_c)^2 + \ldots$$

The second linearly independent solution is of the form,

$$v_B(y) = P_B(y-y_c) + \frac{U''_c}{U'_c} \, (y-y_c) \, P_A(y-y_c) \, \log(y-y_c) \, \Big)$$

$$(4.15)$$

where

$$P_B(y-y_c) = 1 + \left(\frac{U'''_c}{2U'_c} - \frac{U''_c}{U'^2_c} + \frac{1}{2} \alpha^2 \right) (y-y_c)^2 + \ldots$$

In the solution of complete Orr-Sommerfeld equations Heisenberg (1924), made use of the WKB method. We will derive these solutions as follows; let

$$v(y) = \exp \left\{ \int g(y) dy \right\}, \qquad (4.16)$$

then g satisfies the non-linear third order equation,

$$g^4 + 6g^2g' + 4gg'' + 3g'^2 + g''' - 2\alpha^2(g^2 + g') + \alpha^4 \\
= i\alpha R \{(U - c)(g^2 + g' - \alpha^2) - U''\} \qquad (4.17)$$

We will assume an expansion for g of the form,

$$g(y) = (i\alpha R)^{\frac{1}{2}} g_o(y) + g_1(y) + (i\alpha R)^{-\frac{1}{2}} g_2(y) + \dots \qquad (4.18)$$

Substitution into equation (4.17) and equating the coefficients of like powers of $(i\alpha R)^{\frac{1}{2}}$ to zero, leads to

$$g_o^4 = (U - c) g_o^2$$

$$4g_o^3 g_1 + 6g_o^2 g_o' = (U - c)(g_o' + 2g_o g_1) \qquad (4.19)$$

$$- - - - - - -$$

which admits solutions,

$$g_o = \pm(U - c)^{\frac{1}{2}}, \quad g_1 = -\frac{5}{4} \frac{U'}{(U - c)} \dots \qquad (4.20)$$

Retaining the first two terms only of (4.18) we obtain,

$$V_3(y) = \tfrac{1}{2}\pi^{-\frac{1}{2}} (U - c)^{-5/4} \exp \{-(\alpha R)^{\frac{1}{2}} q(y)\}$$

and $$V_4(y) = \tfrac{1}{2}\pi^{-\frac{1}{2}} (U - c)^{-5/4} \exp \{+(\alpha R)^{\frac{1}{2}} q(y)\} \qquad (4.21)$$

where $$q(y) = \int_{y_c}^{y} \{i(U - c)\}^{\frac{1}{2}} \, dy.$$

The choice of the path of integration of the integral is the subject of much analysis and a detailed discussion is given by Wasow (1948). The solutions (4.21) are not valid near the critical point or if the critical point lies close to a boundary, that is,

if $|y_1 - y_c|$ becomes as $0(\alpha R)^{-1/3}$.

It is interesting to note that if $|y - y_c|$ is small compared with unity but large compared with $(\alpha R)^{-1/3}$ then (4.21) is simplified to

$$V_{3,4}(y) \sim \tfrac{1}{2}\pi^{-\frac{1}{2}} \{U_c'(y - y_c)\}^{-5/4} \exp \{\pm \tfrac{2}{3} (i\alpha R U_c')^{\frac{1}{2}}(y - y_c)^{3/2}\} \quad (4.22)$$

It will be seen that this limiting solution agrees with that obtained in subsequent analysis.

In order to obtain approximations to V_3 and V_4 that are valid in the neighbourhood of a critical point we will introduce a stretched independent variable of the form,

$$\xi = (y - y_c)(i\alpha R U_c')^{1/3} \quad , \quad (4.23)$$

and a new dependent variable,

$$\chi^{(o)}(\xi) = v(y) \quad . \quad (4.24)$$

If we substitute these expressions into the Orr-Sommerfeld equation with only the dominant terms for small values of $|y - y_c|$ retained, that is

$$v^{iv} = i\alpha R U_c'(y - y_c)v'' \quad , \quad (4.25)$$

then we obtain,

$$(\frac{d^2}{d\xi^2} - \xi) \frac{d2}{d\xi^2} \chi^{(o)} = 0 \quad (4.26)$$

Equation (4.26) has four solutions which we may write in the form,

$$\chi_1^{(o)} = (y - y_c), \ \chi_2^{(o)} = 1, \ \chi_3^{(o)} \text{ and } \chi_4^{(o)} \ .$$

The first two solutions are identifiable with the leading terms
in the inviscid solutions v_A and v_B, equations (4.14) and (4.15)
The two viscous solutions are given by Lin (1955) as

$$\chi_3^{(o)} = \int_\infty^\eta \int_\infty^\eta \eta^{\frac{1}{2}} H_{1/3}^{(1)} \left[\frac{2}{3}(i\eta)^{3/2}\right] d\eta \; d\eta \quad \left.\begin{array}{c} \\ \\ \\ \\ \end{array}\right)$$

and

$$\chi_4^{(o)} = \int_{-\infty}^\eta \int_{-\infty}^\eta \eta^{\frac{1}{2}} H_{1/3}^{(2)} \left[\frac{2}{3}(i\eta)^{3/2}\right] d\eta \; d\eta \quad \left.\begin{array}{c} \\ \\ \\ \\ \end{array}\right)$$

(4.27)

Where $\eta = (y - y_c)(U_c'\alpha R)^{1/3} = -\xi$

Reid notes that in attempting to study flows with two critical
points it is advantageous to use the Airy function notation.
Then the viscous solutions may be written,

$$\chi_3^{(o)}(\xi) = (\varepsilon U_c')^{-5/4} \int \int A_i(\xi) \; d\xi \; d\xi \quad \left.\begin{array}{c} \\ \\ \\ \\ \end{array}\right)$$

and

$$\chi_4^{(o)}(\xi) = (\varepsilon U_c')^{-5/4} \int \int P_2(\xi) \; d\xi \; d\xi \quad \left.\begin{array}{c} \\ \\ \\ \\ \end{array}\right)$$

(4.28)

where $\varepsilon = (i\alpha R U_c')^{-1/3}$ and

$P_2(\xi) = A_i(\xi e^{2\pi i/3})$ and the limits of integration are deter-
mined by analysis similar to that required in the WKB solutions.
The limiting solutions, for $|y - y_c|$ are small compared with
unity but large compared with $|\varepsilon|$, are

$$\chi_{3,4}^{(o)}(\xi) \sim \tfrac{1}{2}\pi^{-\frac{1}{2}} (\varepsilon U_c')^{-5/4} \; \xi^{-5/4} \; \exp(\pm \tfrac{2}{3} \xi^{3/2}) , \qquad (4.29)$$

which is identical to the limiting form of the WKB solutions.
This demonstrates that there exists an overlapping range of
validity of the WKB and Airy function solutions defined by the
conditions $|\varepsilon| \ll |y-y_c| \ll 1$.

Holstein (1950) tabulated the function $\chi_3^{(o)}$ which he denoted by $\phi_{31}(\eta)$ and is given in our notation by,

$$\phi_{31}(\eta) = -2\sqrt{3} \; e^{\frac{-\pi i}{12}} \int \int A_i(\xi) \; d\xi \; d\xi \qquad (4.30)$$

The method of matched asymptotic expansions was used by Graebel (1966) to determine the viscous solutions. He expanded $v(y)$ in the inner and outer regions according to the series,

$$
\begin{aligned}
v(y,\mu) &\sim \sum_{n=0}^{\infty} \varepsilon_n^*(\mu) \; v_n^*(\eta) \text{ for the inner region and} \\
v(y,\mu) &\sim \sum_{n=0}^{\infty} \bar{\varepsilon}_n(\mu) \; \bar{v}_n(\eta) \text{ for the outer region, where}
\end{aligned}
\qquad (4.31)
$$

$\mu\eta = y-y_c$ and $\mu = 0(\alpha R)^{-n}$. Lins method gives $\mu = (\alpha R)^{-1/3}$. The coefficients in (4.31) are made to satisfy,

$$\lim_{\mu \to 0} \left(\frac{\varepsilon_{n+1}^*}{\varepsilon_n^*} \right) = \lim_{\mu \to 0} \left(\frac{\bar{\varepsilon}_{n+1}}{\bar{\varepsilon}_n} \right) = 0.$$

The coefficients ε_n^* and $\bar{\varepsilon}_n$ are determined by a matching procedure.

Eagles (1969) defined certain exact solutions of the Orr-Sommerfeld equation by using well known convergent series. Asymptotic approximations to the exact solutions were then obtained in the form of a composite series by using the matching procedure of Van Dyke (1964) modified by Fraenkel (1969). He found he required no separate expansion near the wall as employed by Graebel. Eagles also discussed the Lin-Heisenberg approximation to the eigenvalue relation. He concluded that

this was correct in general trend but needed to be treated with caution if accuracy is important. However, he noted that for the case of Poiseuille flow very accurate results for the neutral curve could be obtained using this approximation.

As we have seen, in the above discussion of asymptotic solutions, there are regions of inapplicability to separate methods. Also, even when an analytic form of solution has been obtained, a numerical calculation of the functions involved is required. Thus it is now more attractive to attempt a direct numerical solution of the Orr-Sommerfeld equation making use of high-speed digital computers. So we will now discuss the various numerical methods that have been developed for the solution of the Orr-Sommerfeld equation.

4.2 Numerical Methods

The numerical methods of solution may be broadly divided into two groups. The first method involves the finite difference form of the Orr-Sommerfeld equation which leads to a set of linear algebraic equations. The second method involves the use of a stepping procedure using direct numerical integration.

Nearly all developments in numerical methods have been initially applied to flow problems with either one or two boundaries. The difference between these calculations and those for free shear flows lies only in the application of the boundary conditions. Thus we will examine numerical procedures for various flow problems noting that in most cases these methods may be applied to free shear flows.

The numerical solution of Thomas (1953) was based on finite difference equations and applied to Poiseville flow. The finite difference for the stability equation leads to a set of simultaneous linear algebraic equations which may be written in matrix form as,

$$\bar{A}\,\bar{X} = \lambda\,\bar{B}\,\bar{X} \quad , \tag{4.33}$$

where $\bar{A}$ and $\bar{B}$ are coefficient matrices, $\bar{X}$ is the eigenvector and λ the eigenvalue. The dimensions of the matrices depend on the number of steps into which the range of integration is divided. Thomas used 50 steps and had thus to solve a 50 x 50 matrix to obtain the eigenvalues and eigenfunctions. As we will discuss further the accuracy of the computations involving matrix methods depends on the accuracy with which a matrix may be inverted and is limited to low values of α and R. Thomas's method was applied by Kurtz and Crandall (1962) to the Blasius profile and the free convection boundary layer on a vertical plate. Gallagher and Mercer (1962) solved the Couette flow problem employing the Galerkin method . They reported that difficulties were found in their calculations when the value of αR exceeded 1000.

A variational method for investigating the stability of parallel flows has been developed by Lee and Reynolds (1964, 1967) and applied to various bounded and unbounded flow problems. They first defined the differential operator,

$$L[v] = [(D^2 - \alpha^2)^2 - i\alpha R\ \{(U - c)(D^2 - \alpha^2) - D^2 U\}]v = 0 \tag{4.34}$$

where D is the differential operator $\frac{d}{dy}$. The boundary

conditions are

$$v = Dv = 0 \text{ at the two boundaries} \tag{4.35}$$

In order to construc. the adjoint problem, (4.34), is multiplied by v^*, the adjointfunction, then integrated from one boundary to another, i.e.

$$I = \int_{y_1}^{y_2} v^* L[v] \, dy \tag{4.36}$$

Integrating (4.36) by parts we have,

$$
\begin{aligned}
I = & \left[v^* D^3 v - Dv^* D^2 v + D^2 v^* Dv - D^3 v^* v - 2\alpha^2 v^* Dv + 2\alpha^2 Dv^* v \right. \\
& \left. - i\alpha R \{ Uv^* Dv - UDv^* v - DUv^* v - cv^* Dv + cDv^* v \} \right]_{y_1}^{y_2} \\
& + \int_{y_1}^{y_2} v \left[D^4 v^* - 2\alpha^2 D^2 v^* + \alpha^4 v^* - i\alpha R \{ UD^2 v^* - cD^2 v^* - \alpha^2 (U-c) v^* \right. \\
& \left. + 2DUDv^* \} \right] dy
\end{aligned}
\tag{4.37}
$$

If the boundary conditions for the adjoint problem are chosen to be the same as the given problem,

$$v^* = Dv^* = 0 \quad \text{at the boundaries,} \tag{4.38}$$

then (4.37) may be rewritten in the form,

$$I = \int_{y_1}^{y_2} v \, L^*[v^*] \, dy \quad,$$

from which we may write the adjoint differential operator and equation as,

$$L^*[v^*] = \left[(D^2 - \alpha^2)^2 - i\alpha R \{ (U-c)(D^2 - \alpha^2) + 2DUD \} \right] v^* = 0 \tag{4.39}$$

- 76 -

Lee and Reynolds characterised the variational formulation of the problem by the requirement that the integral

$$I = \int_{y_1}^{y_2} v^* \; L[v] \; dy,$$

is stationary under first order variations in the functions v and v* where v and v* are solutions to their respective problems. They then used the Ritz method to reduce the problem to a set of algebraic equations as follows. Let the functions v and v* be expanded as

$$v(y) = \sum_{j=1}^{k} a_j f_j(y)$$

$$v^*(y) = \sum_{i=1}^{k} a_i^* \; f_i^*(y)$$

(4.40)

where a_j and a_i^* are complex coefficients and f_j and f_i^* are carefully chosen functions that fit the boundary conditions. Since the boundary conditions are identical the same approximating functions may be taken for each set. Substituting (4.40) into (4.36) gives

$$I = \sum_{i=1}^{k} \sum_{j=1}^{k} a_i^* \; a_j \int_{y_1}^{y_2} f_i \; L[f_j] \; dy$$

(4.41)

Since I is to be stationary

$$\frac{\partial I}{\partial a_i^*} = 0 \qquad i = 1, k$$

and so we obtain from (4.41) a set of algebraic equations

$$\sum_{j=1}^{k} a_j \int_{y_1}^{y_2} f_i \; L[f_j] \, dy = 0$$

(4.42)

which has non-trivial solutions if

$$\text{Det} \left[\int_{y_1}^{y_2} f_i \ L \ [f_j] \ dy \right] = 0 \tag{4.43}$$

Lee and Reynolds wrote the operator L in the form $L = M - \lambda N$ then the secular equation (4.43) becomes

$$\text{Det} \ [A_{ij} - \lambda B_{ij}] = 0$$

where

$$A_{ij} = \int_{y_1}^{y_2} f_i \ M[f_j] \ dy$$

and

$$B_{ij} = \int_{y_1}^{y_2} f_i \ N[f_j] \ dy$$

$$\left. \begin{array}{l} \\ \\ \\ \\ \\ \\ \\ \\ \end{array} \right\} \tag{4.44}$$

Equation (4.44) was then solved for the eigenvalues λ. The functions f_i chosen by Lee and Reynolds for various flows were

(i) Poiseuille flow, $f_n(y) = (1 - y^2)^2 \ y^{2(n-1)} \ )$

(ii) Couette flow, $\quad f_n(y) = (1 - y^2)^2 \ y^{n-1} \quad)$ (4.45)

(iii) Plane Jet Flow, $\quad f_n(y) = \text{sech}^n(\alpha y) \quad)$

Lee and Reynolds' results showed good agreement with other methods of calculation and the convergence of the eigenvalue calculations was fast.

As has been mentioned, the accuracy of methods involving the solution of matrix equations depends on the accuracy with which a matrix may be inverted. When the matrix is ill-conditioned the task can be very long and so we will now examine numerical methods that use a step-by-step integration procedure.

A scheme for a step-by-step integration method was suggested by Brown (1959), for the Blasius profile. He noted that

when $y > \delta$, where δ is the value of y when the free stream values are reached within a specified amount, then the solution of the Orr-Sommerfeld may be written exactly as,

$$v = c_1 e^{\alpha y} + c_2 e^{-\alpha y} + c_3 e^{\beta y} + c_4 e^{-\beta y} \qquad (4.46)$$

where $\beta = \beta_r + i\beta_i$ and

$$\left.\begin{array}{l} \beta_r = \dfrac{1}{\sqrt{2}} \left[\alpha^2 + \alpha c_i R + \{(\alpha^2 + \alpha c_i R)^2 + (\alpha R)^2 (U_\delta - c_r)^2\}^{\frac{1}{2}} \right]^{\frac{1}{2}} \\[3mm] \\ \beta_i = \pm \dfrac{1}{\sqrt{2}} \left[-(\alpha^2 + \alpha c_i R) + \{(\alpha^2 + \alpha c_i R)^2 + (\alpha R)^2 (U_\delta - c_r)^2\}^{\frac{1}{2}}\right]^{\frac{1}{2}}, \\[3mm] \\ \text{the sign of } \beta_i \text{ being the same as the sign of } (U_\delta - c_r). \end{array}\right\} \quad (4.47)$$

In order to satisfy the boundary conditions at infinity $c_1 = c_3 = 0$. Thus

$$v = c_2 e^{-\alpha y} + c_4 e^{-\beta y} \qquad (4.48)$$

If the subscript 2 denotes values at $y = \delta$ then the function v and its derivatives yield two equations,

$$v_2''' + \alpha v_2'' - \beta^2 (v_2' + \alpha v_2) = 0 \text{ and}$$

$$\qquad (4.49)$$

$$v_2''' + \beta v_2'' - \alpha^2 (v_2' + \beta v_2) = 0$$

for $y < \delta$ the solution can be written

$$v = k_1 v_1 + k_2 v_2 + k_3 v_3 + k_4 v_4$$

If the v's are defined as follows:

$$v_1(o) = 1 + i, \ v_1'(o) = v_1''(o) = v_1'''(o) = 0,$$
$$v_2(o) = 0, \ v_2'(o) = 1+i, \ v_2''(o) = v_2'''(o) = 0,$$

$v_3(o) = v_3{}'(o) = 0, \ v_3{}''(o) = 1+i, \ v_3{}''' = 0$ \qquad and

$v_4(o) = v_4{}'(o) = v_4{}''(o) = 0, \ v_4{}''' = 1+i,$

then insertion of th boundary conditions at the wall,

$v = v' = 0$ \qquad when $y = 0,$ \qquad leads to,

$0 = k_1(1+i)$

$0 = k_2(1+i),$ so that the complete solution can be expressed as,

$$v = k_3 v_3 + k_4 v_4 \qquad\qquad (4.50)$$

At the boundary layer edge the two solutions (4.48) and (4.50) must coincide. The method suggested by Brown first sets $k_3 = 1$. The functions v_3 and v_4 are then integrated from $y = 0$ to $y = \delta$ and this gives the values at $y = \delta$, i.e. v_{32}, v'_{32} etc. Substitution of equation (4.50) into either equation (4.49) will determine k_4. The other equation (4.49) has then to be satisfied by adjusting the parameters α, R and c. Brown found that the digital computers available to him were not accurate to a large enough number of digits and were too slow for accurate enough step-sizes. However, the method developed by Brown of applying boundary conditions, e.g. equation (4.49), corresponds to the method we will use in our own numerical computations.

The reason for Brown's difficulty in the numerical integration can be seen readily if we examine the behaviour of the solutions in a simple flow case. Let us consider the problem where,

$$U = 1, \ U'' = 0. \qquad\qquad (4.51)$$

then the solutions of the Orr-Sommerfeld equation, which correspond to equations (4.46) and (4.47) are,

$$V_{1,2} \sim \exp\left[\mp \alpha y\right]$$

$$V_{3,4} \sim \exp\left[\pm \{\alpha^2 + i\alpha R(1-c)\}^{\frac{1}{2}} y\right]$$
(4.52)

The boundary conditions only permit the solutions with negative exponents for $y > 0$, i.e. V_1 and V_3. Examination of the form of (4.52) shows that the V_3 solution depends on the Reynolds number and will grow rapidly in comparison with the V_1 solution which is dependent on α. Thus the parasitic error from the rapidly growing V_3 solution will soon dominate the V_1 solution if integration is performed. We therefore need a numerical method to inhibit this contamination.

A scheme developed by Kaplan (1964) provided the first attempt at preventing the contamination of the V_1 solution. His procedure divided the range of integration into a number of segments and then the solution was purified at the start of each segment. Kaplan's method and its modification by Betchov and Criminale (1967) is summarised here.

The solution of the Orr-Sommerfeld equation is written in the form,

$$v(y) = \sum_{j=1}^{4} A_j \, e^{p_j y}$$
(4.53)

where, at any thin slice of the boundary layer, for large Reynolds number

$$p_1 \simeq \left(\alpha^2 + \frac{U''}{U-c}\right)^{\frac{1}{2}} \quad , \qquad p_2 \simeq -\left(\alpha^2 + \frac{U''}{(U-c)}\right)^{\frac{1}{2}} \Big)$$

$$\left.\begin{array}{c} \\ \\ \\ \end{array}\right) \quad (4.54)$$

$$p_3 \simeq (i\alpha R(U-c))^{\frac{1}{2}} \quad , \qquad p_4 \simeq -(i\alpha R(U-c))^{\frac{1}{2}} \Big)$$

Physically A_1 and A_2 represent inviscid rotational oscillations and A_3 and A_4 correspond to viscous vorticity waves.

The numerical solution is started by integrating across the boundary layer to obtain a solution containing as much as possible of the A_4 mode. This is performed by setting $A_1 = A_2 = A_3 = 0$ and $A_4 = 1$ at $y = 1$ and integrating across the entire region storing the values of v and its derivatives at each step. Let us denote this function as $(v)_{\delta_0}$. The computation is then started again at $y = 1$ with $A_z = 1$ and $A_1 = A_3 = A_4 = 0$. Integration proceeds to a station y_1. The computer then integrates across the region y_1 to y_2 etc. If the solution from $y = 1$ to y_1 is denoted by S_1 and that from y_1 to y_2 by S_2 then we define S_2 as follows,

$$S_2 = S_1 + a_1 S_0, \qquad (4.55)$$

where S_0 is the solution obtained on the first complete pass. The new function v is then related to the two others by

$$(v)_{S_2} = (v)_{S_1} + a_1 (v)_{S_0} \qquad (4.56)$$

The coefficient a_1 is determined by the condition that the vorticity mode A_4 of solution S_2 must vanish at $y = y_1$. This

means that

$$a_1 = - \frac{(A_4)_{S_1}}{(A_4)_{S_o}}$$

(4.57)

Kaplan assumed that except near the critical layer and very close to the wall the eigenfunction satisfies the Rayleigh equation and he thus put

$$A_4 = (U-c)(v'' - \alpha^2 v) - U'' v.$$

(4.58)

Betchov and Criminale obtained A_4 from relation (4.53) and its derivatives. Neglecting A_1 and A_2 the relations for v''' and v^{iv} yield,

$$A_4 = \frac{v^{iv} - p_3 v'''}{2(p_3)^3} e^{p_3 y}$$

(4.59)

The initial values for S_2 at $y = y_1$ may now be obtained by applying equation (4.56) at $y = y_1$. The computation then proceeds to a new station y_3 and the decontamination procedure is repeated. When the wall is reached the final solution will be of the form,

$$S_w = S_1 + (a_1 + a_2 + --- a_{w-1}) S_o$$

(4.60)

At the wall the zero normal velocity condition gives

$$v(o) = (v)_{S_w}(o) + A(v)_{S_o}(o) = 0$$

(4.61)

The zero tangential velocity condition with equation (4.61) gives

$$v'(o) = (v)'_{S_w}(o) - \frac{(v)_{S_w}(o)}{(v)_{S_o}(o)} (v)'_{S_o}(o) = 0$$

(4.62)

This equation provides the eigenvalue criterion and the value of

$v'(o)$ is adjusted to be zero by altering the values of the parameters α, R and c.

This method has been used by Wazzan, Okamura and Smith (1966) in a modified form using a scaling factor when storing the rapidly growing solution. The method is also used by Hussain and Reynolds (1970) in their study of a perturbation wave in turbulent shear flow. However, the method is criticised by Wazzan, Okamura and Smith (1967) because of its limited range of application: up to $R = 10^5$. Both Sharma (1968) and Davey and Nguyen (1971) were unable to obtain accurate results using this method, the former author considering the boundary layer and the latter, pipe flow. In both these papers and that of Wazzan et al. (1967) the authors used the much more elegant technique of orthogonalisation which we will use in our computations. A detailed description of this technique will be given at a later stage.

4.3 Spatial and Temporal Amplification

In our discussion of methods of solution of the Orr-Sommerfeld equation, we have confined ourselves to the problem of temporal amplification. We have defined this model as having real Reynolds number and wave-number and a complex value of c, the real part of c being the phase velocity and the imaginary part the amplification factor.

The experimental investigation of Schubauer and Skramstad (1943) was originally accompanied by theory considering temporal amplification. However, the waves observed experimentally grew spatially with distance from the vibrating ribbon and a trans-

- 84 -

formation had to be used which gave the spatial growth rate

apparent to an observer moving at a speed c_r where c_r is given

by,

$$c_r = \frac{\omega}{\alpha} \quad , \text{ the phase velocity,} \qquad (4.63)$$

where α is the real wave number. Gaster (1965a) observes that

the type of waves generated by Schubauer and Skramstad should

have a complex wavenumber and real frequency, ω, defined by

$$\omega = \alpha c \qquad \qquad . \qquad (4.64)$$

However the correspondence between experimental results

analysed using the transformation (4.63) agreed well with the

theory. The relationship between temporal and spatial para-

meters has been examined by Gaster (1965b, 1962).

The characteristic equation (4.12) may be written in

the form,

$$F(\alpha, \omega) = 0, \qquad \qquad (4.65)$$

for a particular velocity profile and Reynolds, where $\omega = \alpha c = \omega_r + i\omega_i$ is the angular frequency, $\alpha = \alpha_r + i\alpha_i$ is the complex

wavenumber and $c = c_r + ic_i$. For every value of ω a value of

α, $\alpha_r + i\alpha_i$, may be found so that one may map lines of constant

α_r and α_i on the ω-plane. Gaster (1965a) notes that the two

families of curves are orthogonal except at points where there

is a singularity in the solution of (4.65). It will be assumed

that no such singularity occurs in the region of interest near

the real axis.

It will be assumed that ω is an analytic function of α.
The two cases of interest are the spatially increasing modes,
with ω real, and the temporally growing modes with α real. These
modes thus occur on the lines $\omega_i = 0$ and $\alpha_i = 0$ respectively.
Along the line $\omega_i = 0$ we have,

$$\omega_i = \alpha_i c_r + \alpha_r c_i = 0 \tag{4.66}$$

With our assumption of an analytical relationship between ω and
α we may write,

$$\omega = \omega_r(\alpha_r, \alpha_i) + i\omega_i(\alpha_r, \alpha_i) \tag{4.67}$$

and the Cauchy-Riemann relations hold,

$$\frac{\partial \omega_r}{\partial \alpha_r} = \frac{\partial \omega_i}{\partial \alpha_i}$$

and

$$\frac{\partial \omega_r}{\partial \alpha_i} = -\frac{\partial \omega_i}{\partial \alpha_r} \tag{4.68}$$

Now let us integrate these relations from a point on the
temporal curve, $\alpha_i = 0$, to a point on the spatial curve, $\omega_i = 0$,
along a line of constant α_r i.e.

$$\omega_{i_T} = -\int_0^{\alpha_{i_S}} \frac{\partial \omega_r}{\partial \alpha_r} \, d\alpha_i \tag{4.69}$$

and

$$\omega_{r_S} - \omega_{r_T} = -\int_0^{\alpha_{i_S}} \frac{\partial \omega_i}{\partial \alpha_r} \, d\alpha_i \tag{4.70}$$

where the subscripts T and S denote values on the temporal and
spatial curves respectively. Gaster argues that the integrand
in equation (4.70) will be of the order of the maximum value

of ω_i for a given Reynolds number and thus the integral term as a whole will be very small and we may write,

$$\omega_{r_S} = \omega_{r_T} \qquad (4.71)$$

Expanding $\dfrac{\partial \omega_r}{\partial \alpha_r}$ about a point α_i^* on the const. α_r line and substitution in (4.69) leads finally to,

$$\frac{\omega_{i_T}}{\alpha_{i_S}} = - \frac{\partial \omega_r}{\partial \alpha_r}(\alpha_i^*) + 0\{\alpha_{i_S} \cdot \omega_{i_{max}}\} \text{ and to the same}$$

accuracy as (4.71) we have,

$$\frac{\omega_{i_T}}{\alpha_{i_S}} = - \frac{\partial \omega_r}{\partial \alpha_r}(\alpha_i^*) \qquad , \qquad (4.72)$$

where $\dfrac{\partial \omega_r}{\partial \alpha_r}$ may be evaluated at any point on the $\alpha_r = $ const curve between the temporal and spatial curves. Thus we see that for small amplification factors the real parts of ω and the real parts of α calculated from temporal and spatial considerations are equal. From (4.72) we see that the spatial growth rate is equal to the temporal growth rate divided by a factor known as the group velocity, that is

$$\alpha_{i_S} = -\omega_{i_T}/c_g \qquad (4.73)$$

where c_g is the group velocity. Now from (4.63) we see that the spatial amplification may not be calculated from the temporal amplification in this manner unless,

$$\frac{\partial \omega_r}{\partial \alpha_r} = \frac{\omega_r}{\alpha_r} \qquad , \qquad (4.74)$$

and the group velocity then equals the phase velocity. In the boundary layer where waves may be considered non-dispersive, this relationship will be approximately true, which accounts for the apparent suc.ssful comparison of theory and experiment by Schubauer and Skramstad.

Although most previous theoretical investigations have considered temporal amplification the use of numerical techniques enables investigations of spatial amplification directly with no great increase in difficulty.

In this chapter we have examined the development of linearised stability theory which has now reached a stage where comparison with experiments in a number of different flows has produced convincing agreement. However, this theory based on the assumption of infinitessimal disturbances, predicts a very rapid growth rate for unstable modes and so non-linearity and finite amplitude disturbances need to be examined. A review of non-linear effects is given at a later stage when calculations for finite amplitude disturbances in a mixing layer are presented.

CHAPTER 5

The Stability of the Mixing Layer between Two Streams

In this chapter we will describe the numerical method to solve the Orr-Sommerfeld equation. Calculations will then be made of the stability of the mixing layer between two streams of finite velocity using the mean velocity profile calculated in Chapter 3. The effect of divergence of the flow will be discussed and corrections made to the stability eigenvalues.

5.1 Numerical Method of Solution

The Orr-Sommerfeld equation of hydrodynamic stability is written,

$$(U-c) \{ \hat{u}_2{}'' - \alpha^2 \hat{u}_2 \} - U''\hat{u}_2 + \frac{i}{\alpha R} \{ \hat{u}_2{}^{iv} - 2\alpha^2 \hat{u}_2{}''$$

$$+ \alpha^4 \hat{u}_2 \} = 0, \tag{5.1}$$

and the boundary conditions are

$$\hat{u}_2 = \hat{u}_2{}' = 0 \quad \text{as} \quad x_2 \to \pm\infty \quad , \tag{5.2}$$

where the primes denote differentiation with respect to x_2. In equation (5.1) the parameters that are determined by the mean flow are U, the mean velocity profile, U'', its second derivative with respect to x_2, and the Reynolds number R given by,

$$R = \frac{U_d L}{\nu} \quad . \tag{5.3}$$

In order to more readily use the form of mean velocity

profile derived in Chapter 3 we will define the mean velocity as,

$$U(\eta^*) = U + U_d\, f'(\eta^*) \tag{5.4}$$

where $\eta^* = x_2/\theta$ and the momentum thickness θ is defined by

$$\theta = \frac{1}{U_d^2} \int_{-\infty}^{\infty} (U_1 - U)(U - U_2)\, dx_2 \tag{5.5}$$

Substitution of expression (5.4) into equation (5.1) leads to,

$$(f'(\eta^*) - c^*)\{\hat{u}_2'' - \alpha^{*2}\,\hat{u}_2\} - f'''(\eta^*)\,\hat{u}_2 + \frac{i}{\alpha^* R_\theta}$$

$$\{\hat{u}_2^{iv} - 2\alpha^{*2}\,\hat{u}_2'' + \alpha^{*4}\,\hat{u}_2\} = 0, \tag{5.6}$$

where $\alpha^* = \alpha\theta$, $R_\theta = \dfrac{U_d\theta}{\nu}$ and $-c^* = \left[\dfrac{U_s}{U_d} - c\right]$ (5.6a)

primes denote differentiation with respect to η^*. It can be

seen that equations (5.1) and (5.6) are identical in form,

however in equation (5.6) the wavenumber and Reynolds number

are functions of x.

Above the mixing layer $f'(\eta^*)$ attains a constant value 1,

and $f'''(\eta^*)$ is zero. In this region the solution to equation

(5.6) may be written,

$$\hat{u}_2 = \sum_{n=1}^{4} \hat{u}_{2_n} = \sum_{n=1}^{4} A_n e^{p_n \eta^*} , \tag{5.7}$$

where $\qquad p_1 = \alpha^*, \qquad\qquad p_2 = -\alpha^*,$

$$p_3 = \left[\alpha^{*2} + i\alpha^* R_\theta(1-c^*)\right]^{\frac{1}{2}} \text{ and } p_4 = -\left[\alpha^{*2} + i\alpha^* R_\theta(1-c^*)\right]^{\frac{1}{2}}$$

(5.8)

Below the mixing layer $f'(\eta*)$ attains a constant value -1 and $f'''(\eta*)$ is zero. In this region the solution to equation (5.6) may be written,

$$\hat{u}_2 = \sum_{n=1}^{4} \hat{u}_{2_n} = \sum_{n=1}^{4} B_n e^{q_n \eta*}, \qquad (5.9)$$

where $\quad q_1 = \alpha* \qquad , \qquad q_2 = -\alpha*$

$$\left. \begin{array}{l} \\ \\ \\ q_3 = \left[\alpha*^2 - i\alpha* R_\theta (1+c*)\right]^{\frac{1}{2}} \text{ and } q_4 = -\left[\alpha*^2 - i\alpha* R_\theta (1+c)\right]^{\frac{1}{2}} \end{array} \right\} \qquad (5.10)$$

In the solutions above the mixing layer we see that $A_1 = A_3 = 0$ in order that the boundary conditions on $\hat{u}_2$ may be fulfilled. Below the mixing layer we also have $B_2 = B_4 = 0$.

In the above solutions we see that above the mixing layer $\hat{u}_{2_2} = A_2 e^{p_2 \eta*}$ corresponds to the 'inviscid solution' and $\hat{u}_{2_4} = A_4 e^{p_4 \eta*}$ involves the Reynolds number and corresponds to the 'viscous solution'. Similarly, below the mixing layer, the solution $\hat{u}_{2_1} = B_1 e^{q_1 \eta*}$ corresponds to the 'inviscid solution' and $\hat{u}_{2_3} = B_3 e^{q_3 \eta*}$ is the 'viscous solution'. Let us consider the solutions for $\eta* > 0$ as we will numerically integrate from above to below the mixing layer.

It can be seen from the form of $\hat{u}_{2_2}$ and $\hat{u}_{2_4}$ that the viscous solution will vary rapidly with $\eta*$ depending on the value of the Reynolds number, whilst the inviscid solution will be well-behaved. In any numerical integration procedure with starting conditions corresponding to,

$$A_2 e^{-\alpha \eta*} \text{ and } A_4 e^{p_4 \eta*} \qquad (5.11)$$

the parasitic error in the numerical technique will inevitably

produce a viscous solution. The problem is to obtain the in

viscid solution without any viscous influences.

Kaplan (1967) found that accurate results were possible

if the inviscid solution is made free of a part of the parasitic

error due to the viscous solution by satisfying the Rayleigh

equation at each step of the integration. This method does

reduce the error in the inviscid solution and its first deriv-

ative, however as the Rayleigh equation is of second order the

higher derivatives are not as well corrected. The method does

not work at high Reynolds numbers and, due to the filtering

system being the inviscid stability equation, the method also

fails in regions of dominant viscous effects such as critical

layers and wall layers. As we have discussed in Chapter 4

for problems where the critical layers are far from the walls

the Kaplan purification scheme has to be abandoned. In our

calculations, in order to remove restrictions on the Reynolds

number and wavenumbers, a different purification scheme is

used throughout. The method which we will use to prevent the

contamination of the inviscid solution is based on preserving

the linear independence of the solutions.

The set of solutions (5.7) are fundamentally linearly

independent functions. In numerical integration we have

noted that the rapidly varying viscous solution affects the

inviscid solution and eventually dominates it, that is the

solutions are no longer linearly independent. The method we

will adopt to preserve the linear independence of the solutions is to obtain an orthonormal system of vectors corresponding to the linearly indepei l nt solutions.

The formation of a set of orthogonal vectors from a system of vectors is a well-known method in vector analysis. Let us consider the two linearly independent vectors $\underset{\sim}{A}$ and $\underset{\sim}{B}$. We wish to construct a vector orthogonal to $\underset{\sim}{A}$ of the form $\underset{\sim}{B} - k\underset{\sim}{A}$ where k is a scalar variable. Thus we may write

$$\underset{\sim}{A} \cdot (\underset{\sim}{B} - k\underset{\sim}{A}) = 0. \tag{5.12}$$

Rearranging this expression we may see that the scalar variable k is formed by the dot product of the vector $\underset{\sim}{B}$ and the normalised vector $\underset{\sim}{A}$, that is,

$$k = \frac{\underset{\sim}{A}}{|\underset{\sim}{A}|^2} \cdot \underset{\sim}{B} , \tag{5.13}$$

where $|\underset{\sim}{A}|^2$ denotes the absolute squared value of the vector $\underset{\sim}{A}$. From the definition of linear independence the vector $(\underset{\sim}{B} - k \cdot \underset{\sim}{A})$ cannot vanish. Thus we have constructed a pair of orthogonal vectors from our original pair of linearly independent vectors.

The adaptation of this procedure to the solution of differential equations was made by Bellman and Kalaba (1965). Let us write the inviscid solution $\hat{u}_{2_2}$ as the vector $\underset{\sim}{V}_2$ where $\underset{\sim}{V}_2$ is given by

$$\underset{\sim}{V}_2 = (\hat{u}_{2_2}, \hat{u}_{2_2}', \hat{u}_{2_2}'', \hat{u}_{2_2}'''), \tag{5.14}$$

and the viscous solution $\hat{u}_{2_4}'$ as $\underset{\sim}{V}_4$ where $\underset{\sim}{V}_4$ is given by,

$$\underset{\sim}{V}_4 = (\hat{u}_{2_4}, \hat{u}_{2_4}{}', \hat{u}_{2_4}{}'', \hat{u}_{2_4}{}''') \tag{5.15}$$

The method of solution is to first obtain the viscous solution $\underset{\sim}{V}_4$. This can either be evaluated for one integration step or across the range of integration and the values stored. The viscous solution is then normalised which we will denote by $\overline{\underset{\sim}{V}}_4$, that is,

$$\overline{\underset{\sim}{V}_4} = \frac{\underset{\sim}{V}_4}{|\underset{\sim}{V}_4|} \tag{5.16}$$

We now form the purified inviscid solution by setting,

$$\overline{V}_2 = \frac{\underset{\sim}{V}_2 - \lambda \underset{\sim}{V}_4}{|\underset{\sim}{V}_2 - \lambda \underset{\sim}{V}_4|} \tag{5.17}$$

where the complex scalar λ is given by,

$$\lambda = \underset{\sim}{V}_2 \cdot \overline{\underset{\sim}{V}}_4{}^*$$

where the star denotes the complex conjugate. The value of λ may be evaluated at each step of the integration. The solutions $\overline{V}_2$ and $\overline{\underset{\sim}{V}}_4$ now represent the linearly independent inviscid and viscous solutions to the equation.

A numerical example of the above technique for a wholly real differential equation is given in Appendix A.

5.2 Numerical Calculation Procedure

The numerical integration method chosen was the standard Runge-Kutta scheme with error minimisation developed by Fyfe (1965). It was found that the accuracy of the integration

could be easily checked by altering the step size and comparing calculations. Two numerical procedures were used in all; the first which checked e step length accuracy and recorded the required step length: the second used this information in an unchecked numerical integration which saved computation time.

The integration is started from above the mixing layer where the exact solutions are known. To start the integration the coefficients A_2 and A_4, (equation (5.7)), are set equal to unity. If the starting value of η^* is η_1^* then the starting conditions on $\hat{u}_{2_2}$ and $\hat{u}_{2_4}$ are

$$\hat{u}_{2_2} = e^{-\alpha^* \eta_1^*} \;, \quad \hat{u}_{2_2}{}' = -\alpha^* \hat{u}_{2_2} \;, \quad \hat{u}_{2_2}{}'' = \alpha^{*2} \hat{u}_{2_2} \;, \quad \hat{u}_{2_2}{}''' = -\alpha^{*3} \hat{u}_{2_2} \;, \quad (5.18)$$

and

$$\hat{u}_{2_4} = e^{p_4 \eta_1^*} \;, \quad \hat{u}_{2_4}{}' = p_4 \hat{u}_{2_4} \;, \quad \hat{u}_{2_4}{}'' = p_4^2 \hat{u}_{2_4} \;, \quad \hat{u}_{2_4}{}''' = p_4^3 \hat{u}_{2_4} \;, \quad (5.19)$$

where primes denote differentiation with respect to η^*.

For large values of Reynolds number the starting values of $\hat{u}_{2_4}$ and its derivatives are very small. To prevent floating-point overflow occurring when the vector $\underset{\sim}{V}_4$ is normalised it is convenient to multiply (5.19) by a suitably large constant throughout. The solution $\underset{\sim}{V}_4$ tends to grow very rapidly as the integration proceeds unless some scaling procedure is introduced. The normalisation of $\underset{\sim}{V}_4$ at every integration step, which is required for the orthonormalisation procedure, prevents overflow of the viscous solution and no scaling factors are required.

When an integration step is completed the solution $\bar{y}_4$ is normalised and the new orthogonal vector $\bar{y}_2$ is calculated. If the eigenfunctions are required the same transformations have to be performed on the preceding values of $\bar{y}_2$ and $\bar{y}_4$. However if only the eigenvalues are required the time is saved if this backward transformation is not performed.

When the linearly independent solutions $\bar{y}_2$ and $\bar{y}_4$ have been calculated completely across the layer the boundary conditions below the layer must be applied to form the eigenvalue problem. Let the value of η^* at the finish of integration below the layer be η_2^*. Then at this point we have from equation (5.9)

$$
\begin{vmatrix} \hat{u}_2 \\ \hat{u}_2{}' \\ \hat{u}_2{}'' \\ \hat{u}_2{}''' \end{vmatrix} = \begin{vmatrix} 1 & 1 & 1 & 1 \\ \alpha^* & -\alpha^* & q_3 & -q_3 \\ \alpha^{*2} & \alpha^{*2} & q_3{}^2 & q_3{}^2 \\ \alpha^{*3} & -\alpha^{*3} & q_3{}^3 & -q_3{}^3 \end{vmatrix} \begin{vmatrix} B_1 \, e^{\alpha^* \eta_2^*} \\ B_2 \, e^{-\alpha^* \eta_2^*} \\ B_3 \, e^{q_3 \eta_2^*} \\ B_4 \, e^{-q_3 \eta_2^*} \end{vmatrix} \qquad (5.20)
$$

Equation (5.20) may be inverted to give four equations for B_n in terms of u_2 and its derivatives. The equations for B_2 and B_4 are

$$
B_2 = \frac{e^{(\alpha^* \eta_2^*)}}{(2\alpha^*(q_3{}^2 - \alpha^{*2}))} \{ \hat{u}_2{}''' - \alpha^* \hat{u}_2{}'' - q_3{}^2 \hat{u}_2{}' + \alpha^* q_3{}^2 \hat{u}_2 \} \qquad (5.21)
$$

and

$$
B_4 = \frac{-e^{(q_3 \eta_2^*)}}{(2q_3(q_3{}^2 - \alpha^{*2}))} \{ \hat{u}_2{}''' - q_3 \hat{u}_2{}'' - \alpha^{*2} \hat{u}_2{}' + q_3 \alpha^{*2} \hat{u}_2 \} \qquad (5.22)
$$

The values of $\overline{\underset{\sim}{V}}_2$ are substituted into equations (5.21) and
(5.22) giving values of B_2 and B_4 which we will denote by (B_2)
and $(B_4)_I$. Similar substitution of $\overline{\underset{\sim}{V}}_4$ leads to values of B_2
and B_4 of $(B_2)_{II}$ and $(B_4)_{II}$. Because the Orr Sommerfeld equation
is linear solutions may be obtained by addition of the two
solutions $\overline{\underset{\sim}{V}}_2$ and $\overline{\underset{\sim}{V}}_4$. The constants B_n in the lower stream are
thus given by

$$B_n = A_2 (B_n)_I + A_4 (B_n)_{II}, \qquad (5.23)$$

for arbitrary values of A_2 and A_4. We may set $A_2 = 1$ which is
equivalent to dividing equation (5.7) throughout by A_2. We
require to find the values of A_2 and A_4 which will enable the
boundary conditions to be satisfied below the mixing layer.
Thus we first set

$$A_4 = \frac{-(B_2)_I}{(B_2)_{II}}, \qquad (5.24)$$

which determines the value of A_4 for which $B_2 = 0$. The constant
B_4 then becomes

$$B_4 = (B_4)_I - \frac{(B_2)_I}{(B_2)_{II}} (B_4)_{II} \qquad (5.25)$$

For the boundary conditions to be met B_4 must vanish. The value
of B_4 is set by the choice of parameters α, R and c or ω, R and
c, and these values must be altered in order to set $B_4 = 0$.
This minimisation constitutes the numerical eigenvalue problem.

In the case of temporal amplification it is convenient to
keep α and R constant and alter the value of c. For the spatial

case we keep ω and R constant and again alter the value of c.
We may rewrite equation (5.25) as

$$B_4(R, \alpha, c) = (B_4)_I - \frac{(B_2)_I}{(B_2)_{II}} \cdot (B_4)_{II} \qquad (5.25a)$$

The search for the zero of B_4 can be found by linear interpolation.
As we are altering the value of c only for a specific set of
values of α and R, or ω and R, we find the change in B_4 made by
a small change in c of δc. Then for any other small change in
c of Δc we may write the value of B_4 as,

$$B_4(c + \Delta c) = B_4(c) + \frac{B_4(c + \delta c) - B_4(c)}{\delta c} \cdot \Delta c. \qquad (5.26)$$

In order to make $B_4(c + \Delta c)$ zero we must therefore choose Δc
such that

$$\Delta c = - \lambda \left\{ \frac{B_4(c + \delta c)}{B_4(c)} - 1 \right\} \delta c, \qquad (5.27)$$

where λ is a factor that enables the computer to take large or
small steps towards the minimum depending on the variation of
B_4 with c. The value of c is then replaced by $c + \Delta c$ and δc by
$\mu \Delta c$ where μ acts in the same way as λ to reduce to step size
as the minimum is reached.

When the computations were performed it was found to be
very difficult to make B_4 exactly zero. Instead the program
compares successive values of c and when two such values are
within a specified limit then the interpolation is stopped.
It was also found that for high Reynolds number the program
would only converge if the initial guess at the eigenvalue is

very close to the actual eigenvalue. This problem was also

encountered by Sharma (1968) who developed the following scheme

of inverse Langrangian interpolation which proved to give

higher accuracy and faster convergence of the eigenvalue.

A number of values of B_4 for various values of c are

calculated and these values are used to generate a power series

of the form,

$$c_n = \sum_n a_n B_4{}^n \tag{5.28}$$

An approximating series for c_n is formed using Lagrange's inter-

polation polynomial and is of the form,

$$c_{n+1} = \sum_{j=0}^{n} L_j{}^{(n)}(B_4) \cdot c_j, \tag{5.29}$$

$$\text{where} \quad L_j{}^{(n)}(B_4) = \frac{\prod\limits_{i=0}^{n} (B_4 - B_{4i}) \; i \neq j}{\prod\limits_{i=0}^{n} (B_{4j} - B_{4i}) \, i \neq j} \tag{5.30}$$

$L_j{}^{(n)}$ is the nth Lagrangian coefficient formed for the (n+1)

pairs (c_o, B_{4_o}), (c_1, B_{4_1}), ..., (c_n, B_{4_n}).

We are seeking the value of c for which B_4 is zero. Thus

we set $B_4 = 0$ in (5.30) and substitute into (5.29) giving,

$$c_{n+1} = \sum_{j=0}^{n} c_j \, (-1)^n \, \frac{\prod\limits_{i=0}^{n} B_{4i} \quad i \neq j}{\prod\limits_{j=0}^{n} (B_{4j} - B_{4i}) \; i \neq j} \tag{5.31}$$

Equation 5.31) provides the next value of c to be used in the

solution of equation (5.1).

In the computations three values of c are used to start
giving three corresponding values of B_4 and equation (5....
used to determine the new value of c. The corresponding value
of B_4 is calculated and the four sets of values are then used
to determine another value for c. The convergence in our
calculations appears to have been more rapid than that of Sharma.
An example of the convergence of B_4 to a minimum is shown in
Figure 10 for a typical set of values of R and α. The surface
$|B_4|$ as a function of complex variable c exhibits a sharp
minimum at the eigenvalue but outside the minimum the surface
gradually slopes away. If points are chosen outside the
immediate area of the minimum then the interpolated new value
of c will not be closer to the eigenvalue and the procedure
will not converge.

In the next section we will review previous work on the
stability of free shear layers.

5.3 Review of Studies of the Stability of Free Shear Layers

The investigation of the stability of free shear layers
was initiated by Lord Rayleigh (1880). He considered the
inviscid shear layer with a mean velocity profile given by,

$$U = \begin{cases} 1 & y > 1, \\ y & -1 < y < 1, \\ -1 & y < 1. \end{cases} \quad (5.32)$$

He assumed that the value of U'' was finite within the layer
$y = 1 \pm \varepsilon$ and that $\hat{u}_2$ was constant. Integrating the inviscid

- 100 -

stability equation showed that the value of $(U-c)\hat{u}_2' - U'\hat{u}_2$

at $y = 1 - \varepsilon$ must equal its value at $1 + \varepsilon$. This lead to

an expression for c of the form,

$$c^2 = (1 - \frac{1}{2\alpha})^2 - (\frac{1}{4\alpha^2}) e^{-4\alpha} .$$ (5.33)

These values of c agree qualitatively with those obtained for

continuous mean velocity profiles. The eigenvalues and ampli-

fications for the profile (5.32) are sketched below.
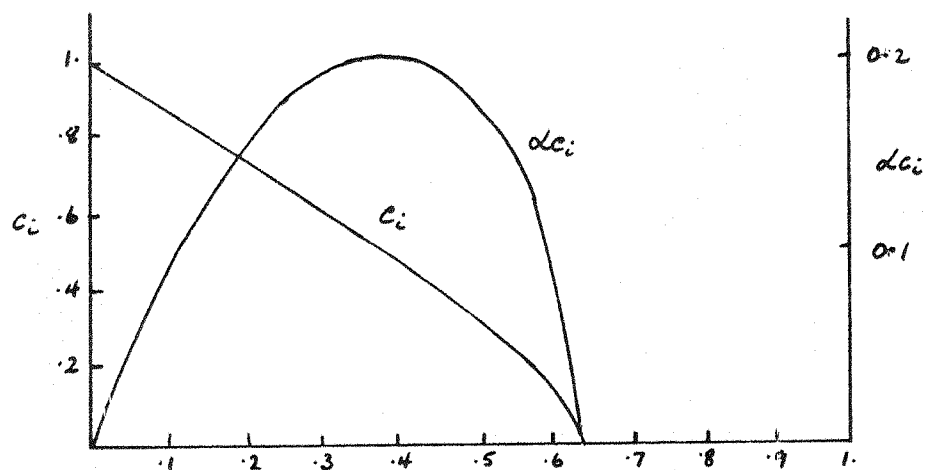
Eigenvalues and amplifications for discontinuous profile,
equation (5.32)

Following Rayleigh's work the problem was not tackled again

until 1950, when Lessen (1950) considered the free boundary

layer between parallel streams. He solved the complete Orr-

Sommerfeld equation using an expansion method similar to the

one used to obtain the mean velocity profile. His calculations,

and those of subsequent workers, showed that the unstable

properties of the shear layer were very nearly independent of

Reynolds number for large values of Reynolds number. Esch (1957)

considered the stability of a free shear layer with a piecewise mean velocity profile. He showed that the neutral curve approached the origin with $\alpha = R \times$ const. This indicates that there exists no critical Reynolds number for the free shear layers. However for low values of Reynolds number the assumption of parallel mean flow is not valid as the variation in the mean velocity profile in the x-direction may be important. We will discuss this problem in more detail a little later. The inviscid shear layer has also been studied by Michalke (1964) who considered the disturbance vorticity distribution. He showed that for neutral disturbances a single concentration of vorticity existed within a single wave length forming a stable cell-like structure. However, for the case of maximum temporal amplification two distinct concentrations existed within one wavelength. If these vorticity distributions are considered in terms of eddies then the instability may be seen as the rolling over of one eddy on another. The preceding investigations have all considered temporally growing disturbances as were assumed in the classical stability theory. In order to compare the results for temporal growth rates obtained theoretically with experimental results, a number of researchers, Schade and Michalke (1962) and Sato (1959) have used the disturbance phase speed to obtain spatial growth rates. The agreement was fair comparing wave-numbers and growth rates, other factors such as the eigenfunction for temporal amplification, was contrary to that predicted from experiment. As we have seen in Chapter 4, Gaster concluded that

the phase velocity would only be used when the wave system is non-dispersive, which is nearly the case in boundary layers.

Direct numerical calculations of the spatial growth rates involving complex wavenumber and real frequency have been made by Michalke (1965) for the inviscid shear layer, Betchov and Criminale (1966) for the inviscid jet and wake, Lessen and Ko (1966) for the viscous incompressible half jet flow and Ko and Lessen (1969) for the viscous full jet. The calculations by Michalke compared very well with the experimental results of Freymuth (1966) and Browand (1966). The growth rates and wavenumbers corresponded to the transformed values using temporal amplification. However, the essential features of the instability such as the distribution of the u_1-fluctuation, which exhibits a phase reversal for one stream having zero velocity, were also predicted. As we have noted, no critical Reynolds number is predicted using a parallel mean flow assumption. We will now discuss the modification in the growth rates caused by a non-parallel mean flow.

5.4   The Stability of Non-Parallel Flows

The non-parallel mean flow problem was treated analytically by Lanchon and Eckhaus (1964). They concluded that for free shear flows only the inviscid limit obtained from the quasi-parallel flow assumption was correct and it would be essential to take account of flow divergence when viscous terms are included. They also noted that the asymptotic theory of weakly divergent flows is analytically little more complicated than the classical theory.

In our direct numerical integration of the stability
equation we need to take account of the effect of flow diver-
gence. Lessen and Ko (1966) and Lessen, Harpavat and Zien
(1969) proposed a relatively simple method of correcting the
stability curves in non-parallel flows. Though we shall note
that some of their results are anomolous, it is felt that
their basic argument is justified.

Lessen et. al. argue that in linear stability theory it
is the interaction energy between the disturbance and the main
flow that plays a role in the stability of the flow. Let us
denote this interaction energy by $E(x,y,t)$ which will depend
on the products of the disturbances. If we denote two such
disturbance terms as $p(x,y,t)$ and $q(x,y,t)$ then their Fourier
transforms are,

$$\hat{p}(y;k,\omega) = \frac{1}{(2\pi)^2} \int\limits_{-\infty}^{\infty}\int \exp\{-i(kx - \omega t)\}\, p(y;x,t)\, dx\, dt$$

and

$$\hat{q}(y;k,\omega) = \frac{1}{(2\pi)^2} \int\limits_{-\infty}^{\infty}\int \exp\{-i(kx - \omega t)\}\, q(y;x,t)\, dx\, dt,$$

where k is the wavenumber in the x-direction and ω is the
angular frequency. The Fourier transform of the energy term
will be of the form of the product of the two disturbances,

$$\hat{q}(y;k,\omega).\hat{p}(y;k,\omega)$$

$$= \frac{1}{(2\pi)^4} \int\limits_{-\infty}^{\infty}\int \exp\{-i(kx - \omega t)\, dx\, dt \int\limits_{-\infty}^{\infty}\int p(x',y,t').$$

$$\qquad\qquad\qquad\qquad\qquad\qquad q((x-x'),y\ (t-t'))\, dx'\, dt'$$

(5.34)

Thus we may write the transform of the interaction energy as,

$$\hat{E}(y;k,\omega) = \frac{1}{(2\pi)^2} \int\limits_{-\infty}^{\infty}\int\limits^{\infty} \exp\{-i(kx - \omega t)\}\ E(y;x,t)\ dx\ dt \qquad (5.35)$$

Let the energy density per unit width be given by $\varepsilon(y;x,t)$ with its transform $\hat{\varepsilon}(y;k,\omega)$.

Then we may write,

$$\frac{1}{\varepsilon}\frac{d\varepsilon}{dx} = \frac{1}{E}\frac{dE}{dx} - \frac{1}{V}\frac{dV}{dx} \quad, \qquad (5.36)$$

where V is the volume occupied by the disturbances. Let us assume that as the change in the volume V depends on the growth of the layer then we may write,

$$\frac{1}{V}\frac{dV}{dx} = \frac{1}{\ell}\frac{d\ell}{dx} \quad, \qquad (5.37)$$

where ℓ is the width of the mixing layer for laminar flow such that,

$$\ell = (\frac{\nu x}{U_d})^{\frac{1}{2}} \qquad . \qquad (5.38)$$

From (5.37) and (5.38) we have,

$$\frac{1}{\ell}\frac{d\ell}{dx} = \frac{1}{2x} \qquad . \qquad (5.39)$$

Making use of equation (5.35) we see that

$$\frac{1}{E}\frac{dE}{dx} = -k_i \qquad , \qquad (5.40)$$

where k_i is the imaginary part of the wavenumber k.

Substituting equations (5.39) and (5.40) into equation (5.36) we obtain,

$$\frac{1}{\hat{\varepsilon}} \frac{d\hat{\varepsilon}}{dx} = -k_i - \frac{1}{2x} \qquad (5.41)$$

Non-dimensionalising this equation with respect to the reference length ℓ and a reference energy density ε_o we obtain,

$$\frac{1}{\hat{\varepsilon}^*} \frac{d\hat{\varepsilon}^*}{dx^*} = -\alpha_i - \frac{1}{2R_\ell} \qquad (5.42)$$

where $\hat{\varepsilon}^* = \hat{\varepsilon}/\varepsilon_o$, $\quad \alpha_i = k_i \ell$ and

$$R_\ell = \frac{U_d \ell}{\nu} \quad .$$

From equation (5.42) we see that the growth of the region has led to the inclusion of a term, $(2R_\ell)^{-1}$, which reduces the amplification factor found from parallel flow assumptions. Thus for spatial amplification we may write,

$$(\alpha_i)_{\text{non-parallel}} = (\alpha_i)_{\text{parallel}} + \frac{1}{2R_\ell} \qquad (5.43)$$

This result is the same as that obtained by Lessen and Ko (1966). However, it is interesting to note that if one assumes a wave-like form for the disturbances a priori, then the interaction energy will have an exponent of twice that of the disturbance. However, making use of the Fourier transform, as we have seen above, eliminates this problem.

Let us now consider the effect of a divergent flow when one considers temporal amplification. Using a similar technique to that above we may write

$$\frac{1}{\hat{\varepsilon}^*} \frac{d\hat{\varepsilon}^*}{dt^*} = \alpha c_i - \frac{1}{2R_\ell} \cdot \frac{dx^*}{dt^*} \qquad (5.44)$$

In their discussion of the problem, Lessen et. al. (1969) set $\frac{dx^*}{dt^*}$ equal to unity which implies that the disturbances are travelling at the mean reference velocity.

Let us set $\frac{dx^*}{dt^*} = c^*$, a non-dimensionalised velocity which represents the translation speed of the disturbances. We may then write,

$$(\alpha c_i)_{\text{non-parallel}} = (\alpha c_i)_{\text{parallel}} - \frac{c^*}{2R_\ell} \qquad (5.45)$$

The neutral stability curves for either spatial or temporal amplification must be identical in the non-divergent case as well as the parallel case. Making use of our discussion of spatial amplification in Chapter 4, we may usefully multiply equation (5.43) by $-\frac{\partial\omega_r}{\partial\alpha_r}$ to obtain,

$$\left(\alpha_i \frac{\partial\omega_r}{\partial\alpha_r}\right)_{\text{non-parallel}} = \left(\alpha_i \frac{\partial\omega_r}{\partial\alpha_r}\right)_{\text{parallel}} + \frac{1}{2R_\ell} \frac{\partial\omega_r}{\partial\alpha_r} \qquad (5.46)$$

Now from equation (4.72) we have,

$$\frac{\omega_{i_T}}{\alpha_{i_s}} = -\frac{\partial\omega_r}{\partial\alpha_r} , \qquad (4.72)$$

where the subscripts T and s refer to temporal and spatial amplification respectively. From equations (5.45) and (5.46) with (4.72) we may see that

$$c^* = \frac{\partial\omega_r}{\partial\alpha_r} = c_g, \text{ the group velocity.} \qquad (5.47)$$

In the case of a non-dispersive wave system the group velocity will equal the wave speed given by

$$c_r = \frac{\omega_r}{\alpha_r} \tag{5.48}$$

Thus we may see from the preceding discussion that we may only calculate the correction in amplification factor for the temporal case when the system is non-dispersive and then we have,

$$(\alpha c_i)_{non-parallel} = (\alpha c_i)_{parallel} - \frac{c_r}{2R_\ell} \tag{5.49}$$

5.5 Results and Discussion

In this section we will present the numerical results for the stability of a mixing layer between two streams. Calculations have been performed for the two cases of temporal and spatial amplification. The results for the temporal case will be presented first and comparison will be made, where possible, with the results of other researchers.

5.5.1 Eigenvalues and Eigenfunctions for the Temporal Case

Calculation of the eigenvalues for the temporal case were made for the laminar velocity profile calculated in Chapter 3 for the mixing of two streams with finite velocity. The velocity ratio of the two streams was 0.61. The eigenvalues for various wavenumbers and Reynolds numbers are tabulated below. The results of Esch (1957) indicated that for values of $\alpha R > 100$ the results of inviscid theory were found to be a good approximation to the viscous results. Calculations were thus made at a value of $R_\theta = 500$ so that comparison with the results of inviscid theory

- 108 -

and calculation could be made. The value of 500 was chosen
so as to clearly meet the requirement of Esch and also so that
computations could be faster than if a higher value of Reynolds
number had been chosen. The eigenvalues were evaluated by
integrating between values of y/θ of +2 and -2, with a step
size of .005. In all cases the computation was completed when
successive values of the interpolated eigenvalue differed by
less than 10^{-7}.

Table III. Numerical Results of the Calculations. Temporal Case

R_θ	α	c_r	c_i	αc_i
5.0	.2	4.068748	.349364	.069873
5.0	.4	4.070216	.189218	.075687
5.0	.55	4.071635	.073067	.040187
10.0	.2	4.068189	.474343	.094869
10.0	.4	4.070206	.350662	.140265
10.0	.6	4.072800	.223019	.133811
10.0	.8	4.075939	.098330	.078664
12.5	.2	4.068031	.509870	.101974
12.5	.4	4.070301	.392735	.157094
12.5	.6	4.073127	.269509	.161705
12.5	.8	4.076464	.148938	.119151
15.0	.2	4.067927	.537436	.107487
15.0	.4	4.070428	.424085	.169634
15.0	.6	4.073447	.303373	.182024
15.0	.8	4.076943	.185258	.148207
15.0	1.0	4.080973	.071291	.071291

R_θ	α	c_r	c_i	αc_i
500.0	0.1	4.068741	.876765	.087676
500.0	0.2	4.072069	.808464	.161693
500.0	0.4	4.076671	.667809	.267124
500.0	0.6	4.081002	.538959	.323375
500.0	0.8	4.085574	.421458	.337166
500.0	1.0	4.090603	.312914	.312914
500.0	1.2	4.096279	.211166	.253399
500.0	1.3	4.099424	.162251	.210927
500.0	1.4	4.102813	.114379	.160131
500.0	1.5	4.106474	.067347	.101020
500.0	1.6	4.110444	.020994	.033591
500.0	1.7	4.114761	-.024834	-.042218

The temporal amplification factors αc_i, are shown graphically in Figure 11 as a function of the wavenumber. The calculations of Betchov and Szewczyk (1963) for a hyperbolic tangent representation of the mean profile are shown as a dotted line. The results of Rayleigh (1880) for the mean velocity profile given by equation (5.32) are also plotted. These two calculations are for the inviscid shear layer. It can be seen that for low wavenumbers the amplification factors are nearly independent of the mean profile shape. This agrees with the work of Esch (1957)

and Michalke (1969). Esch comments that at low wavenumbers the wavelength of the disturbance will be large compared with the width of the shear layer and the disturbance motion will spread deeply into the uniform streams outside the shear layer. Under these conditions the individual mean velocity profiles will all appear the same and the amplification will be independent of the profile shape. However, at high wavenumbers the individual mean velocity profile greatly affects the stability characteristics of the shear layer. It can be seen that at a Reynolds number of 15 the maximum amplification factor is 55% of the maximum value at the high Reynolds number. It will be seen later that when corrections are made for the flow divergence then the amplification factors at low Reynolds numbers are reduced.

Curves of constant amplification factor are plotted in Figure 12. It can be seen from the figure that there exists no critical Reynolds number, that is no Reynolds number below which no amplification occurs. In his analysis of the instability of the shear layer with mean velocity profile given by equation (5.32), Esch (1957) showed that for small wavenumbers a form of the secular determinant equation (4.11) led to a series in $(\alpha R_\theta)^{\frac{1}{2}}$, for the neutral stability case. Equating the first non-vanishing term in the series to zero yielded the equation,

$$2i\delta\left[\delta + (\delta^2 - i)^{\frac{1}{2}}\right]\left[\delta + (\delta^2 + i)^{\frac{1}{2}}\right] + (\delta^2 - i)^{\frac{1}{2}} - (\delta^2 + i)^{\frac{1}{2}} = 0, \quad (5.50)$$

where $\delta = \alpha/(\alpha R_\theta)^{\frac{1}{2}}$. For positive real δ this equation has the single root,

$$\delta = .380.$$

The equation, $\alpha = .380 \, (\alpha R_\theta)^{\frac{1}{2}}$, $\qquad\qquad\qquad$ (5.51)

is plotted in Figure 13 and compared with our calculated neutral stability curve replotted as a function of (αR_θ). It can be seen that for values of $\alpha R_\theta < 1$ the agreement is good. This also serves to demonstrate that for low wavenumbers the velocity profile shape does not affect the overall stability of the shear layer. It is interesting to note that our calculations give no indication of a peak in the neutral stability curve about (αR_θ) 15 as was calculated by Esch. The monotonicity of the curve is later demonstrated again for the case of spatial amplification.

The wave speed $c_r = \omega_r / \alpha_r$ is plotted as a function of wave-number in Figure 14. It can be seen that for the case of an assymmetric velocity profile the wave speed is a function of wave number. For symmetric profiles it may be shown that the value of $c_r = \frac{1}{2}\{U(\infty) + U(-\infty)\} = U_s$. That is that for a symmetric profile $c_r = 0$. In this case $U(-y) = -U(y)$ and if we replace y by $-y$ in the Orr-Sommerfeld equation we obtain,

$$\hat{u}_2^{iv}(-y) - 2\alpha^2 \, \hat{u}_2{}''(-y) + \alpha^4 \, \hat{u}_2(-y)$$

$$= -i\alpha R\left[(U+c) \{\hat{u}_2(-y) - \alpha^2 \, \hat{u}_2(-y)\} - U'' \, \hat{u}_2(-y)\right] \quad (5.52)$$

Then if we put $\chi(y) = \hat{u}_2^*(-y)$, (see Tatsumi and Gotoh (1959)), where the star denotes the complex conjugate, then taking the complex conjugate of equation (5.52) leads to,

$$\chi^{iv} - 2\alpha^2 \, \chi'' + \alpha^4\chi = i\alpha R\{(U + c^*)(\chi'' - \alpha^2\chi) - U''\chi\}, \quad (5.53)$$

which equation in $\chi(y)$ is identical with the Orr-Sommerfeld equation for $\hat{u}_2(y)$ when $c = -c^*$. If for a given α and R there exists a unique solution then the eigensolutions χ and ϕ must be equal and $c = -c^*$, which leads to

$$c_r = 0. \tag{5.54}$$

From Figure 14 we may see that for low wavenumbers the value of c_r is approximately equal to the average velocity of the two streams, again showing the lack of influence of the profile shape at low wave numbers.

The eigensolutions $\hat{u}_2(y/\theta)$ and their first derivatives are plotted in Figures 15(a) and (b) and 15(c) and (d) for several wavenumbers and a value of $R_\theta = 500$. The functions have been normalised such that $\hat{u}_{2_r} = 1$ and $\hat{u}_{2_i} = 0$ when $(y/\theta) = 0$. It is interesting to note that the distributions are not symmetric about the x-axis in the temporal case. The derivative of the eigenfunction is related to the axial velocity disturbance through the transformed equation of continuity,

$$\hat{u}_1 = \frac{i\hat{u}_2{}'}{\alpha} \tag{5.55}$$

The amplitude distributions of axial and transverse velocity fluctuations are shown in Figures 16 and 17 respectively. The distributions have been normalised such that the value of $|\hat{u}_1|^2$ is unity for y/θ equal to zero. We can see that the axial velocity fluctuation distributions exhibit three distinct peaks. The magnitude of these peaks increases as the wavenumber increases. By comparing Figures 16 and 17 we can see that the relative magnitudes of the axial to the transverse fluctuations decrease as the wavenumber increases.

- 113 - A.

The relative phase and amplitude of the computed eigen-functions and derivatives for two wavenumbers are shown in Figures 18 and 19. For a wavenumber of 1.0 the two outside peaks which occur on the $|\hat{u}_1|^2$ distribution may be seen to be approximately π radians out of phase with each other. For the same wavenumber the central peak in the distribution is $\pi/2$ radians leading the peak at negative y/θ and $\pi/2$ radians lagging the peak at positive y/θ. As the wavenumber decreases so the phase difference between the three peaks increases.

We will now consider the results of the calculations for spatial amplification. Subsequently we will evaluate the corrections to the stability curves for divergent flow, then, where possible, compare the results of computations in both the temporal and spatial cases with other theory and experiment.

5.5.2. Eigenvalues and Eigenfunctions for the Spatial Case

Calculations made for the spatial case were performed at similar Reynolds numbers to those of the temporal case. For the reasons given in the previous section, the maximum value of Reynolds number chosen was 500. The eigenvalues were evaluated by integrating between values of y/θ of $+2$ and -2, with a step size of .005. The same limits of convergence were used as for the temporal case. The eigenvalues for various frequencies and Reynolds numbers are tabulated below.

Table IV Numerical Results of Calculations – Spatial Case

R_θ	ω	c_r	c_i	α_r	α_i
5.0	.25	4.059658	.468662	.060772	-.007016
5.0	.50	4.057460	.414033	.121960	-.012445
5.0	.75	4.055135	.362751	.183482	-.016413
5.0	1.00	4.053769	.312416	.245227	-.018899
5.0	1.25	4.053587	.262667	.807079	-.019898
5.0	1.50	4.054612	.213512	.368926	-.019427
5.0	1.75	4.056799	.165028	.430662	-.017519
5.0	2.00	4.060076	.117287	.492191	-.014218
5.0	2.25	4.064363	.070344	.553426	-.009578
5.0	2.50	4.069582	.024235	.614292	-.003658
5.0	2.75	4.075657	-.021022	.674720	.003480
10.0	.25	4.063003	.542055	.060454	-.008065
10.0	.50	4.059945	.516489	.121193	-.015418
10.0	.75	4.055824	.484400	.182319	-.021775
10.0	1.00	4.052309	.448453	.243787	-.026979
10.0	1.25	4.049801	.410550	.305520	-.030957
10.0	1.50	4.048382	.371126	.367431	-.033683
10.0	1.75	4.048026	.331424	.429431	-.035159
10.0	2.00	4.048665	.291658	.491440	-.035402
10.0	2.25	4.050216	.252093	.553382	-.034444
10.0	2.50	4.052601	.212900	.615190	-.032318
10.0	2.75	4.055743	.174189	.676802	-.029068
10.0	3.00	4.059576	.136027	.738165	-.024734

R_θ	ω	c_r	c_i	α_r	α_i
10.0	3.25	4.064043	.098454	.799227	-.019362
10.0	3.50	4.069093	.061492	.859946	-.012996
10.0	3.75	4.074684	.025147	.920282	-.005679
10.0	4.00	4.080779	-.010582	.980198	.002542
12.50	.75	4.056048	.519310	.181927	-.023293
12.50	1.50	4.047024	.412710	.366828	-.037409
12.50	2.25	4.047373	.297750	.552924	-.040677
12.50	3.00	4.055179	.185103	.738257	-.033699
15.0	.25	4.064982	.584232	.060256	-.008660
15.0	.50	4.061245	.571603	.120724	-.016991
15.0	.75	4.056151	.546030	.181607	-.024470
15.0	1.00	4.051677	.515140	.242885	-.030881
15.0	1.25	4.048266	.480384	.304487	-.036132
15.0	1.50	4.045994	.443854	.366328	-.040187
15.0	1.75	4.044815	.406472	.428327	-.043044
15.0	2.00	4.044645	.368801	.490404	-.044716
15.0	2.25	4.045386	.331190	.552486	-.045231
15.0	2.50	4.046950	.293861	.614509	-.044621
15.0	2.75	4.049252	.256952	.676414	-.042923
15.0	3.00	4.059920	.149433	.860920	-.031688
15.0	3.75	4.064553	.114756	.921876	-.026028
20.0	.75	4.056111	.587137	.181111	-.026217
20.0	1.50	4.044434	.488145	.365555	-.044121
20.0	2.25	4.042706	.377540	.551746	-.051526

R_θ	ω	c_r	c_i	α_r	α_i
20.0	3.00	4.048436	.268907	.737772	-.049004
20.0	3.75	4.059543	.165211	.922222	-.037532
20.0	5.00	4.086860	.004075	1.223432	-.001220
500.0	0.10	4.068019	.881803	.023478	-.005089
500.0	0.15	4.067089	.894179	.035181	-.007735
500.0	0.25	4.062960	.895915	.058678	-.012939
500.0	0.50	4.053139	.865303	.117984	-.025188
500.0	0.75	4.045608	.823418	.178012	-.036231
500.0	1.50	4.033164	.692261	.361273	-.062010
500.0	2.25	4.031221	.569186	.547234	-.077266
500.0	3.00	4.035964	.456336	.733934	-.082984
500.0	3.75	4.045310	.352752	.920004	-.080225
500.0	5.00	4.067968	.196176	1.226263	-.059136
500.0	5.25	4.073400	.166850	1.286691	-.052704
500.0	5.50	4.079111	.138093	1.346790	-.045594
500.0	5.75	4.085103	.109884	1.406536	-.037834
500.0	6.00	4.091371	.082173	1.465910	-.029442
500.0	6.25	4.097918	.054944	1.524891	-.020445
500.0	6.50	4.104746	.028175	1.583458	-.010869
500.0	6.75	4.111857	.001846	1.641594	-.000737

The spatial amplification factor, $-\alpha_i$, is plotted against frequency for several Reynolds numbers in Figure 20. Also shown in the figure is the amplification curve for the temporal case simply transformed for comparison with the spatial case.

The spatial amplification factor, $-\alpha_i$, and the temporal factor $-\alpha c_i/c_r$ may be seen to coincide very closely. This, as we will discuss later, is unlike the results of Michalke (1965) whose calculations produced only broadly similar curves for the case of an anti-symmetric mean velocity profile and one free stream at rest. Curves of constant amplification factor are shown in Figure 21 as a function of wavenumber and Reynolds number. As may be seen from an inspection of the eigenvalue problem in both the temporal and spatial cases, the neutral stability curve is the same in both. In the neutral case the wavenumber, frequency and eigenvalue are all real. Also shown in the figure is the curve

$$\alpha = \frac{1}{4\sqrt{3}} R_\theta \quad , \tag{5.56}$$

which is the neutral stability curve at low wavenumbers derived in this form by Tatsumi and Gotoh (1960) being equivalent to equation (5.51).

The wave speed ω_r/α_r is plotted in Figure 22 as a function of frequency for several Reynolds numbers. Also shown for the high Reynolds number case is the corresponding wave speed curve for the temporal amplification case. The noticeable difference between the two cases is the rise in the magnitude of the wave speed in the spatial case at low frequencies. However, it is to be noticed that there exists a maximum value of wave speed of 4.2633. In fact the wave speed in the spatial case varies between 50 and 60 percent. of velocity difference above the velocity of the lower velocity free stream. In his calculations

for the separated shear layer, i.e. $U_2 = 0$, Michalke (1965), using inviscid theory, calculated that at zero frequency the wave speed equalled the velocity of the free stream U_1.

The eigenfunctions and their derivatives are shown in Figures 23(a) and (b) and 23(c) and (d) respectively. As in the temporal case the eigenfunctions have been normalised such that $\hat{u}_{2_r} = 1$ and $\hat{u}_{2_i} = 0$ when $y/\theta = 0$. It is interesting to note the close correspondence between the eigenfunctions in the temporal and spatial cases at approximately corresponding wavenumber and frequencies. This may also be seen in the amplitude distributions of axial and transverse velocity fluctuations shown in Figures 24 and 25 respectively. The relative phase of the $\hat{u}_1$ fluctuation is shown in Figure 26 for several frequencies. It can be seen that the overall phase difference across the layer is less for the higher frequencies than the lower. Also the major phase change, which occurs towards the centre of the mixing layer, takes place over a narrower region for the higher frequency fluctuations than for the lower frequency disturbances. Also shown in the figure is the calculated phase distribution of Freymuth (1966) and Michalke (1965) for the case of $U_2 = 0$ and inviscid flow. In their calculations of the spatial case they found a sharp phase reversal corresponding to the sharp minimum in the $\hat{u}_1$ magnitude distribution. This they also observed experimentally and the reversal occurred at all frequencies. In our calculations of the spatial case we have found no phase reversal.

It may be argued that the case of a mixing layer with one stream at rest is the special case in the general problem of the mixing of two streams with finite velocity. Only when both streams have finite velocity can the assumption that the disturbances are much smaller than the mean quantities be applied everywhere in the flow. Thus one must question the validity of linearised theory in the special case. However, the calculations and observations of Freymuth do coincide. We may argue that by posing the eigenvalue problem as in equation (5.6) the results for spatial and temporal calculations will coincide as U_2 tends to equal U_1. We may see this if we consider the imaginary part of the frequency which, for spatial amplification, is to be zero. The imaginary part of the frequency is

$$\omega_i = \alpha_i c_r + \alpha_r c_i$$

Making use of equation (5.6a) we may write this as,

$$\omega_i = \alpha_i \frac{U_s}{U_d} + \alpha_i c_r^* + \alpha_r c_i^* \tag{5.57}$$

For spatial amplification $\omega_i = 0$, α_i is negative and c_i^* is positive. Thus for positive real part of wavenumber we have,

$$\alpha_i = -(\alpha_r c_i^* + \alpha_i c_r^*) \cdot \frac{U_d}{U_s}$$

Now for antisymmetric or nearly antisymmetric mean velocity profiles the value of c_r^* is either identically zero or close to zero respectively. Thus we obtain

$$\alpha_i = -\alpha_r c_i^* \frac{U_d}{U_s} \tag{5.58}$$

Assuming, as the calculations indicate, the values of α_r and c_i^* remain finite as U_2 tends to U_1 then towards the limit as U_2 tends to U_1, α_i tends to zero. That is the spatial and temporal cases tend to coincide. Thus one would expect that the results for the spatial case will change from those for the spatial case of $U_2 = 0$, calculated by Michalke, to those of the temporal case as U_2 tends to U_1. As of yet there exists no experimental verification of this as all experiments on the transition of a free shear layer have dealt with the case of $U_2 = 0$.

Experimental results have indicated that the mode which dominates the flow in the region of validity of the linearised theory corresponds to the mode at the frequency at which maximum amplification occurs. From the results of Michalke (1965) and Sato (1956, 1959) for the case of one stream at rest, it may be inferred that the spatial amplification case is to be considered. The distributions of the magnitude of the axial and transverse velocity fluctuations are shown in Figures 27 and 28 respectively for cases of both temporal and spatial amplification. The results have been normalised such that $|\hat{u}_1|^2$ is unity when y/θ is zero. It can be seen that the differences between the two cases of amplification are slight. The maximum amplitude of the axial velocity fluctuation is larger in the spatial case, though the maximum amplitude of the transverse velocity fluctuation is greater in the temporal case. We may also note that the minimum in the $|\hat{u}_1|^2$ distribution occurring towards the lower velocity stream has a lower value in the spatial than in the temporal case. This may suggest that, as

we have argued above, this minimum will continue to decrease as the value of U_2 decreases until, when $U_2 = 0$, a phase reversal will be evident. The two outside peaks in the $|\hat{u}_1|^2$ distribution occur at the very edges of the mixing layer as may be seen from the mean velocity profile plotted in Figure U. The peaks occur at 8.5 percent. and 99.5 percent. of the velocity difference. This corresponds to the results of Freymuth who also noted that the outside peaks move inward as the frequency increased. The maximum value of the $|\hat{u}_1|^2$ fluctuation is approximately twice the maximum value of the $|\hat{u}_2|^2$ fluctuation in both cases.

From equations (5.7) and (5.8) we may see that for high Reynolds numbers the eigenfunction will behave as $u_2 \propto e^{\pm \alpha y}$ as the mean velocity approaches that of either stream. The sign of the exponent is chosen such that the function is bounded. From equation (5.55) we may then write

$$\hat{u}_1 = i\,\hat{u}_2$$

i.e. $\qquad |\hat{u}_1|^2 = |\hat{u}_2|^2 .$ $\hspace{3cm}$ (5.59)

This result holds in our calculations for $y/\theta > 1.3$ and $y/\theta < 1.3$. The values of $f'(y/\theta)$ at these values of y/θ are +1.0 and −0.9 respectively.

5.5.3. Corrections for Non-Parallel Flow

The eigenvalues obtained for the parallel flow case are modified for the non-parallel flow case according to equation (5.43) and the modified curves of constant amplification factor for the spatial case are plotted in Figure 29. As may be seen

from equation (5.43) the correction is a function of the Reynolds
number and decreases as the Reynolds number increases. It may be
seen that the modification for non-parallel flow has led to a
non-zero value for the critical Reynolds number. This value is
12.3 and agrees with the value of R_{CRIT} of 12 calculated by Lessen
and Ko (1966) for the half-jet flow. We have seen from the
comparison of the spatial amplification factors and the temporal
amplification factors divided by the wave speed that the argument
leading to equation (5.49) may be tentatively applied in these
calculations. Making use of equation (5.49) the curves of constant
amplification, modified for non-parallel flow in the temporal case,
are plotted in Figure 29. As in the spatial case a non-zero value
of critical Reynolds number of 12.3 is obtained. This is to be
expected due to the coincidence of the neutral curves in the
parallel flow case and the correspondance of the spatial and
temporal amplification factors.

5.6 Conclusions

In this chapter we have examined the stability of a mixing
layer between two parallel streams. We have seen that for the
case of both free streams having finite velocity the corresponding
eigenvalues and eigenfunctions for both temporal and spatial
amplification are similar. When the two streams tend to have
equal velocity then the temporal and spatial cases tend to
coincide. We have noted that viewed in this way the problem of
U_2 being zero is a special case of the general mixing problem
and its results do not apply when U_2 is non-zero. Making use

of a non-parallel flow correction based on the energy of the
interaction between the disturbances and the flow a critical
Reynolds number of 12.3 has been calculated.

In the next chapter we will consider the fully turbulent
mixing problem. It will be seen that equations of the type used
in this chapter to determine the stability of a laminar flow
may also occur in the turbulent case.

CHAPTER 6

A Model of the Turbulent Mixing Layer Between Two Streams

In this chapter we will propose a model for the structure of a turbulent mixing layer between two streams. Although the mathematical analysis is similar to that in our previous discussion of the stability of the mixing layer, this analysis will be duplicated in part in order that the two problems may be considered entirely separately.

Firstly we will state the physical structure of the model to be used. In our subsequent mathematical derivation the points will be reiterated where they enter the mathematical model. It is considered that the large scale eddies in the shear flow will dominate the flow structure. These large scale motions are related to the most amplifying disturbances in the flow. The action between the large eddies and the mean flow causes further growth of this scale of motion. The interaction between the large scale motion is then considered to produce smaller scales which contribute to a background turbulence. This background motion may be connected with a turbulent eddy viscosity, which may or may not take the same value as the eddy viscosity used in mean flow analysis. The effect of the eddy viscosity is to reduce the effective Reynolds number of the flow which has a stabilising or amplitude limiting effect on the large scale motions. Thus we see the model is closed and demonstrates the dual rôle of non-linearity in turbulence. Primarily the action between mean flow and large scale motions has a forcing

function effect on the turbulence. Secondly the interaction between eddies leads to a background turbulence which reduces the effective Reynolds number and limits the amplitude of the disturbances.

Let us now derive the governing differential equations for the problem.

6.1 Governing Differential Equations

Let us consider the mixing of two parallel streams of velocity U_1 and U_2 above and below the mixing layer. Let the x_1-co-ordinate lie in the initial direction of flow of the two streams and the x_2-co-ordinate be across the mixing layer. We will assume that the mixing begins at the origin and that the mean flow is two-dimensional. As the analysis associated with the derivation of our final equations is very complicated it is thought to be useful to introduce two assumptions at this stage.

We will firstly assume that the mean flow is parallel. In our discussion of the stability of the mixing layer we have seen that the growth and form of fluctuations in a non-parallel flow are very similar to that in a parallel flow except at low Reynolds numbers. In the case of a turbulent mixing layer the Reynolds number of the flow is high enough such that the assumption of parallel mean flow will not affect our predictions of the turbulent structure. We will also assume that the disturbances in the flow are two-dimensional. Though it is recognised that the fluctuations in the flow are three-dimensional it will be assumed that the dominating motions are in two dimensions.

We have seen that in the problem of stability in a mixing layer the dominating disturbances are two-dimensional, that is the more oblique the wave is the less fast will it grow. We will see in our discussion of the turbulent flow case that similar differential equations govern the fluctuations in a turbulent flow and in a laminar flow on the point of transition. Michalke (1969) has shown numerically that this dominance of the two dimensional mode applies whether fluctuations are considered as having growth or decay with time or space. This assumption of two-dimensionality could be introduced subsequent to our derivation of the equations rather than here, but the increased complexity of the analysis is not considered to justify this exactness.

With the assumption of two dimensional disturbances, i.e. $u_3 = 0$ and $\frac{\partial}{\partial x_3} = 0$, and the assumption of parallel flow, we may write down the two-dimensional vorticity equation in the form,

$$\{\frac{\partial}{\partial t} + U \frac{\partial}{\partial x_1} - \nu \nabla^2\} \omega_3 + u_2 \Omega_3{'} = - \frac{\partial}{\partial x_i} (u_i \omega_3 - \overline{u_i \omega_3}), \quad (6.1)$$

where we have introduced the fluctuating component of vorticity

$$\omega_3 = \frac{\partial u_2}{\partial x_1} - \frac{\partial u_1}{\partial x_2} \quad , \quad (6.2)$$

and the mean vorticity vector Ω_3. For two dimensional parallel mean flow we have $\Omega_1 = \Omega_2 = 0$, and for two dimensional disturbances we have $\omega_1 = \omega_2 = 0$.

Let us introduce a fluctuating stream function ψ defined by,

$$u_1 = \frac{\partial \psi}{\partial x_2} \qquad \text{and} \qquad u_2 = - \frac{\partial \psi}{\partial x_1} \qquad\qquad (6.3)$$

Then the fluctuating component of vorticity ω_3 is given by,

$$\omega_3 = -\nabla^2 \psi. \qquad\qquad (6.4)$$

For two dimensional parallel mean flow the mean vorticity vector Ω_3 is given by

$$\Omega_3 = -U' \qquad\qquad (6.5)$$

Equation (6.1) written in terms of the fluctuating stream function is then,

$$\left(\frac{\partial}{\partial t} + \frac{U \partial}{\partial x_1} - \nu\nabla^2\right) \nabla^2 \psi - U'' \, \frac{\partial \psi}{\partial x_1} = - \frac{\partial}{\partial x_1} \left(\nabla^2 \psi \, \frac{\partial \psi}{\partial x_2} - \overline{\nabla^2 \psi \, \frac{\partial \psi}{\partial x_2}}\right)$$
$$+ \frac{\partial}{\partial x_2} \left(\nabla^2 \psi \, \frac{\partial \psi}{\partial x_1} - \overline{\nabla^2 \psi \, \frac{\partial \psi}{\partial x_1}}\right) \qquad (6.6)$$

Equation (6.6) is a fourth order partial differential equation for the fluctuating stream function ψ. The boundary conditions on the velocity fluctuations are

$$u_1 = u_2 = 0 \text{ when } u_2 \to \mp\infty \qquad\qquad (6.7)$$

The boundary conditions on the stream function may be more clearly defined later, however, making use of equations (6.3) we have,

$$\frac{\partial \psi}{\partial x_2} = 0 \quad \text{as } x_2 \to \pm\infty \qquad)$$
$$\qquad\qquad\qquad\qquad\qquad\qquad)$$
$$\qquad\qquad\qquad\qquad\qquad\qquad) \qquad (6.8)$$
$$\text{and} \qquad \psi = \psi(x_2) \quad \text{as } x_2 \to \pm\infty \qquad)$$

Let us introduce the Fourier transform of the fluctuating stream function of the form,

$$\hat{\psi}(x_2; k_1, \omega) = \frac{1}{(2\pi)^2} \int_{-\infty}^{\infty} \int_{-\infty}^{\infty} e^{-i(k_1 x_1 - \omega t)} \psi(x_2, x_1, t) \, dx_1 dt \quad (6.9)$$

where $\hat{\psi}$ is the Fourier transform of ψ, k_1 is the wave number in the x_1-direction and ω is the frequency. In order to assure that the above integral exists we will assume that the fluctuating vorticity, ω_3, is zero outside a region defined by $x_1 = \pm X_1$ and $t = \pm T$. Then $\psi = 0$ outside this region.

The Fourier transform of equation (6.6) is

$$(U - c)(\hat{\psi}'' - k_1^2 \hat{\psi}) - U'' \hat{\psi} - \frac{\nu}{ik_1} \left[\hat{\psi}^{iv} - 2k_1^2 \hat{\psi}'' + k_1^4 \hat{\psi}\right]$$

$$= -\frac{1}{k_1} \int_{-\infty}^{\infty} \int_{-\infty}^{\infty} \kappa_1 (\hat{\psi}'' - \kappa_1^2 \hat{\psi}) \, \hat{\psi}(k_1 - \kappa_1, \omega - w) \, d\kappa_1 dw$$

$$- \frac{1}{k_1} \int_{-\infty}^{\infty} \overline{\kappa_1 (\hat{\psi}'' - \kappa_1^2 \hat{\psi}) \, \hat{\psi}'(k_1 - \kappa_1, \omega - w)} \cdot \delta(\omega - w) d\kappa_1$$

$$+ \frac{1}{k_1} \int_{-\infty}^{\infty} \int_{-\infty}^{\infty} (k_1 - \kappa_1)(\hat{\psi}''' - \kappa_1^2 \hat{\psi}') \hat{\psi}(k_1 - \kappa_1, \omega - w) d\kappa_1 dw$$

$$+ \frac{1}{k_1} \int_{-\infty}^{\infty} (k_1 - \kappa_1)(\hat{\psi}''' - \kappa_1^2 \hat{\psi}') \hat{\psi}(k_1 - \kappa_1, \omega - w) \, \delta(\omega - w) \, d\kappa_1$$

Following Sharma (1968) we then obtain,

$$(U - c)(\hat{\psi}'' - k_1 \hat{\psi}) - U'' \hat{\psi} - \frac{\nu}{ik_1} \left[\hat{\psi}^{iv} - 2k_1^2 \hat{\psi}'' + k_1^4 \hat{\psi}\right]$$

$$= \frac{1}{k_1} \int_{-\infty}^{\infty} \int_{-\infty}^{\infty} [\hat{\psi}'''(k_1 - \kappa_1, \omega - w)\, \kappa_1 \hat{\psi}(\kappa_1, w) -$$

$$\kappa_1 \hat{\psi}(\kappa_1, w)\, \hat{\psi}'(k_1 - \kappa_1, \omega - w)] \, d\kappa_1 dw$$

$$+ \frac{1}{k_1} \int_{-\infty}^{\infty} \overline{[\hat{\psi}'''(k_1 - \kappa, \omega - w)\, \kappa_1 \hat{\psi}(\kappa_1, w) -}$$

$$\overline{\kappa_1 \hat{\psi}''(\kappa, w)\, \hat{\psi}(k_1 - \kappa_1, \omega - w)]} \; \delta(\omega - w) \, d\kappa_1$$

$$= \int_{-\infty}^{\infty} \int_{-\infty}^{\infty} \hat{\psi}'''(\kappa_1, w)\, \hat{\psi}(k_1 - \kappa_1, \omega - w) \, d\kappa_1 dw$$

$$+ \int_{-\infty}^{\infty} \overline{\hat{\psi}'''(\kappa_1, w)\, \hat{\psi}(k_1 - \kappa_1, \omega - w)} \; \delta(\omega - w) \, d\kappa_1$$

$$- \frac{1}{k_1} \int_{-\infty}^{\infty} \int_{-\infty}^{\infty} \kappa_1 \frac{d}{dx_2} \hat{\psi}''(\kappa_1, w)\, \hat{\psi}(k_1 - \kappa_1, \omega - w) \, d\kappa_1 dw -$$

$$\frac{1}{k_1} \int_{-\infty}^{\infty} \overline{\kappa_1 \frac{d}{dx_2} \hat{\psi}''(\kappa_1, w)\, \hat{\psi}(k_1 - \kappa_1, \omega - w)} \; \delta(\omega - w) \, d\kappa_1$$

$$= - \frac{1}{k_1} \int_{-\infty}^{\infty} \int_{-\infty}^{\infty} (k_1 - \kappa_1)(\hat{\psi}''(k_1 - \kappa_1, \omega - w) - (k_1 - \kappa_1)^2$$

$$\hat{\psi}(k_1 - \kappa_1, \omega - w))\, \hat{\psi}'(\kappa_1, w) \, d\kappa_1 dw$$

$$- \frac{1}{k_1} \int_{-\infty}^{\infty} \overline{(k_1 - \kappa_1)(\hat{\psi}''(k_1 - \kappa_1, \omega - w) - (k_1 - \kappa_1)^2}$$

$$\overline{\hat{\psi}(k_1 - \kappa_1, \omega - w))\, \hat{\psi}'(\kappa_1, w)} \; \delta(\omega - w) \, d\kappa_1$$

$$+ \frac{1}{k_1} \int_{-\infty}^{\infty} \int_{-\infty}^{\infty} \kappa_1 \left(\hat{\psi}^{\prime\prime\prime}(k_1 - \kappa_1, \omega - w) - (k_1 - \kappa_1)^2 \hat{\psi}^{\prime}(k_1 - \kappa_1, \right.$$

$$\left. \omega - w) \right) \hat{\psi}(\kappa_1, w) \, d\kappa_1 dw$$

$$+ \frac{1}{k_1} \int_{-\infty}^{\infty} \overline{\kappa_1 \left(\hat{\psi}^{\prime\prime\prime}(k_1 - \kappa_1, \omega - w) - (k_1 - \kappa_1)^2 \hat{\psi}^{\prime}(k_1 - \kappa_1, \omega - w) \right)}$$

$$\overline{\hat{\psi}(\kappa_1, w)} \, \delta(\omega - w) \, d\kappa_1$$

$$= - \int_{-\infty}^{\infty} \int_{-\infty}^{\infty} \hat{\psi}^{\prime}(\kappa_1, w) \left(\hat{\psi}^{\prime\prime}(k_1 - \kappa_1, \omega - w) - (k_1 - \kappa_1)^2 \hat{\psi}(k_1 - \kappa_1 \right.$$

$$\left. \omega - w) \right) \, d\kappa_1 dw$$

$$+ \frac{1}{k_1} \int_{-\infty}^{\infty} \int_{-\infty}^{\infty} \kappa_1 \hat{\psi}(\kappa_1, w) \left(\hat{\psi}^{\prime\prime}(k_1 - \kappa_1, \omega - w) - (k_1 - \kappa_1)^2 \right.$$

$$\left. \hat{\psi}(k_1 - \kappa_1, \omega - w) \right) \, d\kappa_1 dw$$

$$+ \frac{1}{k_1} \int_{-\infty}^{\infty} \int_{-\infty}^{\infty} \kappa_1 \hat{\psi}(\kappa_1, w) \left(\hat{\psi}^{\prime\prime}(k_1 - \kappa_1, \omega - w) - (k_1 - \kappa_1)^2 \right.$$

$$\left. \hat{\psi}^{\prime}(k_1 - \kappa_1, \omega - w) \right) \, d\kappa_1 dw$$

$$+ (\overline{})$$

where $(\overline{})$ denotes the time average of the preceding terms. The delta functions arise in the time averaged integrals as these then lead to the Fourier transforms of constants.

Let us consider the right hand side of equation (6.10). The integrand of the first integral is the product of the u_1-fluctuation and the vorticity fluctuation. The integrand of the second integral corresponds to the product of the vorticity fluctuation and the derivative with respect to x_1 of the u_1-fluctuation. The final integrand represents the product of the gradient of the vorticity fluctuation and the u_2-fluctuation. We also notice that if the right hand side of equation (6.10) is set equal to zero the homogeneous equation is the well known Orr-Sommerfeld equation we have previously derived in our consideration of the stability of the mixing layer.

The solution of equation (6.10) in the form written is a formidable task, the difficulty lying in the presence of the non-linear terms on the right-hand side. We will discuss the various previous treatments of the non-linear problem when we introduce the problem of finite amplitude disturbances in the next chapter. However, we will introduce a number of those ideas here as an explanation in part of our method of solution for the free shear layer.

A method of solution involving a perturbation of the mean profile was used by Sharma (1968) in his work on the boundary layer. If we assume that the vorticity fluctuations in equation (6.10) may be taken out from the integrals then the velocity fluctuations and derivatives alone remain in the integrands. Then the integrals may be evaluated and combined with the terms on the left hand side of equation (6.10). This can be shown

to be equivalent to perturbing the mean velocity profile. Let us return to our two-dimensional model. The vorticity equation is,

$$\left(\frac{\partial}{\partial t} + U\frac{\partial}{\partial x_1} - \nu\nabla^2\right)\omega_3 - u_2\frac{\partial^2 U}{\partial x_2^2} = -\frac{\partial}{\partial x_i}\left(u_i\omega_3 - \overline{u_i\omega_3}\right)$$

$$= -\left(u_1\frac{\partial\omega_3}{\partial x_1} + u_2\frac{\partial\omega_3}{\partial x_2}\right) + \overline{\left(u_1\frac{\partial\omega_3}{\partial x_1} + u_2\frac{\partial\omega_3}{\partial x_2}\right)} \tag{6.11}$$

We may rewrite this equation as,

$$\left(\frac{\partial}{\partial t} + (U + u_1)\frac{\partial}{\partial x_1} - \nu\nabla^2\right)\omega_3 - u_2\left(\frac{\partial^2 U}{\partial x_2^2} - \frac{\partial\omega_3}{\partial x_2}\right)$$

$$= \overline{\left(u_1\frac{\partial\omega_3}{\partial x_1} + u_2\frac{\partial\omega_3}{\partial x_2}\right)} \tag{6.12}$$

Writing this equation in terms of the stream function we have,

$$\left(\frac{\partial}{\partial t} + (U + u_1)\frac{\partial}{\partial x_1} - \nu\nabla^2\right)\nabla^2\psi - \frac{\partial\psi}{\partial x_1}\left(\frac{\partial^2 U}{\partial x_2^2} + \frac{\partial^2 u_1}{\partial x_2^2} - \frac{\partial^2 u_2}{\partial x_1\partial x_2}\right)$$

$$= -\left(\frac{\partial u_1\omega_3}{\partial x_1} + \frac{\partial u_2\omega_3}{\partial x_2}\right) \tag{6.13}$$

The right hand side of equation (6.13) represents the time-averaged convection of vorticity by the turbulent fluctuations. The relative magnitudes of these time averaged terms may be judged by assuming that the vorticity is a transferable quantity and may be expressed as,

$$\overline{u_2\omega_3} = -\overline{\left(u_2^2\right)}^{\frac{1}{2}} L_2\frac{d^2 U}{dx_2^2} \quad,$$

- 132 -

$$\overline{u_1 \omega_3} = - \left(\overline{u_1^2}\right)^{\frac{1}{2}} L_1 \frac{d^2 U}{dx_2^2}$$

where L_1 and L_2 are length scales. The values of $\left(\overline{u_2^2}\right)^{\frac{1}{2}}$ may be considered small at the points of maximum $\frac{d^2 U}{dx_2^2}$ and the gradient of $\overline{u_2 \omega_3}$ may be considered much smaller than the gradient of $u_2 \omega_3$. The variation of $\left(\overline{u_1^2}\right)^{\frac{1}{2}}$ with x_1 is small for parallel or nearly parallel flows and the variation of $\overline{u_1 \omega_3}$ with x_1 can be neglected in comparison with the gradient of $u_1 \omega_3$. Thus we may neglect the terms on the right hand side of equation (6.13) in comparison to the terms representing the convection of vorticity by the turbulence on the left hand side. The remaining homogeneous equation is still too complicated for useful solution. Sharma solved the homogeneous equation by assuming that the solution to the linear problem, that is the problem neglecting all non-linear terms, was the first approximation to the general solution. He was then able to modify the mean profile to obtain the next approximation. If we write

$$\tilde{U} = U + u_1,$$

where u_1 is the solution of the linear homogeneous equation then the second approximation is a solution of the equation,

$$\left(\frac{\partial}{\partial t} + \tilde{U} \frac{\partial}{\partial x_1} - \nu \nabla^2\right) \nabla^2 \psi - \frac{\partial \psi}{\partial x_1} \left(\frac{\partial^2 \tilde{U}}{\partial x_2^2}\right) = 0. \qquad (6.14)$$

The results obtained by Sharma for the first iteration of the modified mean profile led to enhanced amplification. He showed that a perturbation in the mean profile excited large

- 133 -

scale motions in the boundary layer. In the boundary layer case, however, the disturbances are either stable, neutral or only very slightly amplified. The inclusion of the perturbation on the mean profile leads clearly to an inflexional instability on the outer part of the boundary layer. This inflexional instability leads to much higher values of amplification. Thus we see that considered in this way the non-linear terms have acted as a destabilising influence. However, we must consider that the non-linear terms have a stabilising effect as well for it is known that there is a limiting value to the turbulence intensity. Let us consider that the background turbulence may be associated with an eddy viscosity term. We must be clear here that this eddy viscosity 'may' or may not take the same value as that used in our mean flow analysis (Chapter 3). The eddy viscosity used there was contributed to by the large scale turbulent motions. We are here dealing with a turbulent eddy viscosity associated with the small scale background turbulence. We may write the eddy viscosity such that,

$$T_i = - \frac{\partial}{\partial x_j} \nu_T \left(\frac{\partial u_i}{\partial x_j} + \frac{\partial u_j}{\partial x_i} \right) , \qquad (6.15)$$

where T_i is the Reynolds stress function defined by,

$$T_i = \frac{\partial}{\partial x_j} (\overline{u_i u_j} - u_i u_j) \qquad (6.16)$$

Then the new form of the transformed equation (6.10) is

$$(U-c)(\hat{\psi}'' - k^2 \hat{\psi}) - U'' \hat{\psi}$$

$$= - \frac{i}{k} \left(\frac{1}{R} + \frac{1}{R_T} \right)(\hat{\psi}^{iv} - 2k^2 \hat{\psi}'' + k^4 \hat{\psi}) - \frac{2}{k} i (\hat{\psi}''' - k^2 \hat{\psi}') \cdot \frac{d\nu_T}{dx_2}$$

$$- \frac{i}{k} \cdot (\hat{\psi}'' - k^2\hat{\psi}) \, \frac{d^2\nu_T}{dx_2^2} \qquad \left. \begin{matrix}) \\ ) \end{matrix} \right.$$

We have seen from our calculations for the mean velocity profile
that the assumption of a constant eddy viscosity distribution
does lead to a representation not unlike the measured values.
Thus we may ascribe a constant value to ν_T to obtain a repre-
sentation of the effect of its introduction on the equation's
solution. With ν_T constant the equation (6.17) leads to the
homogeneous Orr-Sommerfeld equation with the kinematic viscosity
enhanced by an eddy viscosity. This leads to a net effect of
a reduction in the effective Reynolds number. As we have seen
from our calculation of the stability of a mixing layer a
reduction in Reynolds number has the effect of stabilising the
flow. Though we have performed no calculations using an eddy
viscosity it does not seem unreasonable to tentatively suggest
the dual role of the turbulence in the flow. We have seen from
equation (6.14) that a perturbation in the instantaneous velocity
profile has a destabilising effect whereas as the turbulence
level increases the formation of an eddy viscosity has a
stabilising or amplitude limiting effect.

We have noticed however that the role of the turbulence
in enhancing the growth of disturbances, by modifying the mean
velocity profile, was chiefly successful in Sharma's work,
for the case of the boundary layer, owing to the introduction
of an inflection point in the mean profile. The boundary
layer does not have an inflexion point in the mean profile,

except for special cases such as at the separation point. Thus it is clear that in this case modification of the mean profile will have a dominating effect on the growth of disturbances. However, we must question whether the effect would be as great if the same formulation of the problem were used in the case of the mixing layer between two streams. In this case there already exists a strong inflexional instability in the mean velocity profile which leads to strong amplification of disturbances. Thus we may argue that the former role of the turbulence expressed above as a destabilising influence will not be best considered by perturbing the mean velocity profile. That is to say that for the case of the mixing layer the first approximation, the linear solution, to the non-linear equation (6.14) will not be modified greatly by a perturbation of the mean velocity profile. In view of this a different formulation of the non-linear problem for the case of the mixing layer has been used and this is presented in the next chapter. However we must expect that our first linear approximation will adequately represent the fluctuations in the turbulent mixing layer.

From the preceding discussion it would appear that the solutions to the homogeneous linear equation plays an important role in the description of fluctuations in the turbulent mixing layer. Eckhaus (1965) expanded the solution to the non-linear problem in terms of solutions to the linearised equation. If the solution to the non-linear problem is given by $\Phi'(x_i, t)$ then at any instant of time it may be represented

by the series expansion

$$\Psi'(x_i,t) = \sum_{m=0}^{\infty} A_m(t)\,\Psi_m(x_i) \qquad (6.18)$$

where $\Psi_m(x_i)$ are the solutions of the linearised problem and $A_m(t)$ are 'amplitude functions' which may be determined from the relation,

$$A_m = \frac{1}{(c - c_m)} \int_{-\infty}^{\infty} f(x_2)\,\overset{\vee}{\Psi}_m(x_2)\,dx_2 \qquad (6.19)$$

where c_m represents the complex eigenvalues for given values of k_1 and R in the solution of the linearised homogeneous equation (6.10), $f(x_2)$ represents the non-linear right hand side of this equation and $\overset{\vee}{\Psi}_m(x_2)$ are the corresponding eigenfunctions of the adjoint problem given by,

$$(U-c)(\overset{\vee}{\psi}'' - k_1^2\overset{\wedge}{\psi}) + 2U'\overset{\vee}{\psi}' + \frac{i\nu}{k_1}(\overset{\vee}{\psi}{}^{iv} - 2k_1^2\overset{\vee}{\psi}'' + k_1^4\overset{\vee}{\psi}) = 0 \;)$$

$$\text{with}\quad \overset{\vee}{\psi}(+\infty) = \overset{\vee}{\psi}(-\infty) = \overset{\vee}{\psi}'(+\infty) = \overset{\vee}{\psi}'(-\infty) = 0 \qquad \Bigg)\;(6.20)$$

In equation (6.19) the adjoint eigenfunction and non-linear terms are functions of x_2 only. In the preceding analysis we have introduced the concept that for given values of k_1 and R there exists no unique eigenvalue c. In stability theory we seek the lowest eigenvalue of the sequence. Eckhaus, interpreting the results of Corcos and Sellars (1959), stated that 'in the first asymptotic approximation for R → ∞ the number of eigenvalues is found to be finite for every fixed value of R

- 137 -

and increasing without limit as $R \to \infty$.' In chapter 4 we dis-
cussed methods of solution of the Orr-Sommerfeld equation
which involved variational techniques. It is clear that in
this case the solution of the matrix problem will give rise
to a sequence of eigenvalues. Thus numerically we may evaluate
the eigenvalue sequences.

In our approach to the solution of this problem we will
make use of the first term in the eigenfunction analysis, that
is the solution involving the lowest eigenvalue. A similar
approach has been used by Landahl (1967) in his wave-guide model
for the turbulent boundary layer. In his formulation he sought
the lowest eigenvalue to the Orr-Sommerfeld problem. However
it is thought probable that his failure to find any amplifying
modes to the boundary layer problem was due to the inaccuracies
in his purification scheme for the numerical solution at high
Reynolds numbers. Landahl considered that the cross-spectral
density of the pressure fluctuations will be dominated by
lightly damped waves. This can be seen as these waves will
correlate over a larger distance. However in the case of the
free shear layer there exists strong amplification and it
does not seem reasonable to describe the structure of the
flow in terms of lightly damped or neutral disturbances.

We have already seen in our discussion of the stability
of free shear layers that the most amplifying mode dominates
the local flow structure. This is clearly seen in the work
of Michalke (1965). Thus we propose to describe the structure
of the turbulent flow in terms of the most amplifying eigen-

function solution of the homogeneous equation,

$$(U-c)(\hat{\psi}'' - k_1^2\hat{\psi}) - U''\hat{\psi} + \frac{i\nu}{k_1}(\hat{\psi}^{iv} - 2k_1^2\hat{\psi}'' + k_1^4\hat{\psi}) = 0 \qquad (6.21)$$

In the light of the correspondence between theory and measurements in stability work on the free mixing layer using spatial amplification we will consider the spatial mode in our calculations. That is we will consider a real frequency and complex wavenumbers and eigenvalues.

In the next section we will describe the method of solution of equation (6.21) and the numerical values of parameters chosen to correspond with experiment. We will later discuss how the introduction of the most amplifying eigenfunction is compatible with our previous discussion of amplitude limitation.

6.2 Numerical Calculation Procedure for the Solution of the Homogeneous Equation of Turbulent Shear Flow

Let us first non-dimensionalise equation (6.21) with respect to a reference length L_o^*, and a reference velocity U_o^*. Equation (6.21) then yields,

$$(U-c)(\hat{\psi}'' - \alpha^2\hat{\psi}) - U''\hat{\psi} + \frac{i}{\alpha R}(\hat{\psi}^{iv} - 2\alpha^2\hat{\psi}'' + \alpha^4\hat{\psi}) = 0, \qquad (6.22)$$

where $\alpha = k_1 L_o^*$, $R = \dfrac{U_o^* L_o^*}{\nu^*}$ and all other quantities in equation (6.22) are non-dimensional. Let us write the mean velocity in the form, as in Chapter 3,

$$U^* = \frac{U_1^* + U_2^*}{2} + \frac{U_1^* - U_2^*}{2} f'(y/\theta) \qquad (6.23)$$

where θ is the momentum thickness and dimensional quantities are starred. Then letting $U_o^* = \dfrac{U_1^* - U_2^*}{2}$ and referring all

lengths to 0 we obtain from (6.22),

$$(f' - c^*)(\hat{\psi}'' - \alpha^2 \hat{\psi}) - f''' \hat{\psi} + \frac{i}{\alpha R} (\hat{\psi}^{iv} - 2\alpha^2 \hat{\psi}'' + \alpha^4 \hat{\psi}) = 0,)$$

$$\text{where} \quad c^* = c - (\frac{U_1 + U_2}{2}) \ . \qquad \qquad) \quad (6.24)$$

The detailed solution of equation (6.24) has been dealt with in Chapter 5 and Appendix II, however we will describe again here the main features.

Above the mixing layer $U^* = U_2$ and $f' = 1$. The solutions to the equation are then

$$\hat{\psi} = \sum_{n=1}^{4} A_n e^{p_n y / \theta} \qquad , \qquad (6.25)$$

where $\qquad p_1 = \alpha \qquad , \qquad p_2 = -\alpha \qquad)$

$$\qquad \qquad \qquad \qquad \qquad \qquad \qquad \qquad \qquad) \quad (6.26)$$

$$p_3 = (\alpha^2 + i\alpha R(1-c^*))^{\frac{1}{2}} \quad , \qquad p_4 = -(\alpha^2 + i\alpha R(1-c^*))^{\frac{1}{2}})$$

Below the shear layer the solutions are of the form,

$$\hat{\psi} = \sum_{n=1}^{4} B_n e^{q_n y / \theta} \qquad , \qquad (6.27)$$

where $\qquad q_1 = \alpha \qquad , \qquad q_2 = -\alpha \qquad)$

$$\qquad \qquad \qquad \qquad \qquad \qquad \qquad \qquad \qquad) \quad (6.28)$$

$$q_3 = (\alpha^2 - i\alpha R(1+c^*))^{\frac{1}{2}} \quad , \qquad q_4 = -(\alpha^2 - i\alpha R(1+c^*))^{\frac{1}{2}})$$

The computation is started with $A_2 = 1$ and $A_4 = 0$ and the integration is performed from above to below the layer. At some point below the layer we may evaluate the values of B_n

for this solution. The quantities B_n may be obtained by inverting the equation (6.27) which leads to,

$$B_1 = \frac{-e^{-\alpha \, y/\theta}}{2\alpha(q_3^2 - \alpha^2)} \, (\hat{\psi}''' + \alpha\hat{\psi}'' - q_3^2\hat{\psi}' - \alpha q_3^2\hat{\psi}),$$

$$B_2 = \frac{e^{\alpha \, y/\theta}}{2\alpha(q_3^2 - \alpha^2)} \, (\hat{\psi}''' - \alpha\hat{\psi}'' - q_3^2\hat{\psi}' + \alpha q_3^2\hat{\psi}),$$

$$B_3 = \frac{e^{-q_3 \, y/\theta}}{2q_3(q_3^2 - \alpha^2)} (\hat{\psi}''' + q_3\hat{\psi}'' - \alpha^2\hat{\psi}' - \alpha^2 q_3\hat{\psi}) \quad \text{and}$$

$$B_4 = \frac{-e^{q_3 \, y/\theta}}{2q_3(q_3^2 - \alpha^2)} (\hat{\psi}''' - q_3\hat{\psi}'' - \alpha^2\hat{\psi}' + \alpha^2 q_3\hat{\psi}).$$

The values of the constants B_n evaluated using the values of the computations with $A_2 = 1$ and $A_4 = 0$ we will call B_{n_I}. A second integration is then performed with $A_2 = 0$ and $A_4 = 1$ as the starting conditions and the corresponding values of B_n are called $B_{n_{II}}$. As the equation is linear we have that for any arbitrary values of A_2 and A_4 the values of B_n are given by $B_n = A_2 B_{n_I} + A_4 B_{n_{II}}$. We require that for a bounded solution below the mixing layer $B_2 = B_4 = 0$. We may find the value of A_4 for which $B_2 = 0$ for A_2 set arbitrarily equal to unity from the above equation. The equation for B_4 is then

$$B_4 = B_{4_I} - \frac{B_{2_I}}{B_{2_{II}}} \circ B_{4_I} \tag{6.29}$$

Equation (6.29) leads to the numerical method for calculating the eigenvalue for fixed values of ω and R. For any value

of ω and R the value of c^* is altered such that the value of B_4 is set as near zero as possible. Further details of the numerical purification scheme needed for large Reynolds numbers and the interpolation procedure may be found in chapter 5 and Appendix II.

In our calculations we will consider the problem of a mixing layer for which $U_2/U_1 = 0.61$. This corresponds to the experiments of Yule (1970). The value of R used is 6,000, which corresponds to a reference velocity $(U_1 - U_2)/2$ of 3.55 m/sec and a reference thickness of 10^{-2}M.

In the next section we will describe the results of our calculations for the mixing layer between two streams. The results will be compared, where possible, with the experimental results of Yule.

6.3 Discussion of Results

The mean velocity profile used in the numerical calculations was found theoretically by the method of solution given in Chapter 3. We saw there that this gave excellent agreement with the experimental profile. A numerical solution was used, rather than the experimental values, for the mean velocity profile as it was found to be difficult to obtain a smooth second derivative from the measured values. However for the case of the mixing layer neither the mean velocity nor its second derivative have very high values, as is the case for the boundary layer, and it is unlikely that very small differences between theoretical and measured profiles will greatly affect the calculations.

We will now present the results of our calculations for the turbulent mixing layer. In a number of cases quantities which are predicted theoretically have not been measured by Yule for this particular velocity ratio of 0.61. In this case we will attempt to relate certain experimental results for different velocity ratios.

6.3.1. The phase velocity and the convection velocity

The phase velocity is shown in Figures 31 for both cases of spatial and temporal amplification respectively. Although we will concentrate most of our succeeding discussion on the spatial case it is thought useful to include both here for comparison. It is clear that the phase velocity is a function of frequency. In his calculations for the boundary layer Sharma (1968) found that as the frequency increased so the phase velocity becomes independent of the frequency. In our calculations for the mixing layer this is not the case. In the instance of spatial amplification the phase velocity has a peak value at low frequency then decreases to a minimum with increasing frequency and finally begins to increase with frequency. For temporal amplification the phase velocity is increasing monotonically with frequency with a large range of near independence of frequency in the middle wavenumber regions. If we recall the results of the stability analysis of Chapter 5 we noticed that at low frequencies the calculations were independent of the mean profile shape and at high frequencies the profile shape was a critical factor. Thus it

is clear that our particular choice of velocity profile accounts for the rise in phase velocity at the higher frequencies. The range of variation of phase velocity in the spatial case is between 49% and 58% of the velocity difference between the two free streams. The experimental results of Davies and Bose (1968) show that the phase velocity is nearly independent of frequency and takes a value approximately equal to the local mean velocity. We must note that measurements of convection velocity depend on the transverse position of the measuring instrument in the mixing layer. In our calculations the phase velocity predicted is not a function of the transverse co-ordinate. It would appear reasonable that our predicted phase velocity should thus lie close to the arithmetic mean of the velocities of the two streams. If we consider the relationship between spatial and temporal variations we may write,

$$\frac{\partial}{\partial t} = -U_c \frac{\partial}{\partial x} \; , \qquad\qquad\qquad (6.30)$$

where U_c is the convection velocity. If we Fourier transform this expression we see that,

$$U_c \; \alpha \; c_r \qquad\qquad , \qquad\qquad\qquad (6.31)$$

where c_r is the phase velocity. As we have previously discussed in considering the relationship between temporally and spatially growing disturbances, the constant of proportionality in equation (6.31) will be a function of the group velocity, $c_g = \frac{\partial \omega_r}{\partial \alpha_r}$. The variation of phase velocity with frequency for the range of

frequencies considered is not great though there exists no region of frequency independence. However the error involved in equating U_c and c_r in equation (6.31) is unlikely to be large. The measurements of Davies, Fisher and Barrett (1963) confirm that the difference between convection velocity and phase velocity in the mixing region of a jet is never greater than 10%. It is interesting to note that the phase velocity in the spatial case reaches a maximum value at low frequencies. In the case of U_2 = 0 the calculations of Michalke (1965) for the stability problem, indicate that the phase velocity increases with decreasing frequency and reaches a value equal to the velocity U_1 at zero frequency. The phase velocity, as we have noted above, is related to the convection of eddies in the flow. If we consider the spatial case it is clear that the large eddies move faster than the smaller although there is an increase in velocity towards the higher frequencies.

The amplification factor, α_i, in the spatial case is plotted as a function of frequency in Figure 32. The amplification is strong as is to be expected for the profile of a mixing layer with an inflection point. The maximum value of amplification factor is -.073699 and occurs at a frequency, ω, of 2.50275. The phase velocity of the maximum amplifying mode is 4.07343 which is 50.15% of the velocity difference of the two streams above the value of U_2.

6.3.2. <u>Rate of growth or decay of eddies</u>

The ratio α_i/α_r, in the spatial case, is related to the

rate of decay of the eddies. The rate of growth, $-\alpha_i/\alpha_r$, is shown against frequency in Figure 33. It may be seen that the rate of growth is largest at low frequencies and the growth rate decreases with increasing frequency until the neutral frequency is reached. This suggests that the rate of growth of the large eddies is much faster than that of the small eddies. The calculations of Sharma (1968) for the boundary layer in which the amplification is very small, show that the larger eddies decay slower than the smaller ones. An extension of our curve in Figure 33 for higher frequencies at which damping takes place would show the same features as Sharma noticed assuming that the curve continued with the same sign of derivative at higher frequencies.

We have only performed calculations in this instance for one Reynolds number. However if we can assume that the results of Sharma for the boundary layer will be analogous to ours for the mixing layer it is to be expected that alteration in the magnitude of the Reynolds number will have only a small effect and then only at the higher frequencies. We may explain this by noting that the larger eddies will be dominated by inertial forces and will be little affected by viscous forces.

6.3.3. <u>The fluctuating velocity and pressure field</u>

In this section we will examine the distributions of fluctuating velocity in the mixing layer by a suitable use of the eigensolutions to equation (6.22). A complete description of the fluctuating velocity field would be obtained by

applying the inverse Fourier transform to the stream function in equation (6.22). This would involve an integration over wave-number and frequency. However, as we have argued above, the flow structure at any axial position in the mixing layer will be dominated by the mode receiving maximum amplification. The eigensolution to equation (6.22) which receives maximum amplification is shown in Figure 34(a) and (b). The solution has been normalised such that the real part of $\hat{\psi}$ is unity at $y/\theta = 0$ and the imaginary part of $\hat{\psi}$ is zero. The relationships between $\hat{u}_2$ and $\hat{\psi}$ and $\hat{u}_1$ and $\hat{\psi}$ are given by the transformed form of equation (6.3); they are

$$
\left.
\begin{aligned}
\hat{u}_2 &= -i\alpha\hat{\psi} \quad \text{and} \\
\hat{u}_1 &= \hat{\psi}'
\end{aligned}
\right\}
\tag{6.32}
$$

The derivative of $\hat{\psi}$, which is related to $\hat{u}_1$ through equation (6.32) is shown in Figures 35(a) and (b). The change of sign and relative magnitudes of real and imaginary parts of $\hat{\psi}$ and $\hat{\psi}'$ makes description of the distributions of velocity fluctuations difficult. We will therefore conside the modulii of squared $\hat{u}_1$ and $\hat{u}_2$. These are shown in Figures 36 and 37 respectively. The results have been normalised in both instances such that the modulus of $\hat{u}_1$ is unity when y/θ is zero. Also shown on Figure 36 are the measurements of Yule (1970) for the mixing layer with $U_2/U_1 = .61$. It may be seen that the agreement over most of the mixing layer is very good.

The experimental results have been modified such that the
maximum experimental value equals the maximum theoretical value.
The measured values do not correspond at the edges of the mixing
layer where the theoretical curves predict two small peaks. The
values of mean velocity at the position of the two minima in the
predictions are 5% and 93% of the velocity difference. The
phase difference of the two smaller peaks is 180° and the maximum
at the centre of the layer is 90° out of phase with both smaller
peaks. The corresponding measured values of $|\hat{u}_2|^2$ are also shown
in Figure 37. It can be seen that the measured values are twice
as large as predicted values. The two peaks in the theoretical
profile correspond, through the continuity equation, with the
two minima of the $|\hat{u}_1|^2$ values. We may see from the results of
the stability analysis of Chapter 5, or from equation (6.32),
that for the magnitude of $|\hat{u}_2|^2$ to correspond to the measured
values, assuming two-dimensional disturbances, the wavenumber,
α, should be of order unity. However as this does not correspond
to the wavenumber for maximum amplification it would appear more
likely that the low values of $|\hat{u}_2|^2$ are due to our assumption
of two dimensional disturbances. The same effect was noticed
by Sharma in his results for the boundary layer. No calculations
have been made for oblique waves, however the effect of obliquity
on the value of the normal velocity fluctuation may be seen
qualitatively by considering a simple example. For high values
of Reynolds number the inviscid solution is a good approximation
to full equation. We will consider a shear layer where the
mean velocity profile is given by

$$U = U_1^* + U_2^* + y/\theta, \quad 0 < y/\theta < 1. \tag{6.33}$$

We may then write the inviscid equation for the $\hat{u}_2$ fluctuation,

$$\hat{u}_2'' = (\alpha^2 + \beta^2)u_2, \tag{6.34}$$

where β is the non-dimensional wavenumber in the x_3-direction.

The admissible solution of equation (6.34) for $y/\theta > 0$ is,

$$\hat{u}_2 \propto e^{-(\alpha^2 + \beta^2)y/\theta}$$

$$= e^{-(\alpha^2 \sec^2\phi)^{\frac{1}{2}}y/\theta}, \tag{6.35}$$

where ϕ is the wave angle given by $\phi = \tan^{-1}\beta/\alpha$.

We may write equation (6.35),

$$\hat{u}_2 \propto e^{-(\alpha/\cos\phi)y/\theta}. \tag{6.35a}$$

Thus we see that the magnitude of $\hat{u}_2$ is dependent on the magnitude of $\cos\phi$. So the magnitude of $\hat{u}_2$ decreases as ϕ increases. This contradicts the result of Sharma who incorrectly interpreted a trigonometric relation. Thus we see that the maximum magnitude of $\hat{u}_2$ occurs when $\phi = 0$ or for two-dimensional disturbances. However we may see from equation (6.32) that the magnitude of $\hat{u}_2$ increases as the wavenumber increases so the magnitude of the $\hat{u}_2$ fluctuation will increase if averaging is performed over wavenumber instead of considering the maximum amplifying mode alone.

The distribution of Reynolds stress function is shown in Figure 38. Also shown in the figure are the results obtained

by Yule. The experimental results have been modified so that
the maximum experimental value corresponds to the theoretical
maximum value. The distribution is very well predicted by the
linear theory in this case. The curve exhibits a peak at a
value of y/θ corresponding to the point of maximum mean shear,
U'. It is interesting to note that the Reynolds stress distri-
bution exhibits no peaks or troughs which are evident in the
fluctuating velocity distributions. The distribution of Reynolds
stress coefficient or shear correlation coefficient is shown in
Figure 39. The distribution appears to take a constant value
over most of the mixing layer. The experiments of Bradshaw et.
al. (1963) give a maximum value of R_{12} of .54 compared with
Liepmann and Laufer of .56. The reason for the high value of
correlation may be seen by comparing the eigenfunction and its
derivative. At $y/\theta = 0$ the function is $\pi/2$ radians out of phase
with the derivatives. Thus, making use of equation (6.32) we
see that the $\hat{u}_1$ and $\hat{u}_2$ components are nearly in antiphase at the
centre of the layer. This is true over all the mixing layer
except for a small region of $y/\theta < 0$. This accounts for the
dip in the correlation curve.

The equation for the fluctuating pressure may be obtained
by returning to our original equation of motion. The Navier-
Stokes equations may be written,

$$\frac{\partial u_i}{\partial t} + \frac{\partial}{\partial x_j} u_i u_j = -\frac{1}{\rho} \frac{\partial p}{\partial x_i} + \nu \nabla^2 u_i \qquad (6.36)$$

Making use of the equation of continuity and taking the

divergence of (6.36) we obtain

$$\nabla^2 p(x_i, t) = -\rho \frac{\partial^2}{\partial x_i \partial x_j} u_i u_j, \tag{6.37}$$

which is the Poisson equation for the pressure. Dividing the velocity and pressure into mean and fluctuating components, substituting into equation (6.37) and subtracting the mean part leads to

$$\nabla^2 p = -2\rho \frac{\partial u_2}{\partial x_1} \frac{\partial U}{\partial x_2} - \rho \frac{\partial}{\partial x_i \partial x_j} (u_i u_j - \overline{u_i u_j}),$$

or $\nabla^2 p = -2\rho \dfrac{\partial u_2}{\partial x_1} \dfrac{\partial U}{\partial x_2} + \rho \dfrac{\partial}{\partial x_i} T_j,$ \hfill (6.38)

where $T_i = \dfrac{\partial}{\partial x_j} (\overline{u_i u_j} - u_i u_j)$ is the divergence of the Reynolds stress tensor. The equations for the fluctuating velocity components are obtained by direct substitution of mean and fluctuating components into equation (6.36) and subtraction of the mean, which leads to

$$\frac{\partial u_i}{\partial t} + U_1 \frac{\partial u_i}{\partial x_j} + u_j \frac{dU_i}{dx_j} - \nu \nabla^2 u_i + \frac{1}{\rho} \frac{\partial p}{\partial x_i} = T_i \tag{6.39}$$

The u_2-component of equation (6.39) is

$$\frac{\partial u_2}{\partial t} + U \frac{\partial u_2}{\partial x_1} = -\frac{1}{\rho} \frac{\partial p}{\partial x_2} + \nu \nabla^2 u_2 + T_2 \tag{6.40}$$

The equation for the fluctuating pressure may then be obtained from (6.38) making use of equation (6.40) so that,

$$\frac{\partial^2 p}{\partial x_1^2} + \frac{\partial^2 p}{\partial x_3^2} = (\frac{\partial}{\partial t} + U \frac{\partial}{\partial x_1}) \frac{\partial u_2}{\partial x_2} - \frac{dU}{dx_2} \frac{\partial u_2}{\partial x_1} -$$

- 151 -

$$\nu \nabla^2 \frac{\partial u_2}{\partial x_2} + \frac{\partial T_1}{\partial x_1} + \frac{\partial T_3}{\partial x_3} \qquad (6.41)$$

Performing a Fourier transformation on equation (6.41) we obtain

the equation for the transform of the pressure fluctuation. The

transformed equation for two dimensional disturbances is

$$\hat{p} = - \frac{i}{\alpha} \left[(U-c)\, \hat{u}_2' - U'\hat{u}_2 + \frac{i}{\alpha R} (\hat{u}_2''' - \alpha^2 \hat{u}_2') \right] - \frac{i}{\alpha} (\hat{T}_1), \qquad (6.42)$$

where $\hat{p}$ is the transform of p and the components of the equation

have been non-dimensionalised with respect to a reference length,

velocity and density. In our analysis we have neglected the

transformed shear stress term. The equation for $\hat{p}$ in terms of the

fluctuating stream function $\hat{\psi}$ is then

$$\hat{p} = - \left[(U-c)\hat{\psi}' - U'\hat{\psi} + \frac{i}{\alpha R} (\hat{\psi}''' - \alpha^2 \hat{\psi}') \right] \qquad (6.43)$$

The magnitude distribution of the fluctuating pressure obtained

from equation (6.43) is shown in Figure 40. The measurements of

Fuchs (1969) for the mixing region of a jet exhausting into still

air show a pronounced peak at the centre of the layer i.e. y/θ

$= 0$. The behaviour of our linearised prediction may be explained

by considering the equation (6.43). The fluctuating pressure

clearly follows the product of the u_1-fluctuation and the mean

velocity towards the outer edges of the mixing. At the centre

of the layer where U approaches the real part of c, the product

of the derivative of mean velocity and the $\hat{u}_2$-fluctuation,

which is of opposite sign to the first term in the right hand

side of (6.43), reduces the magnitude of the pressure fluctuation.

It would appear then that in this region we are unable to

justify our neglect of the non-linear terms. We may say that
as the phase velocity of the fluctuations approaches the local
mean velocity the pressure fluctuations will be produced by
quadratic velocity terms; either squares of velocity fluctuations
or shear stress terms. For the case of isotropic turbulence,
Batchelor (1951) derived the result that,

$$\tilde{p}_{ISOTROPIC} = (0.58 \to 1.0)\bar{\rho} \; \tilde{v}^2$$

where $\tilde{v}^2 = u_1{}^2 = u_2{}^2 = u_3{}^2$.

The products of pressure and velocity fluctuations averaged
over wave length are shown in Figure 41. The products $\overline{\hat{p}\hat{u}_1}$ and
$\overline{\hat{p}\hat{u}_2}$ are of opposite sign over the whole mixing layer. The
magnitude of the $\overline{\hat{p}\hat{u}_1}$ distribution is approximately twice that of
the $\overline{\hat{p}\hat{u}_2}$ distribution except at the positions corresponding to the
sharp minimum in the $\hat{u}_1$ fluctuation distribution. The derivative
of the $\overline{\hat{p}\hat{u}_2}$ product represents the lateral pressure diffusion in
the turbulent energy balance equation. Applying the normal
boundary layer assumptions we may write equation (2.32) as,

$$\frac{U}{2}\frac{\partial}{\partial x_1}(\overline{u_1{}^2} + \overline{u_2{}^2}) + \frac{1}{2}\frac{\partial}{\partial x_2}(\overline{u_1{}^2 u_2} + \overline{u_2{}^3}) + \frac{1}{\rho}\frac{\partial}{\partial x_2}\overline{pu_2} \; -$$

$$(6.44)$$

$$\nu(\overline{u_1 \nabla^2 u_1} + \overline{u_2 \nabla^2 u_2}) + \overline{u_1 u_2}\frac{\partial U}{\partial x_2} = 0.$$

The first term in equation (6.44) represents the convection of
turbulent energy by the mean flow. The second term represents
the diffusion of turbulent energy. The third term denotes the
pressure diffusion, the fourth is the viscous dissipation of
turbulent energy and the fifth represents the production of

- 153 -

turbulent energy. The production terms distribution in the

mixing layer may be seen from the distribution of the shear

term $\overline{u_1 u_2}$ to be negative across the layer and have maximum

magnitude at the position of maximum mean vorticity. The

distribution across the layer of the pressure diffusion term

is shown in Figure 42. Also shown on the figure are the

experimental results of Yule (1970). It may be seen that

agreement is good over most of the mixing layer except on the

lower velocity side of the layer where the predicted pressure

diffusion attains a small positive value and the experimental

results indicate that the term remains negative. The experi-

mental results have been plotted such that the maximum positive

value of $\dfrac{\partial \hat{p} \hat{u}_2}{\partial x_2}$ corresponds to the predicted value. In these

two cases of production and pressure diffusion in the

energy balance, where comparison may be made, the predictions

agree fairly well with the measured values. However, as the

computed eigenfunctions may be multiplied by an arbitrary

constant and still meet the boundary conditions of the problem,

only comparison of distributions of fluctuating quantities may

be made.

6.4   Summary of Results of Linear Analysis

We will now summarise the results of the linear analysis

of the turbulent mixing layer. The linear analysis provides a

useful guide to the large scale structure of the shear flow.

We have seen that the convection and phase velocities of the

fluctuations agree with available experimental results. The

fluctuating components of velocity and pressure have been predicted by considering the most amplifying mode in the spatial case which is considered to have a dominant effect on the local structure of flow. The maximum amplifying mode occurs at a non-dimensional wavenumber, with respect to the shear layer thickness, of 0.6. The distribution of $|\hat{u}_1|^2$ across the mixing layer agrees with experimental results except at the edges of the layer where the theoretical prediction exhibits two minor peaks. The distribution of $|\hat{u}_2|^2$ is small by a factor of two compared with measured values. This is due to the value of wavenumber of the maximum amplifying mode, as the magnitude of the u_2-fluctuation is given by,

$$|\hat{u}_2|^2 = |i\alpha\hat{\psi}|^2 .$$

It may be argued that the low value of the transverse velocity fluctuation may be raised by integrating the fluctuations for all wavenumbers. It has been seen that the pressure fluctuations predicted by linearised theory do not correspond to measured values. The major discrepancy occurs in the centre of the mixing layer where the phase velocity approaches the mean velocity. We have seen that in this region the non-linear terms may not be reasonably neglected and that the pressure fluctuations will contain contributions from the non-linear velocity product terms. We may also see this in another way: the non-linear terms will try to force a sort of isotropy on the fluctuations so that the magnitudes of the components of

velocity become equal. In this way the non-linearity acting

at the critical centre of the mixing layer will remove the dips

in the u_2-fluctuation and the pressure distribution.

The discrepancies in results between the linearised theory

and experiment may serve to highlight those terms where non-

linear motions dominate. We have seen that for a correct

distribution of $\hat{u}_1$-fluctuation we may predict the Reynolds

stress distribution. However, the $\hat{u}_2$-fluctuation and the

pressure fluctuation would appear to require a non-linear

solution. The successful prediction of the $\widehat{p}\widehat{u}_2$ correlation

is almost certainly due to the coincidence of discrepancies

in both cases.

On the basis of the results of the linear analysis it is

clear that a useful description of the large scale motion in

a turbulent shear flow may be obtained. However, the analyses

so far presented have dealt with the growth and amplification

of turbulent fluctuations and we have not considered, in detail,

how these fluctuations are amplitude limited. We have pre-

viously argued that the small scale turbulence will contribute

to an eddy viscosity. This will produce a reduction in the

effective Reynolds number which will have a stabilising effect

on the disturbances. We may also note that as a disturbance

grows its wavenumber decreases, which will again have a

stabilising effect on the fluctuation. In the next chapter

we will consider a more complete analysis of the non-linear

problem. We will show how the shape and rate of growth of

disturbances affects the mean flow as the flow moves from a

laminar to a turbulent region.

CHAPTER 7

Finite Amplitude Effects on the Development of the Mixing Layer

7.1 Introduction

In the previous chapters we have seen how linearised theory may be used in connection with the stability of a mixing layer and the description of turbulent structure of the mixing layer. However, we have seen that the rate of growth of the linear disturbances in either space or time is very rapid and it is clear that the neglect of non-linear terms, allowed by the assumption of infinitessimal disturbances, will not be valid when the disturbances have reached finite amplitude. The added complexity of theoretical models including non-linearity is such that much work has been based on experimental observation. The separated shear layer was studied by Sato (1956, 1959). He observed that after separation the flow remained laminar for some distance until velocity fluctuations of a regular sinusoidal wave form appeared. The magnitude of the fluctuations increased until turbulence developed further downstream. The extent of the areas including sinusoidal fluctuations is sketched below, (from Sato (1959)). Inside the shaded area the wave-form is
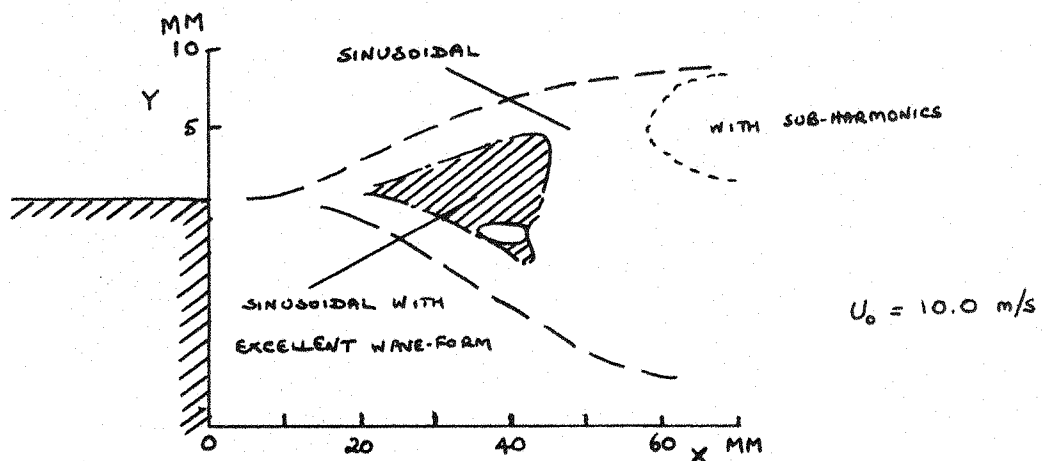
sinusoidal. Within the small region enclosed by a full-line, the amplitude of the fluctuation is very small and the waveform is not sinusoidal. Further downstream the fundamental component is accompanied by a subharmonic component.

When the amplitude of the disturbances has reached a finite value we clearly have to reform the problem of stability to take account of non-linear terms. Let us consider the vorticity equation (2.9) which we write,

$$\frac{\partial \omega_i}{\partial t} + \frac{\partial \omega_i u_j}{\partial x_j} = \frac{\partial u_i \omega_j}{\partial x_j} + \nu \nabla^2 \omega_i \qquad (7.1)$$

where ω_i and u_i are the components of vorticity and velocity respectively. The second and third terms in equation (7.1) represent the convection and stretching of vorticity respectively. For two dimensional flow there is no vortex stretching, however it plays an important part in three-dimensional flow. Stuart (1965) noted that, for a boundary layer, if the vortex stretching terms were omitted no peaking occurred in the vorticity. Thus vortex stretching which creates a greater vorticity locally than that present at any point in the flow plays an important role in flow development.

Let us consider an example of a typical non-linear term, $v \frac{\partial u}{\partial y}$. It is clear that the linearised theory may break down for small amplitudes if the derivative becomes large. Betchov and Criminale (1967) note that if viscosity is allowed to vanish while v retains some small amplitude the derivative

$\partial u/\partial y$ becomes very large at the critical layer. At this point
we may expect the non-linear terms to control the solution in
place of viscous terms. The comments on the development of the
boundary layer by Stuart (1965) make it clear that three-
dimensional effects occur before non-linearity becomes signifi-
cant, however we may usefully consider the two-dimensional
treatment of the non-linear problem.

The study of non-linear stability has been usefully advanced
by the work of Meksyn and Stuart (1951) and Stuart (1958, 1960).
The problem considered by Stuart was that of plane Poiseuille
flow. He defines a stream function for the disturbed flow in
the form,

$$\psi = \phi_0(z,t) + \phi_1(z,t) \, \exp\left[i\alpha(x-c_r t)\right] + \phi_1{}^*(z,t) \qquad)$$

$$)$$
$$\exp\left[-i\alpha(x-c_r t)\right] + \phi_2(z,t) \, \exp\left[2i\alpha(x-c_r t)\right] + \qquad) \qquad (7.2)$$
$$)$$
$$\phi_2{}^*(z,t) \, \exp\left[-2i\alpha(x-c_r t)\right] \qquad)$$

$$+ - - - - , \qquad)$$

where the starred functions denote complex conjugates. The
vorticity equation (7.1) may be written for two dimensional
motion in terms of the stream function as,

$$\frac{\partial \omega_3}{\partial t} + \frac{\partial \psi}{\partial z} \frac{\partial \omega_3}{\partial x} - \frac{\partial \psi}{\partial x} \frac{\partial \omega_3}{\partial z} = \frac{1}{R} \, \nabla^2 \omega_3 \qquad (7.3)$$

where $\omega_3 = -\nabla^2 \psi$.

Let us define the operator $L(\alpha)$, Betchov and Criminale (1967), as

$$L(\alpha) = (U - c_r - \frac{i}{\alpha} \frac{\partial}{\partial t})(\frac{\partial^2}{\partial z^2} - \alpha^2) - U'' + \frac{i}{\alpha R} \cdot$$

$$(\frac{\partial^4}{\partial z^4} - 2\alpha^2 \frac{\partial^2}{\partial z^2} + \alpha^4) \cdot \tag{7.4}$$

Then with the aid of equation (7.4) substitution of equation (7.2) into (7.3) and separation of harmonic components leads to the set of equations,

$$L(\alpha)\phi_1 = \phi_2'(\phi_1^{*''} - \alpha^2\phi_1^*) + 2\phi_2(\phi_1^{*'''} - \alpha^2\phi_1^{*'}) -$$

$$2\phi_1^{*'}(\phi_2'' - 4\alpha^2\phi_2') - \phi_1^*(\phi_2''' - 4\alpha^2\phi_2') \tag{7.5}$$

$$+ 0(\phi_2^*\phi_3),$$

$$L(2\alpha)\phi_2 = -\frac{1}{2}(\phi_1'\phi_1'' - \phi_1\phi_1''') + 0(\phi_1^*\phi_3) , \tag{7.6}$$

$$\frac{\partial U}{\partial t \partial z} + i\alpha \frac{\partial^2}{\partial z^2} \{(\phi_1'\phi_1^* - \phi_1^{*'}\phi_1) + 2(\phi_2'\phi_2^* - \phi_2^{*'}\phi_2) +$$

$$\ldots \} = \frac{1}{R} \frac{\partial^3 U}{\partial z^3} \tag{7.7}$$

Equation (7.7) may be integrated immediately with respect to z such that,

$$\frac{\partial U}{\partial t} + i\alpha \frac{\partial}{\partial z}\{(\phi_1'\phi_1^* - \phi_1^{*'}\phi_1) + 2(\phi_2'\phi_2^* - \phi_2^{*'}\phi_2) + \ldots\}$$

$$= \frac{2}{R} + \frac{1}{R} \frac{\partial^2 U}{\partial z^2} , \tag{7.8}$$

where the constant of integration is given the value (2/R), the pressure gradient in laminar flow. If the $\partial/\partial t$ term in (7.8) may be neglected then this equation may be viewed as a distortion in the mean profile. Stuart notes that this distortion modifies

the transfer of energy from the mean flow to the disturbance.
He applied these ideas to the problem of Poiseuille flow. Sharma
(1968) used the distortion of the mean profile in his study of
the turbulent boundary. He found that the modified profile
introduced stronger rates of growth in the disturbance. It
seems reasonable to attribute this increase in rate of growth
to the appearance of inflection points in the modified profile.
Stuart looked for a solution to equations (7.5) and (7.6), with
the series terminated after the ϕ_2 term, in the form

$$\phi_1 = A(t) \; \psi_1(z) + B(t) \; \psi_{11}(z) \qquad \qquad)$$
$$\qquad \qquad \qquad \qquad \qquad \qquad \qquad \qquad \qquad) \qquad (7.9)$$
$$\phi_2 = A^2(t) \; \psi_2(z) \qquad \qquad \qquad \qquad)$$

In order to obtain a solution where variations in time and z
are separated Stuart writes

$$B(t) = A^2(t) \; A^*(t),$$

which leads to the equation for $A(t)$ in the form,

$$\frac{d(AA^*)}{dt} = 2\alpha c_i (AA^*) - 2\alpha k (AA^*)^2, \qquad (7.10)$$

where k is a complex number which may be determined from the
shape of the functions $\psi_i(z)$ with the aid of the adjoint operator
of (7.4).

The solution to equation (7.10) is,

$$AA^* = \frac{c_i \; C \; \exp(2\alpha c_i t)}{1 + k_i \; C \; \exp(2\alpha c_i t)} \qquad , \qquad (7.11)$$

- 161 -

where k_i is the imaginary part of k and C is an arbitrary, real constant. If $c_i > 0$ the amplitude will increase to a maximum value of c_i/k_i, assuming that k_i is not positive. For $c_i < 0$ and $k_i < 0$ the disturbance takes a value $|c_i|/|k_i|$ as $t \to -\infty$. If $|A|^2 > c_i/k_i$ then the amplitude of the disturbance grows to infinity. Stuart also considered the integral energy equation to obtain an equation of the form of equation (7.10) for the disturbance amplitude but we will consider this later as our subsequent method for the growth with space of the amplitude will be along similar lines.

A class of non-linear problems was considered by Eckhaus (1965) which included the problem of flow stability. He wrote the solution of the non-linear problem as a series in terms of eigenfunctions of the linear problem, i.e.

$$\psi(y,t) = \sum_{n=1}^{\infty} A_n(t)\, \psi_n(y). \tag{7.12}$$

This may also be written,

$$\psi(y,t) = \sum_{n=1}^{\infty} B_n\, \psi_n(y)\, e^{\omega_n t}, \tag{7.13}$$

where ω_n are the eigenfrequencies and $\psi_n(y)$ are the orthonormal eigenfunctions. Making use of the adjoint eigenfunctions $\tilde{\psi}_n(y)$ we may write the orthogonality relationship in the form,

$$\int_0^1 \left[\frac{d\tilde{\psi}_n}{dy}\, \frac{d\psi_m}{dy} + k^2\, \tilde{\psi}_n\, \psi_m \right] dy = \begin{cases} 1 \text{ if } n = m \\ 0 \text{ if } n \neq m \end{cases} \tag{7.14}$$

- 162 -

Application of the eigenfunction expansion (7.12) leads to the result,

$$\frac{dA_n}{dt} - \omega_n A_n = K_n(t) \tag{7.15}$$

As a test of his method Eckhaus considered the model of turbulence proposed by Burgers (1948). In this case the stream function is given by the solution to the equation,

$$\frac{1}{R} \frac{\partial^2 \psi}{\partial y^2} + \psi - \frac{\partial \psi}{\partial t} = \frac{\partial \psi}{\partial y}^2 + R \left[\int_0^1 \psi^2 \, dy \right] \psi \tag{7.16}$$

the boundary conditions on $\psi(y,t)$ being,

$$\psi(o) = \psi(1) = 0. \tag{7.17}$$

The linearised solutions are written as,

$$\psi = \sum_{n=0}^{\infty} b_n e^{\omega_n t} \psi_n(y)$$

and the $\psi_n(y)$ are given by

$$\psi_n = \sin(n + 1) \pi y$$

with eigenfrequencies

$$\omega_n = \left[1 - \frac{\pi^2}{R} (n + 1)^2 \right]$$

This problem is then seen to be analogous to stability theory as there exists a value of $R = R_{CRIT} = \pi^2$, where R is a constant analogous to the Reynolds number. For $R < R_{CRIT}$ there is

stability while for $R > R_{CRIT}$ there is instability. To consider the non-linear problem he introduces the expansion (7.12) and after some calculation he finds

$$\frac{dA_n}{dt} - \omega_n A_n = -\frac{1}{2} R \left[\sum_{k=0}^{\infty} A_k^2 \right] A_n + (n+1)\pi \left[\frac{1}{2} \sum_{k=0}^{n-1} A_k A_{n-k-1} - \sum_{k=0}^{\infty} A_k A_{n+k+1} \right]$$

(7.18)

His calculations for the first few amplitude functions, A_n, agree with those of Burgers (1948). Equation (7.18) is of the form of equation (7.15) which in simple cases leads to the results of Stuart (1960) or Landau and Lifshitz (1953).

Finally, in this short review of non-linear methods we will consider the technique of the energy method. The method was first considered by Orr (1907). Let us define the kinetic energy per unit mass of the perturbation as,

$$e = \frac{1}{2} u_i u_i,$$

(7.19)

where u_i are the perturbations of the mean flow, U_i. We may write the rate of change of energy of the perturbation as,

$$\frac{\partial e}{\partial t} = -u_i u_j \frac{\partial U_i}{\partial x_j} - \frac{1}{R} \frac{\partial u_i}{\partial x_j} \frac{\partial u_i}{\partial x_j} + \frac{\partial}{\partial x_j} \left[\frac{u_i u_i}{2} (U_j + u_j) + \frac{1}{2R} \frac{\partial}{\partial x_j} u_i u_i - p u_j \right]$$

(7.20)

where the components in the equation are suitably non-dimensionalised. If we consider the integral of (7.20) over a volume bounded by walls or the nodes of a periodic velocity field the term in brackets will not contribute and we may write,

$$\frac{\partial E}{\partial t} = \frac{\partial}{\partial t} \int \int_V \int e \, dV = - \int \int_V \int u_i u_j \frac{\partial U_i}{\partial x_j} \, dV - \frac{1}{R} \int \int_V \int \frac{\partial u_i}{\partial x_j} \frac{\partial u_i}{\partial x_j} \, dV \quad (7.21)$$

If the total energy is stationary then $\frac{\partial E}{\partial t} = 0$ and the production term will equal the dissipation. We then have,

$$R = \frac{\int \int_V \int \frac{\partial u_i}{\partial x_j} \frac{\partial u_i}{\partial x_j} \, dV}{-\int \int_V \int u_i u_j \frac{\partial U_i}{\partial x_j} \, dV} \quad (7.22)$$

Use may be made of the calculus of variations to find the extreme value of R, that is the critical Reynolds number.

Stuart (1958) used the energy method for two dimensional disturbances in Poiseuille flow. The integral energy equation may then be written,

$$\frac{\partial}{\partial t} \int \int \frac{1}{2} (u_1^2 + u_3^2) \, dx_1 dx_3 = \int \int (-\overline{u_1 u_3}) \frac{\partial U}{\partial z} \, dx_1 dx_3 \quad -$$

$$\frac{1}{R} \int \int (\frac{\partial u_3}{\partial x_1} - \frac{\partial u_1}{\partial x_3})^2 \, dx_1 dx_3 \quad (7.23)$$

The equation for the mean flow is

$$\frac{\partial U}{\partial t} + \frac{\partial}{\partial x_3} (\overline{u_1 u_3}) = \frac{2}{R} + \frac{1}{R} \frac{\partial^2 U}{\partial x_3^2} \quad (7.24)$$

If we assume that $\partial U/\partial t$ may be neglected then equation (7.24) may be integrated for $U(x_3)$ and with equation (7.23) we obtain,

$$\gamma_1 \frac{\partial a^2}{\partial t} = \gamma_2 \alpha a^4 - \gamma_3 \alpha^2 Ra^4 - \frac{\gamma_4 a^2}{R} , \qquad (7.25)$$

where a is the amplitude of the function and,

$$\gamma_1 = \int_0^1 \{|\phi'|^2 + \alpha^2|\phi|^2\}dx_3, \quad \gamma_2 = 4\int_0^1 x_3(\phi_i\phi_r' - \phi_r\phi_i')dx_3 ,$$

$$\gamma_3 = 4\int_0^1 (\phi_i\phi_r' - \phi_r\phi_i')dx_3, \quad \gamma_4 = 2\int_0^1 \{|\phi''|^2 + 2\alpha^2|\phi'|^2 +$$

$$\alpha^4|\phi|^2\}dx_3,$$

the suffixes r and i denote real and imaginary parts and ϕ is

defined as in equation (7.2). We may write equation (7.25) as,

$$\frac{da^2}{dt} = \beta_1 a^2 - \beta_2 a^2 - \beta_3 a^4 \qquad (7.26)$$

The solution to equation (7.26) is in the form,

$$a^2 = \frac{C e^{(\beta_1 - \beta_2)t}}{1 + (\frac{\beta_3}{\beta_1 - \beta_2}) C e^{(\beta_1 - \beta_2)t}} \qquad (7.27)$$

Now $\beta_1 - \beta_2 = 2\alpha c_i$, from linear stability theory. Thus we see that
equation (7.27) is equivalent to equation (7.11). The equilibrium
amplitude of the disturbance occurs when $\frac{da^2}{dt} = 0$ and may be shown
to be,

$$a_e^2 = \frac{\beta_1 - \beta_2}{\beta_3} = \frac{\gamma_2(R - R_{CRIT})}{\gamma_3 \alpha R^2} \qquad (7.28)$$

Thus it may be seen that the equilibrium amplitude is proportional

to the square root of the difference between the flow Reynolds number and the critical Reynolds number. Stuart showed that the critical Reynolds number agreed reasonably with the calculations of Thomas (1953) although the correct eigensolutions were not available for integration.

We will now present our formulation of the non-linear problem. The integral equation of mean and fluctuating components of the flow will be written as ordinary differential equations in x_1 in terms of a number of shape parameters of the mean flow and the amplitude of the disturbances. The distributions for the fluctuations will be calculated using a modified solution of the stability problem. The technique to be used is similar to that successfully applied to the wake by Ru-Sue Ko et. al. (1970).

7.2 Governing Differential and Integral Equations

In Chapter 2 we obtained the integral equations of the mean flow by integrating across the layer the mean momentum and energy equations and the turbulent energy equation. These were then written as ordinary differential equations in the independent variable x by considering the differentiation of integrals. The final equations in Chapter 2 were derived with the assumption that the fluctuations were zero at the limits of the integration. In this chapter we will not use that assumption as it will be seen that the disturbance distributions used in our formulation decrease exponentially outside the layer.

Referring to Chapter 2 we may write the integral equations of the mean flow and fluctuations as (i) the mean momentum equation,

$$\int_{-\delta_2}^{\delta_1} \frac{\partial}{\partial x}\left[(U-U_1)(U-U_2) + (\overline{u^2} - \overline{v^2})\right]dy + \left[V_2 U_1 - U_2 V_1\right] = 0, \qquad (7.29)$$

(ii) the mechanical energy equation,

$$\int_{\delta_2}^{\delta_1} \frac{\partial}{\partial x}\left\{\frac{1}{2}\left[U(U-U_1)(U-U_2)\right] + \left[U - \frac{(U_1 + U_2)}{2}\right](\overline{u^2} - \overline{v^2})\right\}\,dy \qquad)$$

$$\qquad)$$
$$\qquad) \qquad (7.30)$$
$$= \int_{-\delta_2}^{\delta_1}(\overline{u^2} - \overline{v^2})\frac{\partial U}{\partial x}\,dy + \int_{-\delta_2}^{\delta_1}\overline{uv}\;\frac{\partial U}{\partial y}\,dy - \nu\int_{-\delta_2}^{\delta_1}\left(\frac{\partial U}{\partial y}\right)^2\,dy \qquad)$$
$$\qquad)$$

and (iii) the mean fluctuation energy equation,

$$\frac{1}{2}\int_{-\delta_2}^{\delta_1}\frac{\partial}{\partial x}\left[U(\overline{u^2} + \overline{v^2}) + \overline{u^3} + \overline{uv^2} + 2\frac{\overline{up}}{\rho}\right]\,dy = -\int_{-\delta_2}^{\delta_1}(\overline{u^2} - \overline{v^2})\frac{\partial U}{\partial x}\,dy -$$

$$\qquad (7.31)$$

$$\int_{-\delta_2}^{\delta_1}\overline{uv}\;\frac{\partial U}{\partial y} - \nu\int_{-\delta_2}^{\delta_1}\left[\left(\frac{\overline{\partial u}}{\partial x}\right)^2 + \left(\frac{\overline{\partial u}}{\partial y}\right)^2 + \left(\frac{\overline{\partial v}}{\partial x}\right)^2 + \left(\frac{\overline{\partial v}}{\partial y}\right)^2\right]\,dy$$

Making use of equation (2.24) we may write equation (7.29)

$$\frac{d}{dx}\int_{-\delta_2}^{\delta_1}\left[(U-U_1)(U-U_2) + (\overline{u^2} - \overline{v^2})\right]dy - \frac{d\delta_2}{dx}(\overline{u_2}^2 - \overline{v_2}^2) - \qquad)$$

$$\qquad) \qquad (7.32)$$

$$\frac{d\delta_1}{dx}(\overline{u_1}^2 - \overline{v_1}^2) + \left[V_2 U_1 - U_2 V_1\right] = 0 \qquad)$$

where the subscripts 1 and 2 on the fluctuations refer to their

values at the upper and lower limits of integration respectively.

Equation (7.30) becomes,

$$\frac{d}{dx} \int_{-\delta_2}^{\delta_1} \{\frac{1}{2}[U(U-U_1)(U-U_2)] + [U - \frac{(U_1 + U_2)}{2}] (\overline{u^2} - \overline{v^2})\}dy$$

$$+ U_d\{\frac{d\delta_2}{dx} (\overline{u_2^2} - \overline{v_2^2}) - \frac{d\delta_1}{dx} (\overline{u_1}^2 - \overline{v_1}^2)\} \qquad (7.33)$$

$$= \int_{-\delta_2}^{\delta_1} (\overline{u^2} - \overline{v^2}) \frac{\partial U}{\partial x} dy + \int_{-\delta_2}^{\delta_1} \overline{uv} \frac{\partial U}{\partial y} dy - \nu \int_{-\delta_2}^{\delta_1} (\frac{\partial U}{\partial y})^2 dy,$$

where $U_d = \frac{(U_1 - U_2)}{2}$

Equation (7.30) becomes,

$$\frac{1}{2} \frac{d}{dx} \int_{-\delta_2}^{\delta_1} [U(\overline{u^2} + \overline{v^2}) + 2 \frac{\overline{up}}{\rho}]dy + \frac{1}{2} \frac{d}{dx} \int_{-\delta_2}^{\delta_1} (\overline{u^3} + \overline{uv^2})dy$$

$$- \frac{d\delta_2}{dx} [U_2 \frac{(\overline{u_2}^2 + \overline{v_2}^2)}{2} + \frac{\overline{u_2 p_2}}{\rho}] - \frac{d\delta_1}{dx} [U_1 \frac{(\overline{u_1}^2 + \overline{v_1}^2)}{2}$$

$$+ \frac{\overline{u_1 p_1}}{\rho}] - \frac{1}{2} \{\frac{d\delta_2}{dx} (\overline{u_2^3} + \overline{u_2 v_2^2}) + \frac{d\delta_1}{dx} (\overline{u_1^3} + \overline{u_1 v_1^2})\} \qquad (7.34)$$

$$= - \int_{-\delta_2}^{\delta_1} (\overline{u^2} - \overline{v^2}) \frac{\partial U}{\partial x} dy - \int_{-\delta_2}^{\delta_1} \overline{uv} \frac{\partial U}{\partial y} dy - \nu \int_{-\delta_2}^{\delta_1} [(\frac{\overline{\partial u}}{\partial x})^2 +$$

$$(\frac{\overline{\partial u}}{\partial y})^2 + (\frac{\overline{\partial v}}{\partial x})^2 + (\frac{\overline{\partial v}}{\partial y})^2] dy$$

- 169 -

We will now non-dimensionalise equations (7.32), (7.33) and (7.34) with respect to a reference length ℓ and the velocity difference $(U_1 - U_2)/2$. The pressure is non-dimensionalised with respect to $\rho(U_1 - U_2)^2/4$. Equations (7.32), (7.33) and (7.34) may then be written,

$$
\left.
\begin{aligned}
&\frac{d}{dx^*} \int_{\delta_2^*}^{\delta_1^*} \left[(U^* - U_1^*)(U^* - U_2^*) + (\overline{u^*}^2 - \overline{v^*}^2) \right] dy^* - \frac{d\delta_2}{dx^*} \;. \\[2ex]
&(\overline{u_2^*}^2 - \overline{v_2^*}^2) - \frac{d\delta_1}{dx^*}(\overline{u_1^*}^2 - \overline{v_1^*}^2) + \left[V_2^* U_1^* - U_2^* V_1^* \right] = 0
\end{aligned}
\right\} \text{(7.35)}
$$

$$
\left.
\begin{aligned}
&\frac{d}{dx^*} \int_{-\delta_2^*}^{\delta_1^*} \left\{ \frac{1}{2}\left[U^*(U^*-U_1^*)(U^* - U_2^*) \right] + \left[U^* - \frac{(U_1^* + U_2^*)}{2} \right](\overline{u^*}^2 - \overline{v^*}^2) \right\} dy^* \\[2ex]
&+ \left\{ \frac{d\delta_2^*}{dx^*}(\overline{u_2^*}^2 - \overline{v_2^*}^2) - \frac{d\delta_1^*}{dx^*}(\overline{u_1^*}^2 - \overline{v_1^*}^2) \right\} \\[2ex]
&= \int_{-\delta_2^*}^{\delta_1^*} (\overline{u^*}^2 - \overline{v^*}^2)\frac{\partial U^*}{\partial x^*} dy^* + \int_{-\delta_2^*}^{\delta_1^*} \overline{u^* v^*}\,\frac{\partial U^*}{\partial y^*} dy^* \\[2ex]
&- \frac{1}{R_\ell} \int_{-\delta_2^*}^{\delta_1^*} \left(\frac{\partial U^*}{\partial y^*}\right)^2 dy^*,
\end{aligned}
\right\} \text{(7.36)}
$$

and $\dfrac{1}{2}\dfrac{d}{dx^*} \displaystyle\int_{-\delta_2^*}^{\delta_1^*} \left[U^*(\overline{u^*}^2 + \overline{v^*}^2) + 2\overline{u^* p^*} \right] dy^* + \dfrac{1}{2}\dfrac{d}{dx^*} \displaystyle\int_{-\delta_2^*}^{\delta_1^*} (\overline{u^*}^2 + \overline{u^* v^*}^2) dy^*$

$$
- \frac{d\delta_2^*}{dx^*}\left[U_2^* \frac{(\overline{u_2^*}^2 + \overline{v_2^*}^2)}{2} + \overline{u_2^* p_2^*} \right] -
$$

$$\frac{d\delta_1^*}{dx^*} \left[U_1^* \frac{(\overline{u_1^{*2}} + \overline{v_1^{*2}})}{2} + \overline{u_1^* p_1^*} \right] - \frac{1}{2} \left\{ \frac{d\delta_2^*}{dx^*} (\overline{u_2^{*3}} + \overline{u_2^* v_2^{*2}}) + \right.$$

$$\left. \frac{d\delta_1^*}{dx^*} (\overline{u_1^{*3}} + \overline{u_1^* v_1^{*2}}) \right\}$$

$$= - \int_{-\delta_2^*}^{\delta_1^*} (\overline{u^{*2}} - \overline{v^{*2}}) \frac{\partial U^*}{\partial x^*} \, dy^* - \int_{-\delta_2^*}^{\delta_1^*} \overline{u^* v^*} \frac{\partial U^*}{\partial y^*} \, dy^* -$$

$$\frac{1}{R_\ell} \int_{-\delta_2^*}^{\delta_1^*} \left[(\overline{\frac{\partial u^*}{\partial x^*}})^2 + (\overline{\frac{\partial u^*}{\partial y^*}})^2 + (\overline{\frac{\partial v^*}{\partial x^*}})^2 + (\overline{\frac{\partial v^*}{\partial y^*}})^2 \right] dy^*,$$

where all non-dimensional quantities are starred, and the Reynolds number R_ℓ is given by,

$$R_\ell = \frac{(U_1 - U_2)\ell}{2\nu} \tag{7.38}$$

7.3 Shape Assumption for the Mean Flow

In this section we will assume that the unknowns in our equations may be expressed in terms of a number of shape para-meters. These will then be determined from the integral equations. In their study of the incompressible wake Ru-Sou Ko et. al. (1970) were able to express the mean velocity profile in terms of two parameters, the wake half-width and the velocity defect. In Chapter 3 we saw that when the mean velocity profiles for both laminar and turbulent mixing layers were plotted as a function of η, where η is given by,

$$\eta = \frac{y^* - b^*(x^*)}{\theta^*(x^*)} \qquad (7.39)$$

then the profiles coincided. Sato (1956), whose results on the transition of the mixing layer we will use later, noticed this in his measurements of the mean velocity profiles of a mixing layer before and after transition from laminar to turbulent flow. In equation (7.39), $b^*(x)$ is the value of y^* at which $U = \frac{U_1 + U_2}{2}$, and θ^* is the non-dimensional momentum thickness defined by,

$$\theta^* = \int_{-\infty}^{\infty} (U_1^* - U^*)(U^* - U_2^*)dy^* \qquad (7.40)$$

We will then write the mean velocity profile as,

$$U^*(x^*, y^*) = \frac{U_1^* + U_2^*}{2} + f(\eta), \qquad (7.41)$$

and we will further write η as,

$$\eta = \frac{y^* - b^*(\omega)}{\theta_1^*(x^*) + \theta_2^*(x^*)} = \frac{y^* - b^*(x^*)}{\theta^*(x^*)} \qquad (7.42)$$

$$\text{where } \theta_2^*(x^*) = \int_{-\infty}^{0} (U_1^* - U^*)(U^* - U_2^*)dy^* \qquad \left. \begin{array}{c} \\ \\ \\ \\ \\ \end{array} \right\} \qquad (7.43)$$

$$\text{and } \quad \theta_1^*(x^*) = \int_{0}^{\infty} (U_1^* - U^*)(U^* - U_2^*)dy^*$$

In this manner we are able to define more clearly the width of the mixing layer. We will now change the independent variables (x^*, y^*) to (ξ, η) in equations (7.35), (7.36) and

(7.37). The transformation of variables follows the following rules,

$$\xi = x^* \quad ; \quad \eta = \frac{y^* - b^*}{\theta^*} \quad ; \quad)$$

$$\qquad\qquad\qquad\qquad\qquad\qquad\qquad\qquad\qquad) \quad (7.44)$$

$$\frac{\partial}{\partial x^*} = \frac{\partial}{\partial \xi} - \{\frac{1}{\theta^*}\frac{db^*}{dx^*} + \frac{\eta}{\theta^*}\frac{d\theta}{dx^*}\}\frac{\partial}{\partial \eta} \quad ; \quad \frac{\partial}{\partial y^*} = \frac{1}{\theta^*}\frac{\partial}{\partial \eta} \quad . \quad)$$

We will also alter the range of integration to an integration across the momentum thickness. Then equations (7.35) and (7.36) become,

$$\frac{d}{d\xi}\{\frac{\theta^*}{4}[(U_1^* - U_2^*)^2 + 4\beta_2 + 4(I_1 - I_2)]\} - \frac{d\theta_2^*}{d\xi}(\overline{u}_2^{*2} - \overline{v}_2^{*2}) \quad)$$

$$\qquad\qquad\qquad\qquad\qquad\qquad\qquad\qquad\qquad\qquad\qquad)(7.45)$$

$$- \frac{d\theta_1^*}{d\xi}(\overline{u}_1^{*2} - \overline{v}_1^{*2}) + [V_2^*U_1^* - U_2^*V_1^*] = 0 \quad)$$

and

$$\frac{d}{d\xi}\{\frac{\theta^*}{8}[8\beta_3 + 4(U_1^* + U_2^*)\beta_2 - 2(U_1^* - U_2^*)^2\beta_1 (U_1^* - U_2^*)^2 \quad)$$

$$\qquad\qquad\qquad\qquad\qquad\qquad\qquad\qquad\qquad\qquad\qquad)$$

$$(U_1^* + U_2^*) + 8(I_3 - I_4)]\} + \{\frac{d\theta_2^*}{d\xi}(\overline{u}_2^{*2} - \overline{v}_2^{*2}) - \quad)$$

$$\qquad\qquad\qquad\qquad\qquad\qquad\qquad\qquad\qquad\qquad)(7.46)$$

$$\frac{d\theta_1^*}{d\xi}(\overline{u}_1^{*2} - \overline{v}_1^{*2})\} \quad)$$

$$\qquad\qquad\qquad\qquad\qquad\qquad\qquad\qquad\qquad\qquad)$$

$$= \frac{-db^*}{d\xi}I_5 - \frac{d\theta^*}{d\xi}I_6 + I_7 - \frac{1}{R_\theta}\beta_4 \quad , \quad)$$

where,

$$\beta_1 = \int_{-\eta_2}^{\eta_1} f(\eta)d\eta \quad ; \quad \beta_2 = \int_{-\eta_2}^{\eta_1} f^2(\eta)d\eta \quad ;$$

- 173 -

$$\beta_3 = \int_{-\eta_2}^{\eta_1} f^3(\eta)\,d\eta \qquad ; \qquad \beta_4 = \int_{-\eta_2}^{\eta_1} \left(\frac{df}{d\eta}\right)^2 d\eta \qquad ;$$

$$I_1 = \int_{-\eta_2}^{\eta_1} \overline{u^*}^2\,d\eta \qquad ; \qquad I_2 = \int_{-\eta_2}^{\eta_1} \overline{v^*}^2\,d\eta \qquad ;$$

$$I_3 = \int_{-\eta_2}^{\eta_1} f\overline{u^*}^2\,d\eta \qquad ; \qquad I_4 = \int_{-\eta_2}^{\eta_1} f\overline{v^*}^2\,d\eta \qquad ;$$

$$I_5 = \int_{-\eta_2}^{\eta_1} (\overline{u^*}^2 - \overline{v^*}^2)\,\frac{df}{d\eta}\,d\eta \quad ; \qquad I_6 = \int_{-\eta_2}^{\eta_1} (\overline{u^*}^2 - \overline{v^*}^2)\,\eta\,\frac{df}{d\eta}\,d\eta$$

$$I_7 = \int_{-\eta_2}^{\eta_1} \overline{u^*v^*}\,\frac{df}{d\eta}\,d\eta \qquad ;$$

$$\eta_1 = \frac{\theta_1^* - b^*}{\theta^*} \qquad ; \qquad \eta_2 = \frac{\theta_2^* - b^*}{\theta^*} \qquad ;$$

and

$$R_\theta = \frac{(U_1 - U_2)\theta}{2\nu}$$

Equation (7.37) becomes,

$$\frac{d}{d\xi}\left\{\theta^*\left[\frac{(U_1^* + U_2^*)}{2}(I_1 + I_2) + (I_3 + I_4) + 2I_8 + I_9\right]\right\} -$$

$$\frac{d\theta_2^*}{d\xi}\left[U_2^*\,\frac{(\overline{u_2^*}^2 + \overline{v_2^*}^2)}{}+ 2\overline{u_2^* p_2^*}\right] - \frac{d\theta_1^*}{d\xi}\left[U_1^*\,(\overline{u^*}^2 + \overline{v^*}^2) + \right.$$

$$2u_1^* p_1^*] - \{\frac{d\theta_2^*}{d\xi}(\overline{u_2^*}^3 + \overline{u_2^* v_2^*}^2) + \frac{d\theta_1^*}{d\xi}(\overline{u_1^*}^3 + \overline{u_1^* v_1^*}^2)\}$$

$$= 2\frac{db^*}{d\xi} I_5 + 2\frac{d\theta^*}{d\xi} I_6 - 2I_7 - \frac{2}{R_\theta} I_{10} , \qquad (7.47)$$

where $I_8 = \int_{-\eta_2}^{\eta_1} \overline{u^* p^*}\ d\eta$; $I_9 = \int_{-\eta_2}^{\eta_1} (\overline{u^*}^3 + \overline{u^* v^*}^2)\ d\eta$;

and $I_{10} = \int_{-\eta_2}^{\eta_1} \{(\overline{\frac{\partial \tilde{u}^*}{\partial \eta}})^2 + (\overline{\frac{\partial \tilde{u}^*}{\partial \xi^*}})^2 + (\overline{\frac{\partial \tilde{v}^*}{\partial \eta}})^2 + (\overline{\frac{\partial v^*}{\partial \xi^*}})^2\}\ d\eta$

where ξ^* is the axial co-ordinate non-dimensionalised with respect to the local thickness, i.e.

$$\xi^* \theta^* = \xi.$$

Equations (7.45), (7.46) and (7.47) are differential equations of the first order in the independent variable ξ. The unknown quantities are $\theta^*(\xi)$, $b^*(\xi)$ and the variation of the I-integrals as functions of ξ. In order to generate the disturbance distributions we will now make use of the results of a linear stability analysis.

7.4 Shape Assumptions for the Fluctuations

Experimental investigations of the transition of a free shear layer from laminar to turbulent flow have shown that the initial development of the flow is dominated by a disturbance of a single frequency. It has been noted, (Browand (1966) ,

Freymuth (1966) and Sato (1956)), that this frequency corresponds
to the frequency at which maximum amplification is predicted using
spatial analysis in linear stability theory. Thus in order to
generate the disturbance terms in the integral equations of the
mean flow we will use a form of linearised stability theory. We
have seen in previous sections that the disturbance distributions
of a single frequency component predicted from the eigensolutions
of the Orr-Sommerfeld equation may be used to represent the
turbulent fluctuations. The integral equations derived above
are exact and the only assumptions to be made in order to solve
the ordinary differential equations are that the mean flow may
be represented in terms of a number of shape parameters and that
the disturbance distributions may be generated from solution
of the Orr-Sommerfeld equation. Thus, as in Chapter 2, we will
introduce a Fourier transform of the velocity and pressure fluctu-
ations such that,

$$\varepsilon(\xi).\hat{u}(\alpha^*,\omega^*;\eta) = \frac{1}{(2\pi)^2} \int\limits_{-\infty}^{\infty}\int \exp\{-i(\alpha^*\xi^* - \omega^*t^*)\}u^*(\xi^*,t^*;\eta)d\xi^*dt^*$$

$$\varepsilon(\xi).\hat{v}(\alpha^*,\omega^*;\eta) = \frac{1}{(2\pi)^2} \int\limits_{\infty}^{\infty}\int \exp\{-i(\alpha^*\xi^* - \omega^*t^*)\}v^*(\xi^*,t^*;\eta)d\xi^*dt^*$$

and

$$\varepsilon(\xi).\hat{p}(\alpha^*,\omega^*;\eta) = \frac{1}{(2\pi)^2} \int\limits_{\infty}^{\infty}\int \exp\{-i(\alpha^*\xi^* - \omega^*t^*)\ p^*(\xi^*,t^*;\eta)d\xi^*dt^*$$

$$(7.48)$$

where $\alpha^* = \alpha\theta^*$, the compex wavenumber and $\omega^* = \omega\theta^*$ is the local
real angular frequency. The amplitude of the disturbances is
then given by,

$$A(\xi) = \varepsilon(\xi) \exp(-\alpha_i^* \xi^*) \tag{7.49}$$

Making use of expressions (7.48) we obtain, as in Chapter 2, an equation for the distribution of $\hat{v}(\eta)$. This is of similar from to the Orr-Sommerfeld equation,

$$(f-\bar{c})(\frac{\partial^2}{\partial\eta^2} - \alpha^{*2})\hat{v} - \frac{\partial^2 f}{\partial\eta^2}\hat{v} + \frac{i}{\alpha^* R_\theta} \{\frac{\partial^4 \hat{v}}{\partial\eta^4} - 2\alpha^{*2}\frac{\partial^2 \hat{v}}{\partial\eta^2} + \alpha^{*4}\hat{v}\} = 0 \tag{7.50}$$

where $\bar{c} = \frac{\omega^*}{\alpha^*} - \frac{(U_1^* + U_2^*)}{2}$.

The boundary conditions on the function $\hat{v}(\eta)$ are,

$$\hat{v} = \frac{\partial\hat{v}}{\partial\eta} = 0 \qquad \text{as} \quad \eta \to \pm\infty \tag{7.51}$$

Equation (7.50), together with the boundary conditions (7.51) constitutes an eigenvalue problem. For a given function $f(\eta)$ we have,

$$\left.\begin{array}{l}\alpha^* = \alpha^*(\omega^*, \theta^*) \\[2mm] \text{and} \quad \hat{v} = \hat{v}(\eta; \omega^*, \theta^*)\end{array}\right\} \tag{7.52}$$

We will now write the integrals I_i, $i = 1 \ldots 10$ as functions of the single parameter θ^* and the amplitude square of the disturbances, $|A|^2$. Then the integrals can be written in the form,

$$I_i = k_i(\theta^*) |A|^2, \quad i = 1, 2 \ldots 10 \tag{7.53}$$

when only the fundamental mode is included the terms associated with the triple correlation will vanish.

Using the definition (7.50), equations (7.45), (7.46) and

(7.47) become three first order differential equations for the

three parameters, θ^*, b^* and $|A|^2$. These equations may be solved

as an initial value problem. In order to define the disturbance

magnitude we will set

$$k_1 + k_2 = 1 \tag{7.54}$$

Using equation (7.53) we may write equations (7.45), (7.46)

and (7.47) as,

$$\frac{1}{4}\Big[-(U_1^* - U_2^*)^2 + 4\beta_2 + 4|A|^2(k_1 - k_2) + 4\theta^*|A|^2 \left(\frac{dk_1}{d\theta^*} - \frac{dk_2}{d\theta^*}\right)\Big]$$

$$\frac{d\theta^*}{d\xi} + \Big[\theta^*(k_1 - k_2)\Big] \frac{d|A|^2}{d\xi} - \frac{|A|^2}{(k_1^* + k_2^*)} \frac{d\theta_2^*}{d\xi} (\bar{u}_2^{*2} - \bar{v}_2^{*2}) -$$

$$\frac{|A|^2}{(k_1^* + k_2^*)} \frac{d\theta_1^*}{d\xi} (\bar{u}_1^{*2} - \bar{v}_1^{*2}) + \Big[V_2^* U_1^* - U_2^* V_1^*\Big] = 0,$$

$$\tag{7.55}$$

$$\frac{1}{8}\Big[8\beta_3 + 4(U_1^* + U_2^*)\beta_2 - 2(U_1^* - U_2^*)^2\beta_1 - (U_1^* - U_2^*)^2(U_1^* + U_2^*)\Big)$$

$$+ 8|A|^2 \{(k_3 - k_4 + k_6) + \theta^*(\frac{dk_3}{d\theta^*} - \frac{dk_4}{d\theta^*})\}\Big] \frac{d\theta^*}{d\xi} + \Big[\theta^*(k_3 - k_4)\Big]$$

$$\frac{d|A|^2}{d\xi} + \Big[|A|^2 k_6\Big] \frac{db^*}{d\xi} + \frac{|A|^2}{(k_1^* + k_2^*)} \{\frac{d\theta_2^*}{d\xi} (\bar{u}_2^{*2} - \bar{v}_2^{*2}) -$$

$$\frac{d\theta_1^*}{d\xi} (\bar{u}_1^{*2} - \bar{v}_1^{*2})\} - \Big[|A|^2 k_7 - \frac{1}{R_\theta}\beta_4\Big] = 0$$

$$\tag{7.56}$$

and

$$\Big[|A|^2\{\frac{U_1^* + U_2^*)}{2} (k_1 + k_2) + (k_3 + k_4 - 2k_6 + 2k_8)\} +$$

$$|A|^2 \theta^* \{ \frac{(U_1{}^* + U_2{}^*)}{2} (\frac{dk_1}{d\theta^*} + \frac{dk_2}{d\theta^*}) + (\frac{dk_3}{d\theta^*} + \frac{dk_4}{d\theta^*} + 2\frac{dk_8}{d\theta^*}) \}] \frac{d\theta^*}{d\xi}$$

$$+ [\theta^* \{ \frac{(U_1{}^* + U_2{}^*)}{2} (k_1 + k_2) + (k_3 + k_4 + 2k_8) \}] \frac{d|A|^2}{d\xi} -$$

$$[2|A|^2 k_5] \frac{db^*}{d\xi} - \frac{|A|^2}{(k_1{}^* + k_2{}^*)} \{ \frac{d\theta_2}{d\xi} [U_2{}^*(\overline{u_2}{}^{*2} + \overline{v_2}{}^{*2}) +$$

$$\overline{2u_2{}^* p_2{}^*}] \} - \frac{|A|^2}{(k_1{}^* + k_2{}^*)} \{ \frac{d\theta_1{}^*}{d\xi} [U_1{}^*(\overline{u_1}{}^{*2} + \overline{v_1}{}^{*2}) + \overline{2u_1{}^* p_1{}^*}] \}$$

$$+ [2|A|^2 k_7 + \frac{2}{R_\theta} |A|^2 k_{10}] = 0,$$

$$(7.57)$$

where $(k_1{}^* + k_2{}^*)$ is the sum of the unnormalised integrals at each station. Let us write,

$$k^* = (k_1{}^* + k_2{}^*) \qquad (7.58)$$

From our calculations for the mean velocity profile we have the values of $\theta_1{}^*$, $\theta_2{}^*$ and θ^*. Thus we may write

$$\theta_1{}^* = \lambda \theta^* \qquad)$$
$$(7.59)$$
and $\qquad \theta_2{}^* = (1 - \lambda)\theta^* \quad)$

Making use of expressions (7.58) and (7.59) we may write the three integral equations in their final form,

$$\frac{1}{4} [-(U_1{}^* - U_2{}^*)^2 + 4\beta_2 + 4|A|^2(k_1 - k_2) + 4\theta^*|A|^2 (\frac{dk_1}{d\theta^*} - \frac{dk_2}{d\theta^*}) -$$

$$\frac{4}{k^*} |A|^2 \{ (1-\lambda)(\overline{u_2}{}^{*2} - \overline{v_2}{}^{*2}) + \lambda(\overline{u_1}{}^{*2} - \overline{v_1}{}^{*2}) \}] \frac{d\theta^*}{d\xi} + [\theta^*(k_1 - k_2)]$$

$$\frac{d|A|^2}{d\xi} + [V_2{}^* U_1{}^* - U_2{}^* V_1{}^*] = 0, \qquad (7.60)$$

$$\frac{1}{8}\bigg[8\beta_3 + 4(U_1{}^* + U_2{}^*)\,\beta_2 - 2(U_1{}^* - U_2{}^*)^2\,\beta_1 - (U_1{}^* - U_2{}^*)^2(U_1{}^* + U_2{}^*)$$

$$+ 8|A|^2\{(k_3 - k_4 + k_6) + \theta^*\,(\frac{dk_3}{d\theta^*} - \frac{dk_4}{d\theta^*})\} + \frac{8}{k^*}\,|A|^2\{(1-\lambda).$$

$$(\overline{u_2}{}^{*2} - \overline{v_2}{}^{*2}) - \lambda(\overline{u_1}{}^{*2} - \overline{v_1}{}^{*2})\}\bigg]\,\frac{d\theta^*}{d\xi} + \bigg[\theta^*(k_3 - k_4)\bigg]\,\frac{d|A|^2}{d\xi} +$$

$$\bigg[\,|A|^2 k_5\bigg]\,\frac{db^*}{d\xi} - \bigg[\,|A|^2\,k_7 - \frac{1}{R_\theta}\,\beta_4\bigg] = 0$$

$$(7.61)$$

$$\bigg[|A|^2\{\frac{(U_1{}^* + U_2{}^*)}{2}\,(k_1 + k_2) + (k_3 + k_4 - 2k_6 + 2k_8)\} + |A|^2$$

$$\theta^*\{\frac{(U_1{}^* + U_2{}^*)}{2}\,(\frac{dk_1}{d\theta^*} + \frac{dk_2}{d\theta^*}) + (\frac{dk_3}{d\theta^*} + \frac{dk_4}{d\theta^*} + \frac{2dk_8}{d\theta^*}) - \frac{|A|^2}{k^*}$$

$$\{(1-\lambda)[(\overline{u_2}{}^{*2} + \overline{v_2}{}^{*2})U_2{}^* + 2\overline{u_2^* p_2^*}] + \lambda[(\overline{u_1}{}^{*2} - \overline{v_1}{}^{*2})U_1{}^* + 2\overline{u_1^* p_1^*}]\}\bigg]\frac{d\theta^*}{d\xi}$$

$$+ \bigg[\theta^*\{\frac{(U_1{}^* + U_2{}^*)}{2}\,(k_1 + k_2) + (k_3 + k_4 + 2k_8)\}\bigg]\,\frac{d|A|^2}{d\xi} -$$

$$\bigg[2|A|^2 k_5\bigg]\,\frac{db^*}{d\xi} + \bigg[2|A|^2 k_7 + \frac{2}{R_\theta}\,|A|^2 k_{10}\bigg] = 0$$

$$(7.62)$$

Equations (7.60), (7.61) and (7.62) are first order differential equations for the three unknowns, θ^*, b^* and $|A|^2$. In the next section we will describe the calculation of the integral functions, k_i.

7.5 Calculation of the Integral Functions

In order to evaluate the integral functions the Orr-Sommerfeld equation (7.50) is solved and the distributions of fluctuating

components are calculated from the eigensolutions. The measurements of Sato (1959) show that the natural frequency of the fundamental mode of the fluctuating field is 242 Hz. The Reynolds number used is 4.2374×10^5 which corresponds to a reference plate length of 150 mm. With the frequency fixed at this value the eigenvalues and eigenfunctions of the Orr-Sommerfeld equation may be determined as functions of the momentum thickness, $\theta*$. The amplification factor, $-\alpha_i*$, is shown as a function of $\theta*$ in Figure 43. The measurements of Sato (1956, 1959) were made for the separated shear layer, i.e. $U_2* = 0$, thus our calculations have been made for one stream stationary. Figure 43 shows that the maximum amplification occurs at a thickness $\theta*$ of approximately .0175. The distribution across the shear layer of $\overline{u*}^2$ shows the features of the disturbance profile measured by Sato (1959), Freymuth (1966) and Browand (1966). We may see that the distribution has a sharp minimum at $y/\theta* = 1.4$ which corresponds to a change in phase of the $\overline{u}*$-fluctuation. The integral functions are then evaluated from the eigensolutions of the Orr-Sommerfeld equation and are normalised such that

$$\int_{-\eta_2}^{\eta_1} (\overline{u*}^2 + \overline{v*}^2) \, d\eta = k_1 + k_2 = 1 \tag{7.63}$$

The integral functions are then known functions of $\theta*$ and the three differential equations for $\theta*$, $b*$ and $|A|^2$ may be solved as an initial value problem.

7.6 Results and Discussion

The solution of equations (7.60), (7.61) and (7.62) presents

a tedious computational problem. However we shall see below that by appropriate simplification of the differential equations much useful information about the influence of finite amplitude disturbances on the growth of the mixing layer may be obtained.

Firstly we will assume that the disturbance functions are zero outside the limits of integration. We have seen from our previous chapter on the turbulent problem that agreement between experiment and theory in, for instance, the case of the $\overline{u*}^2$ distribution is good over the centre of the layer but, whereas the predicted profile exhibits two peaks outside this region the experimental results do not. Secondly, we will simplify the energy equations so as only to consider the kinetic energy of the disturbances and to disregard the ξ-derivatives of certain shape parameters. We know from the measurements of Browand (1966) that the value of $b*$ is small and that, after a period of development, which will be influenced by the experimental situation, the value of $\frac{db*}{d\xi}$ is small. Thus we will write the three differential equations as,

$$\frac{d}{d\xi}\left[(\beta_2 - 1)\theta* + |A|^2(k_1 - k_2)\right] = -2V_2* = \frac{-\gamma_1}{\sqrt{\xi}}. \qquad (7.64)$$

$$\frac{d}{d\xi}\left[\theta*(\beta_3 + \beta_2 - \beta_1 - 1)\right] = |A|^2 k_7 - \frac{\beta_4}{R.\theta*}, \qquad (7.65)$$

$$\frac{d}{d\xi}\left[\theta*|A|^2.(k_1 + k_2)\right] = 2|A|^2 k_7 - \frac{2|A|^2 k_{10}}{R.\theta*} \qquad (7.66)$$

We may see from equation (7.64) that when $|A|^2 \to 0$, i.e. for laminar flow, then $\frac{d\theta*}{d\xi} \alpha \frac{1}{\sqrt{\xi}}$ or,

- 183 -

$$\theta^* = \gamma_3 \sqrt{\xi} \qquad\qquad (7.67)$$

In equations (7.65) the left hand side represents the derivative with ξ of the energy of the mean flow. The value of k_7 is always negative and we can see that the disturbed flow is extracting energy from the mean flow. In equation (7.66) the left hand side represents the derivative with ξ of the energy of the disturbed flow. It may be seen from the right hand side of this equation that the shear stresses are feeding energy to the disturbances whilst the viscous forces are applying damping. Combining equations (7.65) and (7.66) we obtain,

$$\frac{1}{|A|^2} \frac{d|A|^2}{d\xi} = -\frac{k_7}{\theta^*}\{2 - \frac{|A|^2}{\gamma_2}\} - \frac{1}{R_0\theta^{*2}}\{2 k_{10} + \frac{\beta_4}{\gamma_2}\} , \qquad (7.68)$$

where $\gamma_2 = 1 + \beta_1 - \beta_2 - \beta_3$.

Rearranging this equation we may write

$$\frac{d|A|^2}{d\xi} = a_1 |A|^2 - a_2 |A|^4 - \frac{a_3}{R} |A|^2 \qquad\qquad (7.69)$$

where $a_1 = \dfrac{-2k_7}{\theta^*}$, $a_2 = \dfrac{-k_7}{\theta^*\gamma_2}$ and $a_3 = \dfrac{1}{\theta^{*2}}\{2k_{10} + \dfrac{\beta_4}{\gamma_2}\}$ (7.70)

Equation (7.69) is to be compared with equation (2.15) of Stuart (1958) for the temporal growth of the disturbance amplitude. In our case the values of a_1, a_2 and a_3 are functions of ξ. It can be seen that when the disturbance magnitude is of order $R^{-\frac{1}{2}}$ then the disturbance terms may no longer be considered as negligible.

We may also note that the first two terms on the right hand side of equation (7.69) are of opposite sign which means there will be a value of $|A|^2$ for which $\frac{d|A|^2}{d\xi} \to 0$. From equation (7.68) it is clearer that this value is given by $|A|^2 = 2\gamma_2$.

Having evaluated k_i as a function of θ^* we will now solve equations (7.64) and (7.68) simultaneously to evaluate the growth of θ^* and $|A|^2$ with ξ. The required inputs to the computer solution are the starting values of ξ, θ^* and $|A|^2$. A number of different values of parameters have been considered and their effect noted. The equations are solved using a Runge-Kutta integration scheme and linear interpolation to evaluate the co-efficients at each point. The starting value of ξ was set at .01, which corresponds to $x = 1.5$ mm and θ^* was started at a value of .004, which corresponds to a value of θ of 6 mm.

The growth of the disturbance amplitude, $|A|^2$ is shown in Figure 45 for a number of different initial values of $|A|^2$. As is to be expected the smaller the initial value of $|A|^2$ the further downstream will the sudden growth occur. It may also be seen that the amplitude limit is reached as $|A|^2 \to 1.257$ the value of $2\gamma_2$ being 1.2628. The effect of the initial disturbance amplitude on the growth of the mixing layer thickness, θ^* is shown in Figure 46. Once again the smaller the initial magnitude of the disturbance the longer will be the transition. We may also note that the smaller the initial amplitude of the disturbances the smoother is the transition. Up to the point of sudden growth of the mixing layer the rate of growth of θ^* is inversely proportional to $\sqrt{\xi}$.

- 185 -

The two quantities measured by Sato with which

comparisons may be made are the value of θ^* and the energy

density of the $\overline{u^*}$-fluctuation defined by,

$$E_\theta = \int_{-\infty}^{\infty} \overline{u^*}^2 \, d\eta \qquad (7.71)$$

This function is shown in Figure 47 for various initial disturbance

amplitudes. The maximum value reached is approximately .75 for

all initial values of $|A|^2$. The experimental results of Sato give

a value in the region of .6, however in the case of the wake there

existed a possible integration error of 10%. We may also note

that in Sato's experiments the sub-harmonic of the fundamental

occurred at a position short of the longitudinal point at which

the maximum amplitude was reached. The distance over which the

energy density grew from zero to a maximum value in Sato's measure-

ments appears independent of the Reynolds number based on the

plate length and free stream velocity. In our calculations the

equivalent non-dimensional distance is given by $\xi \simeq .1$ which

when dimensionalised with respect to $L^* = 150$ mm gives 15 mm.

The value given by Sato is up to 75 mm and thus we see that the

rapid growth of the disturbances is faster in our calculations.

It is clear that some mechanism is required to damp the growth

of the solutions of the simplified set of equations (7.64) and

(7.68). Before examining the effect of the terms omitted from

the complete equations let us look at the effect of increasing

the viscous dissipation. In order to do this we will examine

the effect on E_θ of increasing and decreasing the Reynolds

number.

The effect on the growth of E_θ for four different values

of Reynolds number is shown in Figure 48. The effect is similar

to that caused by varying the initial value of the disturbance

amplitude. This can be clearly seen from equation (7. .) where

decreasing the Reynolds number has the effect of increasing the

disturbance magnitude in the viscous dissipation term. However

the lower Reynolds number has a continuing effect through the

transition and reduces the eventual equilibrium value of the

energy density. For a reduction of order 10 in the Reynolds

number the equilibrium value of the energy density decreases

from 0.75 to 0.61. This latter value agrees more closely with

the measurements of Sato, however the transition length is still

too small in comparison with measurements. There is a slight

increase in the transition length as the Reynolds number is

decreased. The use of a variable Reynolds number to isolate the

effect of viscous dissipation may be used as at high Reynolds

numbers the disturbance distribution integrals will be nearly

independent of Reynolds number and will approach the inviscid

limit.

Let us consider the possible influence of the terms

omitted in our simplification of the energy equations. The term

omitted from the left hand side of the fluctuating energy

equation is

$$\frac{d}{d\xi} \left[\theta^* |A|^2 (k_3 + k_4 + 2k_8) \right] \tag{7.72}$$

From the calculated values we find that in the range $0 < \theta^* < $ •

.025 the value of k_8 is nearly constant and equals $-.25$. The

sum of k_3 and k_4 is also nearly constant in this range and is

approximately equal to .4. Thus the effect of this term is a factor of 10 smaller than the kinetic energy terms k_1 and k_2. The term omitted from the left hand side of the mechanical energy equation is

$$\frac{d}{d\xi}\left[\theta^*|A|^2(k_3-k_4)\right] = \left[|A|^2\{\theta\frac{d(k_3-k_4)}{d\theta^*} + (k_3-k_4)\}\right]\frac{d\theta^*}{d\xi}$$

$$+\theta^*(k_3-k_4)\frac{d|A|^2}{d\xi} . \tag{7.73}$$

As $\theta^* = .015$ which for $|A|^2_{\xi_0} = 1 \times 10^{-6}$ is in the centre of the fast-growing region, the value of (k_3-k_4) is zero. $d(k_3-k_4)/d\theta^*$ is negative and it is clear that this term will increase the value of γ_2 which will lead to a higher limiting amplitude for the disturbance. However, it will also lead to a decrease in the rate of growth of the momentum thickness. The terms omitted from the right hand side of the equation represent the integrated product of $\frac{\partial U}{\partial x}$ and $(\overline{u^*}^2 - \overline{v^*}^2)$. Experimental results show that $\overline{u^*}^2$ and $\overline{v^*}^2$ are nearly equal in the mixing layer and as the value of $\partial U/\partial x$ will be small those terms are unlikely to affect the solution.

The phase velocity of the disturbances given by $c_r = \omega_r/\alpha_r$ is shown in Figure 49. The measurements of Browand (1966) give the phase velocity as $1.16 \pm .22$, in our calculations the phase velocity varies between 1.7 and 1.1. There appears to be no consistency in the measurements of Browand as to the relationship between phase velocity and longitudinal distance. The measurements of Sato for the wake show a sharp change in the phase

velocity from the laminar to the turbulent regions.

Let us return to the amplitude growth of the disturbances. The experiments of Freymuth (1966) show that the growth rate of the main peak in the $\overline{u^*}$ fluctuation is independent of the applied sound pressure and increases ten times in a distance of approximately 30 θ_m where θ_m is the momentum thickness of the layer at the separation point. Our definition of θ^* is different from that of Freymuth, the relation between the two being $\theta^* = 4\theta$. Thus our calculations should show a tenfold increase in a distance of approximately $8\theta_o^*$. With $\theta_o^* = .004$ this distance is .032, and, as is shown on our Figure 45 for a value of $|A|_o^2 = 1 \times 10^{-6}$ the distance is .038. The same growth distance is found for the other values of initial disturbance magnitude. However this calculation may only be used as a quantitative check on the growth rate as calculations performed with different values of θ_o^* gave similar growth distances suggesting that the rate of growth is independent of the initial thickness. The smaller the initial thickness, the longer the longitudinal distance before transition. This may be seen in a plot of momentum thickness against ξ for various values of θ_o^* in Figure 50. A decrease in the value of θ_o^* results in an initial decrease in the Reynolds number based on momentum thickness and, as may be seen from Eqn. (7.65), a consequent increase in the value of the viscous dissipation term.

7.7. Conclusions

We have seen how the development of the mixing layer from laminar to turbulent flow may be determined from a simplified set

of momentum and energy equations. The growth of the mixing layer

is shown to be proportional to $\xi^{+\frac{1}{2}}$ for infinitessimal disturbances.

The point of transition occurs at a point which is a function of

the initial amplitude of the disturbances, the flow Reynolds number

and the initial momentum thickness. A decrease in Reynolds number

leads to a lower limiting value for the energy density. The

amplitude of the disturbances is shown to grow very rapidly and

reaches a limiting value which, in the simplified equations, is

a function of the mean velocity integrals. The limiting magnitude

of the disturbances does not occur at a value of θ^* corresponding

to the neutral mode as was the case for the wake, Ko, Kubota and

Lees (1970). The rate of growth of the disturbance amplitude

was shown to be of the same order as the measurements of Freymuth

(1966) but independent of the initial thickness of the layer.

The results of Sato (1956), however, indicate a rate of growth

of the energy density less than our calculated values. The

limiting value of energy density is a function of the Reynolds

number and agreement between Sato's value and the calculations

occurs for a value of R of one-tenth of the real value. The

maximum amplitude of the energy density is independent of the

initial values of disturbance magnitude and momentum thickness.

The phase velocity of the disturbances decreases from a value

of 1.7 to a value of 1.1 through the transition region.

8. Conclusions

The following conclusions may be drawn from our study of
the laminar and turbulent mixing of two parallel streams which
has been considered in four separate sections.

The analysis of the mean equations of laminar mixing may
be solved numerically using an iterative solution. No assumptions,
other than the normal boundary layer assumptions are required.
For the solution of the mean turbulent mixing problem assumptions
have to be made as to the description of the Reynolds stresses.
It is found that the assumption of an eddy viscosity connecting
Reynolds stresses to mean shear may be successfully employed. An
exponential distribution of eddy viscosity of the form
$\nu_T = \nu_0 \exp(-A\xi^2)$ is used, where ξ is a similarity co-ordinate.
A value of the constant A of 0.7 is found to give good agreement
between measured and calculated velocity profiles. The assumption
that the eddy viscosity distribution is symmetric about a point
corresponding to the position of maximum shear gives better results
than an assumption of symmetry about the x axis. The distribution
of eddy viscosity coincides with the distribution of intermittency
which indicates that the eddy viscosity may be considered constant
in regions of the flow which are fully turbulent. The relationship
between turbulent Reynolds number and velocity ratio of the two
streams is found on the basis of the size of eddies in various shear
flows. The same analysis leads to a relationship between rate of
spread of the layer and velocity ratio the result of which agrees
with the analysis of Abramovitch. The ratio of maximum value of
eddy viscosity to kinematic viscosity is taken from experimental
results and is a function of velocity ratio. The similarity form

- 191 -

of the momentum equation is solved numerically, using the above assumptions, and the results agree with experimental results for cases of zero and finite velocity of one stream.

The stability of the mixing layer between two streams may be studied by considering the growth of small disturbances in the laminar flow. The equation for the calculation of stability is formed by considering the triple Fourier transform of the fluctuating equations of momentum and continuity. The solution of the resulting boundary value problem determines whether disturbances will grow or decay. The stability problem may be posed as either a spatial or temporal one. In the former case disturbance frequency is real and wavenumber and eigenvalue are complex. In the temporal case the wavenumber is real and the frequency and eigenvalue are complex. The results of the analysis show that the laminar shear layer is unstable, in both spatial and temporal senses, to infinitesimal disturbances at all Reynolds numbers. This result is found to be a consequence of the assumption of parallel flow. It is found that for the case of two streams having finite velocity the results of spatial and temporal analyses lead to similar results for eigenfunctions and amplification factors. It may be shown that the case of one stationary stream is a special case of the general problem of the mixing of two streams and that as the velocity of the two streams tends to an equal value the results of spatial and temporal analyses coincide. A correction to the amplification factors for non-parallel flow may be made by considering the interaction energy between mean flow and disturbances. The resulting correction factor is found to be a function of Reynolds number and

the corrected values of amplification lead to a critical

Reynolds number of 12.3.

The structure of the turbulent mixing layer is examined on

the basis of a linear model. This provides a useful guide to

the structure of the flow. The calculated convection and phase

velocities agree with available experimental results. The rate

of growth or decay of eddies as a function of wavenumber

follows the trend exhibited in the boundary layer where the

larger eddies decay more slowly than the smaller. For the shear

layer the higher wavenumber disturbances grow more slowly than

the lower. The fluctuating velocity field is predicted from the

eigensolution of the homogeneous equation for turbulent shear flow

corresponding to the fastest growing mode. The distribution of

longitudinal velocity fluctuation agrees with experimental results

but the transverse velocity fluctuation exhibits a trough at the

centre of the layer and is a factor of two smaller than experimental

results. The same feature is exhibited by the distribution of

linear fluctuating pressure. It is shown that the effect of obli-

quity of the waves only reduces the magnitude of the transverse

velocity fluctuation. It is shown that at the critical layer where

the phase velocity equals the local mean velocity the non-linear

terms in the equations of motion may not be neglected. It may be

argued that the non-linear term will force a form of isotropy on

the fluctuating field. The calculated distributions of shear

stress and pressure diffusion agree well with measured or indi-

rectly measured experimental values. The distribution of the

shear correlation coefficient is nearly a constant value of

unity across the mixing layer. The reason for this high value
is the antiphase of u and v velocity fluctuations predicted by
linearised theory. The pressure diffusion predicted by linear
analysis is close to the expected experimental results. The
linear analysis serves as a guide to those components of the
turbulence governed by non-linearity.

The development of the mixing layer is examined from a
simplified solution of equations of momentum and energy. The
mean and fluctuating components of the flow may be expressed in
terms of a number of shape parameters. The initial growth of the
mixing layer is proportional to the square root of longitudinal
distance. The point of transition from laminar to turbulent flow
is a function of the initial amplitude of the disturbances, the
initial momentum thickness and the flow Reynolds number. The
amplitude of the disturbances grows very rapidly to reach a
limiting value which is a function of integrals of the mean flow.
The rate of growth of the disturbances predicted follows experi-
mental results in one instance but the measurements are not con-
clusive. The limiting value of energy density is predicted to be
higher than measured results though a reduction in flow Reynolds
number reduces the predicted value. The phase velocity falls from
a value of 1.7 to 1.1 through the transition region.

This work has indicated those processes in turbulent flow
governed by linear and non-linear processes. The role of the non-
linear terms is shown as both amplifying and amplitude limiting.
The work may be seen to be readily extendable to compressible flows
which will only add to the complexity of the equations to be solved.

It is to be hoped that an analysis of the sort presented above will aid the understanding of turbulence and its effects. The application to noise generation by turbulence of this analysis presents an interesting problem.

APPENDIX I

Discussion of the Third Boundary Condition for the Mixing of Two Parallel Streams.

We have noted in our analysis in Chapter 3 that the equation for the stream function describing the mixing of two parallel streams is of the third order. It will thus require three boundary conditions. Two of these are immediately apparent, namely that the x-component of velocity must reach that of the free stream on each side of the mixing layer,

$$U \to U_1 \quad \text{as} \quad y \to \infty \tag{AI.1}$$

$$U \to U_2 \quad \text{as} \quad y \to -\infty, \tag{AI.2}$$

where U_1 and U_2 are the velocities of the upper and lower streams respectively. The third boundary condition necessary for the complete solution of the third-order differential equation has been considered by a number of workers. Kuethe (1935) made use of the third boundary condition proposed by von Karman based on the balancing of transverse momentum, though Kuethe made no attempt to justify this proposition. The most complete discussion, of the proper determination of the third boundary condition, so far presented was by Ting (1959). Ting made use of matched asymptotic expansions to derive the appropriate boundary conditions for compressible and incompressible mixing. In his paper he found it necessary to match second order pressures across the mixing layer, for the case of incompressible mixing, in order to derive the third boundary condition. It

is shown below that this was not necessary and was due to an
analytical error in Ting's paper.

Let us first consider a laminar mixing region and write
the velocity components and pressure in the free stream above
the mixing layer as series in powers of ε where $1/\varepsilon$ is of
the order of the square root of the Reynolds number.

$$U_1(x,y) = U_s\{(U_1/U_s) + \varepsilon\ U_1^{(1)}\ (x/L,y/L) + \varepsilon^2\ U_1^{(2)}\ (x/L,y/L) + ...\} \quad (AI.3)$$

$$V_1(x,y) = U_s\{\varepsilon\ V_1^{(1)}\ (x/L,\ y/L) + \varepsilon^2\ V_1^{(2)}\ (x/L,y/L) + ...\} \quad (AI.4)$$

$$P_1(x,y) = P_o\{1 + \varepsilon\ p_1^{(1)}\ (x/L,y/L) + \varepsilon^2\ p_1^{(2)}\ (x/L,y/L) + ...\} \quad (AI.5)$$

where, $U_s = \dfrac{U_1 + U_2}{2}$, L is a reference length, $\varepsilon^2 = \dfrac{\nu_o}{U_s L}$,

ν_o is the kinematic viscosity of the parallel streams

and P_o is the pressure of the parallel streams.

The corresponding expansions for the lower stream are,

$$U_2(x,y) = U_s\{(U_2/U_s) + \varepsilon\ U_2^{(1)}\ (x/L,y/L) + \varepsilon^2\ U_2^{(2)}(x/L,y/L) + ...\} \quad (AI.6)$$

$$V_2(x,y) = U_s\{\varepsilon\ V_2^{(1)}(x/L,y/L) + \varepsilon^2\ V_2^{(2)}\ (x/L,y/L) + ... \quad \} \quad (AI.7)$$

$$P_2(x,y) = P_o\{1 + \varepsilon\ P_2^{(1)}\ (x/L,y/L) + \varepsilon^2\ P_2^{(2)}\ (x/L,y/L) + ... \quad \} \quad (AI.8)$$

In the preceding expansions the subscripts 1 and 2 refer to
quantities in the upper and lower streams respectively and the
superscripts define the order of the term in the series expansion
in powers of ε.

The flow outside the mixing layer is irrotational and
inviscid and we may write Bernoulli's equation for the upper

stream in terms of the series (AI.3, 4, 5),

$$\frac{P_o}{\rho_o} + \frac{U_1^2}{2} = \frac{P_o}{\rho_o} + \frac{\epsilon \ P_o P_1^{(1)}}{\rho_o} + \frac{\epsilon^2 \ P_o P_1^{(2)}}{\rho_o} + \ \cdots$$

$$+ \frac{U_s^2}{2} \{ (\frac{U_1}{U_s})^2 + \frac{2\epsilon U_1 U_1^{(1)}}{U_s} + \epsilon^2 U_1^{(1)^2} + \frac{2\epsilon^2 U_1 U_1^{(2)}}{U_s} + \cdots \} \qquad \text{(AI.9)}$$

$$+ \frac{U_s^2}{2} \{ \epsilon^2 V_1^{(1)^2} + \ \cdots \cdots \}$$

where ρ_o is the density of the two parallel streams.

Collecting coefficients of like powers of ϵ we obtain,

$$\frac{P_o}{\rho_o} + \frac{U_1^2}{2} = \frac{P_o}{\rho_o} + \frac{U_1^2}{2}$$

$$P_1^{(1)} = -\{ \frac{\rho_o U_1 U_s}{P_o} \} \ U_1^{(1)} \ (x/L, y/L), \qquad \text{(AI.10)}$$

$$P_1^{(2)} = - \frac{\rho_o U_s^2}{2 P_o} \{ [U_1^{(1)}]^2 + [V_1^{(1)}]^2 \} - \{ \frac{\rho_o U_1 U_o}{P_o} \} \ U_1^{(2)} \ (x/L, y/L), \text{(AI.11)}$$

$$\circ \bullet \circ \bullet \circ \bullet \circ \bullet \circ \bullet \circ \bullet \circ \bullet \circ \bullet \circ \bullet$$

Similar expressions will exist for the pressure terms in the lower stream. We note in particular that

$$P_2^{(1)} = - \{ \frac{\rho_o U_2 U_s}{P_o} \} \ U_2^{(1)} \ (x/L, y/L) \qquad \text{(AI.12)}$$

It can be seen from equations (AI.10) and (AI.12) that the first order pressures on each side of the layer are proportional to the product of axial velocity and the first order x-component of velocity. It will be shown that the first order x-component of velocity is a function of the transverse velocity at the edge of the layer and in this way the boundary condition proposed by von Karman is satisfied.

Let us expand the velocity components and pressure inside the mixing layer as follows.

$$U(x,y) = U_s\{U^{(o)}(x,Y) + \varepsilon\, U^{(1)}(x,Y) + \ldots \} \qquad \text{(AI.13)}$$

$$V(x,y) = \varepsilon U_s\{V^{(o)}(x,Y) + \varepsilon\, V^{(1)}(x,Y) + \ldots \} \qquad \text{(AI.14)}$$

and

$$P(x,y) = P_o\{P^{(o)}(x,Y) + \varepsilon P^{(1)}(x,Y) + \ldots \} \qquad \text{(AI.15)}$$

where $Y = y/\varepsilon$ is the stretched co-ordinate inside the mixing layer.

The relationships between quantities within the layer and those in the flow above the mixing layer are,

$$\lim_{Y\to\infty} U^{(o)}(x/L,\, Y/L) = U_1/U_o \qquad \text{(AI.16)}$$

$$\lim_{Y\to\infty} U^{(1)}(x/L,\, Y/L) = U_1^{(1)}(x/L, +0) \qquad \text{(AI.17)}$$

$$\bullet\,\circ\,\bullet\,\circ\,\bullet\,\circ\,\bullet\,\circ\,\bullet\,\circ\,\bullet\,\circ\,\circ\,\bullet\,\circ\,\bullet\,\circ\,\bullet\,\circ\,\bullet\,\circ\,\circ\,\bullet$$

$$\lim_{Y\to\infty} V^{(o)}(x/L,\, Y/L) = V_1^{(1)}(x/L, +0) \qquad \text{(AI.18)}$$

$$\bullet\,\circ\,\bullet\,\circ\,\bullet\,\circ\,\bullet\,\circ\,\bullet\,\circ\,\circ\,\bullet\,\circ\,\circ\,\bullet\,\circ\,\circ\,\bullet\,\circ\,\circ\,\bullet\,\circ\,\circ$$

and

$$\lim_{Y\to\infty} P^{(o)}(x/L,\, Y/L) = 1 \qquad \text{(AI.19)}$$

$$\lim_{Y\to\infty} P^{(1)}(x/L,\, Y/L) = P_1^{(1)}(x/L, +0) \qquad \text{(AI.20)}$$

$$\bullet\,\circ\,\bullet\,\circ\,\bullet\,\circ\,\bullet\,\circ\,\bullet\,\circ\,\circ\,\circ\,\bullet\,\circ\,\circ\,\bullet\,\circ\,\circ\,\bullet\,\circ\,\bullet\,\circ$$

The corresponding relationships between the quantities inside the layer and those in the flow below the mixing layer are,

$$\lim_{Y \to -\infty} U^{(o)}(x/L, Y/L) = U_2/U_o \qquad \text{(AI.21)}$$

$$\lim_{Y \to -\infty} U^{(1)}(x/L, Y/L) = U_2^{(1)}(x/L, -0) \qquad \text{(AI.22)}$$

$$\bullet \circ \circ \circ \circ \bullet \bullet \bullet \bullet \bullet \circ \circ \circ \circ \circ \circ \circ \circ \circ \circ \circ \bullet \bullet$$

$$\lim_{Y \to -\infty} V^{(o)}(x/L, Y/L) = V_1^{(1)}(x/L, -0) \qquad \text{(AI.23)}$$

$$\bullet \circ \circ \circ \circ \circ \bullet \bullet \bullet \bullet \bullet \circ \circ \circ \bullet \bullet \circ \bullet \bullet \bullet \circ \bullet \bullet$$

and

$$\lim_{Y \to -\infty} P^{(o)}(x/L, Y/L) = 1 \qquad \text{(AI.24)}$$

$$\lim_{Y \to -\infty} P^{(1)}(x/L, Y/L) = P_2^{(1)}(x/L, -0) \qquad \text{(AI.25)}$$

$$\circ \bullet \bullet \bullet \bullet \bullet \bullet \bullet \circ \circ \circ \circ \circ \circ \bullet \bullet \circ \bullet \bullet \bullet \circ$$

Substituting the series (AI.13, 14, 15) into the Navier-Stokes equations and collecting coefficients of like powers of ε then we obtain from the y-component equation,

$$\frac{\partial P^{(o)}}{\partial Y} = 0 , \qquad \text{(AI.26)}$$

$$\frac{\partial P^{(1)}}{\partial Y} = 0 , \qquad \text{(AI.27)}$$

and $U^{(o)} \dfrac{\partial V^{(o)}}{\partial x} + V^{(o)} \dfrac{\partial V^{(o)}}{\partial Y} = - \dfrac{P_o}{\rho_o U_s^2} \dfrac{\partial P^{(2)}}{\partial Y} + \dfrac{\partial^2 V^{(o)}}{\partial Y^2}$ $\qquad \text{(AI.28)}$

A.I.5.

Then equation (AI.27), together with the matching conditions (AI.20) and (AI.25), leads to,

$$P_1^{(1)}(x/L, +0) = P_2^{(1)}(x/L, -0) \qquad (AI.29)$$

Equation (AI.29) states the condition that there is no net first order pressure difference across the mixing layer. This compatability condition serves to provide the necessary third boundary condition.

In a linear theory we may represent the shear layer as a distribution of sinks lying on the x-axis. Then according to thin aerofoil theory we have,

$$U^{(1)} - iV^{(1)} = \frac{1}{\pi} \int_0^\infty \left\{ \frac{V^{(o)}(\omega/L, \infty)}{(z-\omega)} \right\} d\omega, \qquad (AI.30)$$

(see Tsien (1956)), where $z = x + i y$

In order to evaluate the integral in equation (AI.30) we will now introduce a stream function $\psi^{(o)}(x,y)$ given by,

$$\psi^{(o)}(x,y) = \sqrt{x\, U_s\, \nu_o}\; f(\eta), \qquad (AI.31)$$

where η is a similarity variable given by,

$$\eta + (Y/\sqrt{xL}) - \eta_o \qquad (AI.32)$$

The asymptotic behaviour of the stream function and the velocity components are,

$$f(\eta) \to \left(\frac{U_1}{U_s}\right)(\eta + \alpha),$$

A.I.6.

$$U^{(o)} \to U_1, \qquad\qquad\qquad \eta \to +\infty \qquad (AI.33)$$

$$V^{(o)} \to \tfrac{1}{2}\sqrt{\frac{\nu U_s}{x}} \, (\eta_o - \alpha)\left(\frac{U_1}{U_s}\right),$$

$$f(\eta) \to \left(\frac{U_2}{U_s}\right)(\eta + \beta),$$

$$U^{(o)} \to U_2, \qquad\qquad\qquad \eta \to -\infty \qquad (AI.34)$$

$$\text{and} \qquad V^{(o)} \quad \tfrac{1}{2}\sqrt{\frac{\nu U_s}{x}} \, (\eta_o - \beta)\left(\frac{U_2}{U_s}\right),$$

where α and β are known constants of the similar solution and the inclusion of η_o permits $f'(o) = 1$.

Then for the flow above the mixing layer from (AI.30) and (AI.33) we have,

$$U_1^{(1)} - i\, V_1^{(1)} = -\frac{U_1 \alpha_1}{\pi} \int_0^\infty \frac{d\omega}{\sqrt{\omega}\,(z-\omega)}, \qquad (AI.35)$$

where $\alpha_1 = -\dfrac{1}{2U_s}(\eta_o - \alpha)\sqrt{\dfrac{\nu_o}{U_s}}$

The solution of equation (AI.35) is

$$U_1^{(1)} - i\, V_1^{(1)} = \frac{-iU_1\alpha_1}{\sqrt{z}} + \frac{U_1\alpha_1}{\pi\sqrt{z}} \log\left\{\frac{1+\sqrt{z}}{1-\sqrt{z}}\right\} \qquad . \qquad (AI.36)$$

It is to be noted that in his analysis Ting only noted the singularity at $\omega = z$ in the integrand of (AI.35) and not the singularity where $\sqrt{\omega} = 0$. This led in the limit as $y \to 0$, $U_1^{(1)} = 0$ as the right hand side of equation (AI.36) is then entirely imaginary. As $y \to +0$ we have from equation (AI.36) that

A.I.7.

$$U_1^{(1)}(x/L, +0) = \frac{U_1 \alpha_1}{\pi \sqrt{x}} \log \left\{ \frac{1 + \sqrt{x}}{1 - \sqrt{x}} \right\} \qquad \text{(AI.37)}$$

Making use of equation (AI.10) with (AI.37) we obtain,

$$P_1^{(1)}(x/L, +0) = -\left\{ \frac{\rho_o U_s}{P_o} \right\} \frac{U_1^2 \alpha_1}{\pi \sqrt{x}} \log \left\{ \frac{1 + \sqrt{x}}{1 - \sqrt{x}} \right\} \qquad \text{(AI.38)}$$

Similarly when $y \to -0$ we may obtain,

$$P_2^{(1)}(x/L, -0) = \left\{ \frac{\rho_o U_s}{P_o} \right\} \frac{U_2^2 \alpha_2}{\pi \sqrt{x}} \log \left\{ \frac{1 + \sqrt{x}}{1 - \sqrt{x}} \right\} \qquad \text{(AI.39)}$$

where $\alpha_2 = -\frac{1}{2U_s} (\eta_o - \beta) \sqrt{\frac{\nu_o}{U_s}}$.

Then from equations (AI.38) and (AI.39) with the compatability condition (AI.29) we have,

$$\frac{U_2^2 \alpha_2}{U_s \sqrt{x}} + \frac{U_1^2 \alpha_1}{U_s \sqrt{x}} = 0,$$

with equations (AI.33) and (AI.34) we may finally write this condition

$$U_1 V^{(o)}(x/L, \infty) + U_2 V^{(o)}(x/L, -\infty) = 0. \qquad \text{(AI.40)}$$

This equation constitutes the third boundary condition on our third-order differential problem. It may be seen that this agrees with the proposition of von Karman equation (3.2). However, it is to be noted that this condition is not necessarily correct for higher order matching of pressures across

A.I.8.

the mixing layer. We may also note that if we introduce an

eddy viscosity solution for the turbulent mixing problem and

then introduce an appropriate similarity factor we may also

derive the result (AI.40) for the turbulent problem.

APPENDIX II

The Use of Orthogonalisation Procedure in Numerical Solution of

Boundary-Value Problems

In this section we will consider a simple procedure for the
numerical solution of ill-conditioned boundary-value problems.
Included in this class of problem is the solution of the Orr-
Sommerfeld equation.

Let us firstly introduce the idea of orthogonalisation of
vectors. A set of vectors are linearly dependent if they may
be written,

$$\sum_{m=1}^{n} \lambda_m \underset{\sim}{V}_m = 0,$$ (A.II.1)

where $\underset{\sim}{V}_m$ are the vectors and λ_m are arbitrary numbers at least
one of which is non-zero. If this relation (A.II.1) is not
satisfied then the vectors are said to be linearly independent.
A system of unit vectors $\underset{\sim}{e}_n$ which satisfy the relation,

$$\underset{\sim}{e}_i^2 = 1, \quad \underset{\sim}{e}_i \underset{\sim}{e}_j = 0, \quad i \neq j,$$ (A.II.2)

form an orthogonal system. We may see that an orthogonal set
is also linearly independent.

We may form an orthogonal set of vectors from any arbitrary
system of linearly independent vectors $\underset{\sim}{V}_i$. Let us first set,

$$\underset{\sim}{e}_i = \underset{\sim}{V}_i / |\underset{\sim}{V}_i|.$$ (A.II.3)

We require to find a scalar λ_i such that $\underset{\sim}{V}_j - \lambda_i \underset{\sim}{e}_i$ and $\underset{\sim}{e}_i$
are orthogonal. It is clear that λ_i is given by the dot

product of $\underset{\sim}{V}_j$ and $\underset{\sim}{e}_i$, that is,

$$\lambda_i = \underset{\sim}{V}_j \circ \underset{\sim}{e}_i \tag{A.II.4}$$

As $\underset{\sim}{V}_j$ and $\underset{\sim}{e}_i$ are linearly independent vectors we may construct a unit vector orthogonal to e_i given by,

$$\underset{\sim}{e}_j = \left| \frac{\underset{\sim}{V}_j - \lambda_i \cdot \underset{\sim}{e}_i}{\underset{\sim}{V}_j - \lambda_i \circ \underset{\sim}{e}_i} \right| \tag{A.II.5}$$

We may apply the same procedure to orthogonalise a set of linearly independent functions.

This technique may be applied to the numerical solution of boundary-value problems where the equation to be solved is ill-conditioned. We will now introduce the numerical technique and explain the main steps in the computer solution. A simple example of the technique will then be given. Let us write two linearly independent solutions, and their $(n-1)$ derivatives, of an nth order linear differential equation as

$$\underset{\sim}{G}_1(y) = \begin{pmatrix} g_1(y) \\ g_1{}'(y) \\ g_1{}''(y) \\ \cdot \\ \cdot \\ g_1{}^{n-1}(y) \end{pmatrix} \quad \text{and} \quad \underset{\sim}{G}_2(y) = \begin{pmatrix} g_2(y) \\ g_2{}'(y) \\ g_2{}''(y) \\ \cdot \\ \cdot \\ g_2{}^{n-1}(y) \end{pmatrix} \tag{A.II.6}$$

The equation may be integrated from some linearly independent starting conditions to a value of $y = y_1$. Then applying the technique of orthogonalisation on the values of $\underset{\sim}{G}_1$ and $\underset{\sim}{G}_2$ at $y = y_1$ we obtain

$$\mathbb{E}_1(y_1) = \frac{\underset{\sim}{G_1}(y_1)}{|\underset{\sim}{G_1}(y_1)|}$$

and

$$\mathbb{E}_2(y_1) = \frac{\underset{\sim}{G_2}(y_1) - (\underset{\sim}{G_2}(y_1) \cdot \underset{\sim}{E_1}(y_1))\underset{\sim}{E_1}(y_1)}{|\underset{\sim}{G_2}(y_1) - (\underset{\sim}{G_2}(y_1) \cdot \underset{\sim}{E_1}(y_1))\underset{\sim}{E_1}(y_1)|} \qquad (A.II.7)$$

The same transformations must then be applied to the initial conditions such that they now become,

$$\mathbb{E}_1(o) = \frac{\underset{\sim}{G_1}(o)}{|\underset{\sim}{G_1}(y_1)|}$$

and

$$\mathbb{E}_2(o) = \frac{\underset{\sim}{G_2}(o) - (\underset{\sim}{G_2}(y_1) \cdot \underset{\sim}{E_1}(y_1))\underset{\sim}{E_1}(o)}{|\underset{\sim}{G_2}(o) - (\underset{\sim}{G_2}(y_1) \cdot \underset{\sim}{E_1}(y_1))\underset{\sim}{E_1}(o)|} \qquad (A.II.8)$$

The integration may then procede from $y = y_1$ to $y = y_2$ with $\underset{\sim}{E_1}(y_1)$ and $\underset{\sim}{E_2}(y_1)$ as the starting conditions. It must be remembered that the transformation applied to orthogonalise each set of vectors at each new step of the integration must be applied to each previous set of vectors.

The steps to be used in the computer solution using this technique may be written in sequence as follows,

(i)   set up initial vectors $\underset{\sim}{G_1}(o)$ and $\underset{\sim}{G_2}(o)$,

(ii) integrate to position $y = y_1$,

(iii) create orthogonal vectors $\underset{\sim}{E_1}(y_1)$ and $\underset{\sim}{E_2}(y_1)$ at $y = y_1$,

(iv) perform same transformation on initial conditions to obtain $\underset{\sim}{E_1}(o)$ and $\underset{\sim}{E_2}(o)$,

(v)   integrate from $y = y_1$ to $y = y_2$ with $\underset{\sim}{E_1}(y_1)$ and $\underset{\sim}{E_2}(y_1)$ as initial conditions,

A.II.3

(vi) create orthogonal vectors $\underset{\sim}{E}_1(y_2)$ and $\underset{\sim}{E}_2(y_2)$ at $y = y_2$,

(vii) perform same transformations on vectors $\underset{\sim}{E}_1(y_1)$, $\underset{\sim}{E}_2(y_1)$

   and $\underset{\sim}{E}_1(o)$, $\underset{\sim}{E}_2(o)$,

(viii) integrate from $y = y_2$ to $y = y_3$ with $\underset{\sim}{E}_1(y_2)$ and $\underset{\sim}{E}_2(y_2)$

   as initial conditions,

(ix) continue procedure until end of range of integration.

Let us now consider a simple example of the solution of an ill-conditioned differential equation which we will write as,

$$f^{iv}(y) - 24\ f'''(y) - 169\ f''(y) - 324\ f'(y)$$
$$- 180\ f(y) = 0. \qquad (A.II.9)$$

Its general solution is,

$$f(y) = a_1 e^{-y} + a_2 e^{-2y} + a_3 e^{-3y} + a_4 e^{30y}. \qquad (A.II.10)$$

We will consider the solution with $a_4 = 0$ with boundary conditions

$$f(o) = 0,\ f'(o) = 0,\ f''(o) = 2,\ f'''(o) = -12, \qquad (A.II.11)$$

so that the solution is,

$$f(y) = e^{-y} - 2e^{-2y} + e^{-3y} \qquad (A.II.12)$$

The values of $f(y)$ and $f'(y)$ at $y = 1$ are then

$$f(1) = .1470$$

and $\qquad f'(1) = .0241$ $\qquad (A.II.13)$

We will now solve this equation (A.II.9) as a boundary value problem with boundary conditions given by $f(o) = f'(o) = 0$ and conditions (A.II.13). Let us start the integration with conditions,

$$G_1(o) = \begin{vmatrix} 0 \\ 0 \\ 1 \\ 0 \end{vmatrix} \qquad \text{and } G_2(o) = \begin{vmatrix} 0 \\ 0 \\ 0 \\ 1 \end{vmatrix} \quad .$$

Integrating from $y = 0$ to $y = y_1$ we obtain,

$$g_1(1) = .196 \times 10^{10} \quad , \quad g_1{}'(1) = .587 \times 10^{11}, \text{)}$$
$$\text{)} \qquad (A.II.14)$$
$$g_2(1) = .326 \times 10^4 \quad \text{and } g_2{}'(1) = .978 \times 10^{10}. \text{)}$$

Now the solution of (A.II.9) is a linear combination of $\underset{\sim 1}{G}$ and $\underset{\sim 2}{G}$ such that

$$f(y) = a \, g_1(y) + b \, g_2(y). \qquad (A.II.15)$$

'a' and 'b' may be calculated from (A.II.15) using (A.II.4) and we then obtain,

$$f''(o) = -.006, \qquad \qquad \text{)}$$
$$\text{)} \qquad (A.II.16)$$
$$\text{and } f'''(o) = .036. \qquad \qquad \text{)}$$

which clearly is not the case. The linear independence of the originally linear independent solutions has been contaminated by the solution with exponent 30 in equation (A.II.11). In order to ensure linear independence of the solutions we may use the orthogonalisation procedure outlined above. Integrating from $y = 0$ to $y = 1$ with a step size of .01 and performing the orthogonalisation after each integration step we finally obtain the result,

$$f''(o) = -2.00000037$$
$$\qquad \qquad (A.II.17)$$
$$\text{and} \quad f'''(o) = 11.9999908.$$

A.II.5

This accuracy may be further increased by a decrease in step size and a consequent increase in the possible number of orthogonalisations.

In the solution of the Orr-Sommerfeld equation, which is ill-conditioned in the above sense, the solutions are complex. No difficulty is experienced in FORTRAN V programming as the functions may be declared as COMPLEX. However, care must be taken in forming the scalar operator λ_i in orthogonalisation as for complex vectors it is the dot product of $\underset{\sim}{V}_j$ and the complex conjugate of $\underset{\sim}{e}_i$. (see equation (A.II.4)).

REFERENCES

Abramovitch, G.N.   (1963)   The theory of turbulent jets.
The M.I.T. Press.

Baker and   (1968)   Analytical investigation of the
Weinstein   mixing of two parallel streams
of dissimilar fluid.
NASA C.R. 956.

Batchelor, G.K.   (1951)   Pressure fluctuations in
isotropic turbulence.
Proc. Cam. Phil. Soc. 47, p. 359

Batchelor, G.K.   (1953)   The theory of homogeneous
turbulence.
Cambridge University Press.

Bellman, R.E. and   (1965)   Quasi-linearisation and non-
Kalaba, R.E.   linear boundary-value problems.
Elsevier, N.Y.

Betchov, R. and   (1966)   Spatial instability of the
Criminale, W.O.   inviscid jet and wake.
Phys. Fluids,$\underline{9}$,p.359.

Betchov, R. and   (1967)   Stability of parallel flows.
Criminale, W.O.   Academic Press, N.Y.

Betchov, R. and   (1963)   Stability of a shear layer
Szewczyk, A.   between parallel streams.
Phys. Fluids,$\underline{6}$,p.1391.

Bradshaw, P.,   (1963)   Turbulence in the noise-
Ferriss, D.H. and   producing region of a circular
Johnson,R.F.   jet.
J. Fluid Mech.,$\underline{19}$,p.591.

Browand, F.K.   (1966)   An experimental investigation of
the instability of an incompressible
separated shear layer.
J. Fluid Mech.,$\underline{26}$,p.281.

Brown, W. Byron.   (1959)   Numerical calculation of the
                                stability of cross-flow profiles.
                                Northrop Aircraft Inc., Rep.NAI 59-5

Chrandrasekhar, S. (1961)   Hydrodynamic and hydromagnetic
                                stability.
                                Oxford University Press.

Corcos, G.M.   (1964)   The structure of the turbulent
                                pressure field in boundary layers.
                                J. Fluid Mech.,18,p.353.

Corcos, G.M. and   (1959)   On the stability of fully developed
Sellars, J.R.   flow in a pipe.
                                J. Fluid Mech.,5,p.97.

Crane, L.J.   (1957)   The laminar and turbulent mixing of
                                jets of compressible fluid. Part II-
                                the mixing of two semi-infinite streams.
                                J. Fluid Mech.,3,p.81.

Davey,   (1971)   Finite-amplitude stability of pipe flow.
Nguyen,   J. Fluid Mech. 45, p. 701.

Davies, P.O.A.L. and (1968)   Convection velocity measurements in
Bose, B.   strong turbulence.
                                Univ. of Southampton,
                                I.S.V.R. Memo. 225.

Davies, P.O.A.L.,   (1963)   The characteristics of the turbulence
Fisher, M.J. and   in the mixing region of a round jet.
Barratt, M.J.   J. Fluid Mech.,15,p.337.

Dolph, C.L. and   (1958)   On the application of infinite systems
Lewis, D.C.   of ordinary differential equations to
                                perturbations of plane Poiseuille flow.
                                Quart. Appl. Math.,16,p.97.

Eagles, P.M.   (1969)   Composite series in the Orr-Sommerfeld
                                problem for symmetric channel flow.
                                Quart. J. Mech. Appl., 22, p. 129

Eckhaus, W.   (1965)   Studies in non-linear stability
                                theory.
                                Berlin: Springer-Verlag.

Esch, R.E.   (1957)   The instability of a shear layer
                                between two parallel streams.
                                J. Fluid Mech.,3,p.289.

Favre, A.J.,   (1958)   Further space-time correlations of
Gaviglio, J.J. and   velocity in a turbulent boundary
Dumas, R.   layer.
                                J. Fluid Mech.,3,p.344.

Foote, J.R. and   (1950)   Some recent investigations in the
Lin, C.C.   theory of hydrodynamic stability.
                                Quart. Appl. Math.,8,p.265.

Fraenkel, L.E.   (1969)   On the method of matched asymptotic
                                expansion.
                                Proc. Camb. Phil. Soc., 65, p. 209

Freymuth, P.   (1966)   On transition in a separated laminar
                                boundary layer.
                                J. Fluid Mech.,25,p.683.

Fuchs, H.V.   (1968)   Uber die Messung von Drockschwankungen
                                mit umstromten Mikrofonen.
                                Tech. Univ., Berlin, Thesis.

Fuchs, H.V.   (1969)   Measurement of pressure fluctuations
                                with microphones in an air-stream.
                                Univ. of Southampton,
                                I.S.V.R. Memo. 281.

Fyfe, D.J.   (1965)   Economical evaluation of Runge-Kutta
                                formulae.
                                Math. Comp.,p.392.

Gallagher, A.P. and (1962) On the behaviour of small
Mercer, A.M.   disturbances in plane Couette flow
                            J. Fluid Mech.,13,p.91.

Gartshore, I.S.   (1965)   The streamwise development of two-
                            dimensional wall jets and other
                            two-dimensional shear flows.
                            Mech. Eng., Ph.D. Thesis,
                            McGill University.

Gaster, M.   (1963)   Anote on the relation between
                            temporally and spatially increasing
                            disturbances in hydrodynamic stability.
                            J. Fluid Mech.,14,p.222.

Gaster, M.   (1965a) The role of spatially growing waves
                            in the theory of hydrodynamic
                            stability.
                            Prog. Aero. Sci.,6,p.251.

Gaster, M.   (1965b) On the generation of spatially
                            growing waves in a boundary layer.
                            J. Fluid Mech.,22,p.433.

Gortler, H.   (1942)   Berechnung von Aufgaben der freien
                            Turbulenz auf Grund eines neuen
                            Naherungsansatzes.
                            ZAMM,22,p.244.

Graebel, W.P.   (1966)   On determination of the characteristic
                            equations for the stability of
                            parallel flows.
                            J. Fluid.Mech.,24,p.497.

Grant, H.L.   (1958)   The large eddies of turbulent motion.
                            J. Fluid Mech.,4,p.149.

Hall, M.G.   (1968)   Impressions of U.S. work on turbulent
                            shear flows.
                            ARC 300 33, FM 3945.

Heisenberg, W.   (1924)   Uber Stabilitat und Turbulenz von
                                   Flussigkeitsstromen.
                                   Ann. Physik,74,p.577.

Helmholtz, H.   (1868)   Uber discontinuirliche Flussigkeits-
                                   Bewegungen.
                                   Akad. Wiss., Berlin, Monatsber. 215.

Hodgson, T.H.   (1962)   Pressure fluctuations in shear flow
                                   turbulence.
                                   Ph.D. Thesis, Univ. of London.

Høiland, E.   (1953)   On two-dimensional perturbations of
                                   linear flow.
                                   Geofys. Publikasjoner, Norske
                                   Videnskaps-Akad., Oslo,18,p.1.

Holstein, H.   (1950)   Uber die aussere und innere
                                   Reibungsschicht bei Storungen laminar
                                   Stronungen.
                                   ZAMM,30,p.25.

Hussain, A and   (1970)   The mechanics of a perturbation wave
Reynolds, W.C.   in turbulent shear flow.
                                   Stanford Univ. Mech. Eng. Rep F.M.6

Kelvin, Lord   (1880)   On a disturbance in Lord Rayleigh's
                                   solution for waves in a plane
                                   vortex stratum.
                                   'Math. and Phys. Papers',4,p.186,
                                   Cambridge University Press.

Kaplan, R.E.   (1964)   The stability of laminar incompressible
                                   boundary layers in the presence of
                                   compliant boundaries.
                                   MIT, Aero-Elastic and Structures Res.
                                   Lab. ASRL-TR116.

Ko, D.R-S.,   (1970)   Finite disturbance effect on the
Kubota, T. and   stability of a laminar incompressible
Lees, L.   wake behind a flat plate.
                                   J. Fluid Mech.,40,p.315.

Ko, S-H., and Lessen, M.   (1969)   Viscous instability of an incompressible full jet. Phys. Fluids,$\underline{12}$,p.2270.

Kuethe, A.M.   (1935)   Investigation of the turbulent mixing regions formed by jets. J. Appl. Mech.,$\underline{2}$,A-87.

Kurtz, E.F. and Crandall, S.H.   (1962)   Computer-aided analysis of hydrodynamic stability. J. Math. Phys.,$\underline{41}$,p.264.

Lanchon, H. and Eckhaus, W.   (1964)   Sur l'analyse de la stabilite des ecoulements faiblement divergents. J. Mecan.,$\underline{3}$,p.445.

Landahl, M.T.   (1967)   A wave-guide model for turbulent shear flow. J. Fluid Mech.,$\underline{29}$,p.441.

Landau, L.D. and Lifshitz, E.M.   (1953)   Mechanics of continuous media. Gostekhizdat, Moscow.

Lee, L.H. and Reynolds, W.C.   (1964)   A variational method for investigating the stability of parallel flows. Stanford Univ. Mech. Eng. Tech. Rep. FM-1.

Lee, L.H. and Reynolds, W.C.   (1967)   On the approximate and numerical solution of Orr-Sommerfeld problems. Quart. Mech. Appl. Math.,$\underline{20}$,p.1.

Lessen, M.   (1950)   On stability of free laminar boundary layer between parallel streams. NACA Report 979.

Lessen, M. and Ko, S-H.   (1966)   Viscous instability of an incompressible fluid half-jet. Phys. Fluids,$\underline{9}$,p.1179.

Lessen, M.,   (1965)   The instability of inviscid jets and
Fox, J.A. and   wakes in compressible fluid.
Zien, H.M.   J. Fluid Mech., $\underline{21}$, p.129.

Lessen, M.,   (1969)   Stability of three-dimensional
Harpavat, G. and   laminar and turbulent shear layers.
Zien, H.M.   J. Fluid Mech., $\underline{38}$, p.39.

Liepmann, H.W. and (1947)   Investigations of free turbulent
Laufer, J.   mixing.
                               NACA T.N. 1257.

Lilley, G.M.   (1967)   The laminar and turbulent mixing of
                               parallel streams.
                               (unpublished).

Lilley, G.M.   (1967)   A note on Reynolds stresses.
                               B.T.M.C.

Lin, C.C.   (1953)   On the stability of the laminar
                               mixing region between two parallel
                               streams in a gas.
                               NACA Tech. Note 2887.

Lin, C.C.   (1955)   Theory of hydrodynamic stability.
                               Cambridge University Press.

Lock, R.C.   (1951)   The velocity distribution in the
                               laminar boundary layer between
                               parallel streams.
                               Quart. J. Mech. Appl. Math., $\underline{4}$, p.42.

Malkus, W.   (1956)   Outline of a theory of turbulent
                               shear flow.
                               J. Fluid Mech., $\underline{1}$, p.521.

Meksyn, D. and   (1951)   Stability of viscous motion between
Stuart, J.T.   parallel planes for finite
                               disturbances.
                               Proc. Roy. Soc., $\underline{A208}$, p.517.

Michalke, A.   (1964)   On the inviscid instability of the
                              hyperbolic tangent velocity profile.
                              J. Fluid Mech.,19,p.543.

Michalke, A.   (1965)   On spatially growing disturbances in
                              an inviscid shear layer.
                              J. Fluid Mech.,23,p.521.

Michalke, A.   (1969)   A note on spatially growing three-
                              dimensional disturbances in a free
                              shear layer.
                              J. Fluid Mech.,38,p.765.

Michalke, A.   (1969)   The influence of the vorticity
                              distribution on the inviscid
                              instability of a free shear layer.
                              'Fluid Dynamics Transactions',4,
                              Polish Acad. Sci., Warsaw, p.751.

Miles, J.W.   (1957)   On the generation of surface waves
                              by shear flow.
                              J. Fluid Mech.,3,p.185.

Mills, R.D.   (1968)   Numerical and experimental
                              investigations of the shear layer
                              between two parallel streams.
                              J. Fluid Mech.,33,p.591.

Moffat, H.K.   (1965)   The interaction of turbulence with
                              rapid uniform shear.
                              Stanford Univ. Res. Rep.,
                              Sudaer 242.

Newman, B.G.   (1967)   Turbulent jets and wakes in a
                              pressure gradient.
                              'Fluid Mechanics of Internal Flow',
                              ed. Sovran, Elsevier.

Orr, W.McF.   (1907)   The stability or instability of the
                              study of motions of a liquid.
                              Proc. Roy. Irish Acad.,A27,p.9.

Phillips, O.M.   (1967)   The maintenance of Reynolds stress
in a turbulent shear flow.
J. Fluid Mech.,27,p.131.

Prandtl, L.   (1925)   Bericht uber Untersuchungen zur
ausgebildeten Turbulenz.
ZAMM,5,p.136.

Prandtl, L.   (1942)   Bemerkung zur Theories der freien
Turbulenz.
ZAMM,22,p.5.

Rayleigh, Lord.   (1878)   On the stability of jets.
'Scientific Papers',1,p.361,
Cambridge University Press.

Rayleigh, Lord.   (1880)   On the stability or instability of
certain fluid motions.
'Scientific Papers',1,p.474,
Cambridge University Press.

Reid, W.H.   (1965)   The stability of parallel flows.
'Basic Developments in Fluid Dynamics'
(ed. M. Holt),1,p.249,
Academic Press, N.Y.

Reynolds, O.   (1883)   An experimental investigation of the
circumstances which determine
whether the motion of water shall be
direct or sinuous.
'Scientific Papers',2,p.51,
Cambridge University Press.

Reynolds, W.C. and   (1967)   Stability of turbulent channel flow,
Tiederman, W.G.   with application to Malkus' theory.
J. Fluid Mech.,27,p.253.

Sabin, C.M.   (1965)   An analytical and experimental study
of the plane incompressible turbulent
free shear layer with arbitrary
velocity ratio and pressure gradient.
Stanford Univ.Mech.Eng.Rep. MD-9.

Sato, H.   (1956)   Experimental investigation on the
                                  transition of the laminar separated
                                  layer.
                                  J. Phys. Soc. Japan,11,p.702.

Sato, H.   (1959)   Further investigation on the
                                  transition of two-dimensional
                                  separated layer at subsonic speeds.
                                  J. Phys. Soc. Japan,14,p.1797.

Schade, H. and   (1962)   Formation of vortices in a free
Michalke, A.   boundary layer.
                                  Z. Flugwiss.,10,p.147.

Schubauer, G.B.and   (1943)   Laminar boundary layer oscillations
Skramstad, H.K.   and transition on a flat plate.
                                  NACA Tech. Rept. 909.

Sharma, R.   (1968)   The structure of turbulent shear
                                  flow.
                                  Ph.D. Thesis, Univ. of Southampton.

Sommerfeld, A.   (1908)   Ein Beitrag zur hydrodynamischen
                                  Erklarung der turbulenten
                                  Flussigkeitsbewegung.
                                  Proc. 4th. Int. Congr. Maths, Rome,
                                  p.116.

Squire, H.B.   (1933)   On the stability of three-
                                  dimensional disturbances of viscous
                                  flow between parallel walls.
                                  Proc. Roy. Soc.,A221,p.189.

Stuart, J.T.   (1958)   On the non-linear mechanics of
                                  hydrodynamic stability.
                                  J. Fluid Mech.,4,p.1.

Stuart, J.T.   (1960)   On the non-linear mechanics of wave
                                  disturbances in stable and unstable
                                  parallel flows. I.The basic
                                  behaviour in Poiseuille flow.
                                  J. Fluid Mech.,9,p.353.

Stuart, J.T.	(1965)	The production of intense shear layers by vortex stretching and convection. N.P.L. Aero. Rept. 1147.
Tatsumi, T. and Gotoh, K.	(1960)	The stability of free boundary layers between two uniform streams. J. Fluid Mech.,$\underline{7}$,p.433.
Taylor, G.I.	(1935)	Statistical theory of turbulence. Proc. Roy. Soc.,$\underline{A151}$,p.421.
Thomas, L.H.	(1953)	The stability of plane Poiseuille flow. Phys. Rev.,$\underline{91}$,p.780.
Ting, Lu.	(1959)	On the mixing of two parallel streams. J. of Math. Phys.,$\underline{38}$,p.153.
Tollmien, W.	(1926)	Calculation of turbulent expansion processes. ZAMM,$\underline{6}$,p.468.,also NACA T.M. 1085 (1945).
Tollmien, W.	(1929)	Uber die Entstehung der Turbulenz. Gessellschaft der Wissenschaften, Gottingen,$\underline{21}$.
Townsend, A.A.	(1956)	The structure of turbulent shear flow. Cambridge University Press.
Townsend, A.A.	(1962)	Remarks on the Malkus theory of turbulent flow. Mechanique de la Turbulence, Paris: CNRS,p.167.
Tsien, H.S.	(1956)	The Poincare-Lighthill-Kuo method. Advances in Appl. Mech.,$\underline{4}$,p.56.
Tu, B.J. and Willmarth, W.W.	(1966)	An experimental study of the structure of turbulence near the wall. Aerospace Eng. Aero. Lab. Rept. 02920-3-T. Univ. of Michigan.

Van Dyke, M.   (1964)   Perturbation Methods in Fluid
                                 Mechanics.
                                 Academic Press, N.Y.

Wasow, W.   (1948)   The complex asymptotic theory of a
                                 fourth order differential equation
                                 of hydrodynamics.
                                 Ann. Math.,$\underline{49}$,p.852.

Wazzan, A.R.,   (1967)   Stability of laminar boundary layer
Okamura, T.T. and   at separation.
Smith, A.M.O.   Phys. Fluids,$\underline{10}$,p.2540.

Wazzan, A.R.,   (1966)   Spatial stability study of some
Okamura, T.T. and   Falkner-Skan similarity profiles.
Smith, A.M.O.   Proc.5th. U.S. Natl. Congr. Appl.
                                 Mech.,p.836.

Willmarth, W.W. and (1965)   Resolution and structure of the wall
Roos, F.W.   pressure field beneath a turbulent
                                 boundary layer.
                                 J. Fluid Mech.,$\underline{22}$,p.81.

Willmarth, W.W. and (1962)   Measurements of the fluctuating
Wooldridge, C.E.   pressure beneath a turbulent boundary
                                 layer.
                                 J. Fluid Mech.,$\underline{14}$,p.187.

Wygnanski, I. and   (1970)   The two-dimensional mixing region.
Fiedler, H.E.   J. Fluid Mech.,$\underline{41}$,p.327.

Yule   (1970)   On the mixing of two parallel streams.
                                 Part II. Ph.D.Thesis,
                                 University of Manchester.

Velocity Ratio $\frac{U_2}{U_1}$	0.0	0.61
$\eta = y / \sqrt{\frac{\nu x}{U_s}}$	f'(η)	f'(η)
-8.	-.9998	-1.0
-7.2	-.9972	-.9999
-6.4	-.9919	-.9999
-5.6	-.9815	-.9994
-4.8	-.9607	-.9968
-4.	-.9196	-.9854
-3.6	-.8863	-.9712
-3.2	-.8404	-.9462
-2.8	-.7777	-.9049
-2.4	-.6934	-.8407
-2.	-.5824	-.7469
-1.6	-.4406	-.6185
-1.2	-.2663	-.4540
-0.8	-.0628	-.2574
-0.4	.1594	-.0389
0.0	.3825	.1860
0.4	.5852	.3995
0.8	.7490	.5856
1.2	.8649	.7341
1.6	.9360	.8421
2.	.9735	.9136
2.4	.9905	.9566
2.8	.9970	.9800
3.2	.9992	.9916
3.6	.9998	.9968
4.	.9999	.9989
4.8	1.0	.9999
5.6	1.0	1.0

TABLE I

Laminar Velocity Distributions.

Velocity Ratio $\frac{U_2}{U_1}$	0.0	0.61
$\eta = y/L(x)$	$f'(\eta)$	$f'(\eta)$
-2.0	-.9999	-.9999
-1.8	-.9992	-.9997
-1.6	-.9920	-.9938
-1.4	-.9656	-.9642
-1.2	-.9039	-.8933
-1.0	-.7965	-.7733
-0.8	-.6393	-.6158
-0.6	-.4341	-.4342
-0.4	-.1874	-.2389
-0.2	.0883	-.0369
0.	.3718	.1671
0.2	.6317	.3688
0.4	.8315	.5611
0.6	.9479	.7329
0.8	.9915	.8687
1.0	.9995	.9547
1.2	.9999	.9916
1.4	1.0	.9994
1.6	1.0	1.0

TABLE II

Turbulent Velocity Distributions.
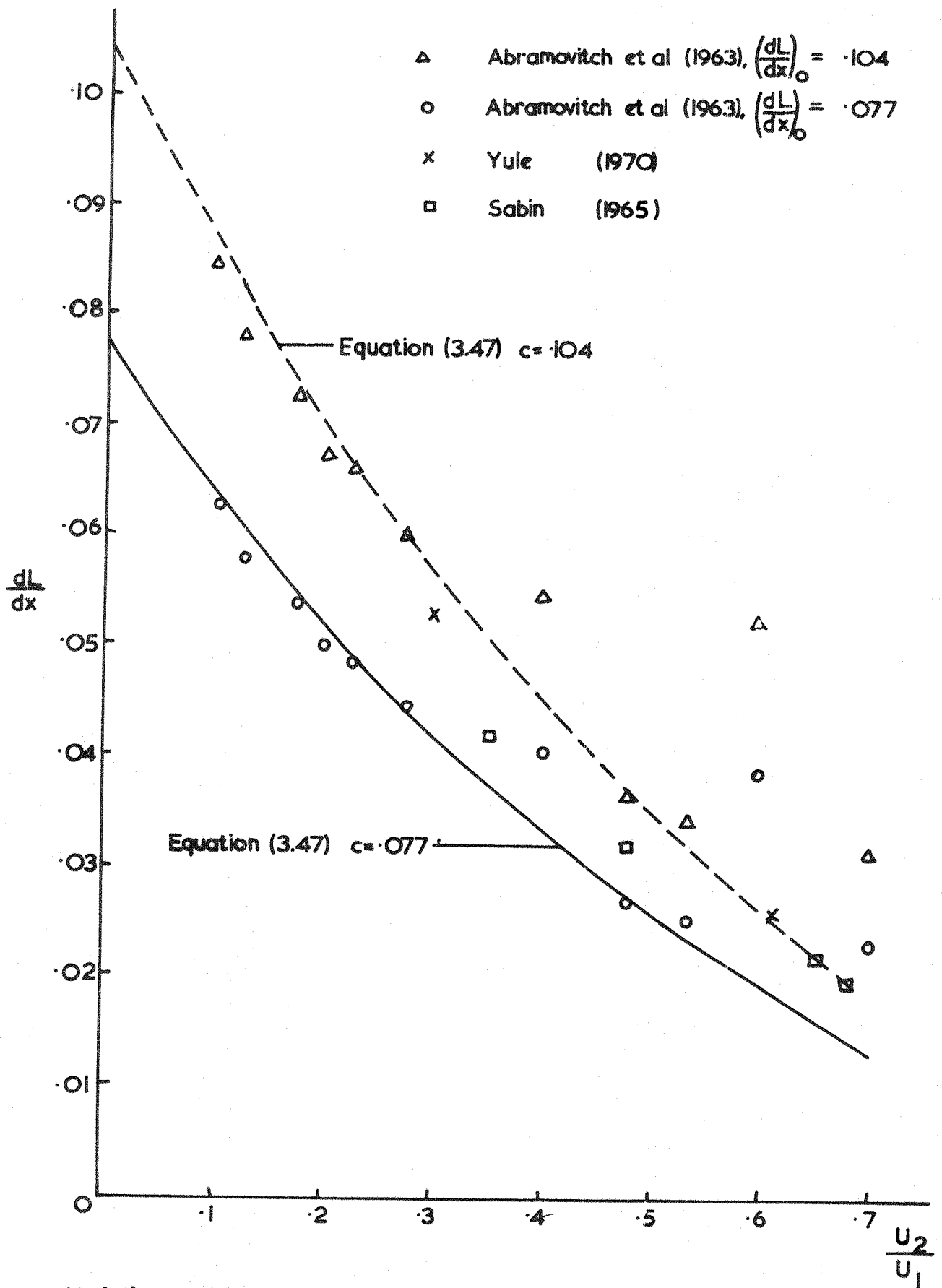
Variation of Rate of Spread with Velocity Ratio   Figure I.
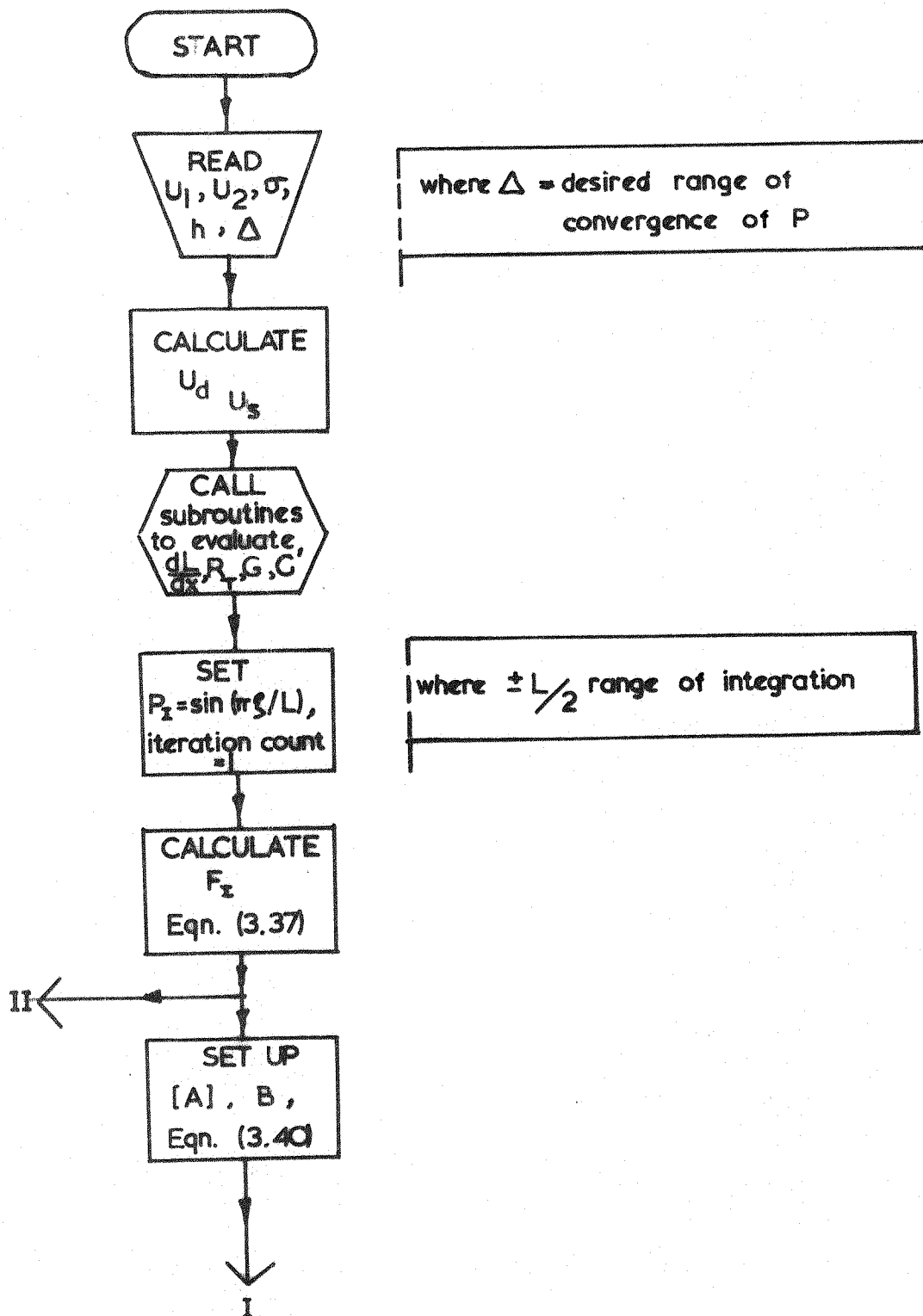
START

READ
$U_1, U_2, \sigma,$
h, Δ

where Δ = desired range of
convergence of P

CALCULATE
$U_d \quad U_s$

CALL
subroutines
to evaluate,
$\frac{dL}{dx}$, R, G, C'

SET
$P_x = \sin(\pi\varsigma/L)$,
iteration count
=

where $\pm L/2$ range of integration

CALCULATE
F_x
Eqn. (3.37)

II

SET UP
[A], B,
Eqn. (3.40)

I

<u>Flow Diagram of Program to Calculate Mean Velocity</u>

<u>Figure 2 Part I</u>

II

I

SET
iteration count
= iter. count+1

SOLVE
for P, using
Gaussian
Elimination

CALCULATE
F_z
Eqns. (3.37),
(3.13),(3.14)

CALCULATE
summed
difference
of $P_{z+1} - P_z = \delta$

CALCULATE
next value of
P_z

IF

$\Delta - \delta$

>0

≤0

CALL
subroutines
to evaluate
V, Eqn.(3.13)
U", V".

WRITE
U, V, U",V",
G, G'

FINISH
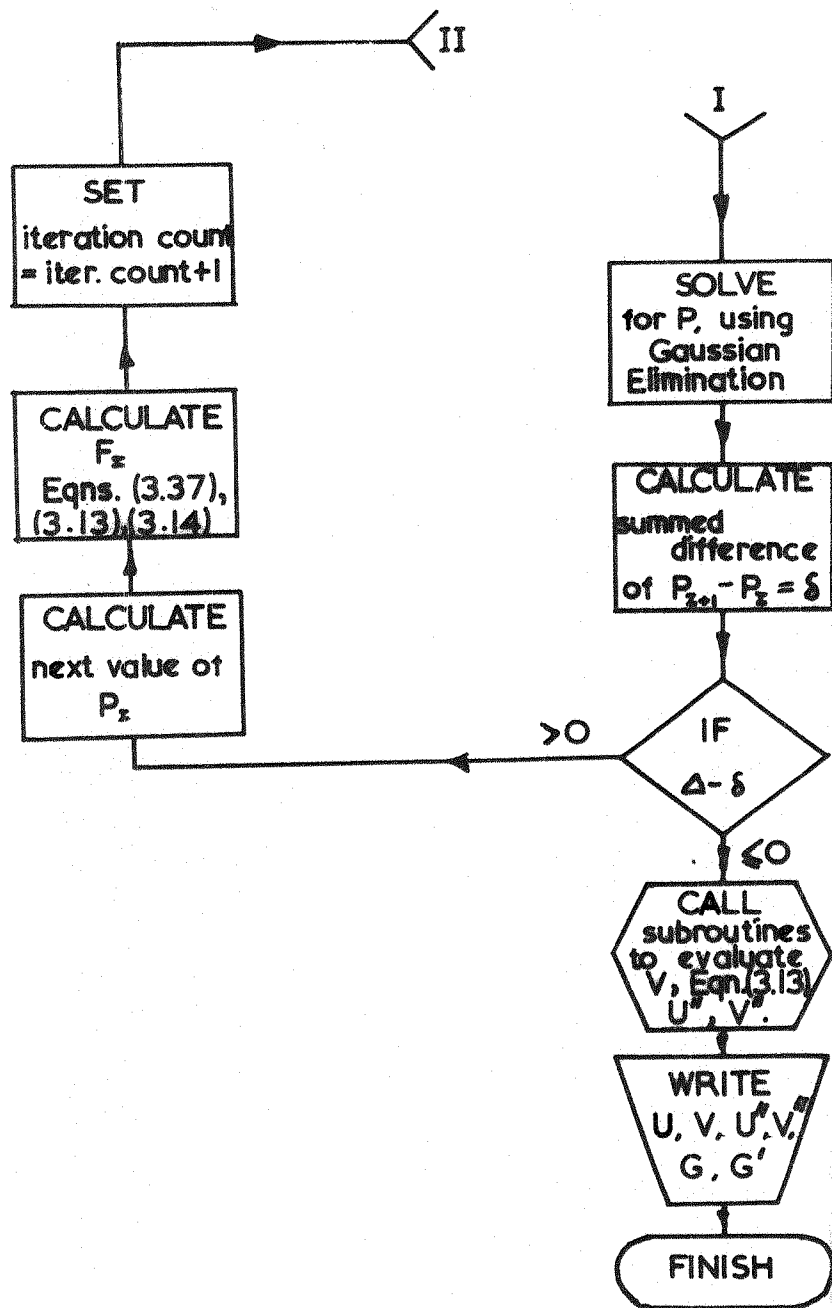
Flow Diagram of Program to Calculate Mean Velocity

Figure 2   Part II
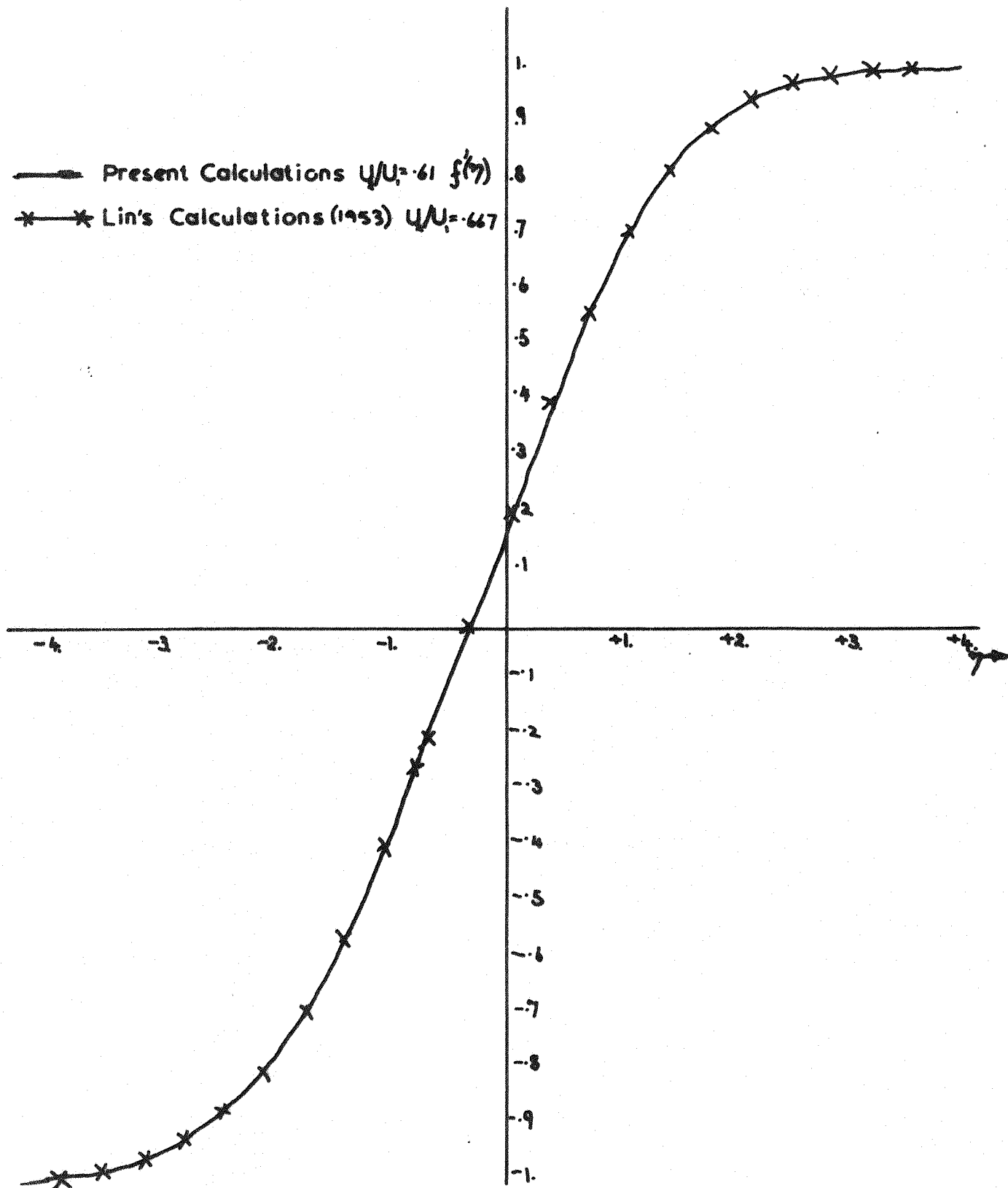
Nondimensional Laminar Velocity Profile   Figure 3.
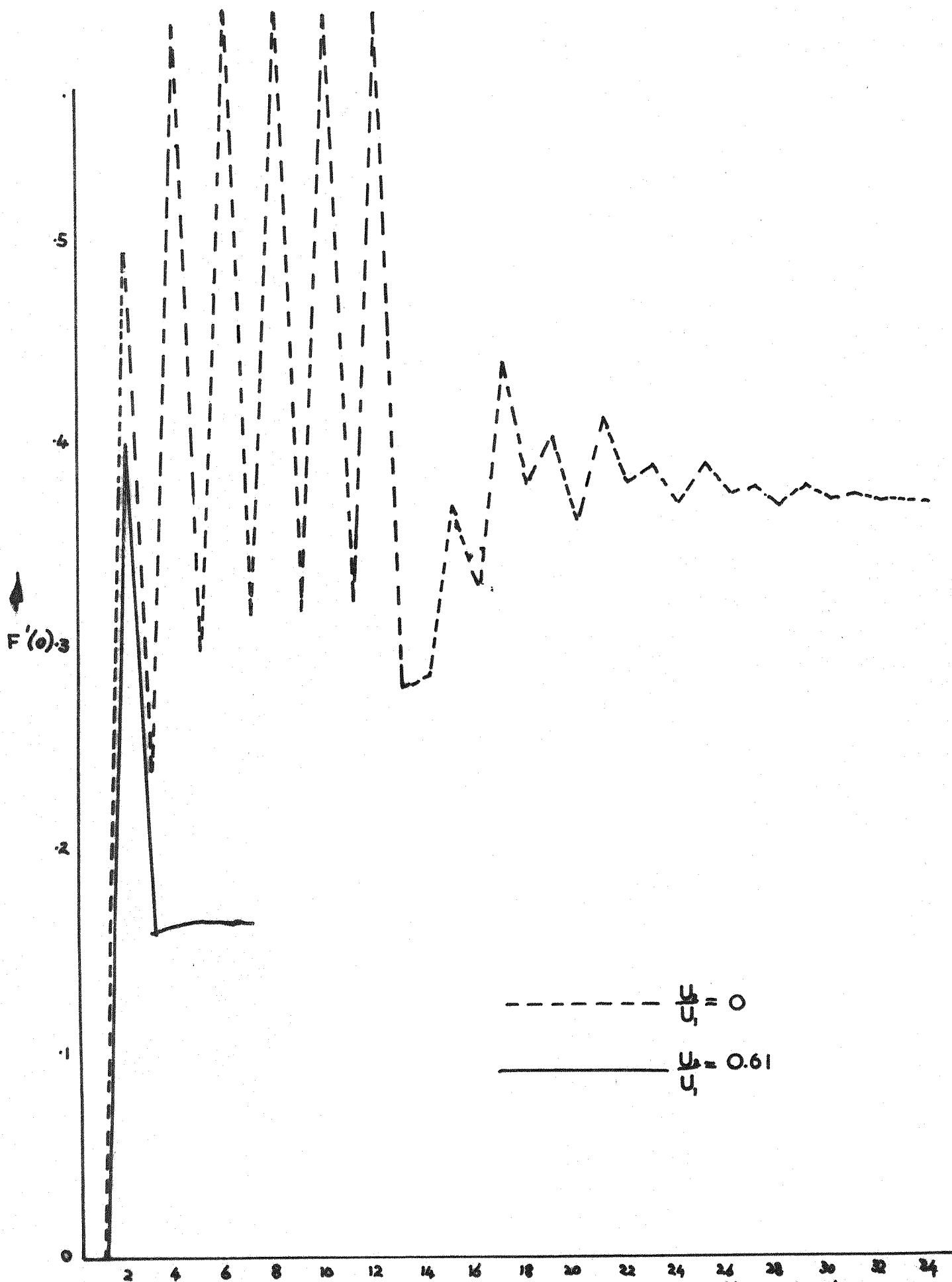
Convergence of F(0) for Different Velocity Ratios

$\frac{U_2}{U_1} = 0$

$\frac{U_2}{U_1} = 0.61$

F'(0)

Iteration Number

Figure 4.

Effect of Eddy Viscosity Distribution on the Non-dimensional Second Derivative of Axial Velocity; $U_2/U_0 = 0.61$

Figure 5

Legend:
- $\nu_T = \nu_0 \exp[.7(\zeta - \zeta_t)^2]$
- $\nu_T = \nu_0 \exp[.7(\zeta)^2]$
- $\nu_T = \nu_0$
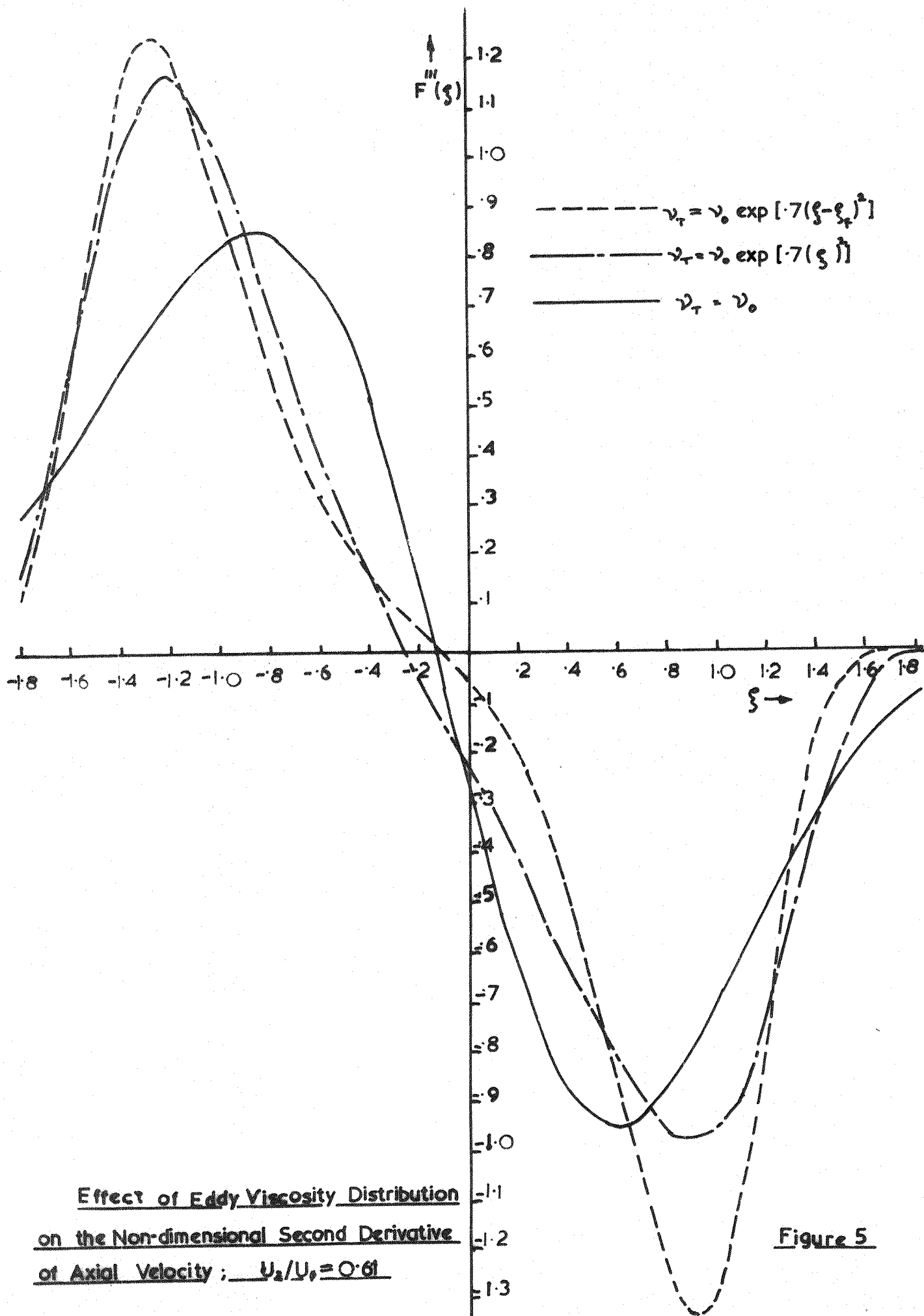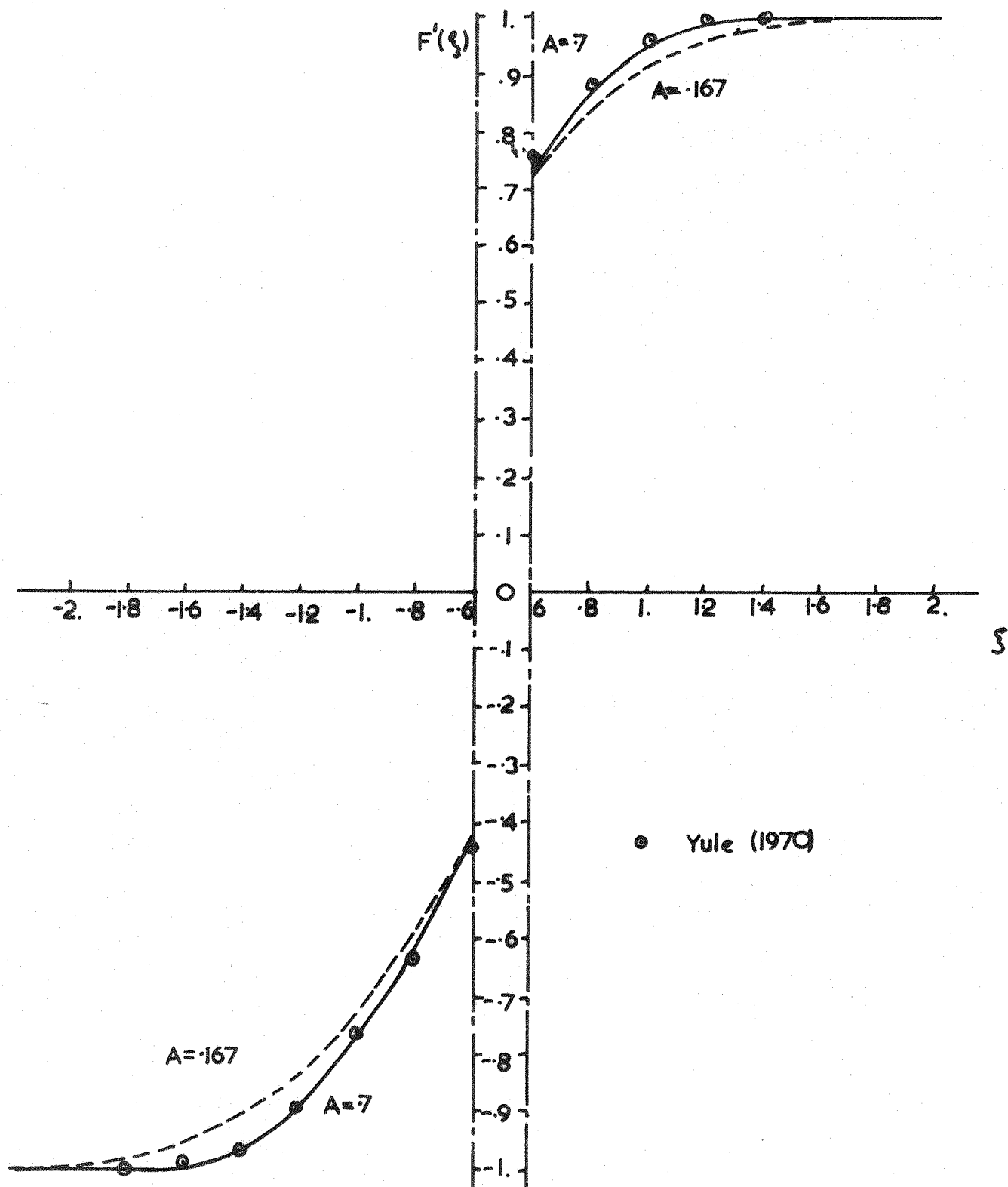
Effect of Choice of Constant A on Numerical Solution $U_2/U_1 = 0.61$

Figure   6
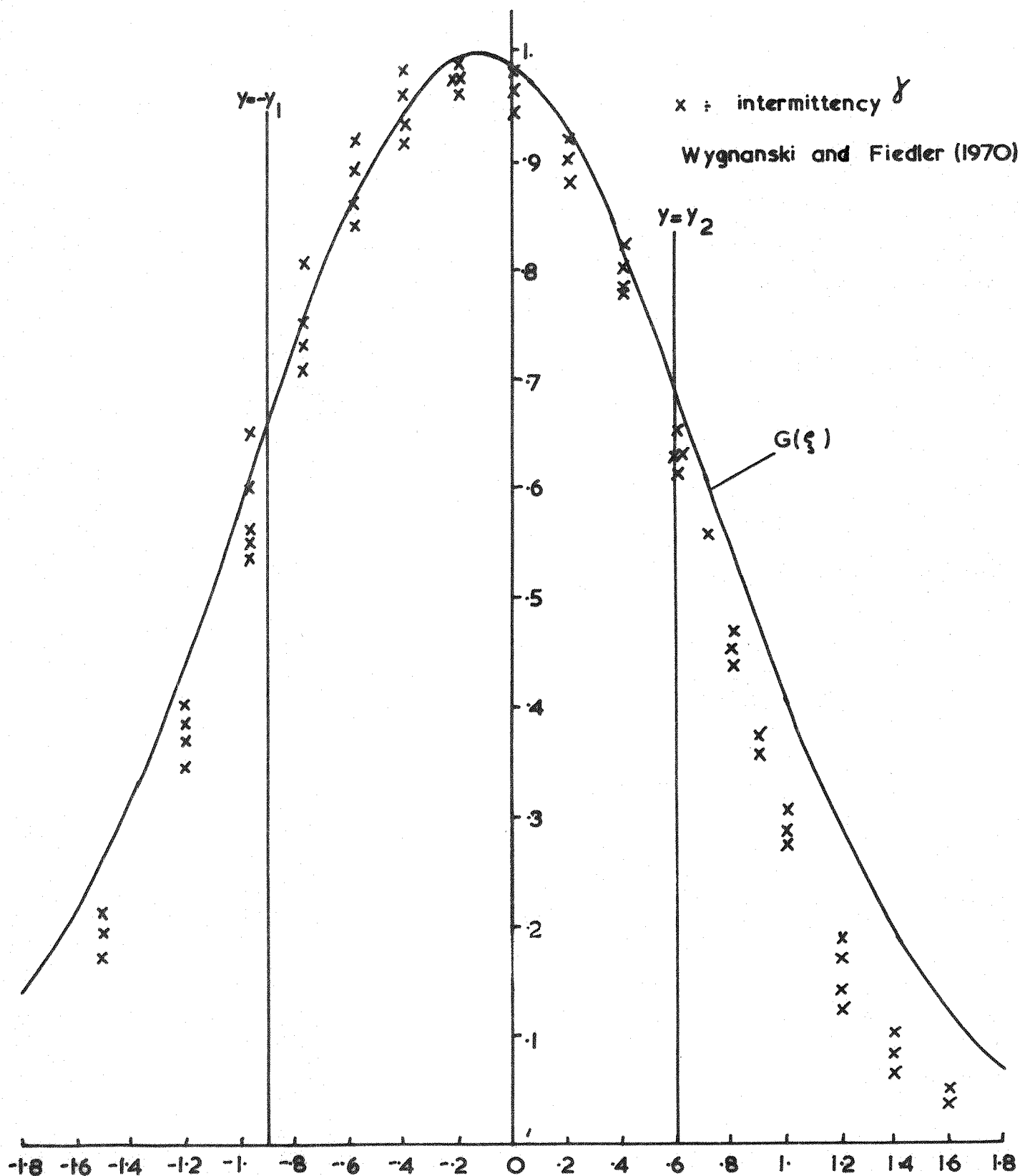
Comparison of the Function $G(\zeta)$ with Experimental Measurements of

Wygnanski and Fiedler   Figure 7.

Legend:
- Experimental results   Yule
- - - - Exponential distribution of eddy viscosity, $A = 0.7$, $\xi_E = -0.13125$, $\sigma = 0.0033$.
- —— Constant eddy viscosity, $\sigma = 0.0033$
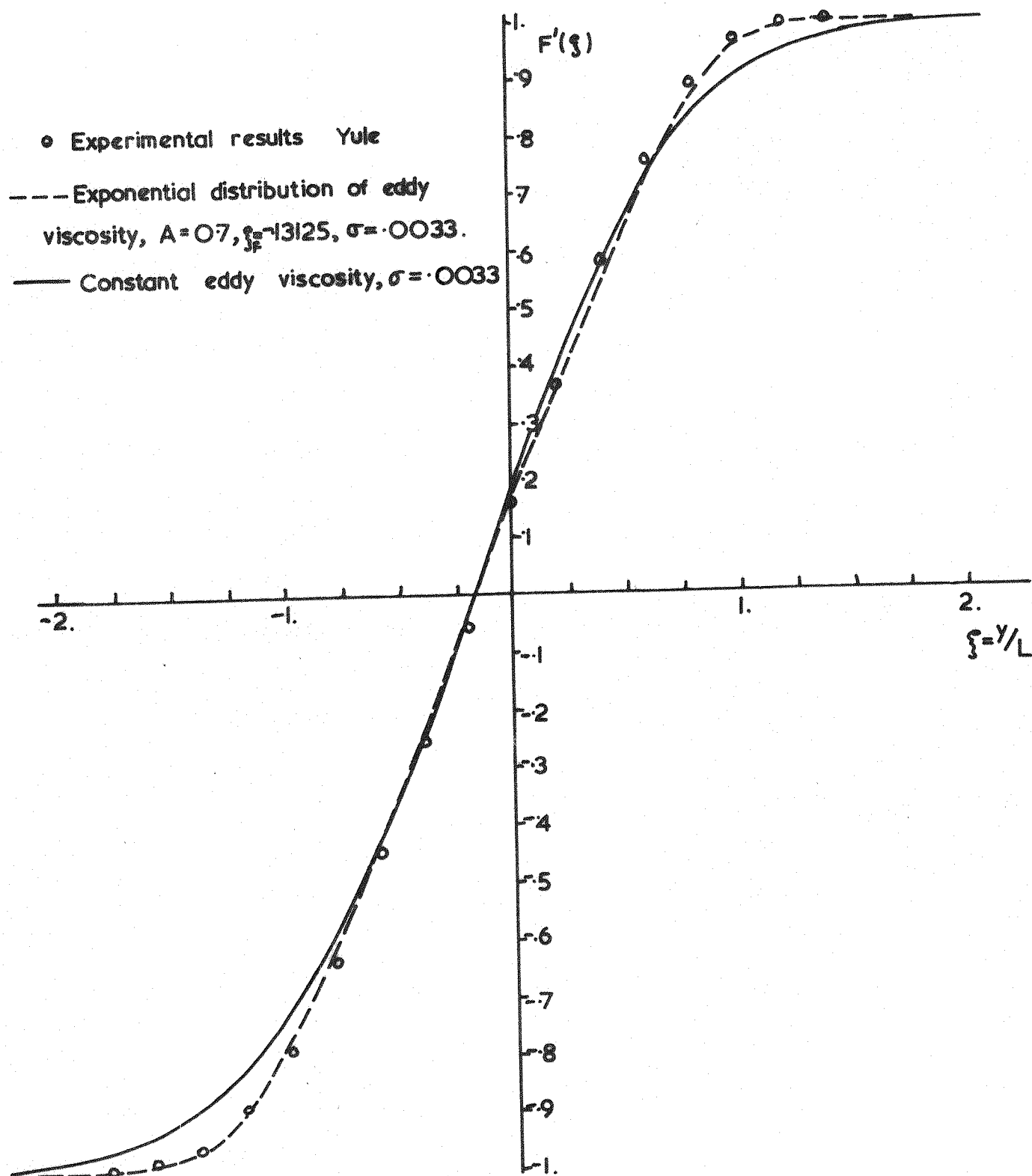
Non-dimensional   Turbulent   Velocity   Profile $U_2 / U_1 = 0.61$
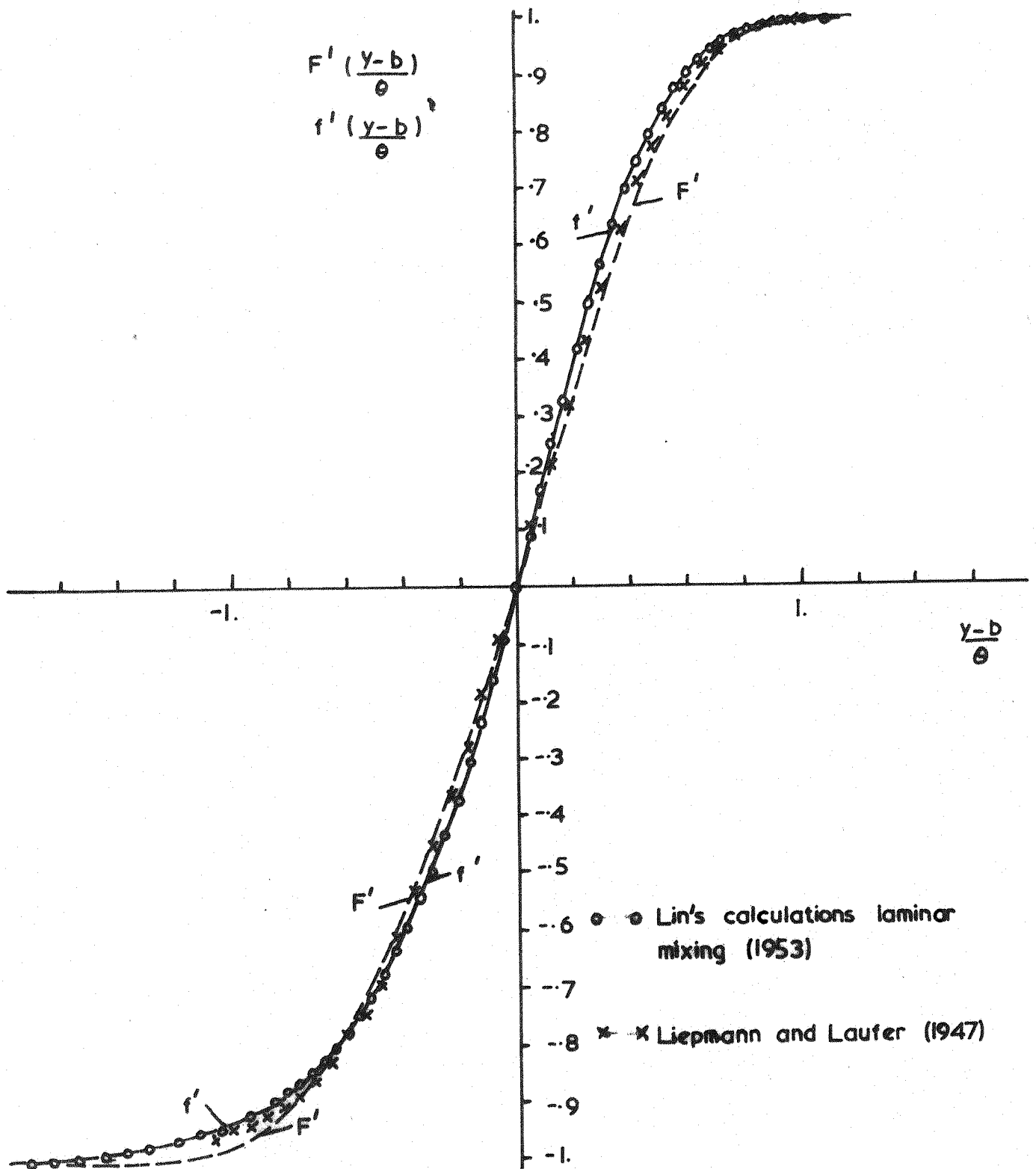
Figure   8

Non-dimensional Turbulent and Laminar Velocity Profiles, $U_2 = 0$, as Functions of $(y-b)/\theta$.   Figure 9
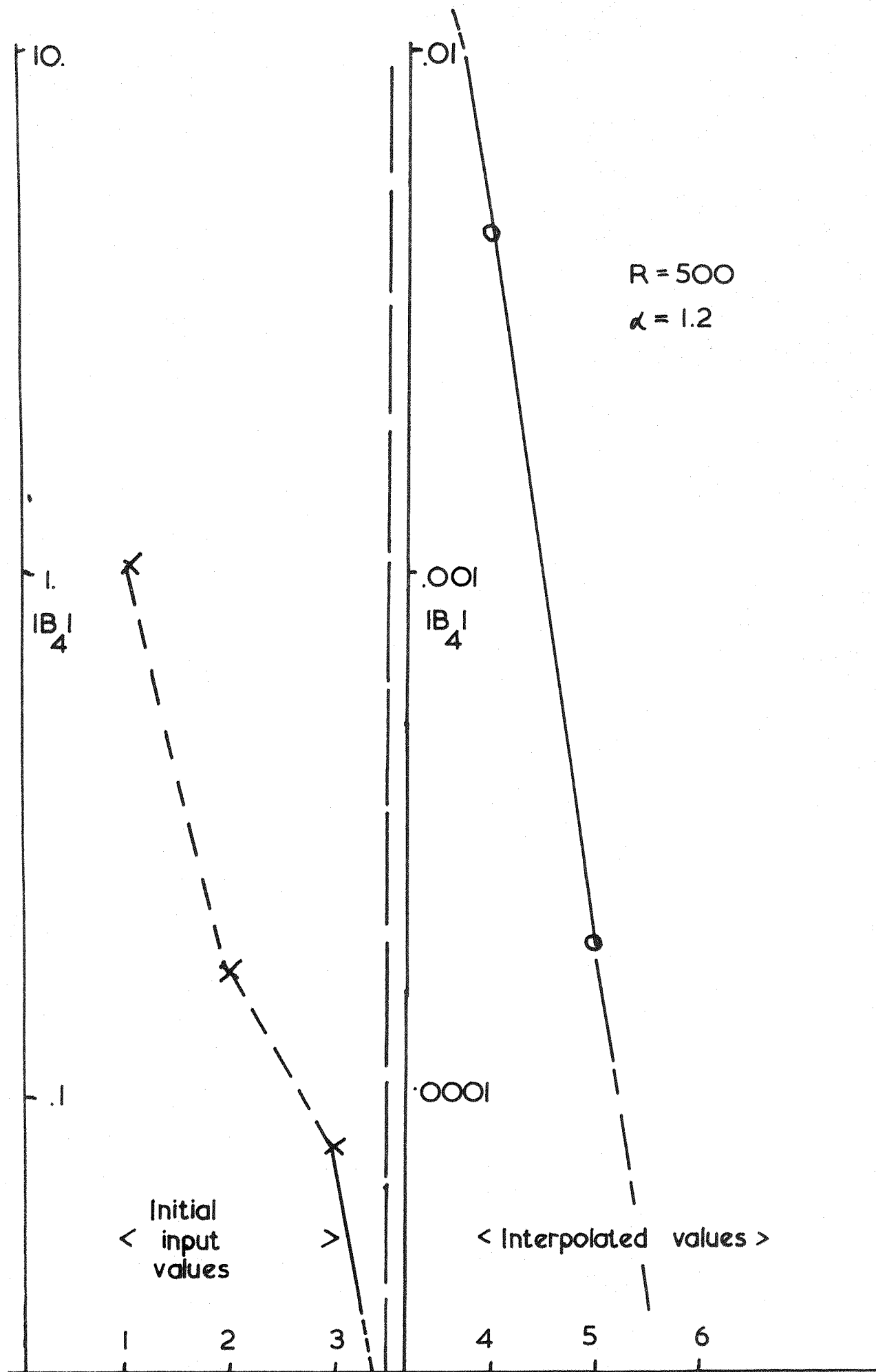
Convergence of Interpolation to Minimise $|B_4|$. Figure 10
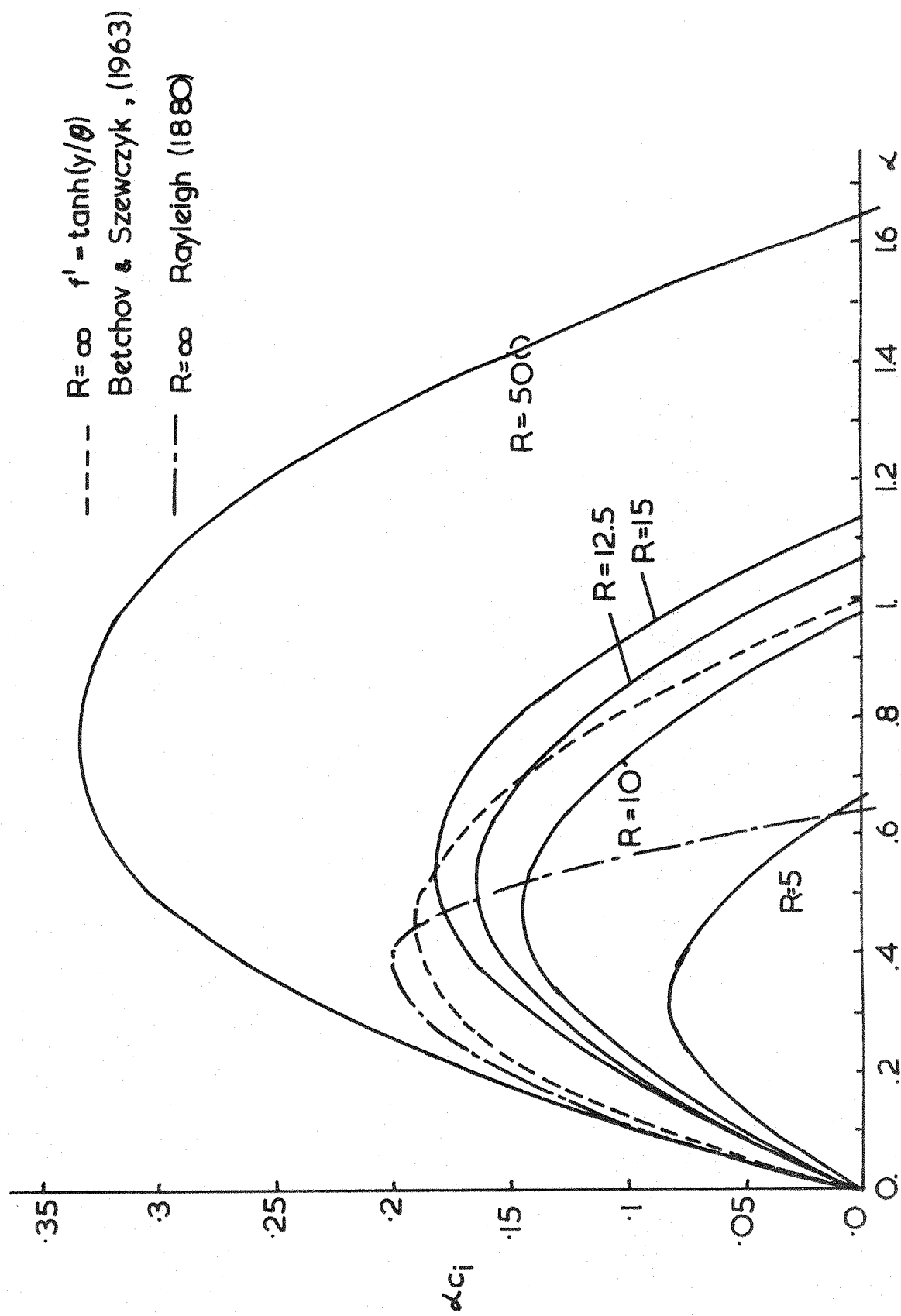
Temporal Amplification against Wavenumber for Several Reynolds Numbers.   Figure 11
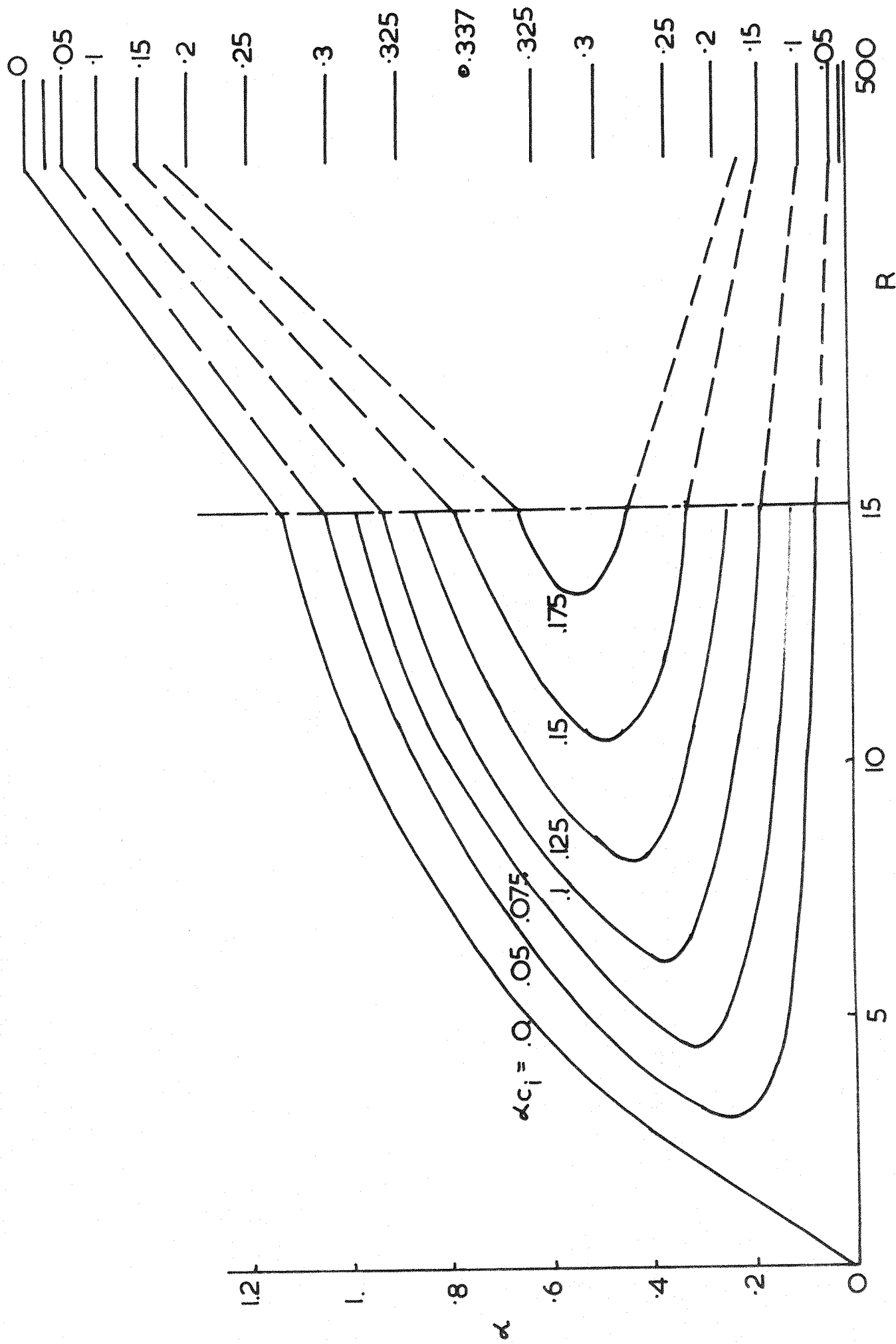
Curves of Constant Amplification Factor for Temporal Amplification

R

Figure 12

Present calculation

— Small analytic result : Esch(1957)

$.380(\alpha R)^{1/2}$
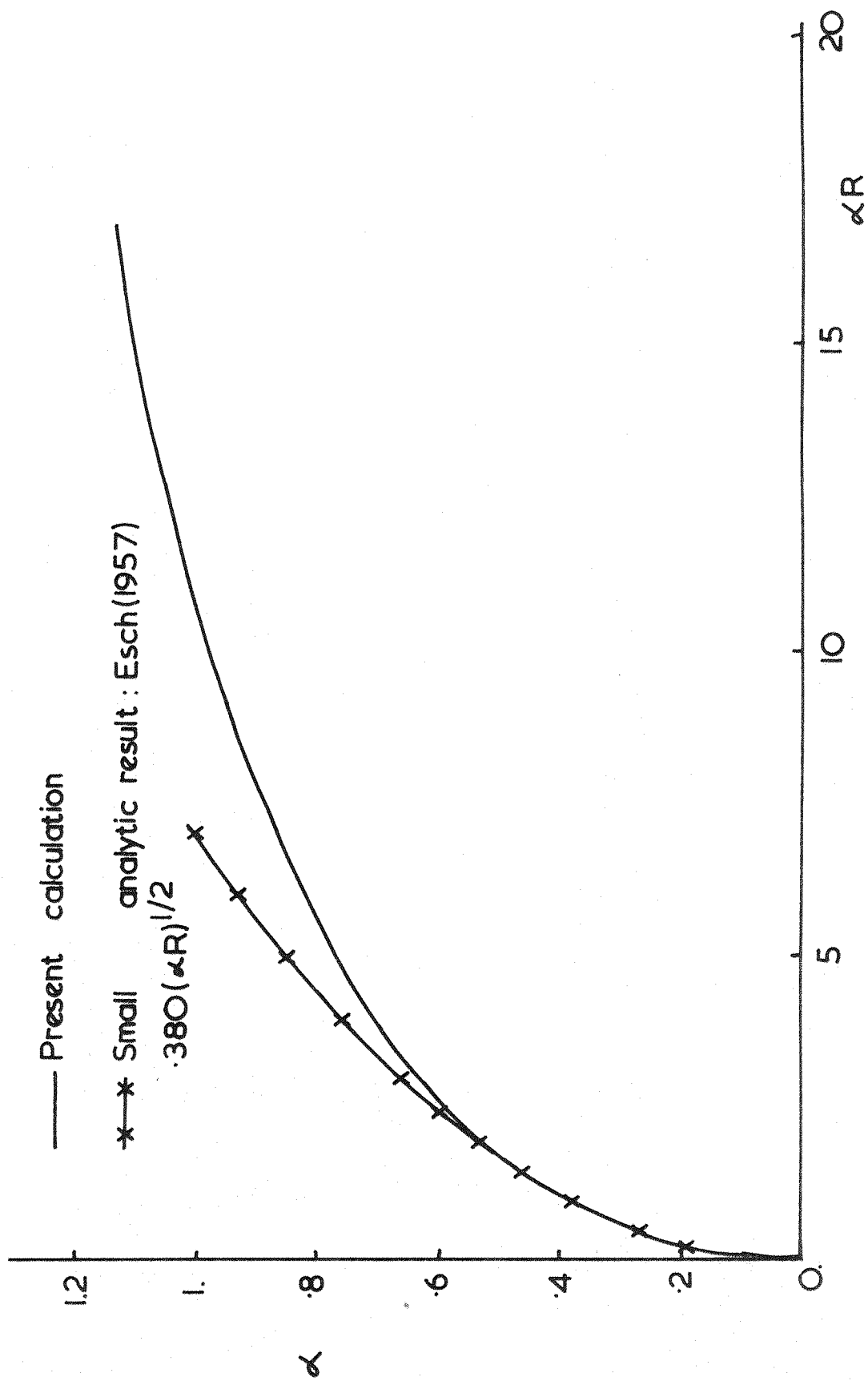
Curves of Neutral Stability against (αR)

Figure 13

Wave-speed against Wavenumber for
Several Reynolds Numbers

Figure 14
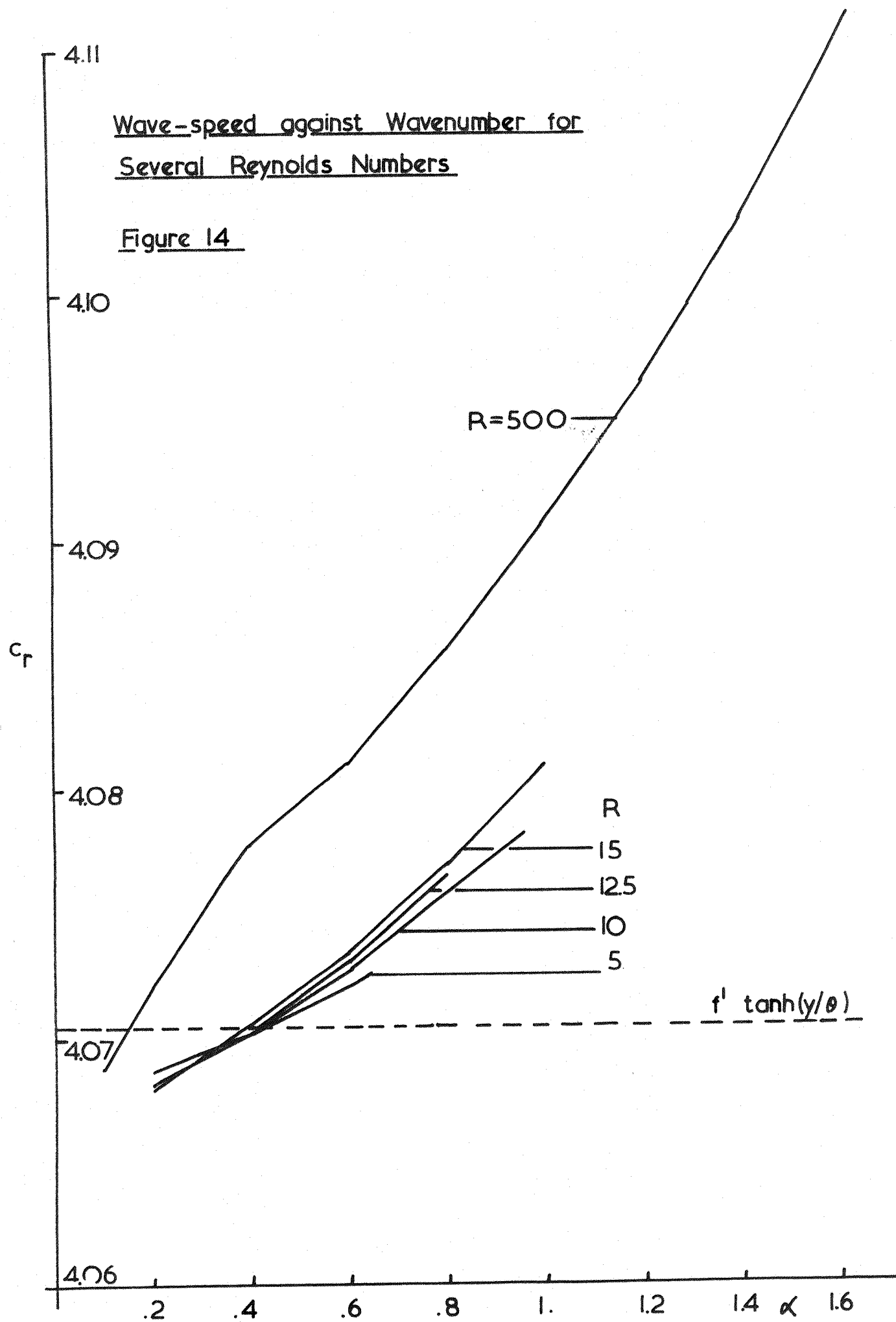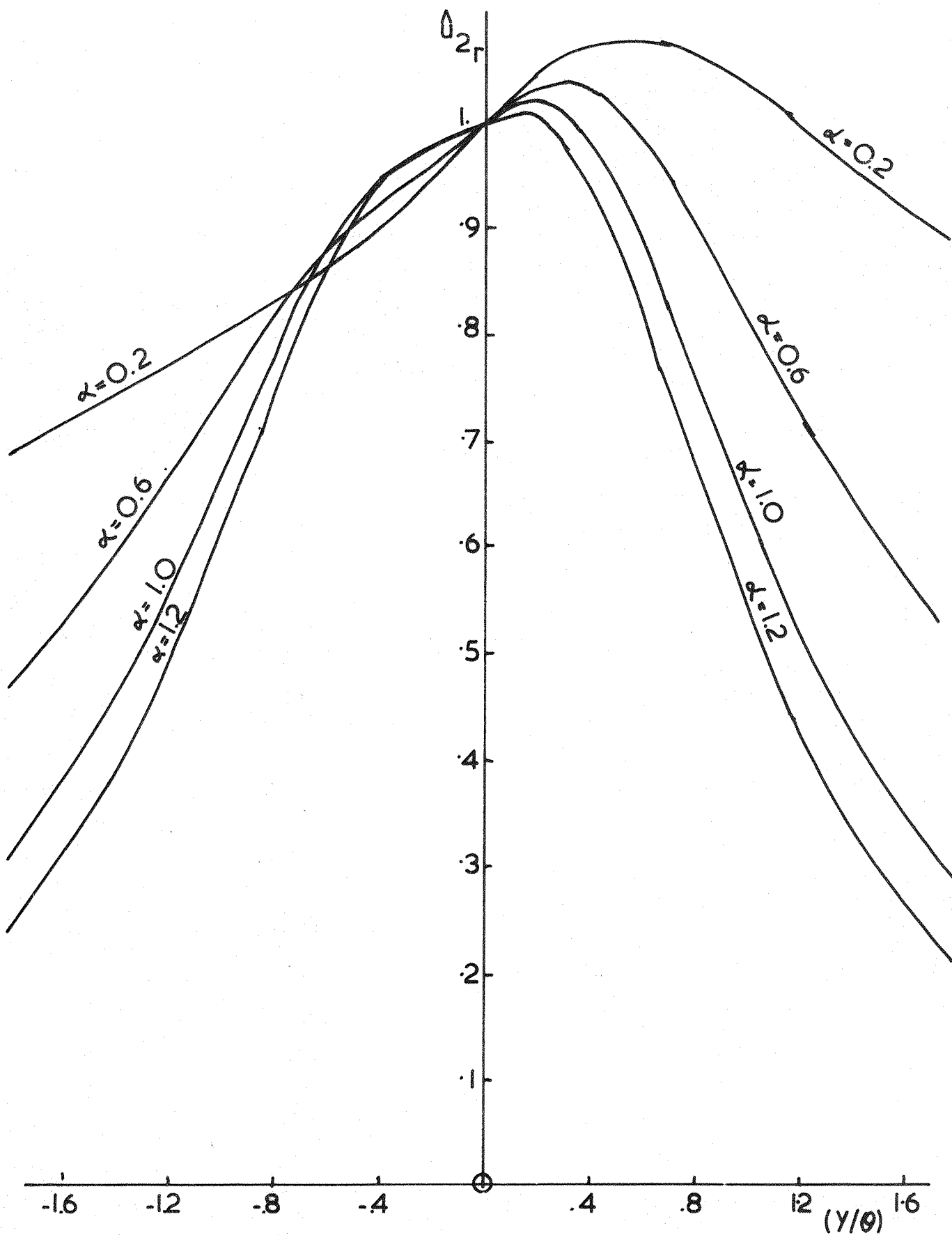
Eigenfunctions $\hat{u}_{2_r} (y/\theta)$ for Temporal Case and Several

Wavenumbers   Figure 15(a)
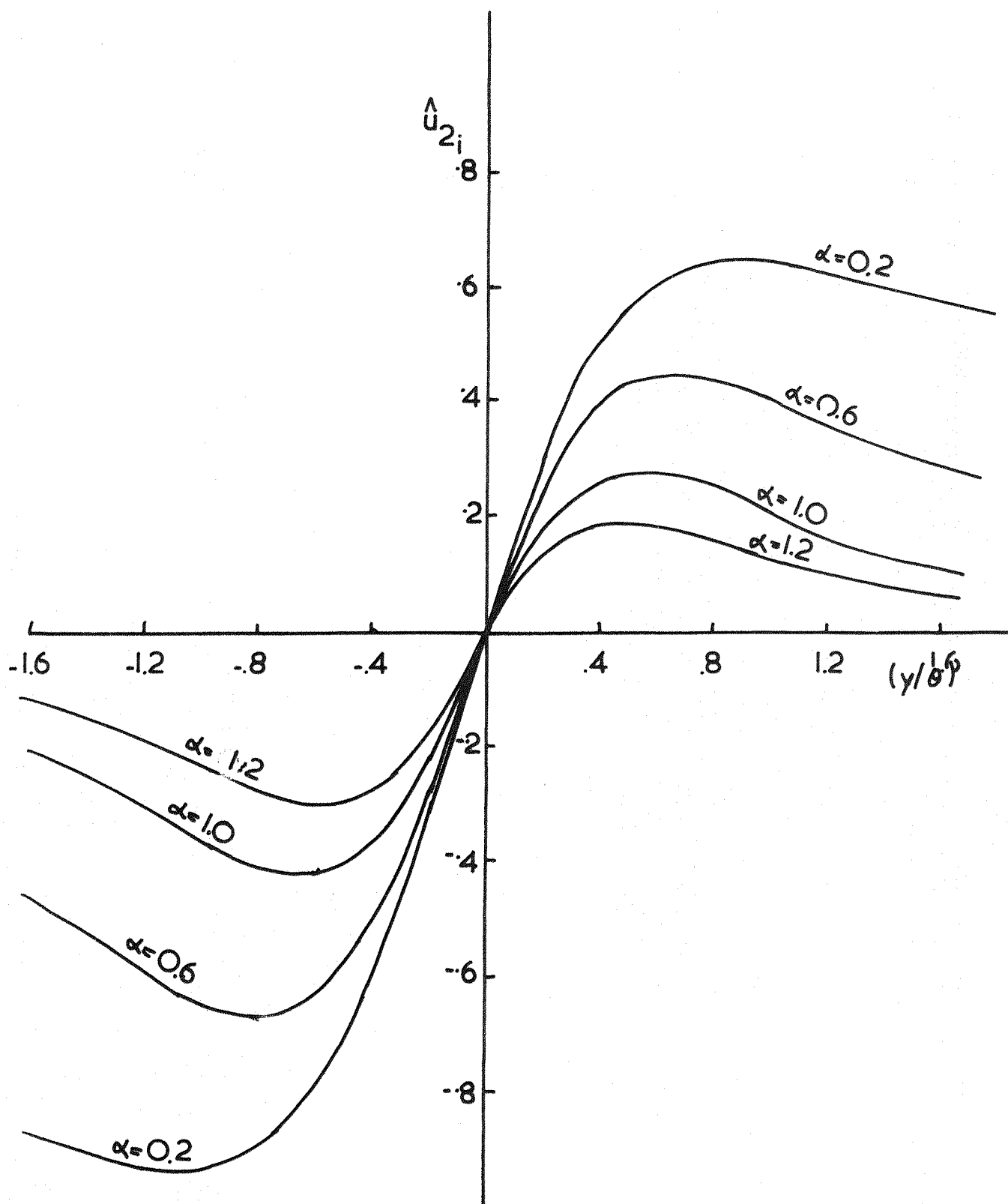
Eigenfunctions $\hat{u}_{2_i}(y/\theta)$ for Temporal Case and Several Wavenumbers   Figure 15(b)
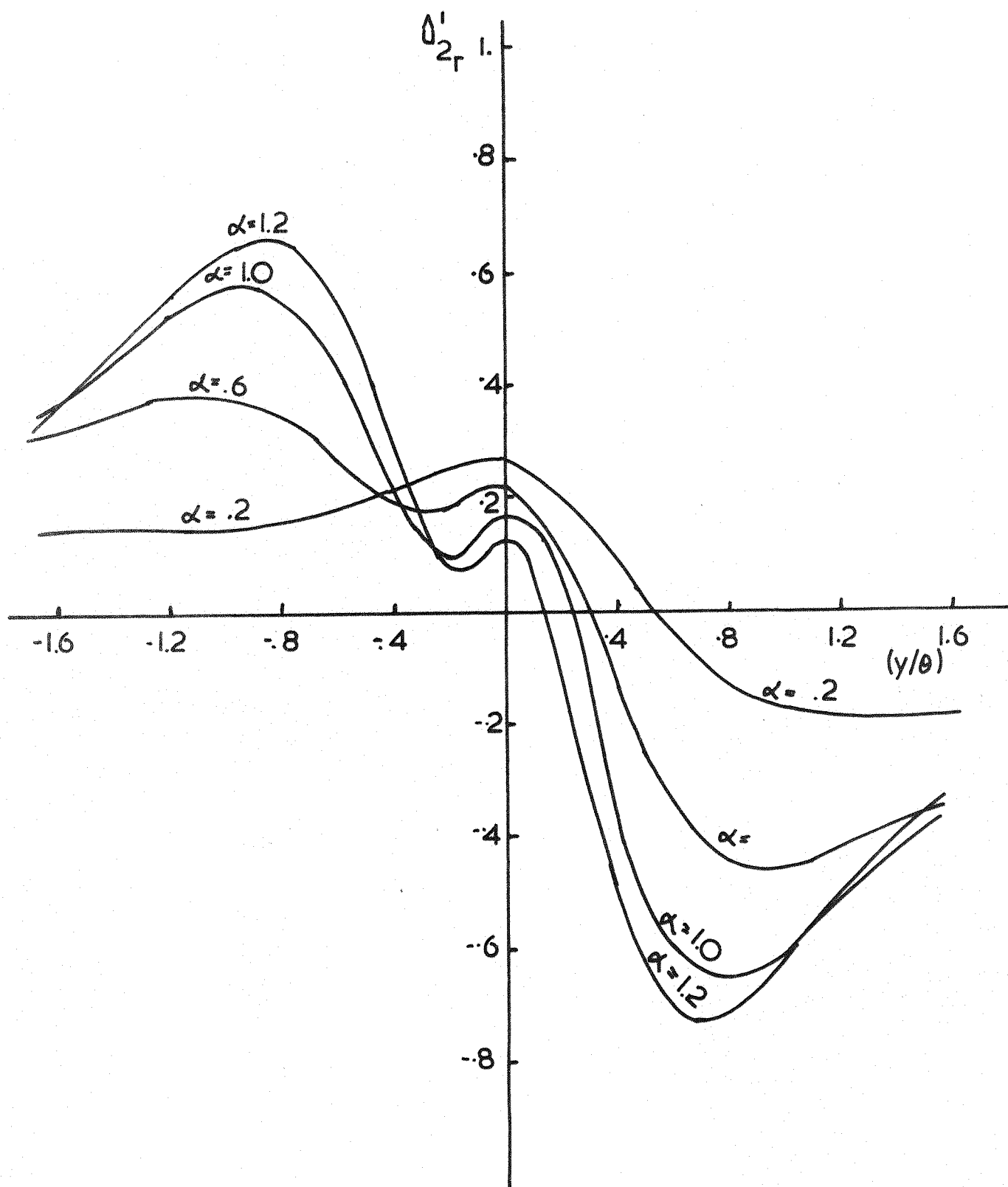
Derivatives $\hat{u}'_{2_r}(y/\theta)$ of Eigenfunctions for Temporal Case

and Several Wavenumbers   Figure 15(c)
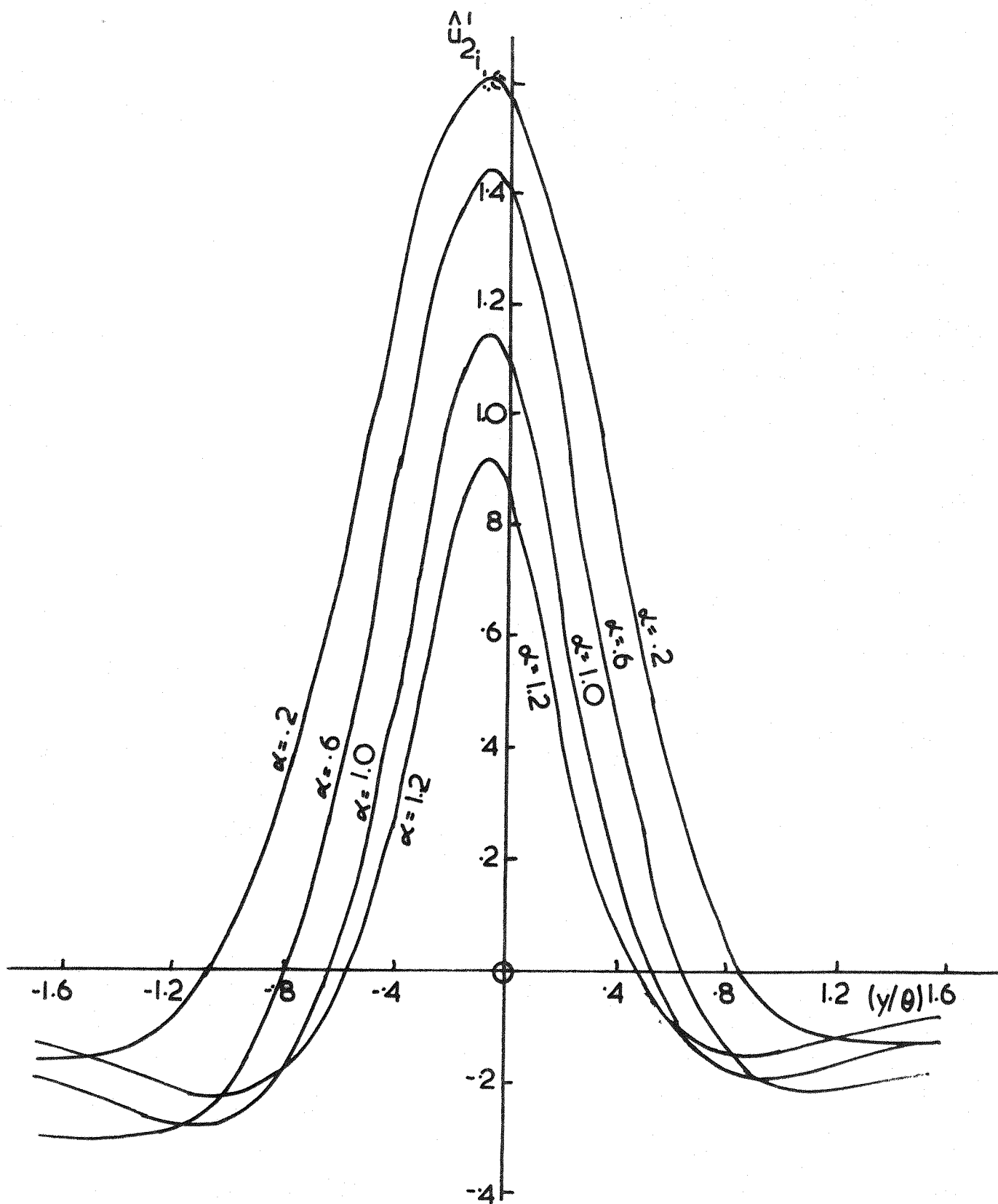
Derivatives $\hat{u}'_{2_i}(y/\theta)$ of Eigenfunctions for Temporal Case

and Several Wavenumbers   Figure 15(d)
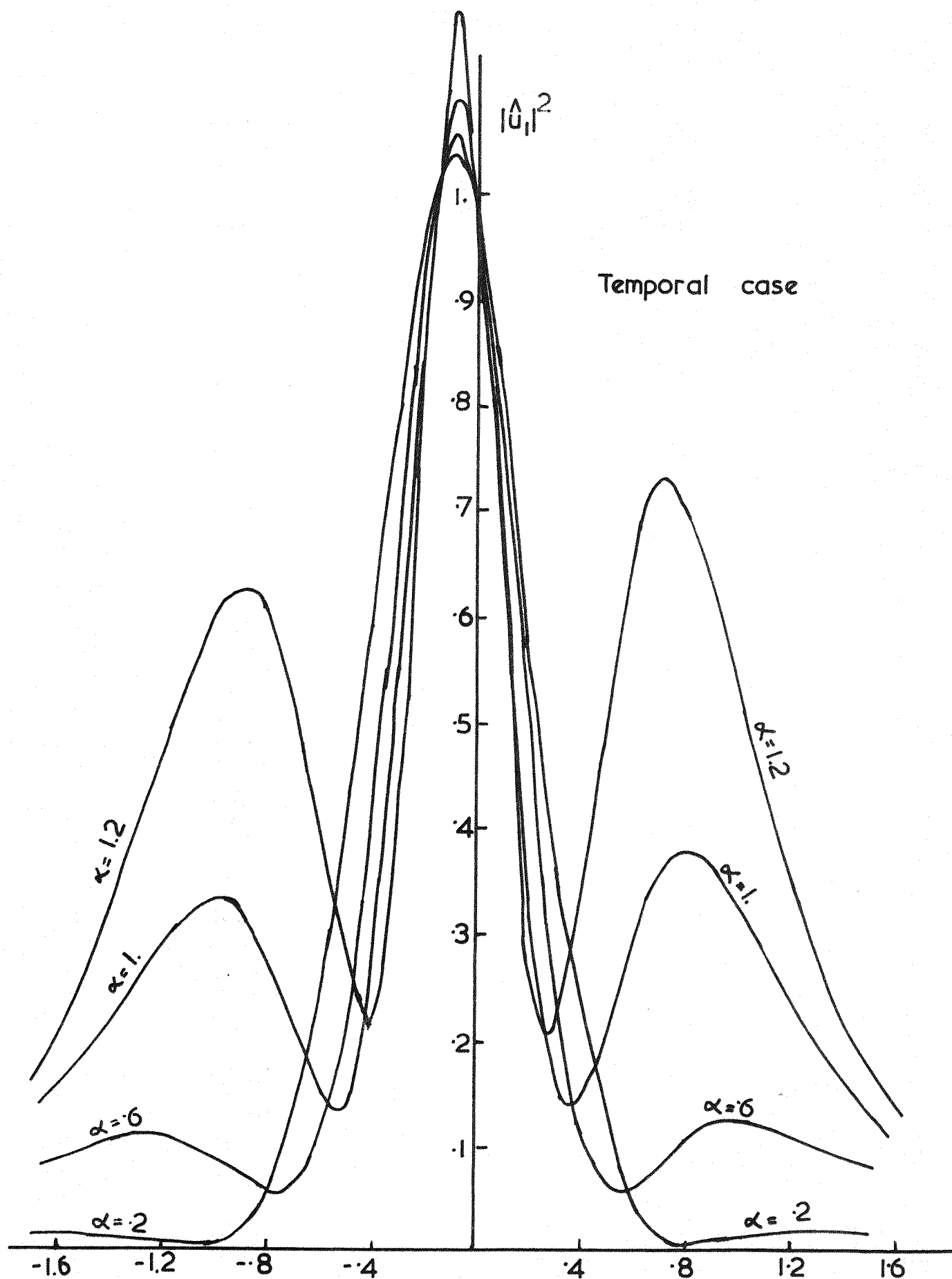
Distribution of $|\hat{u}_1|^2$ for Several Wavenumbers   Figure 16
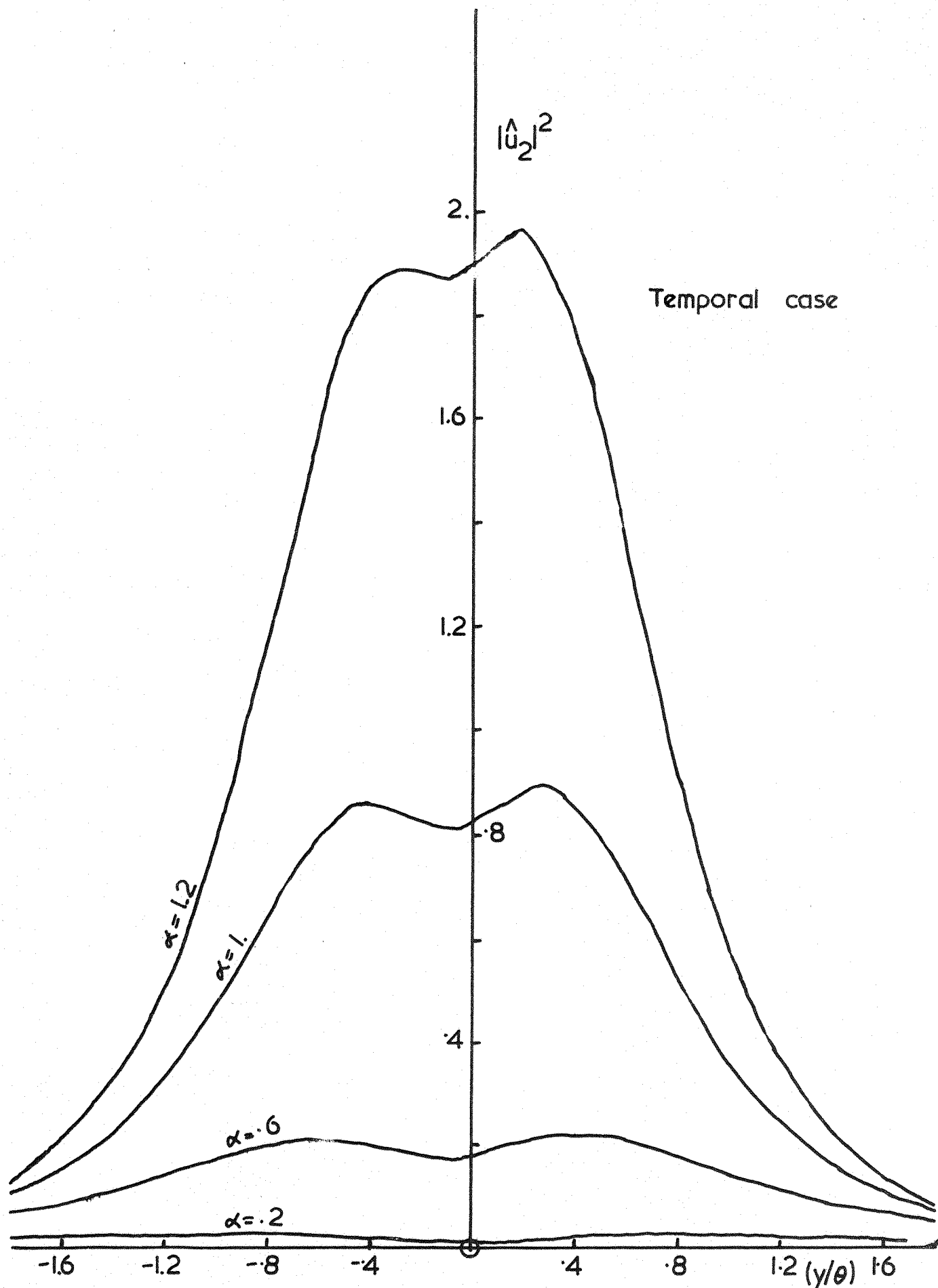
Distribution of $|\hat{u}_2|^2$ for Several Wavenumbers   Figure 17
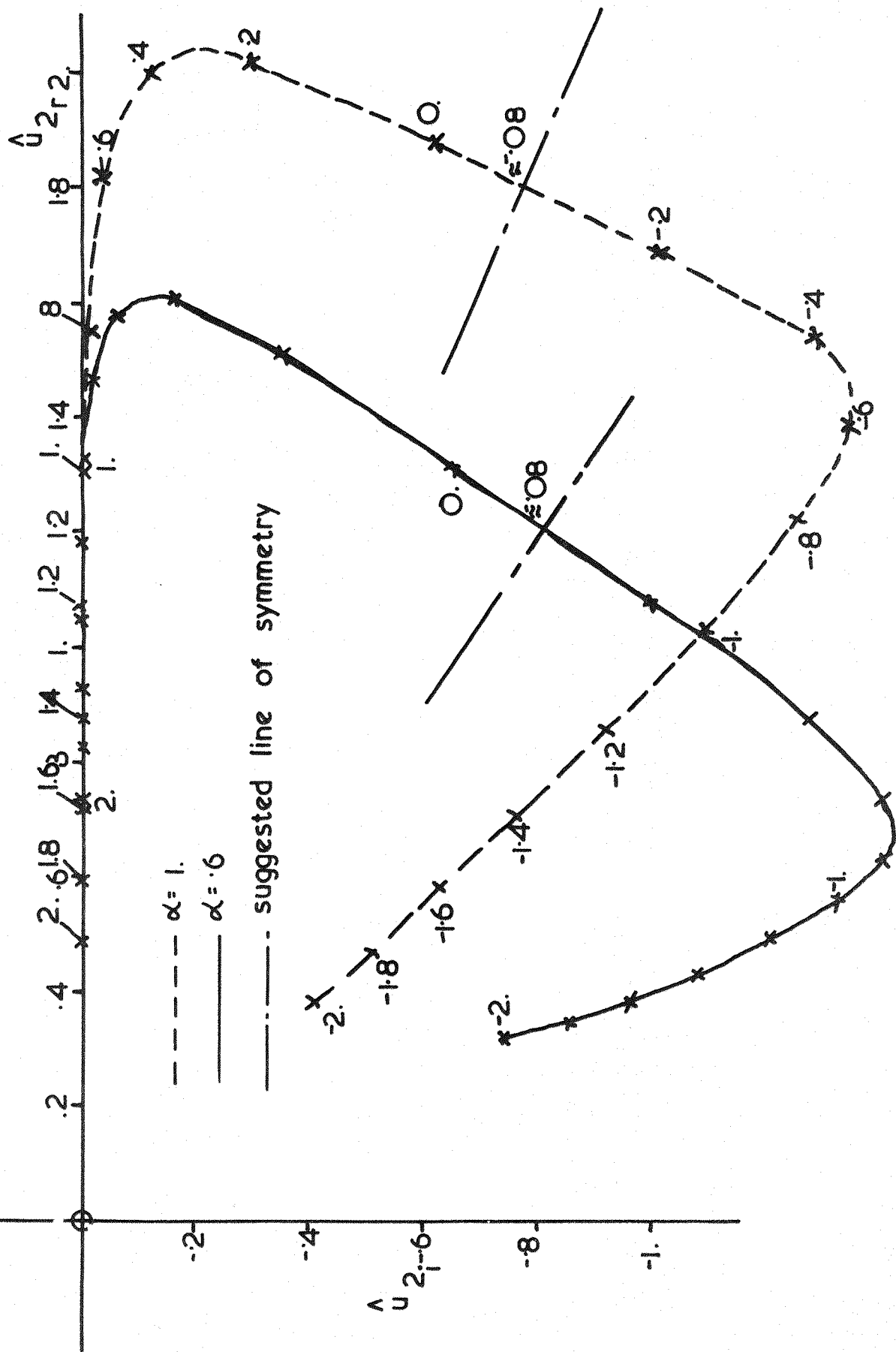
Relative Phase of $\hat{u}_2(y|\theta)$ for Wavenumbers of 0.6 & 1.0   Figure 18

Temporal case
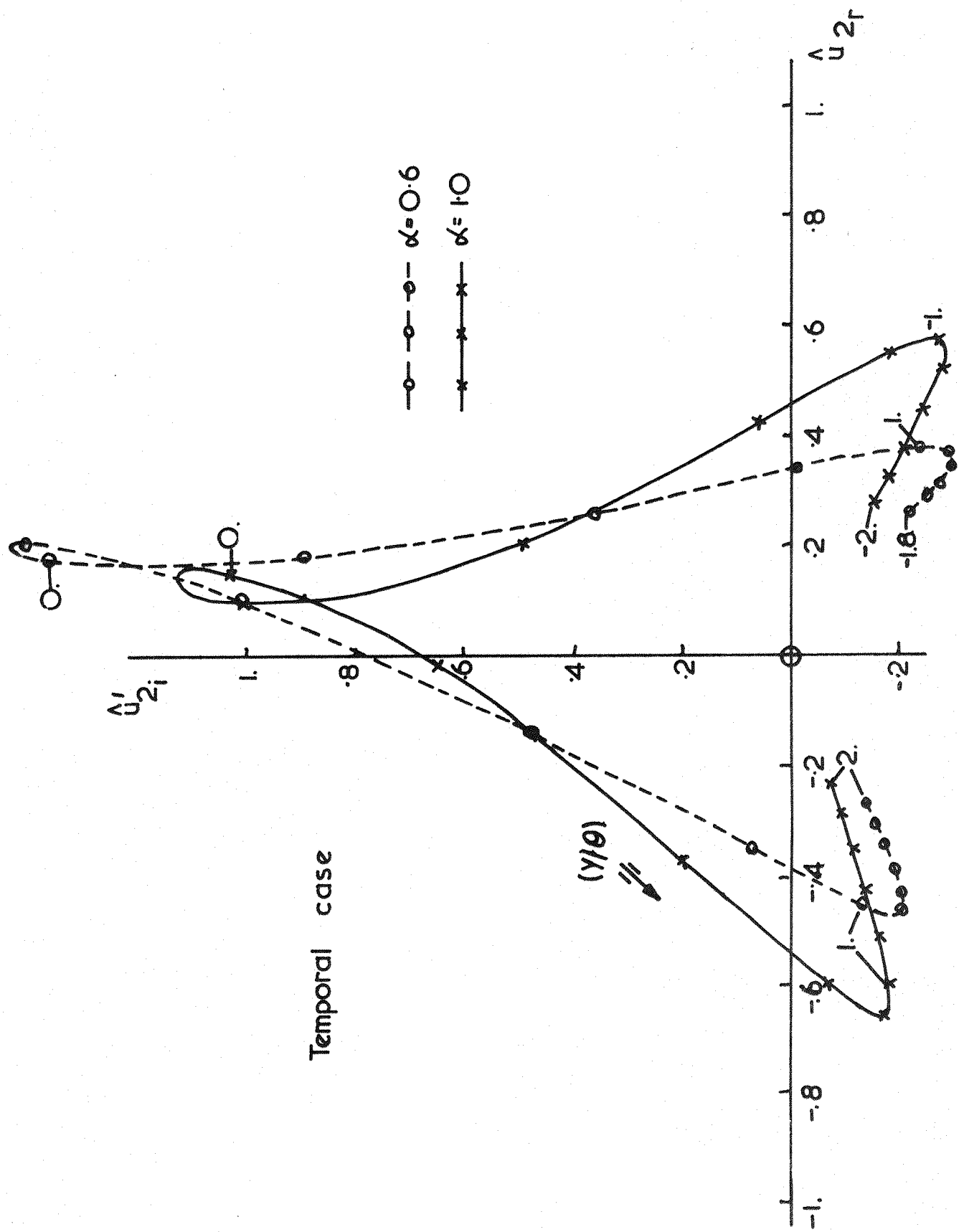
Relative Phase and Amplitude of $\hat{u}_2'$ for Wavenumbers 0·6 & 1·0   Figure 19
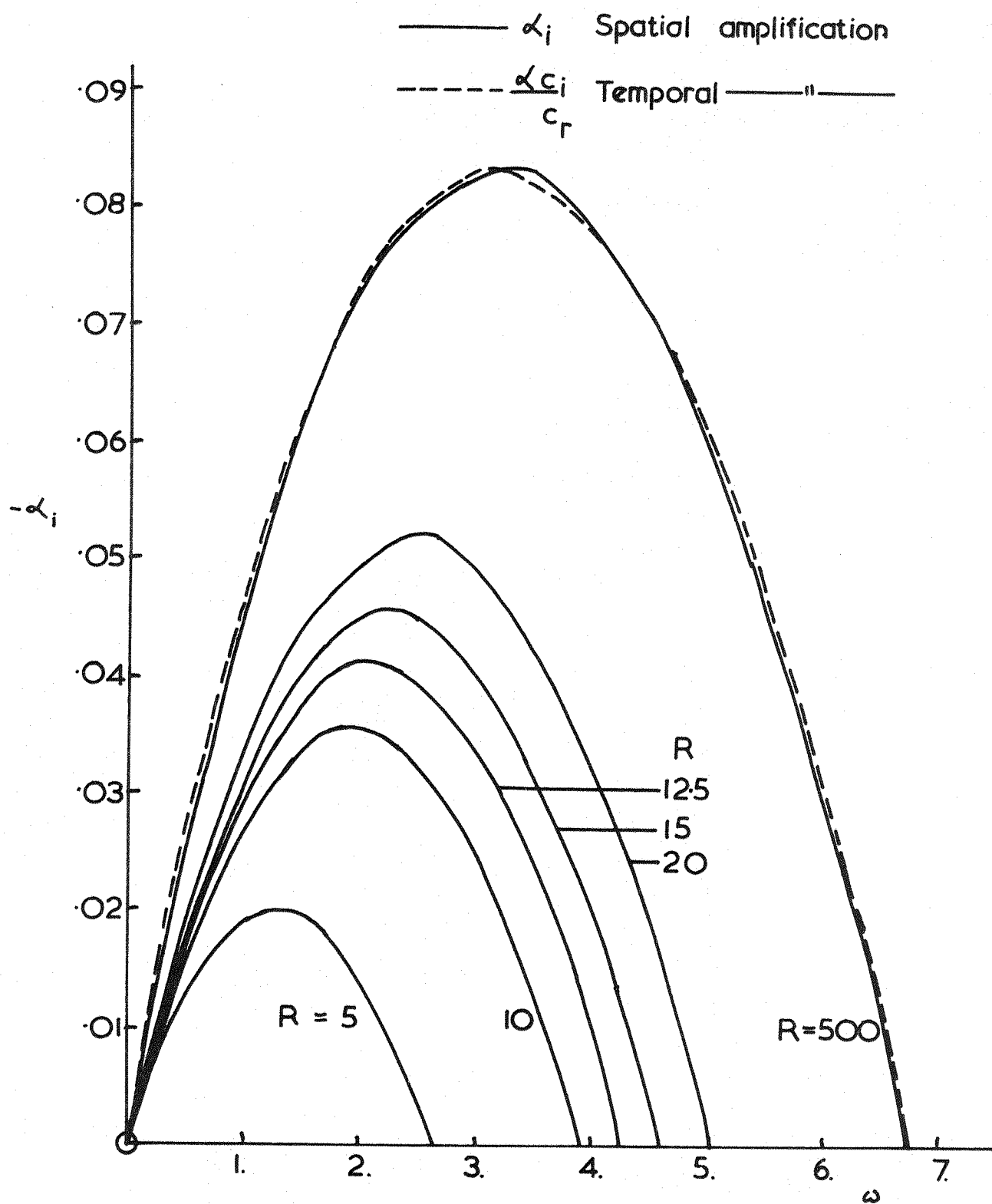
Spatial Amplification against Frequency for
Several Reynolds Numbers   Figure 20
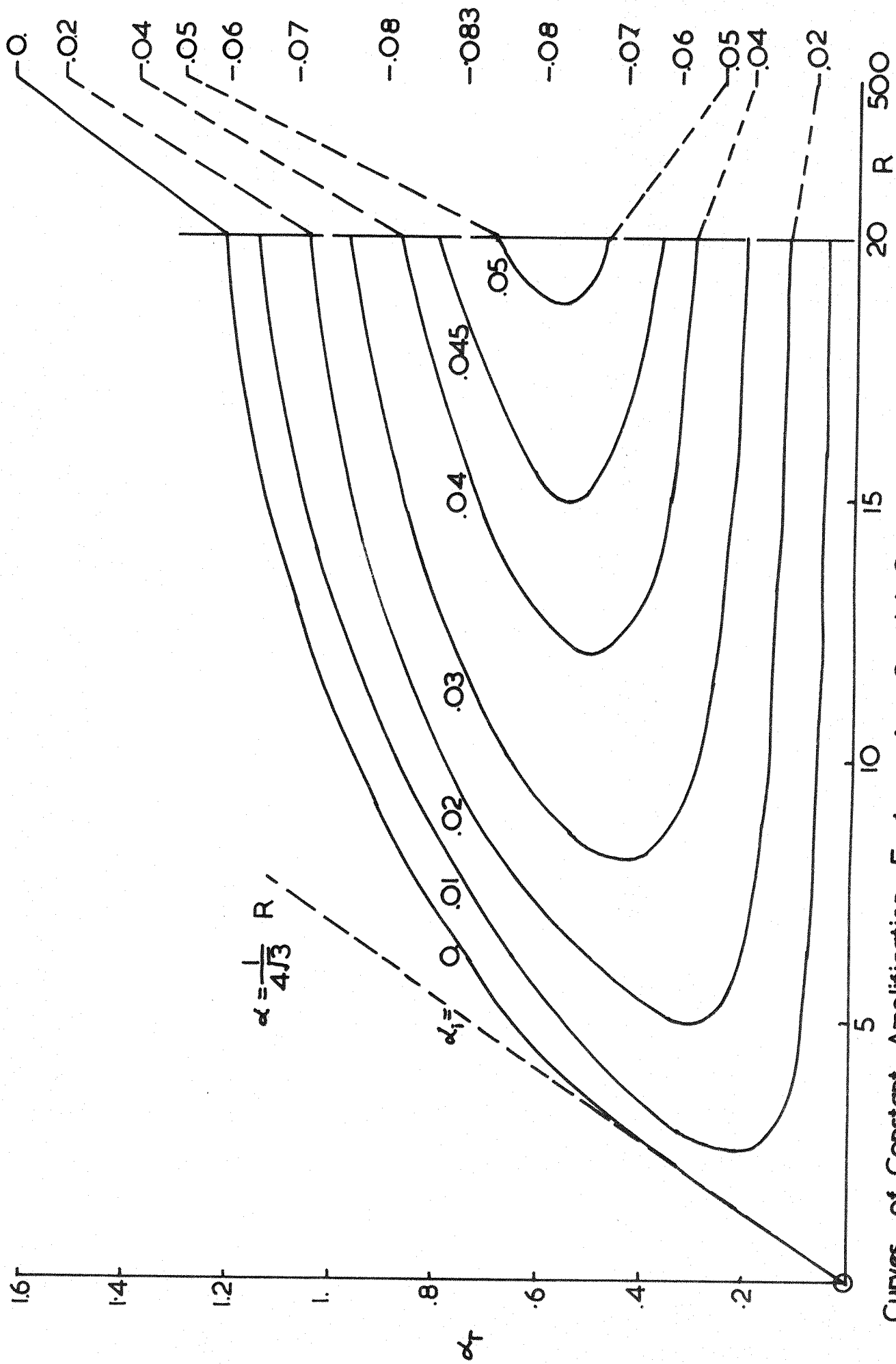
Curves of Constant Amplification Factor for Spatial Case   Figure 21
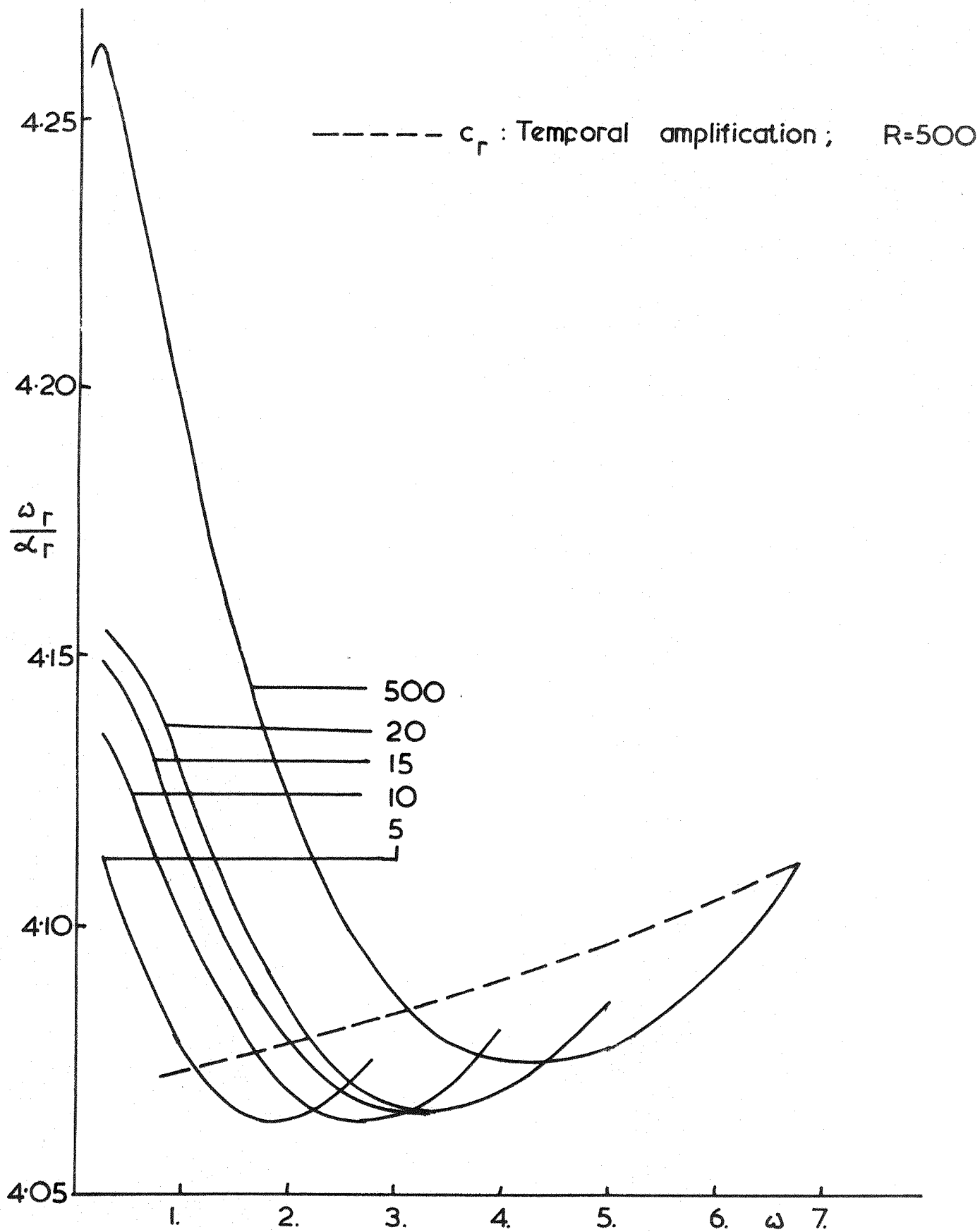
Phase Velocity against Frequency for Several

Reynolds Numbers   Figure 22
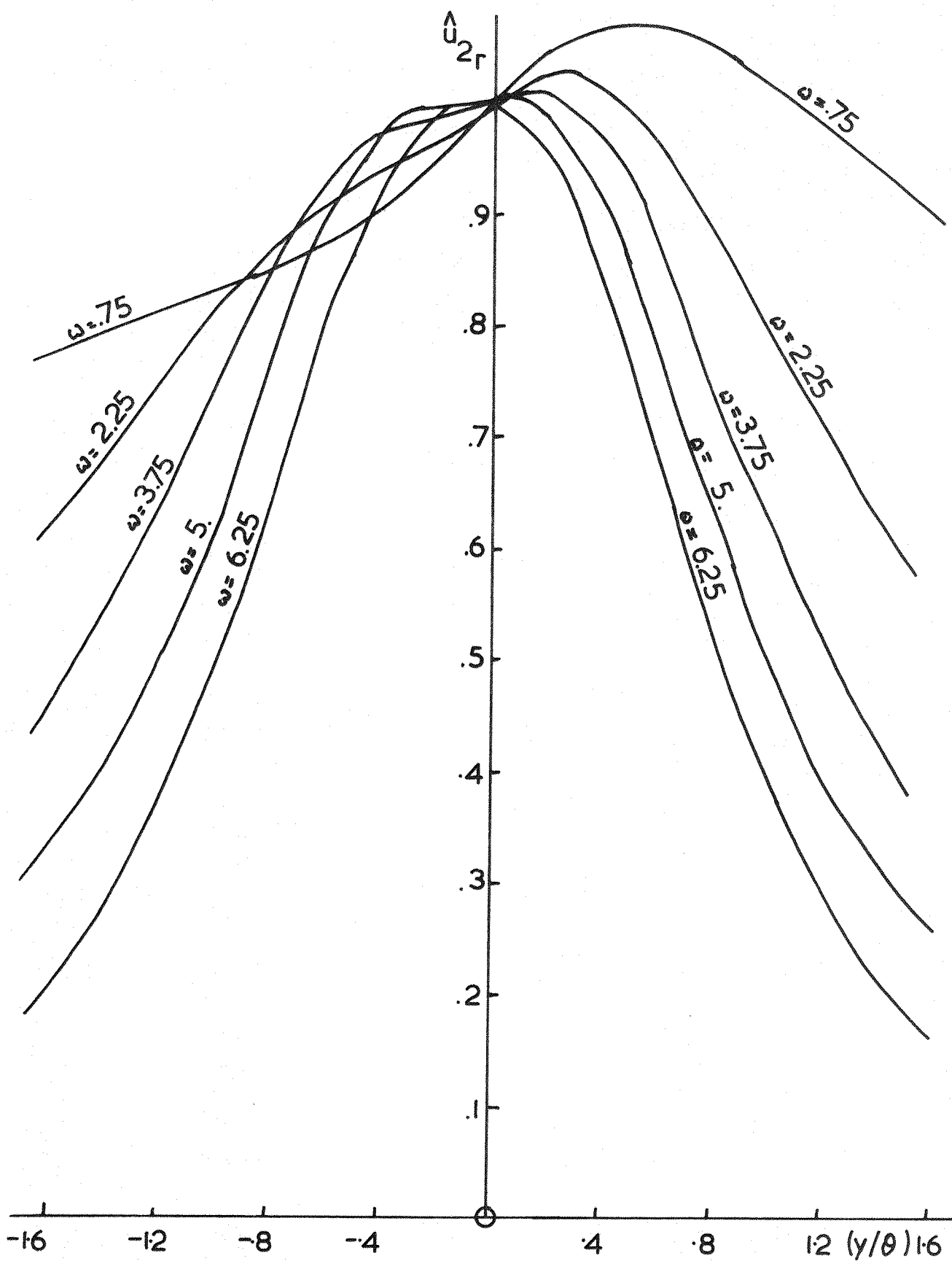
Eigenfunctions $\hat{u}_{2_r}(y/\theta)$ for Spatial Case and Several

Frequencies   Figure 23(a)
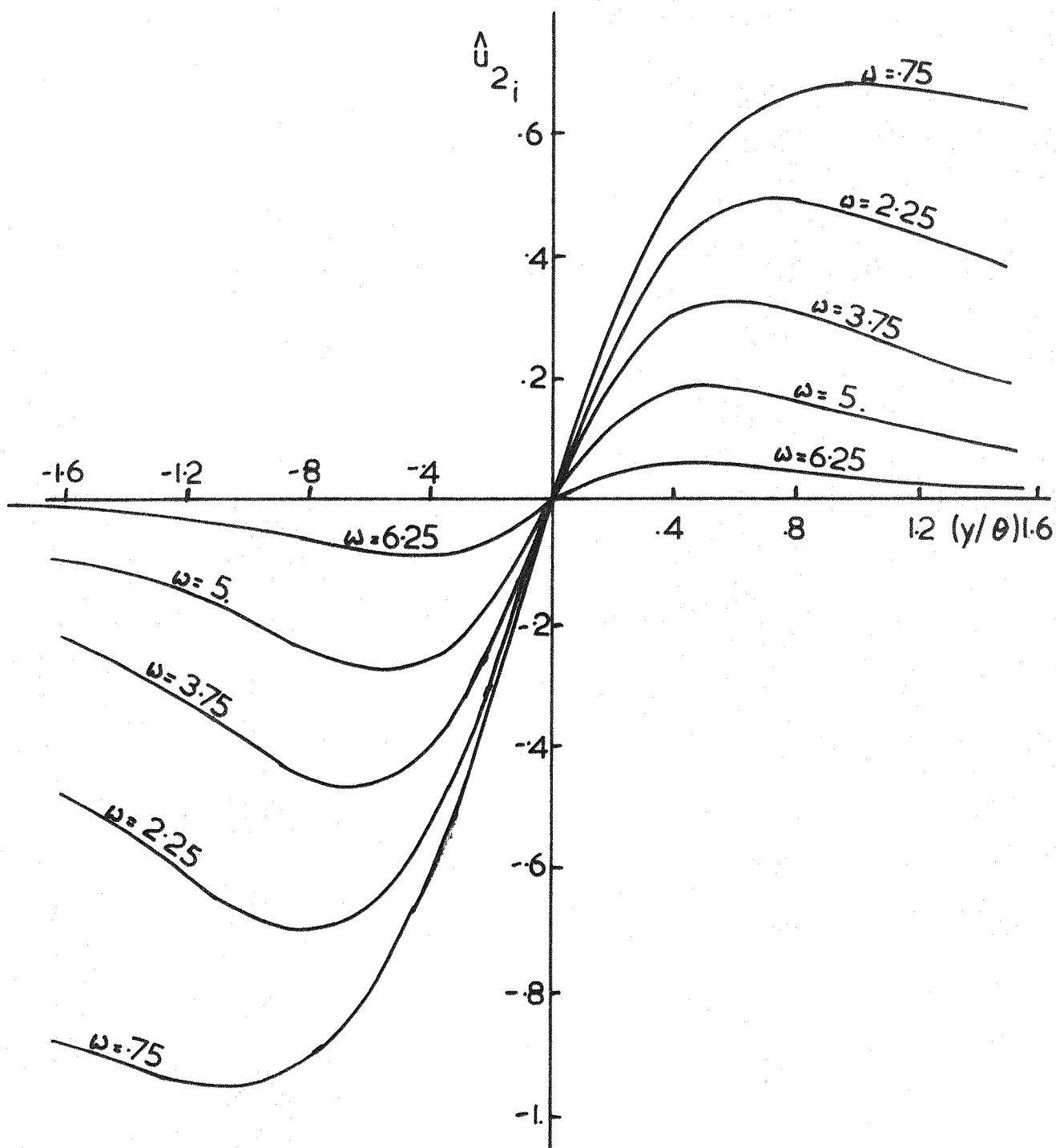
Eigenfunctions $\hat{u}_{2_i}(y/\theta)$ for Spatial Case and Several

Frequencies   Figure   23 (b)
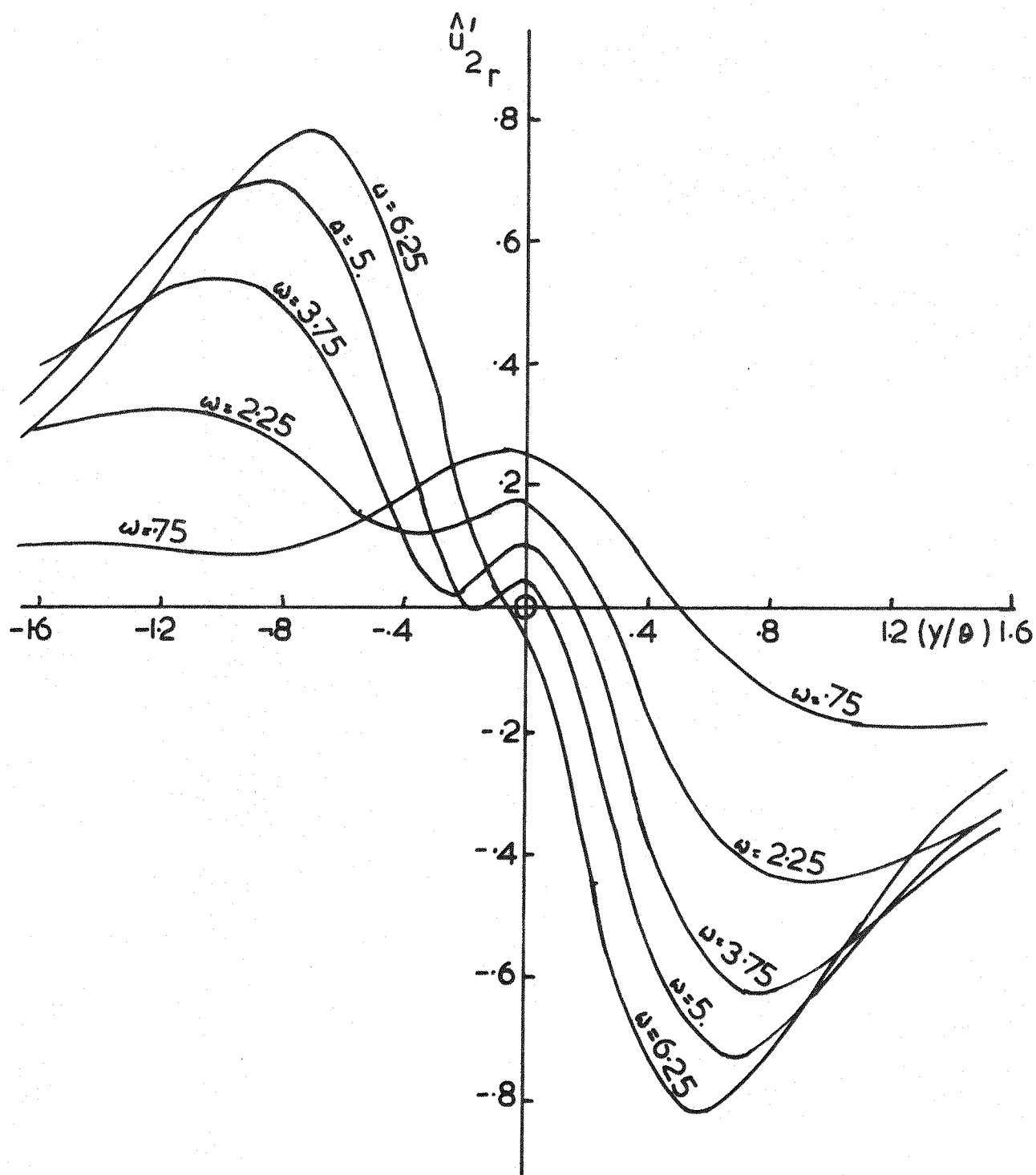
Derivatives $\hat{u}'_{2_r}(y/\theta)$ for Spatial Case and Several Frequencies   Figure 23(c)
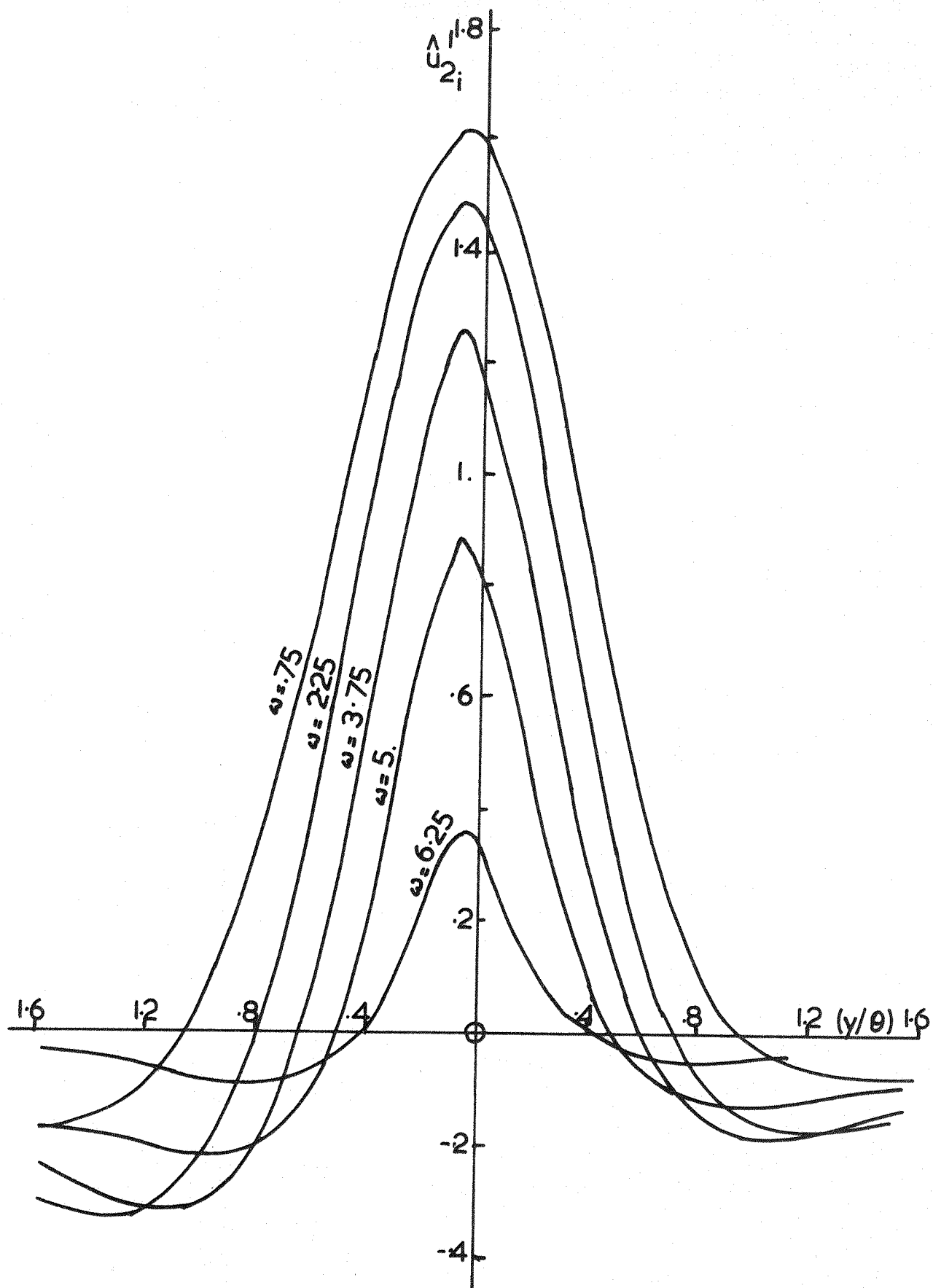
Derivatives $\hat{u}_{2_i}^{I}(y/\theta)$ for Spatial Case and Several

Frequencies   Figure 23(d)

$|\hat{u}_1|^2$

$\omega=5.$

$\omega=3.75$

$\omega=2.25$

$\omega=.75$
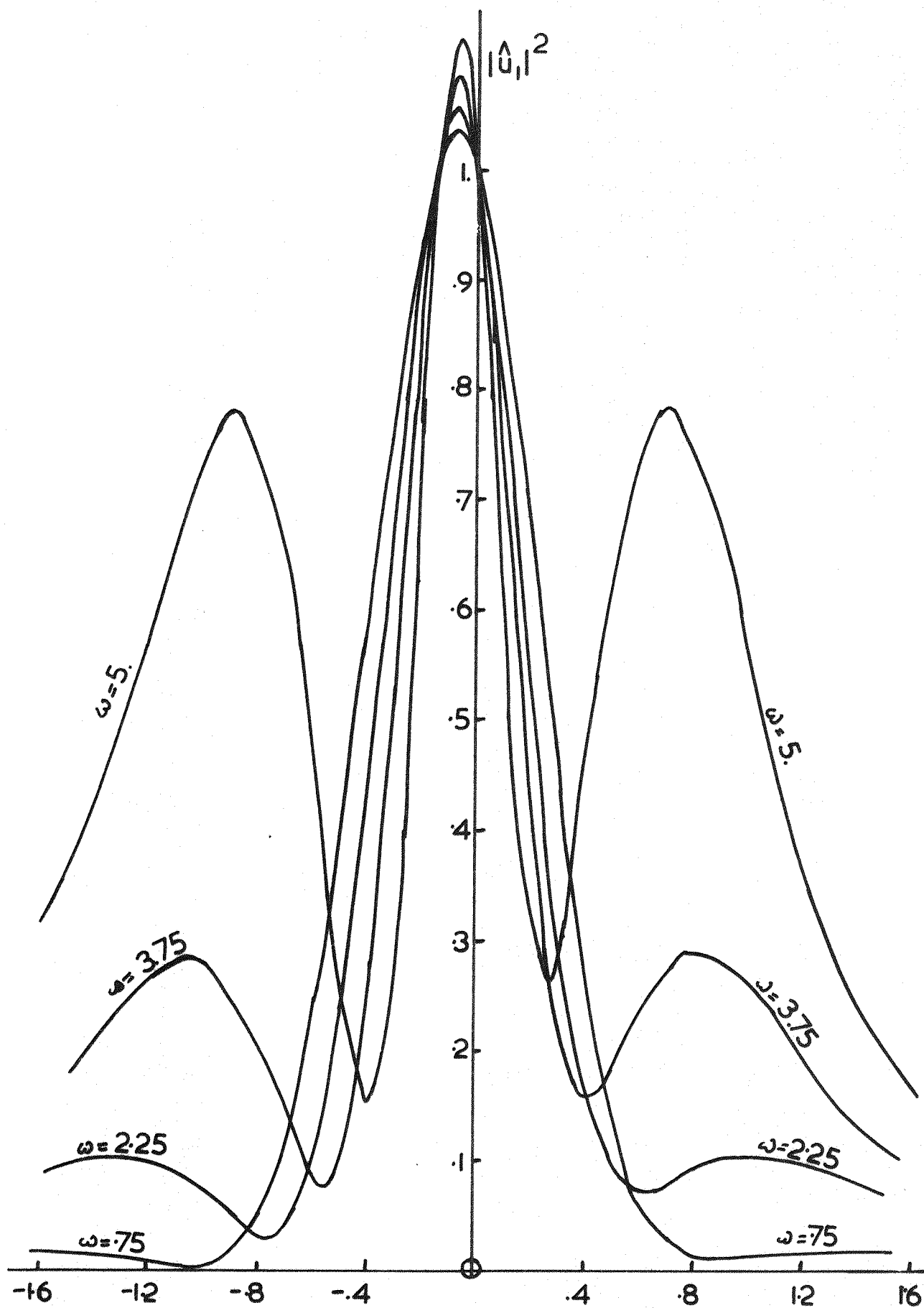
Distribution of $|\hat{u}_1|^2$ for Several Frequencies   Figure 24
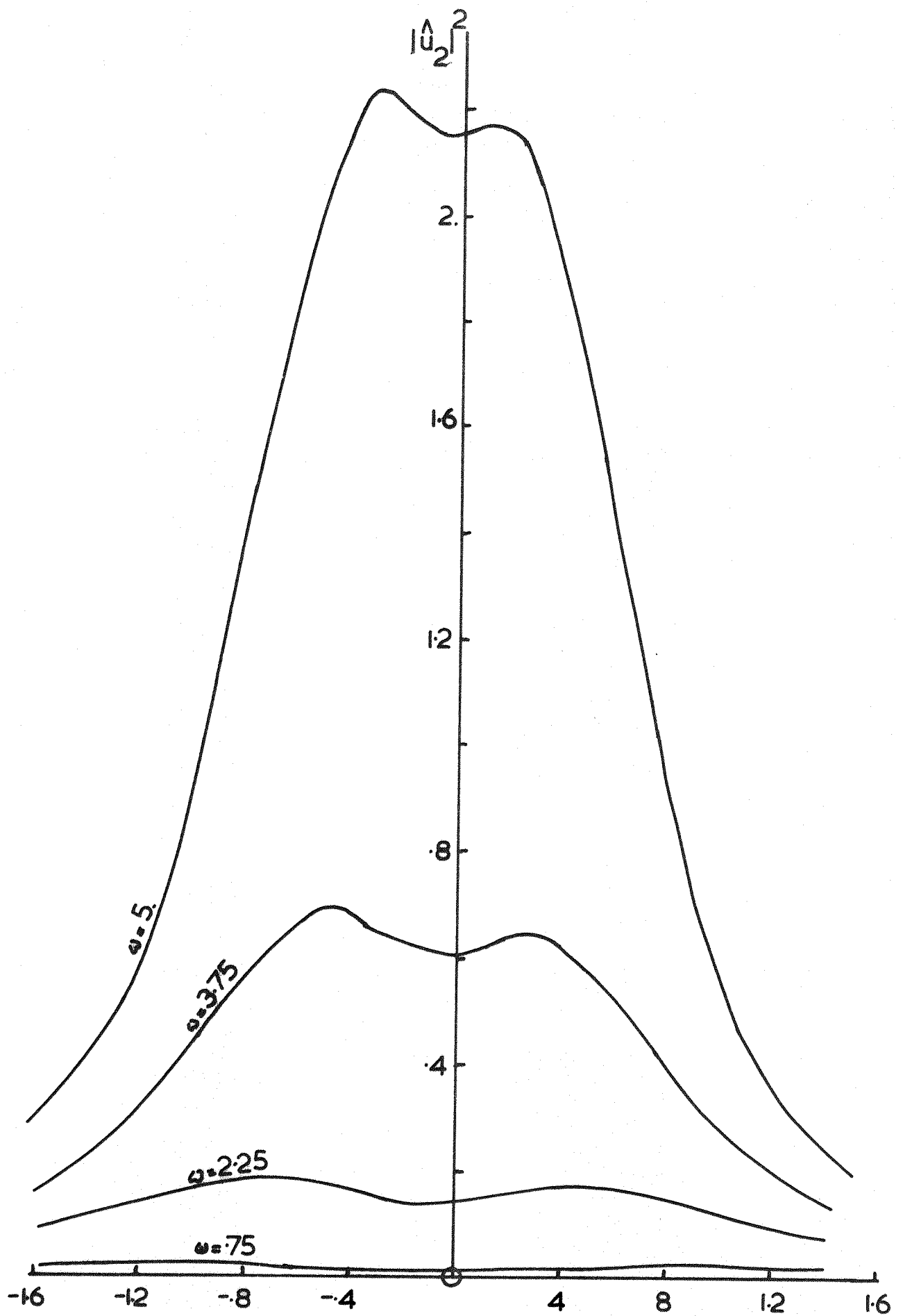
Distribution of $|\hat{u}_2|^2$ for Several Frequencies   Figure 25
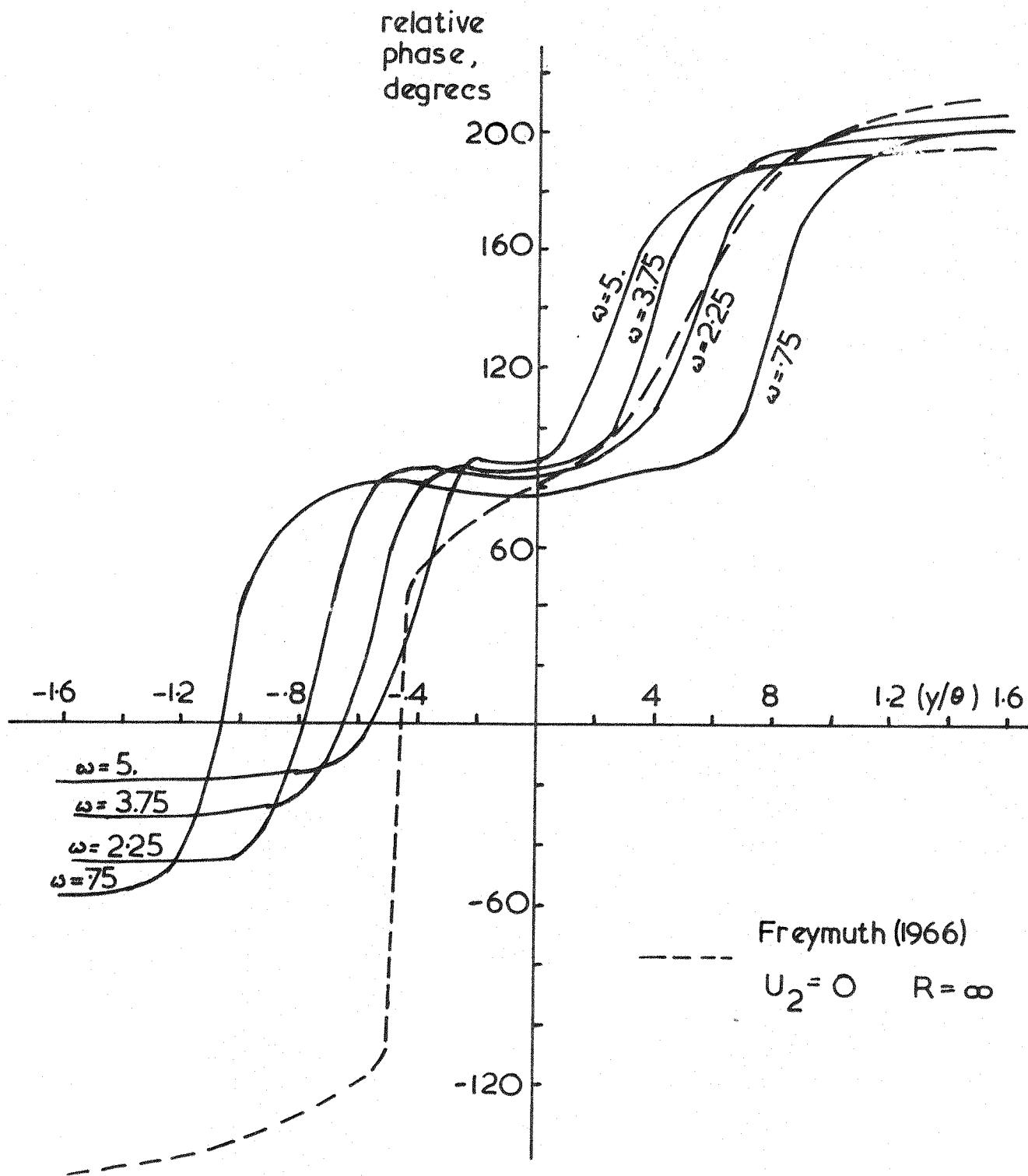
Relative Phase of $\hat{u}_1$ for Several Frequencies

Figure 26
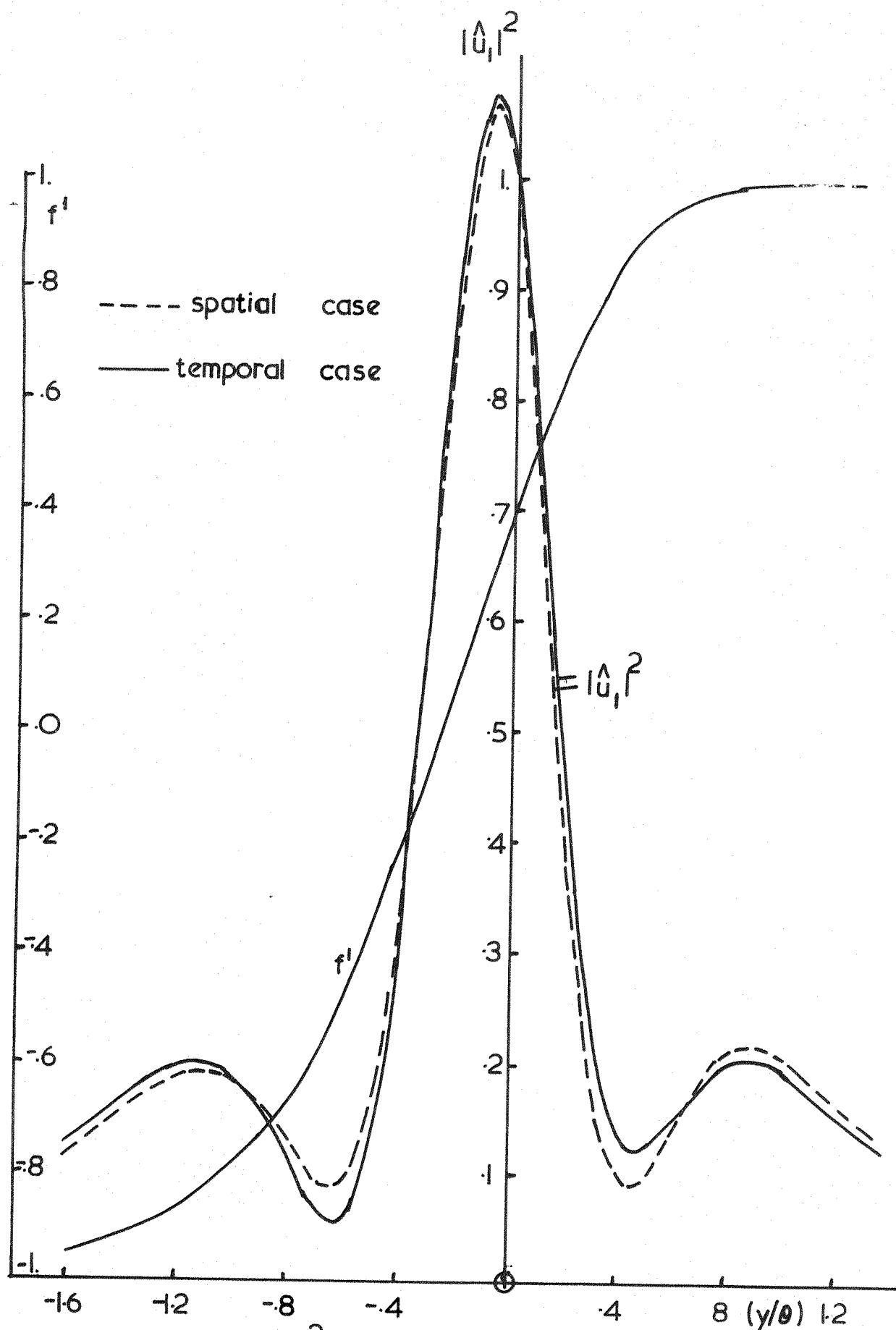
Distribution of $|\hat{u}_1|^2$ for Maximum Spatial and Temporal Amplification

Figure 27
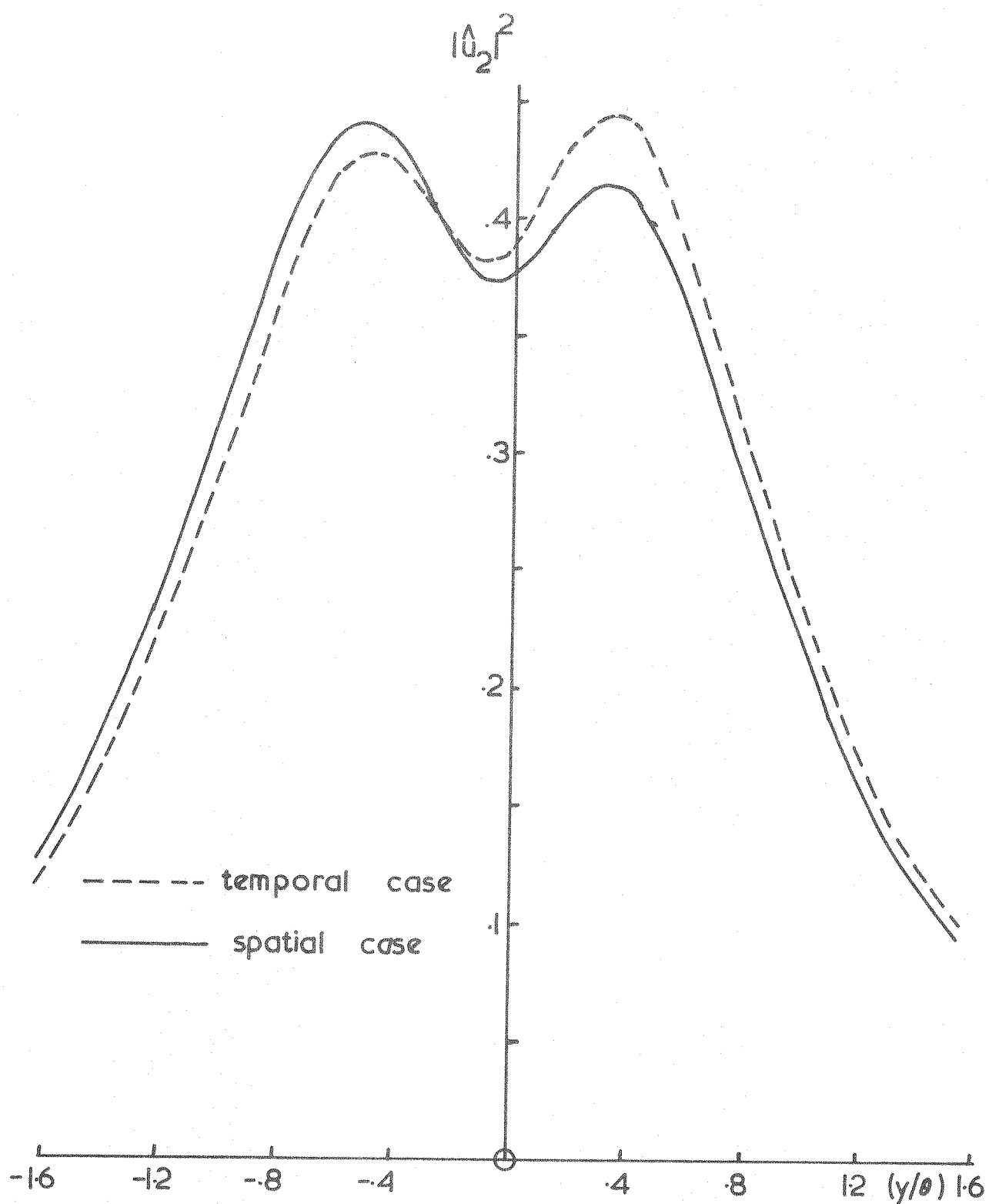
Distribution of $|\hat{u}_2|^2$ for Maximum Spatial and Temporal Amplification

Figure 28
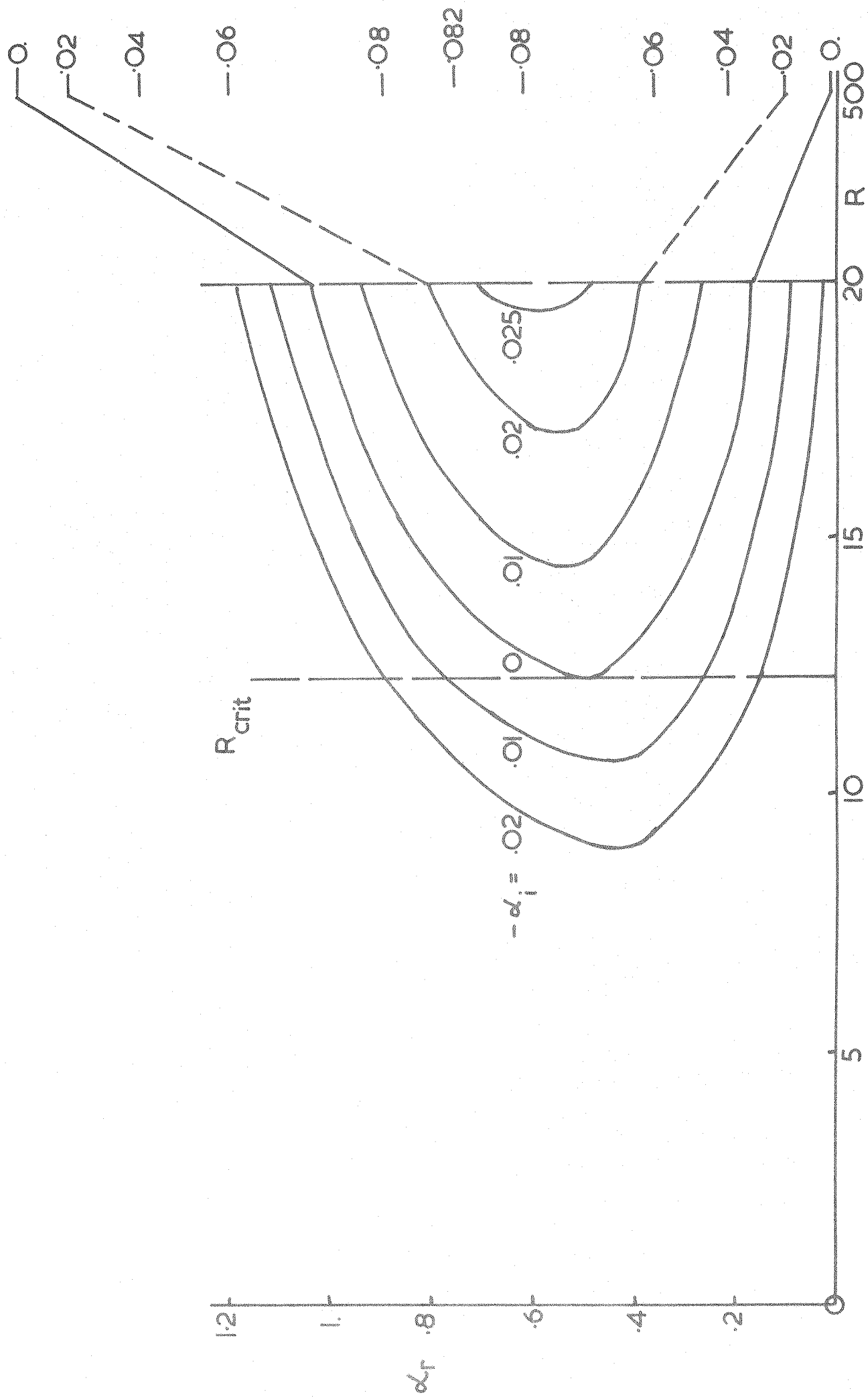
Curves of Constant Spatial Amplification Factor Corrected for Non-parallel Flow

Figure 29
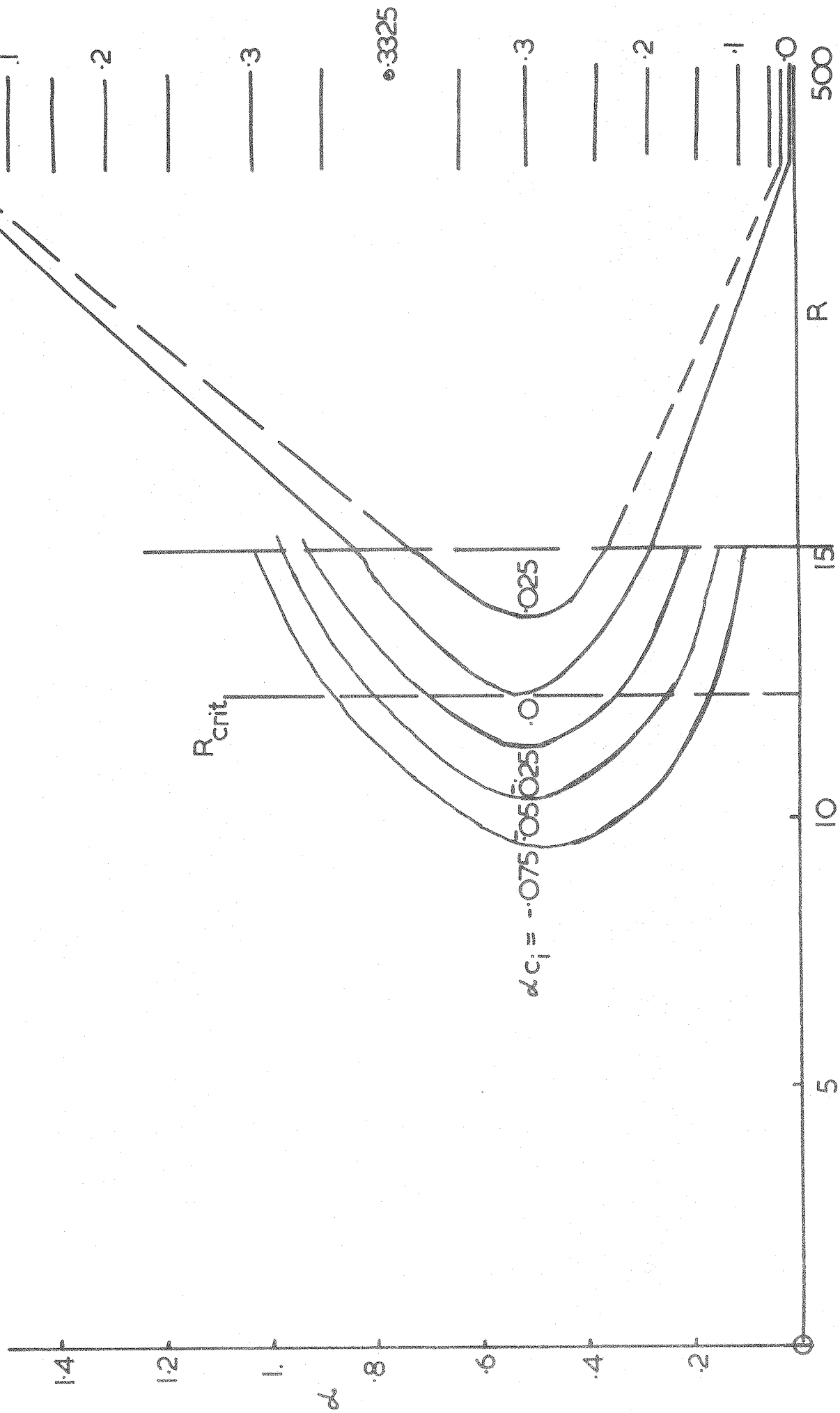
Curves of Constant Temporal Amplification Factor Corrected for Non-parallel Flow   Figure 30

Reynolds Number 6000

U_2/U_1 0.61

spatial case

temporal case

c_r

4.25
4.2
4.15
4.1
4.05
4.0

O 1. 2. 3. 4. 5.

ω

Variation of Phase Velocity with Frequency.

Figure 31

U_2/U_1 0.61

Reynolds Number 6000
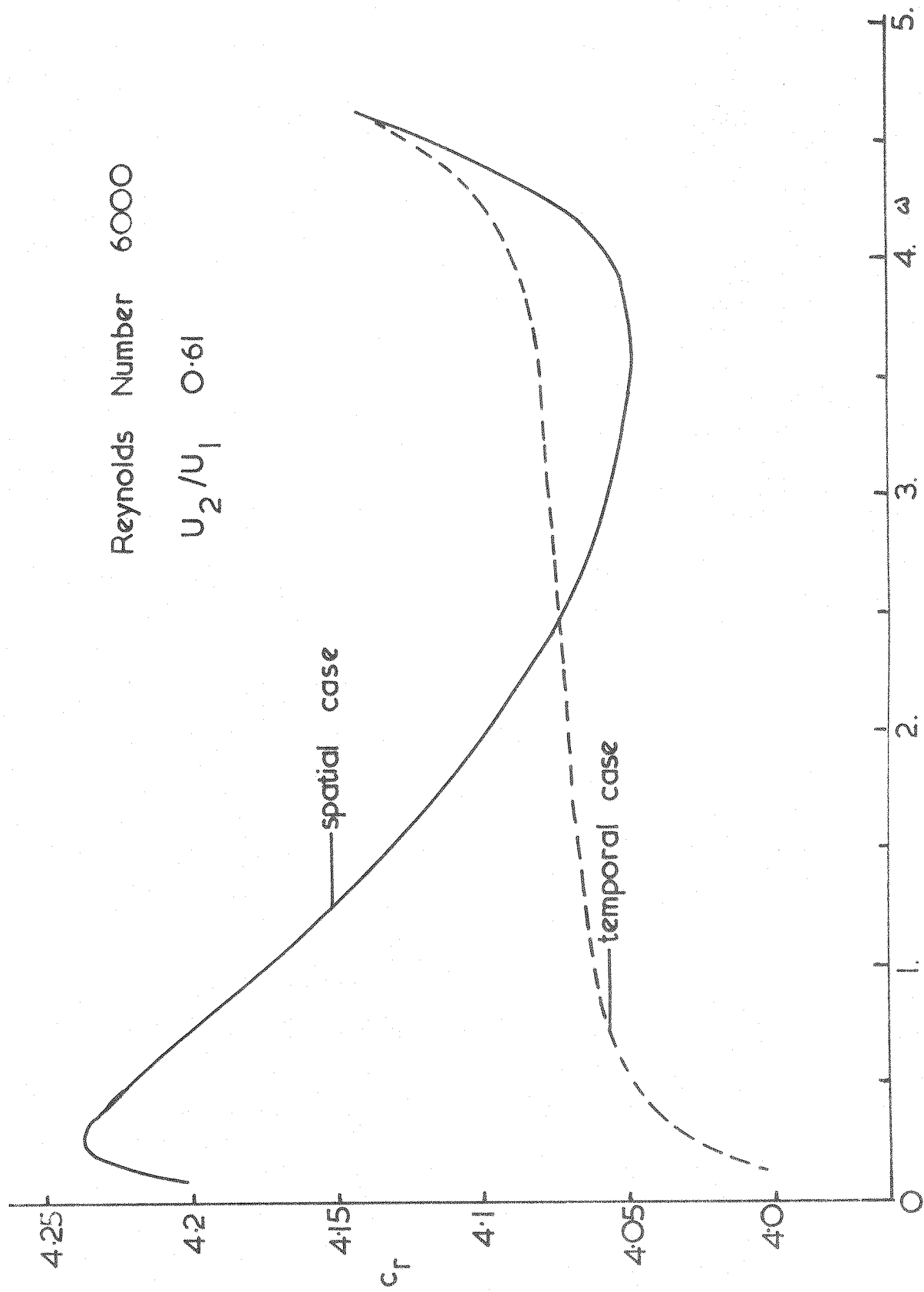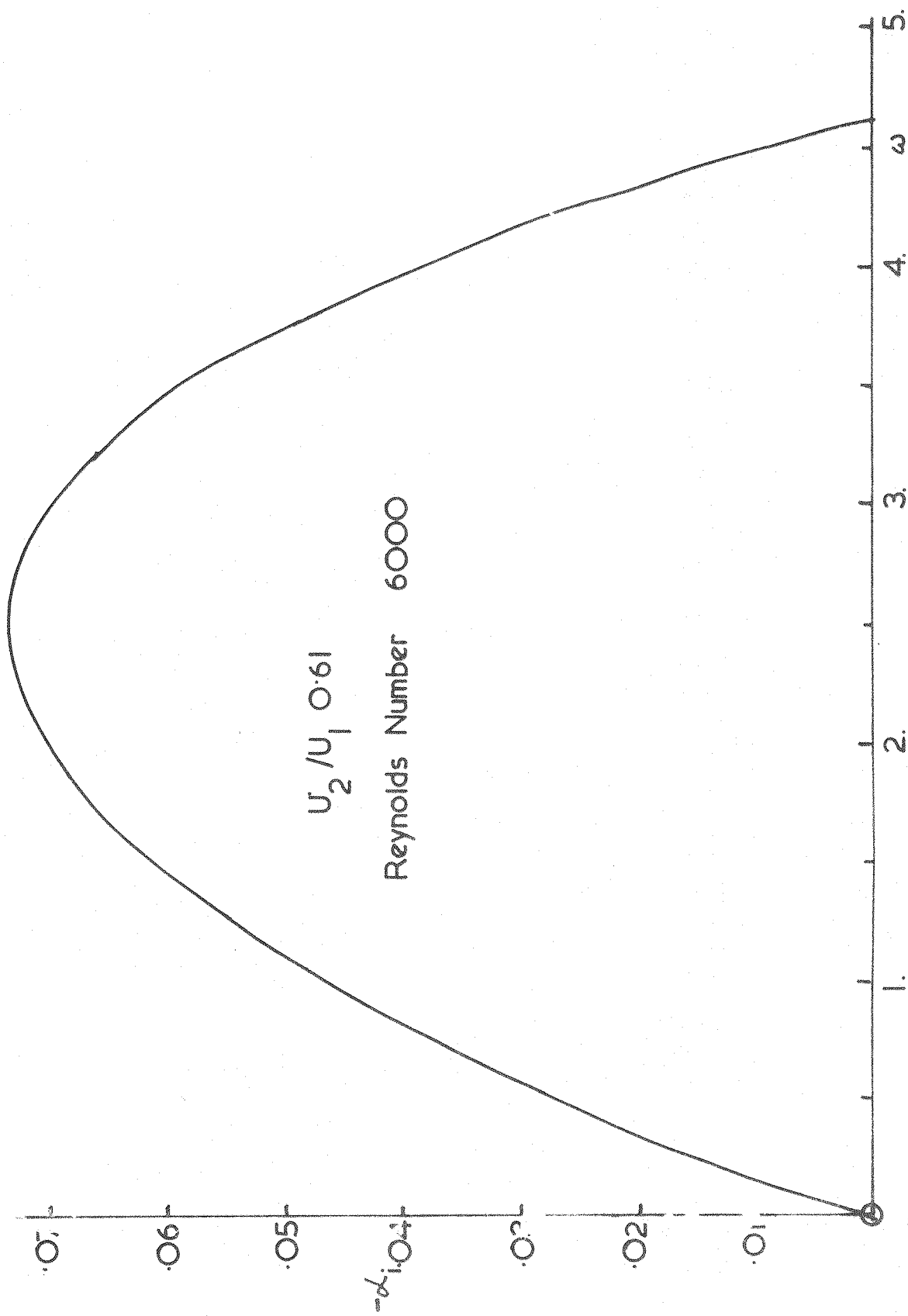
Variation of Spatial Amplification Factor with Frequency.   Figure 32

Reynolds Number 6000

U_2/U_1 0.61
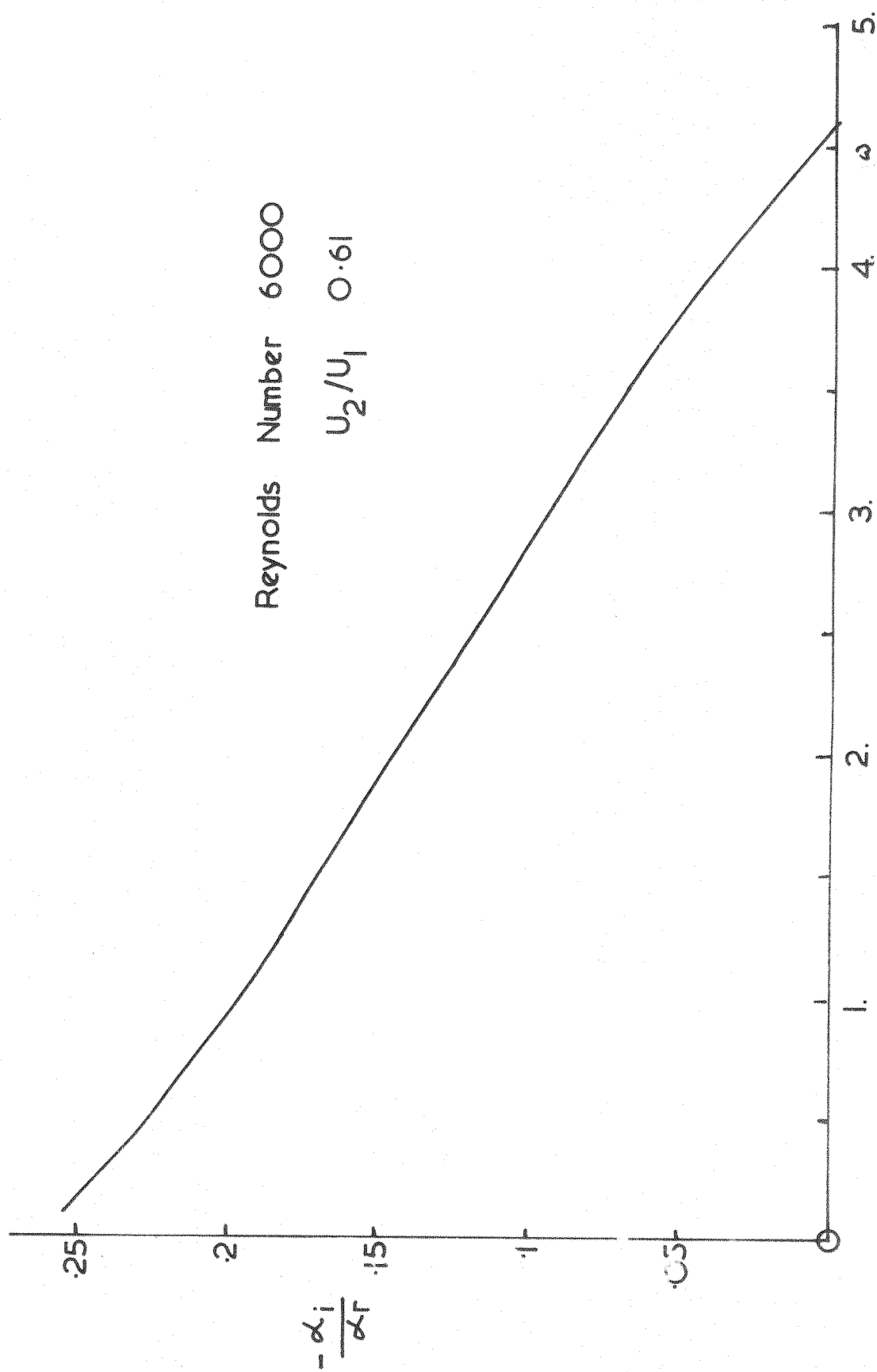
Variation of Rate of Growth of Eddies with Frequency.   Figure 33

R : 6000

ω : 2·50275

$\dfrac{U_2}{U_1}$: 0·61

Distribution of $\hat{\Psi}_r$ (y/θ) for Maximum Spatial Amplification

Figure 34(a)

R : 6000

ω : 2.50275

$\dfrac{U_2}{U_1}$ 0.61
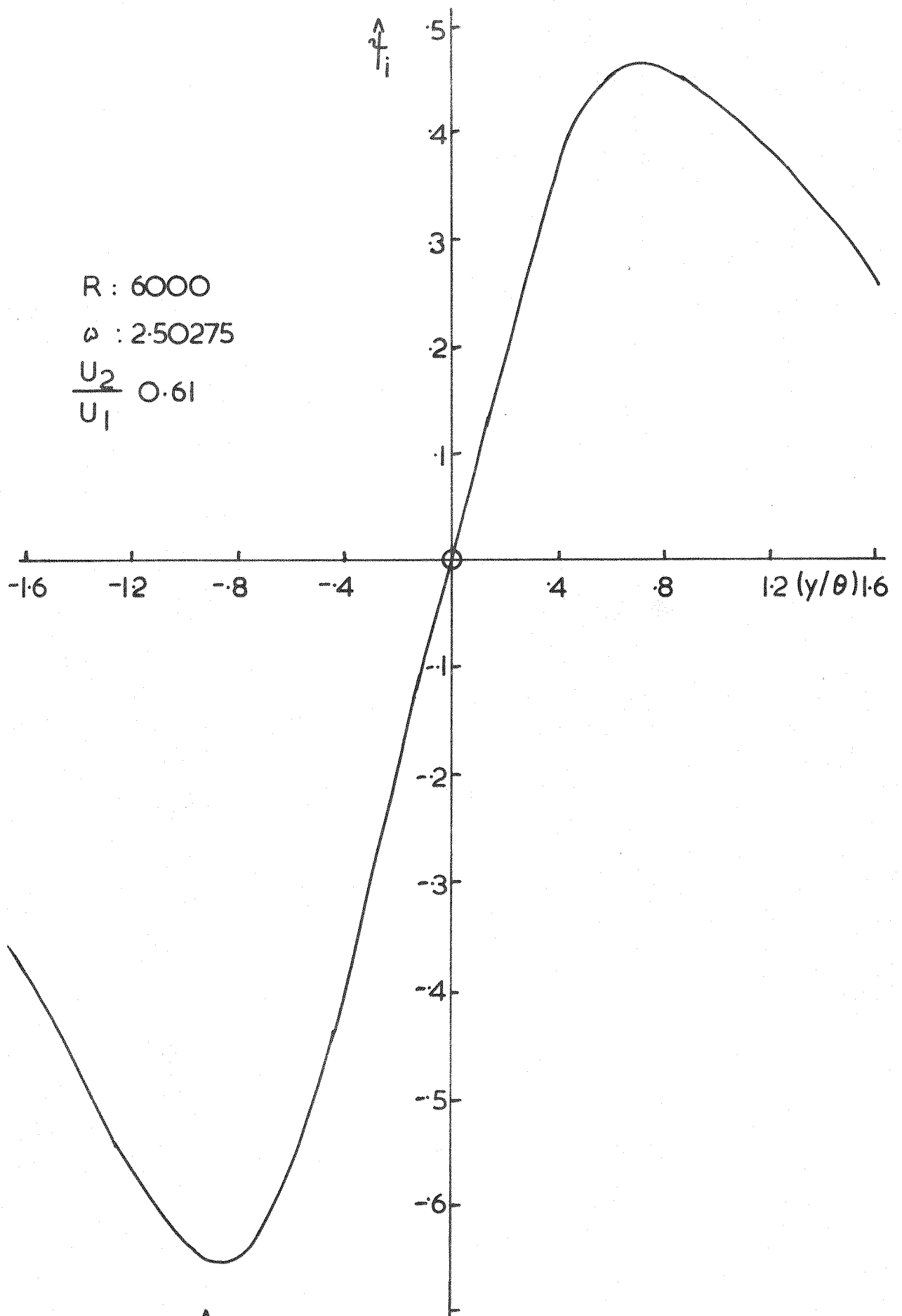
Distribution of $\hat{f}_i$ (y/θ) for Maximum Spatial Amplification
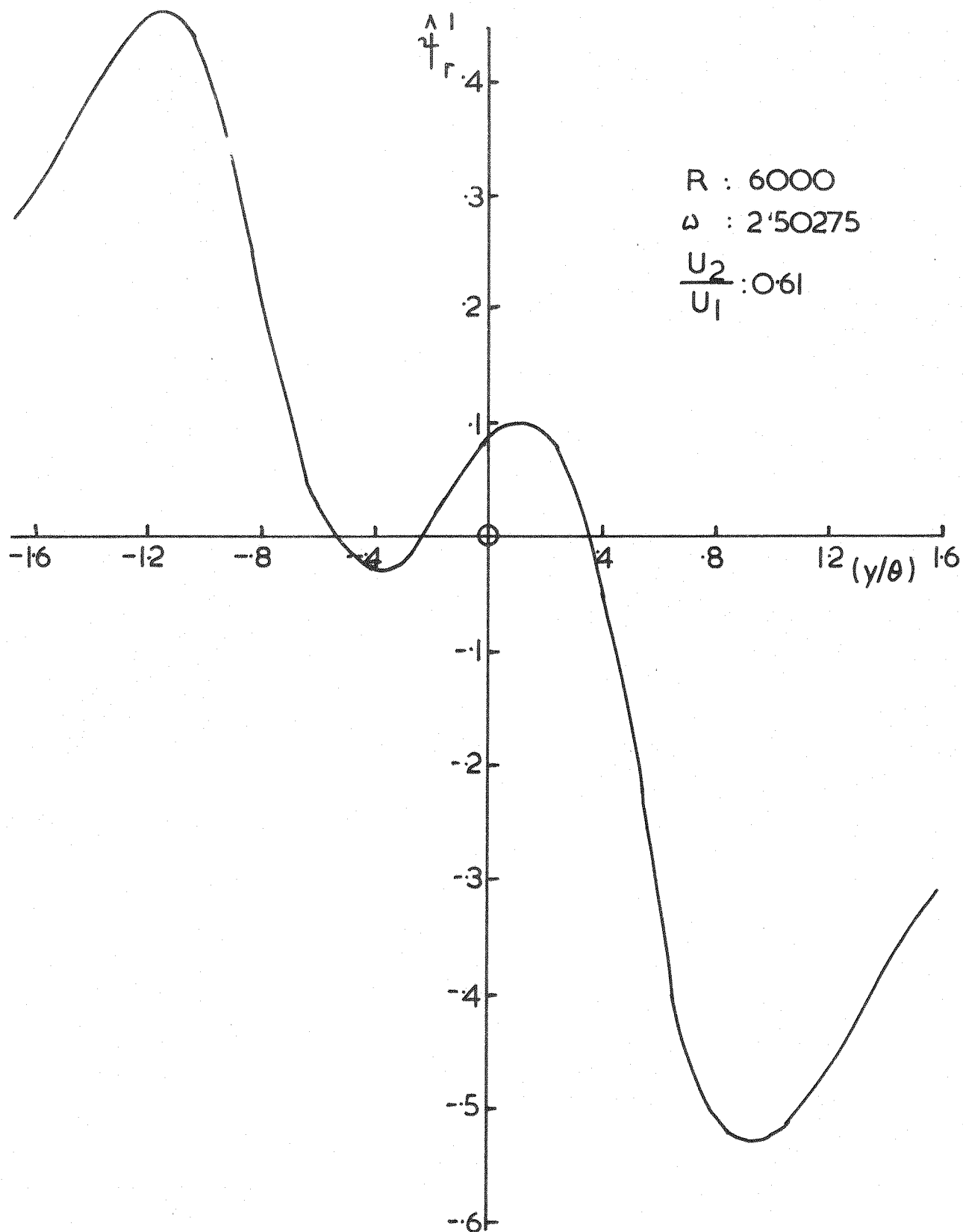
Figure 34(b)

Distribution of $\hat{\psi}'_r(y/\theta)$ for Maximum Spatial Amplification

Figure 35(a)
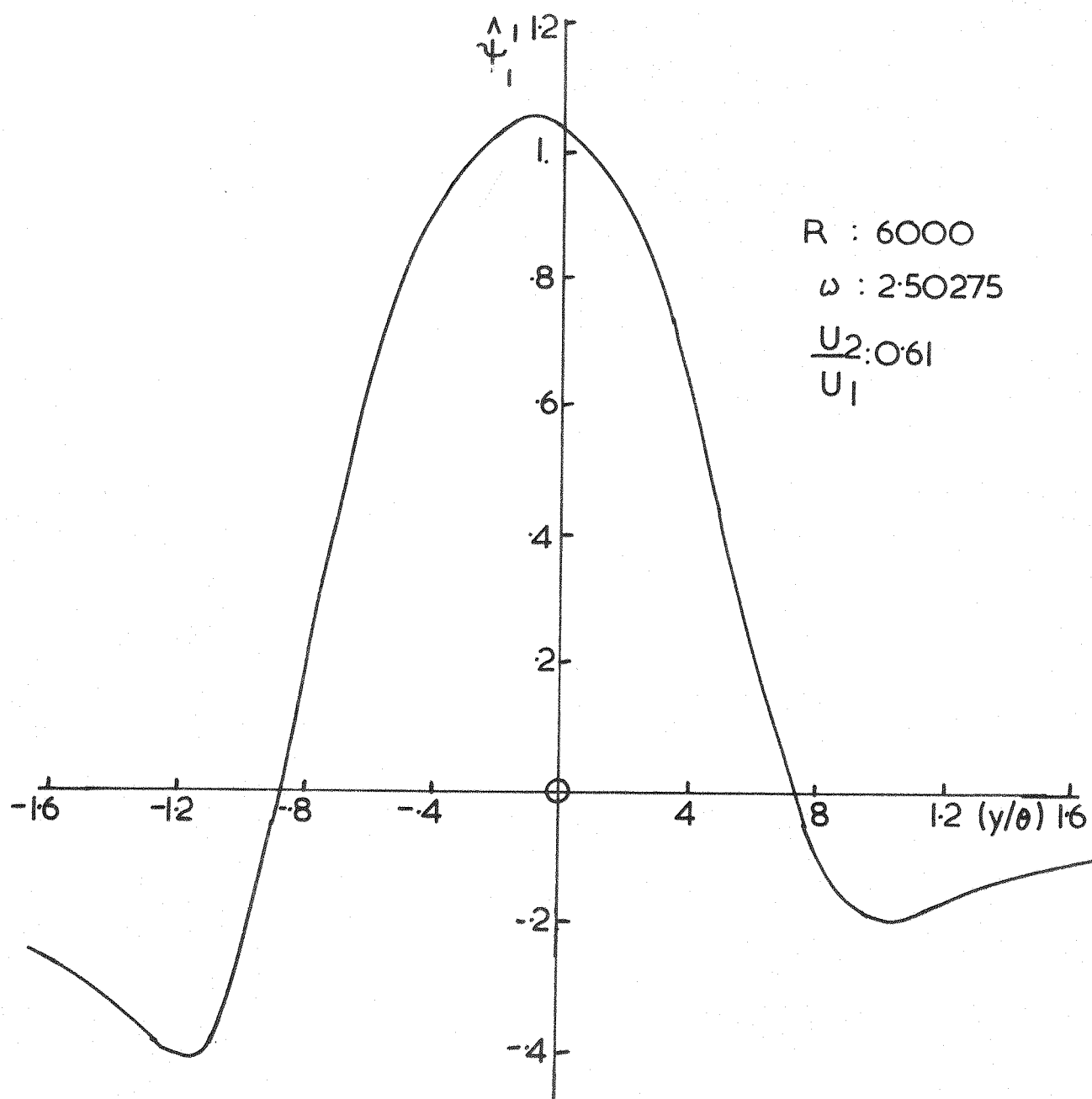
Distribution of $\hat{\psi}'_i$ (y/θ) for Maximum Spatial Amplification

Figure 35(b)
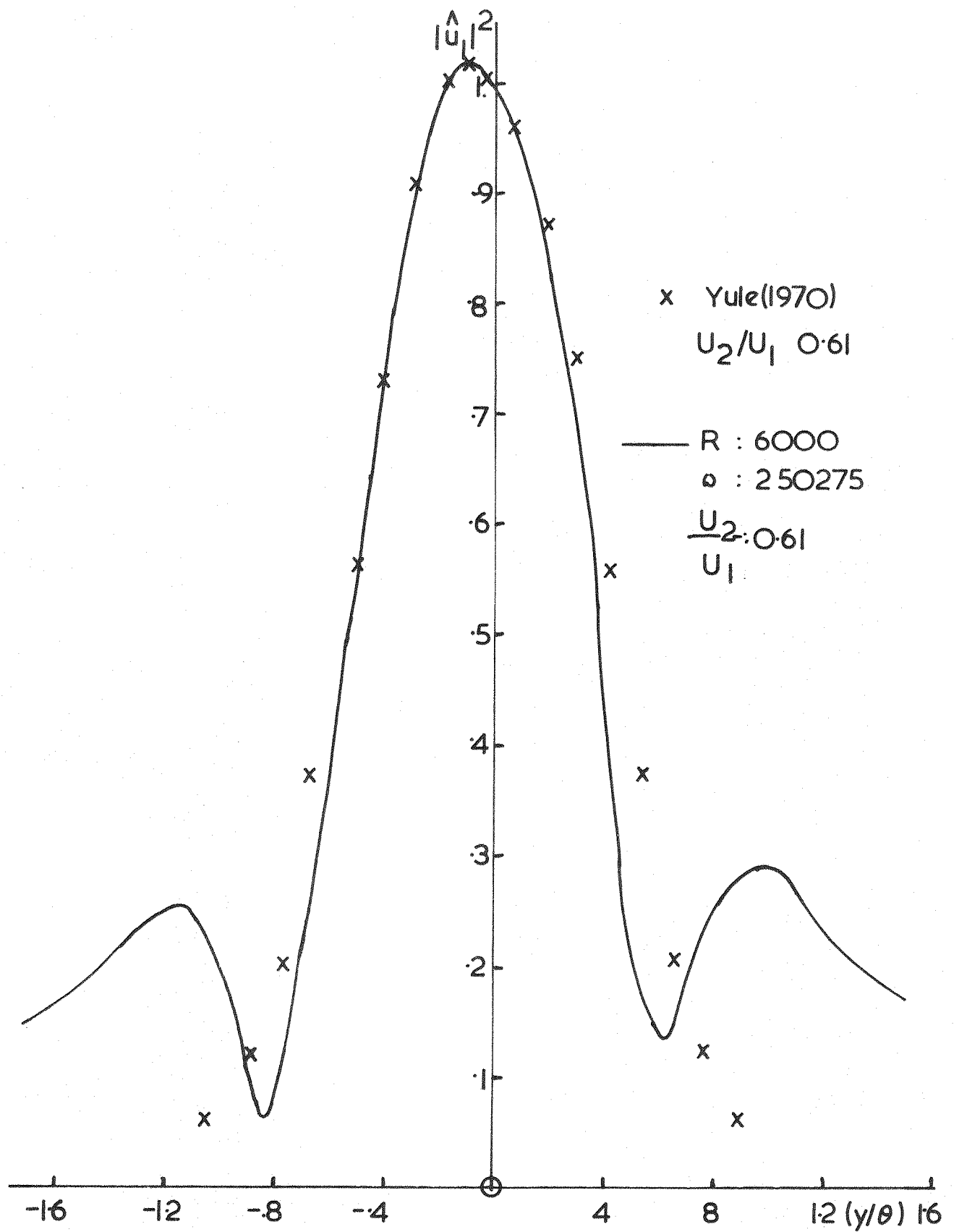
Distribution of $|\hat{u}_1|^2$ for Maximum Spatial Amplification

Figure 36
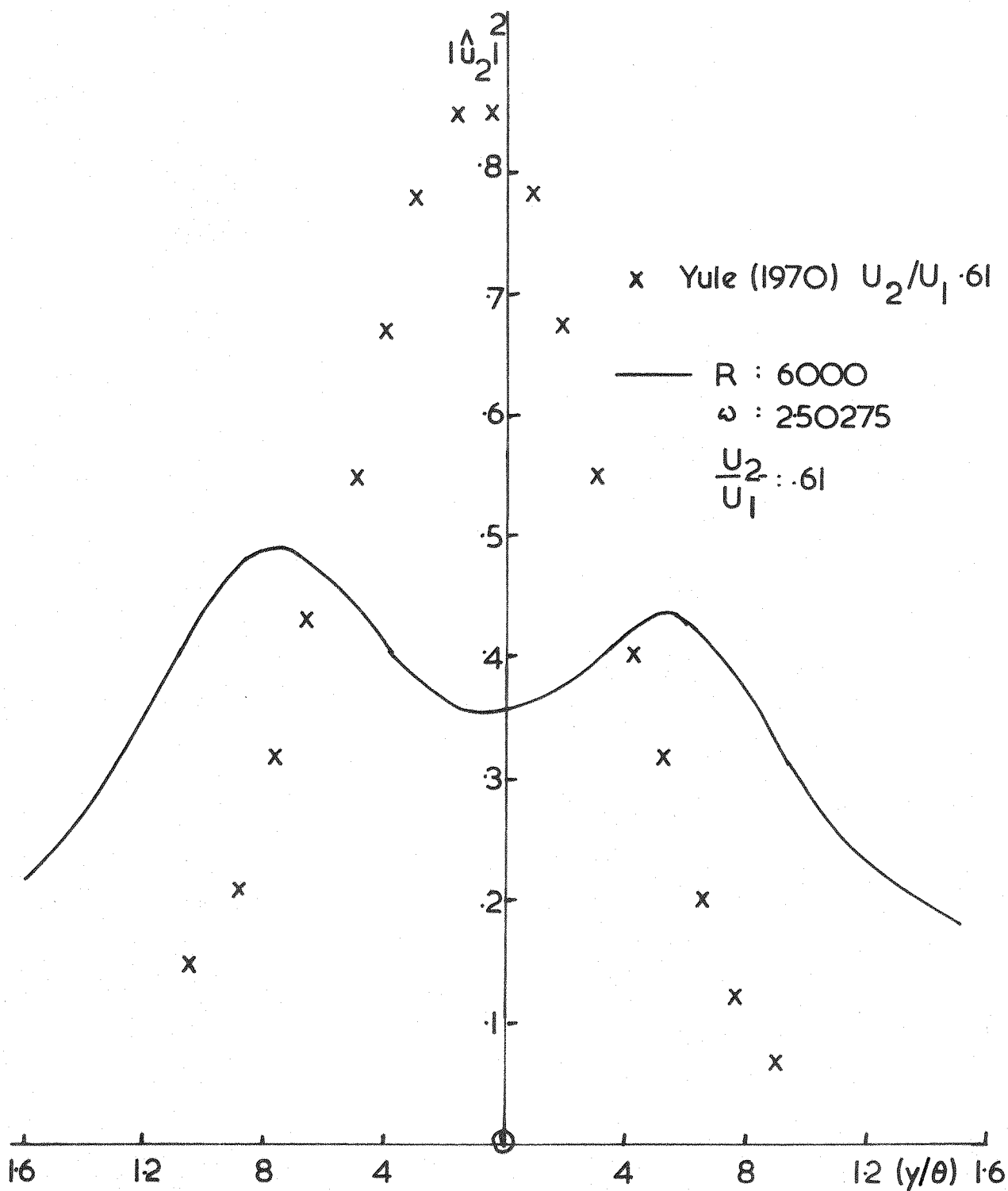
Distribution of $|\hat{u}_2|^2$ for Maximum Spatial Amplification

Figure 37

Distribution of $-\overline{u_1 u_2}$ for Maximum Spatial Amplification

Figure 38

$$\overline{\frac{\hat{u}_1 \hat{u}_2}{\sqrt{\hat{u}_1{}^2}.\sqrt{\hat{u}_2{}^2}}}$$

R : 6000

ω : 2 50 275

$\dfrac{U_2}{U_1}$: 0·61
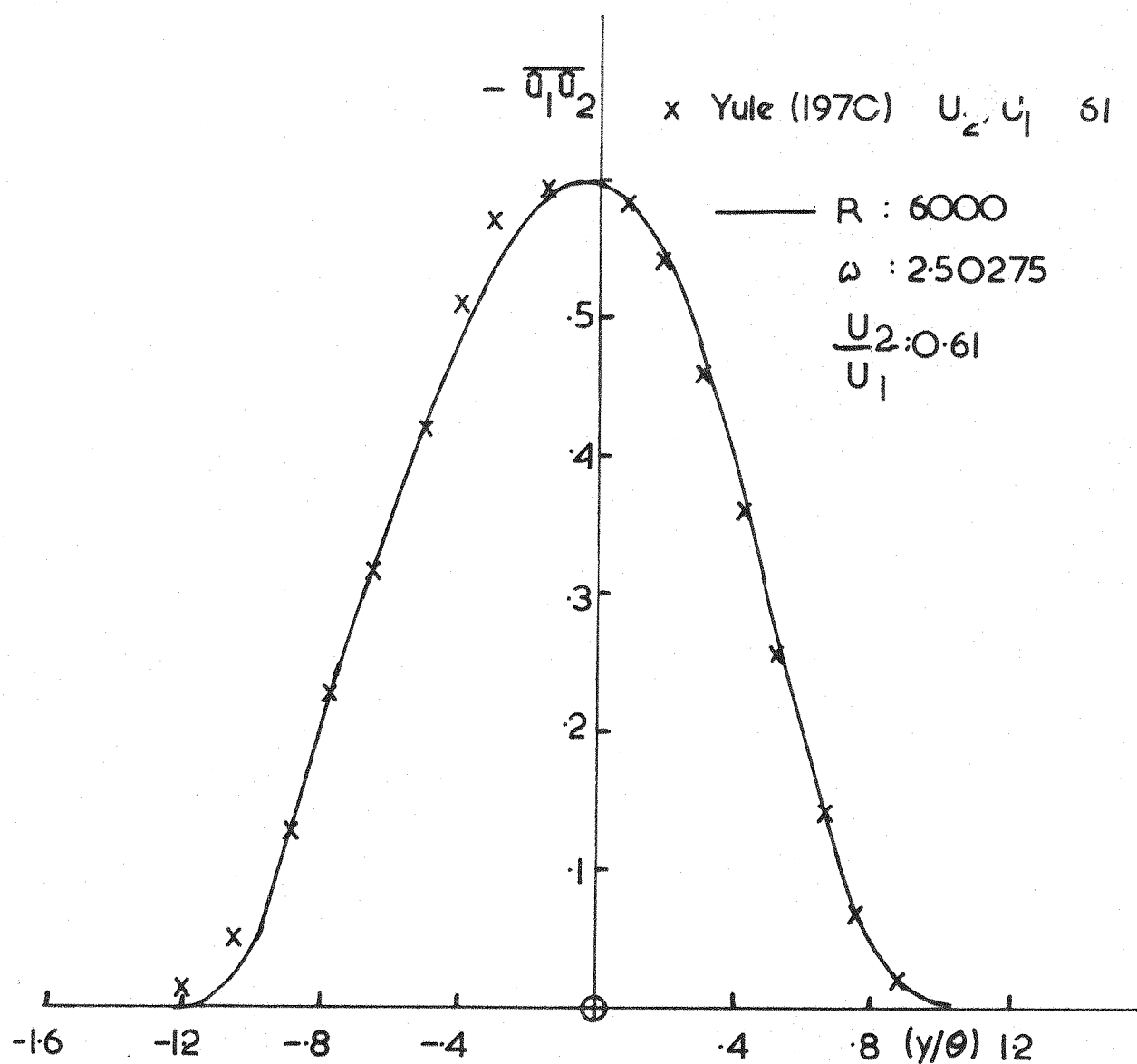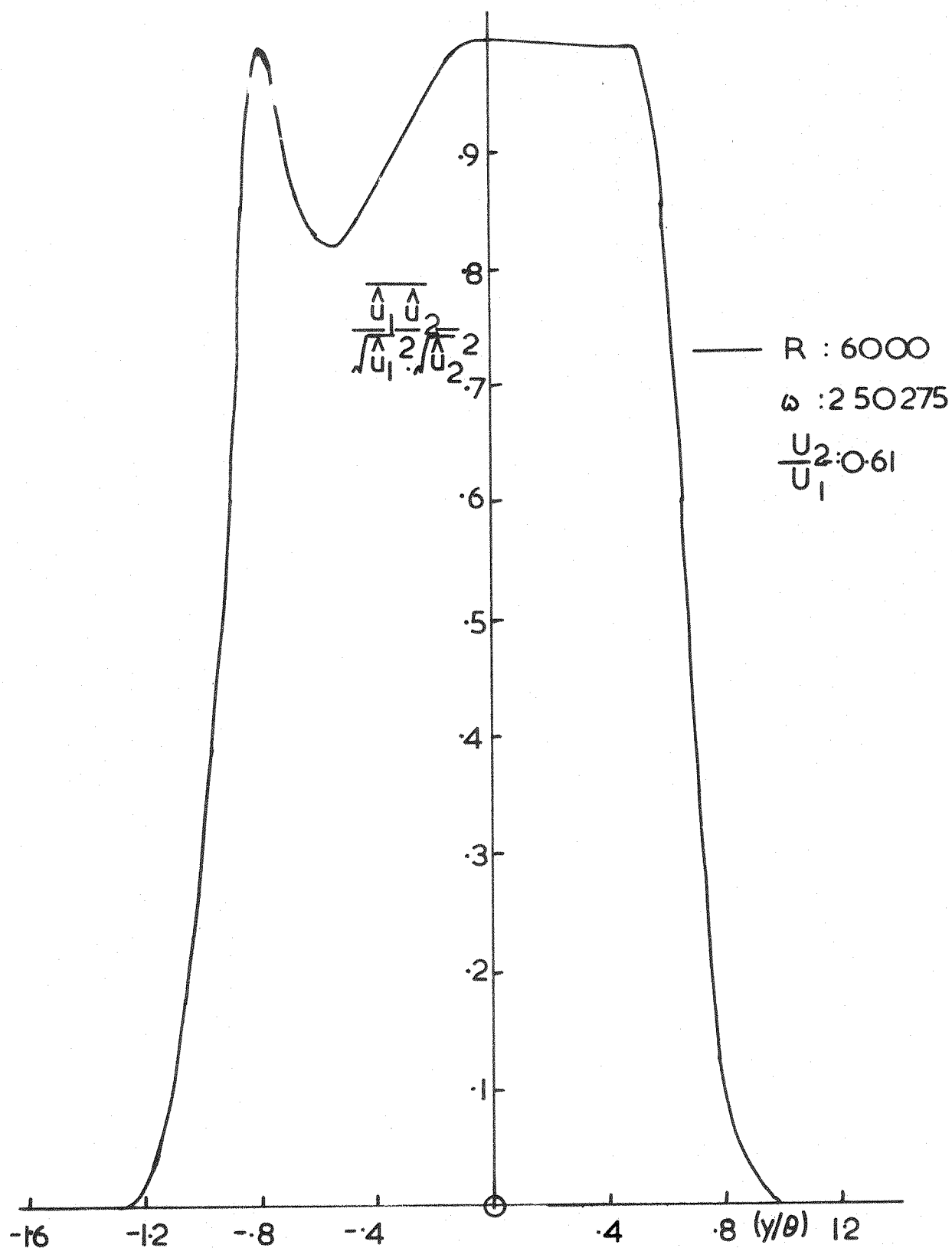
Distribution of Shear Correlation Coefficient for

Maximum Spatial Amplification   Figure 39
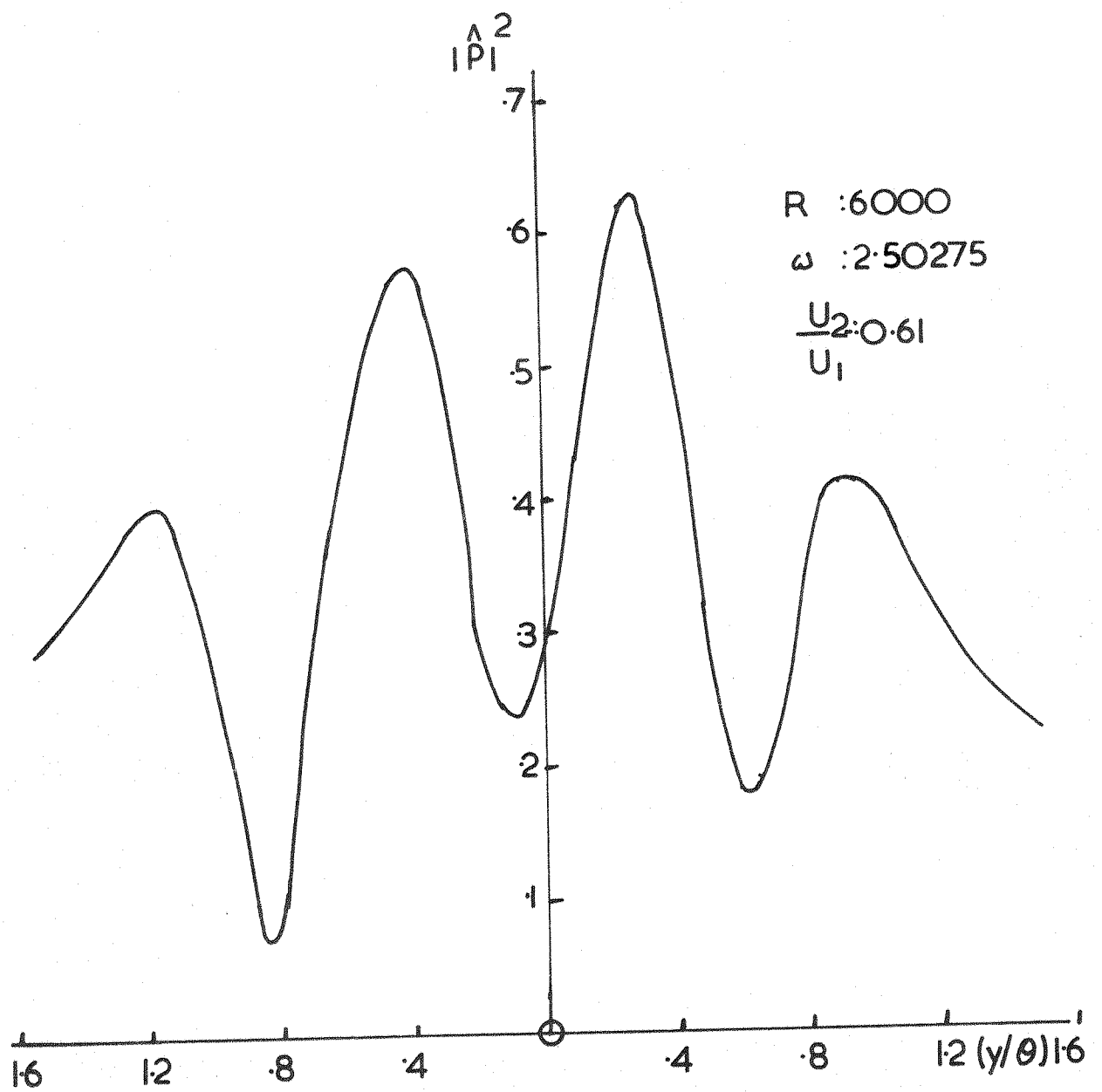
Distribution of $|\hat{p}|^2$ for Maximum Spatial Amplification

Figure 40
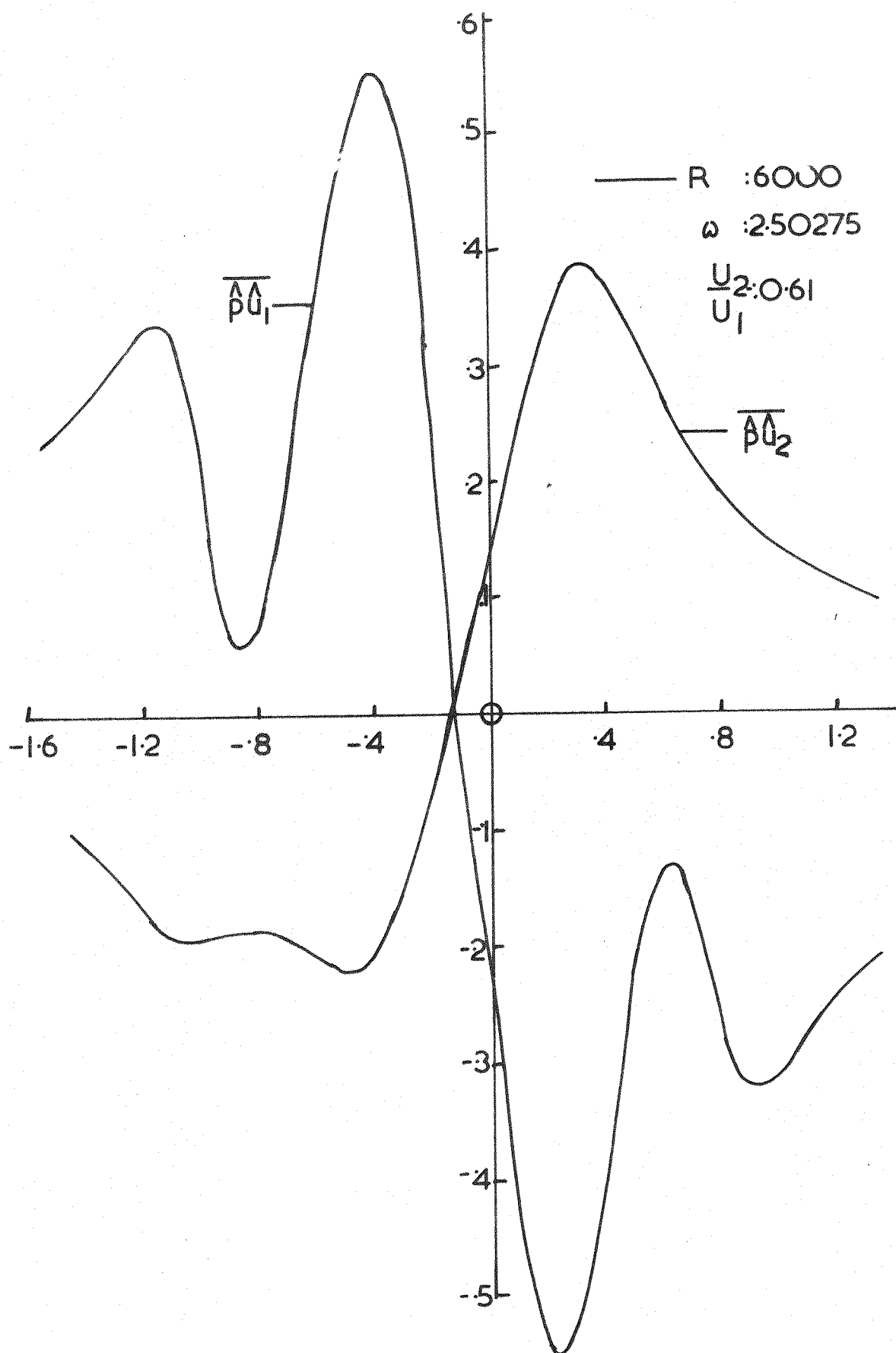
Distributions of $\overline{\hat{p}\hat{u}_1}$ & $\overline{\hat{p}\hat{u}_2}$ for Maximum Spatial Amplification

Figure 41
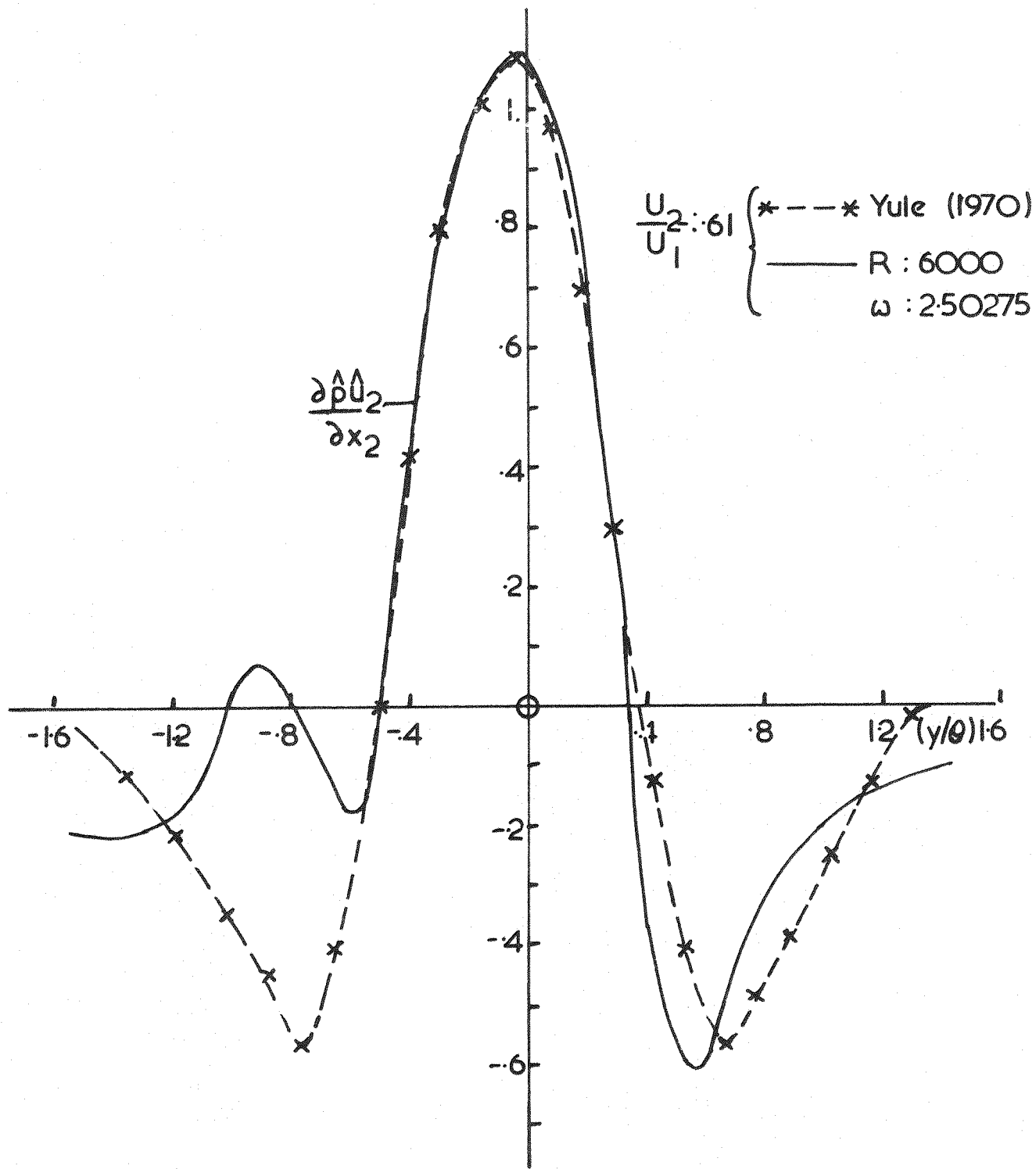
Distribution of $\dfrac{\partial \rho u_2}{\partial x_2}$ for Maximum Spatial Amplification

Figure 42

$R = 423740$

$U_2^* = 0$
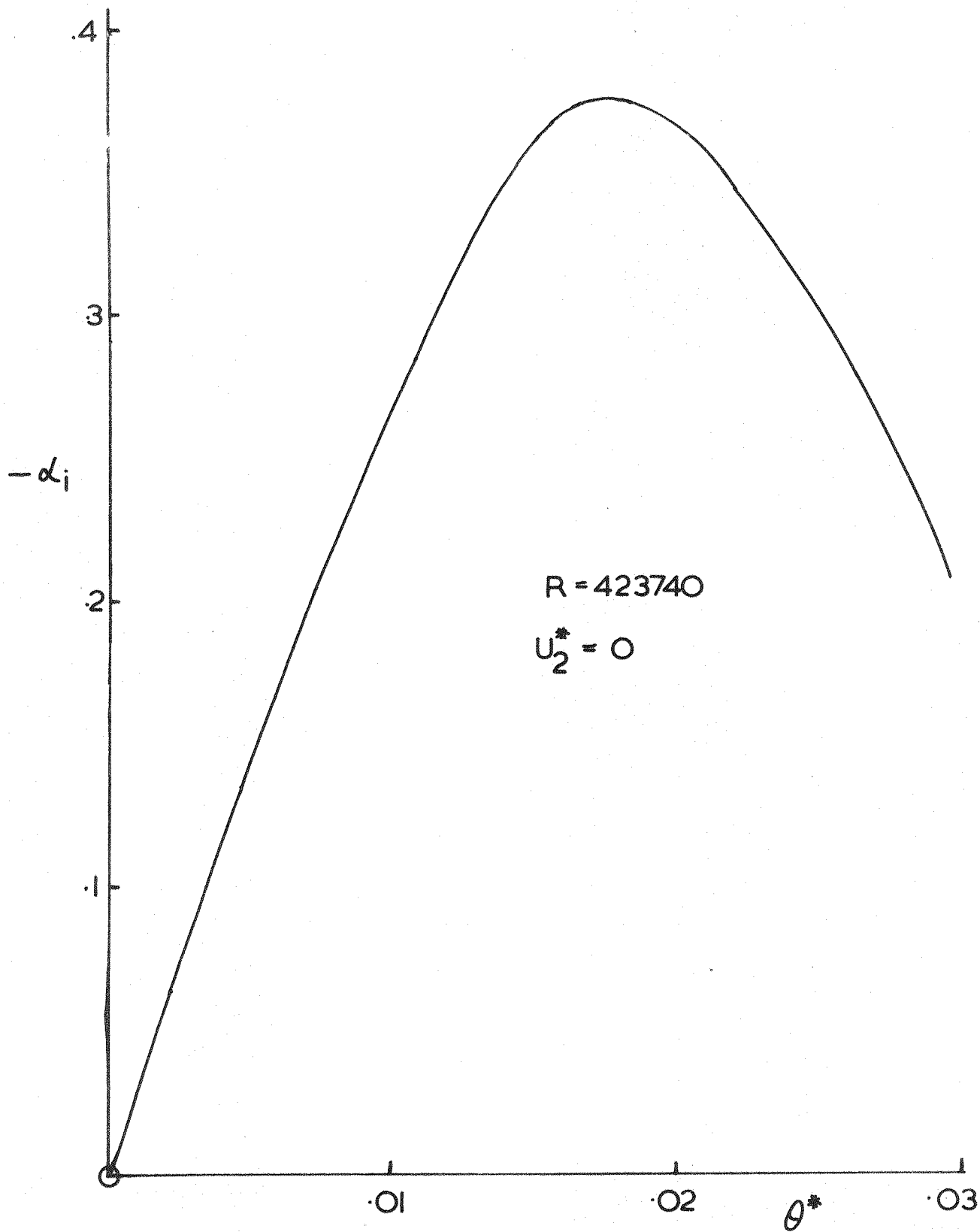
Amplification Factor against θ^* Figure 43
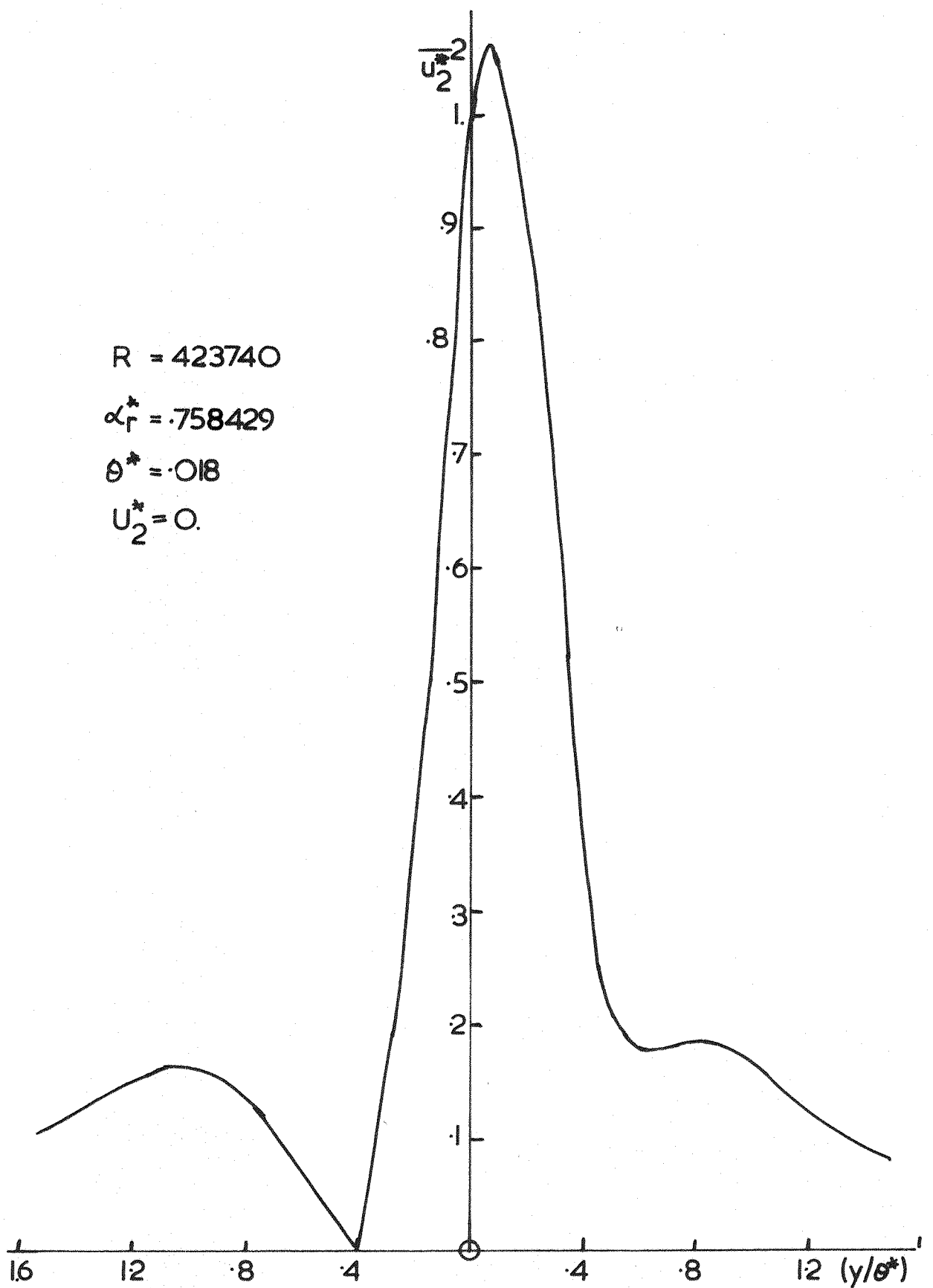
Distribution of $\overline{u_2^*}^2$ for $\theta^* = \cdot018$ Figure 44
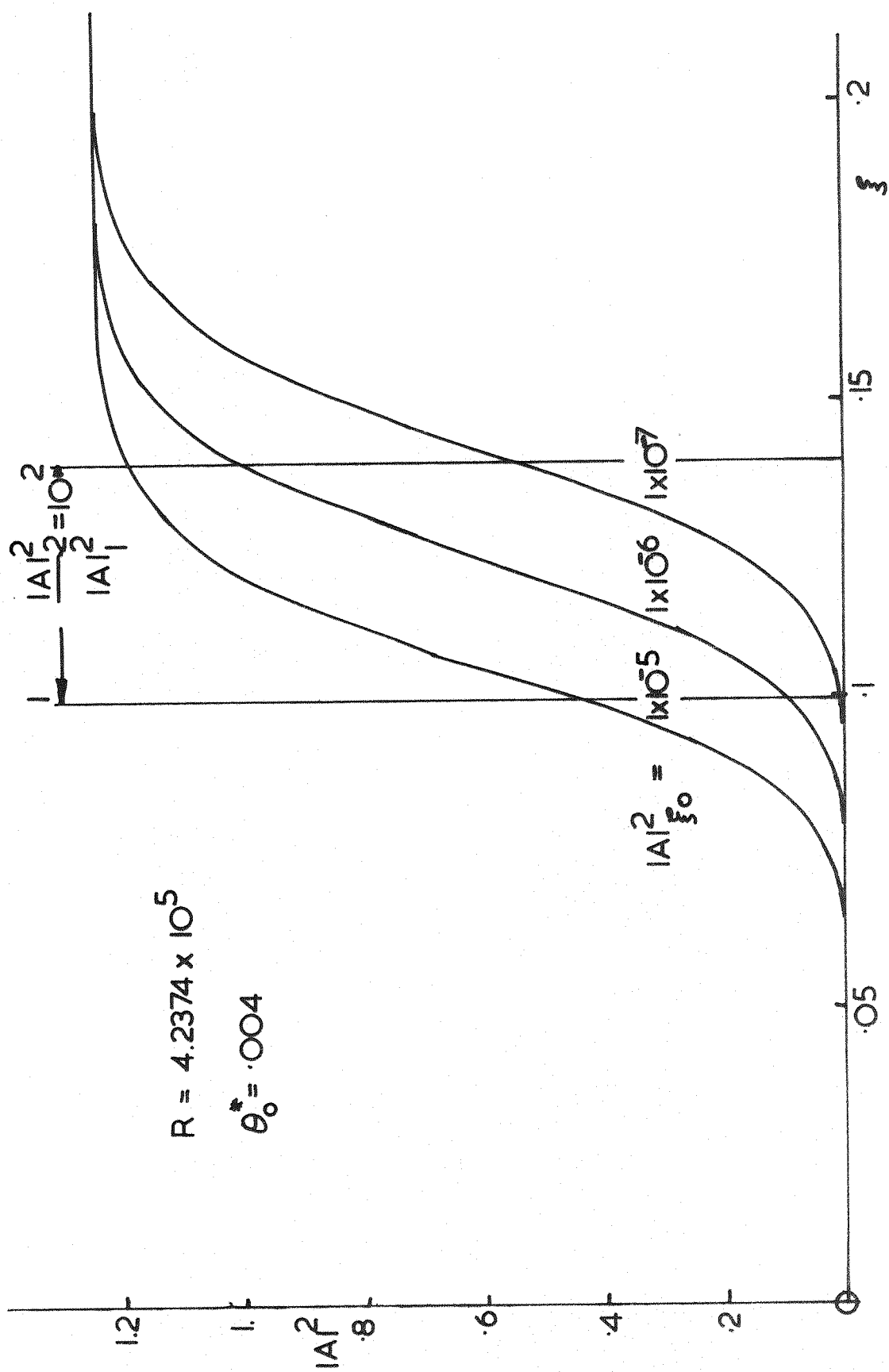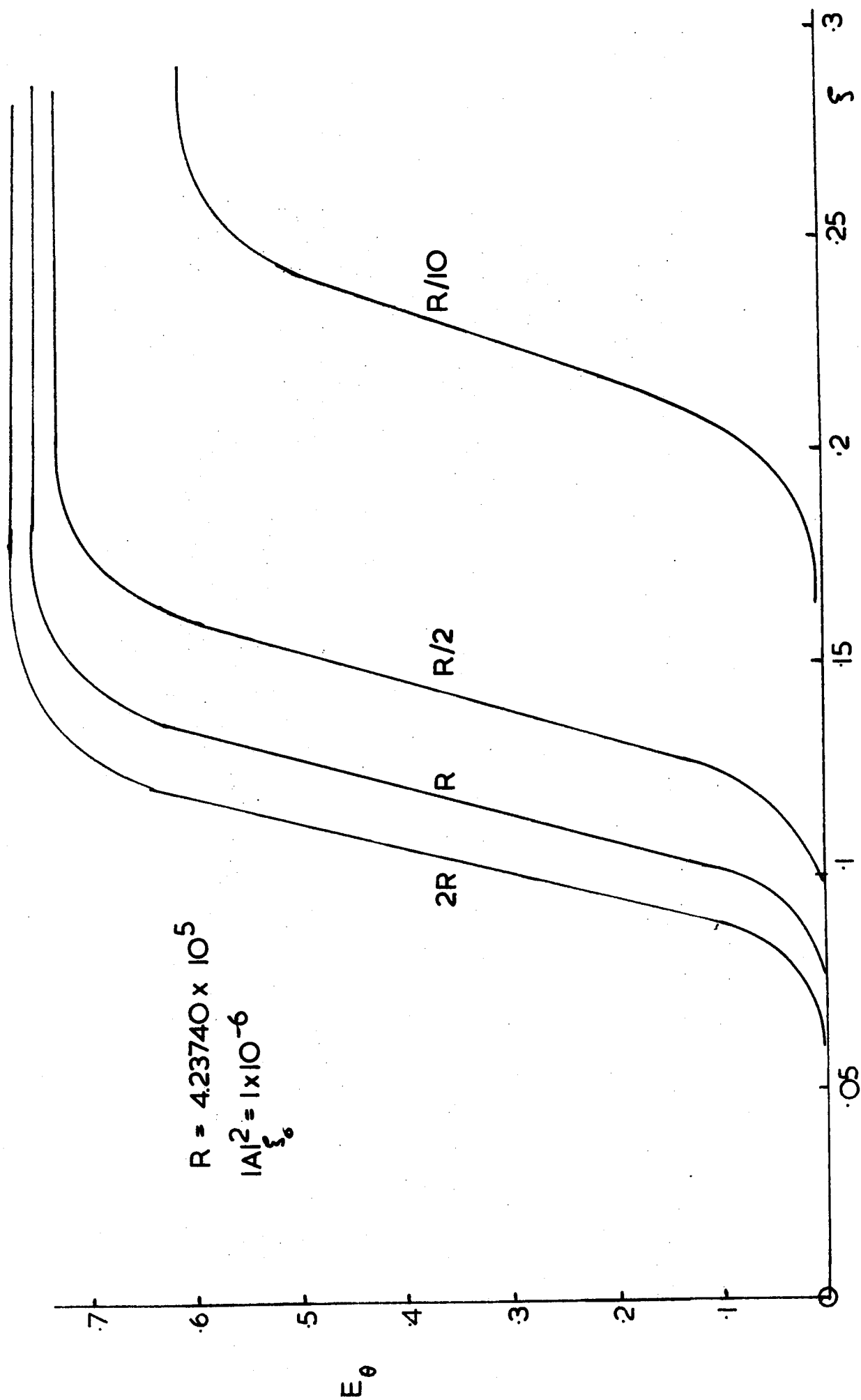
Effect of Initial Value of $|A|^2$ on Growth of $|A|^2$
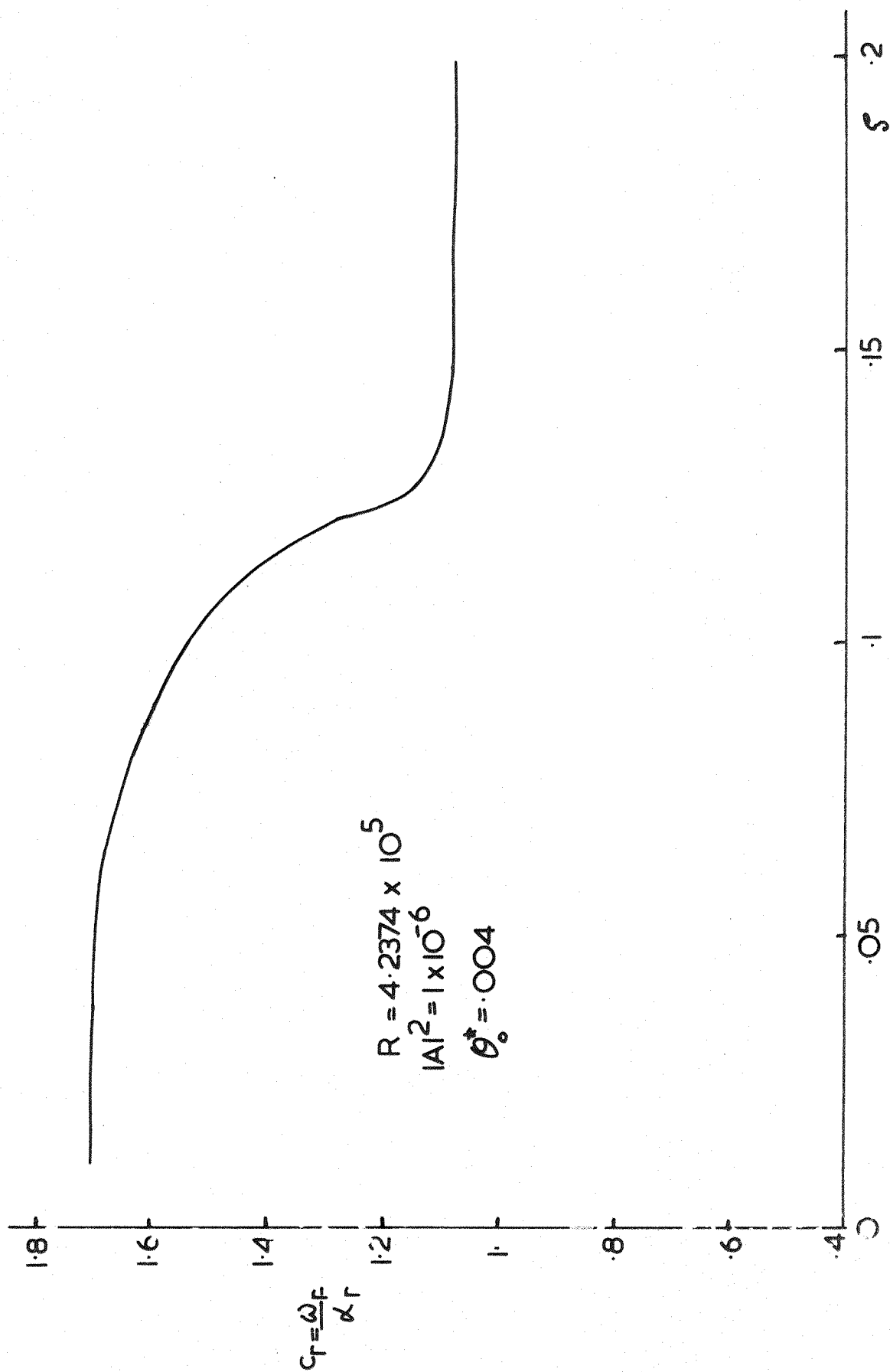
Figure 45
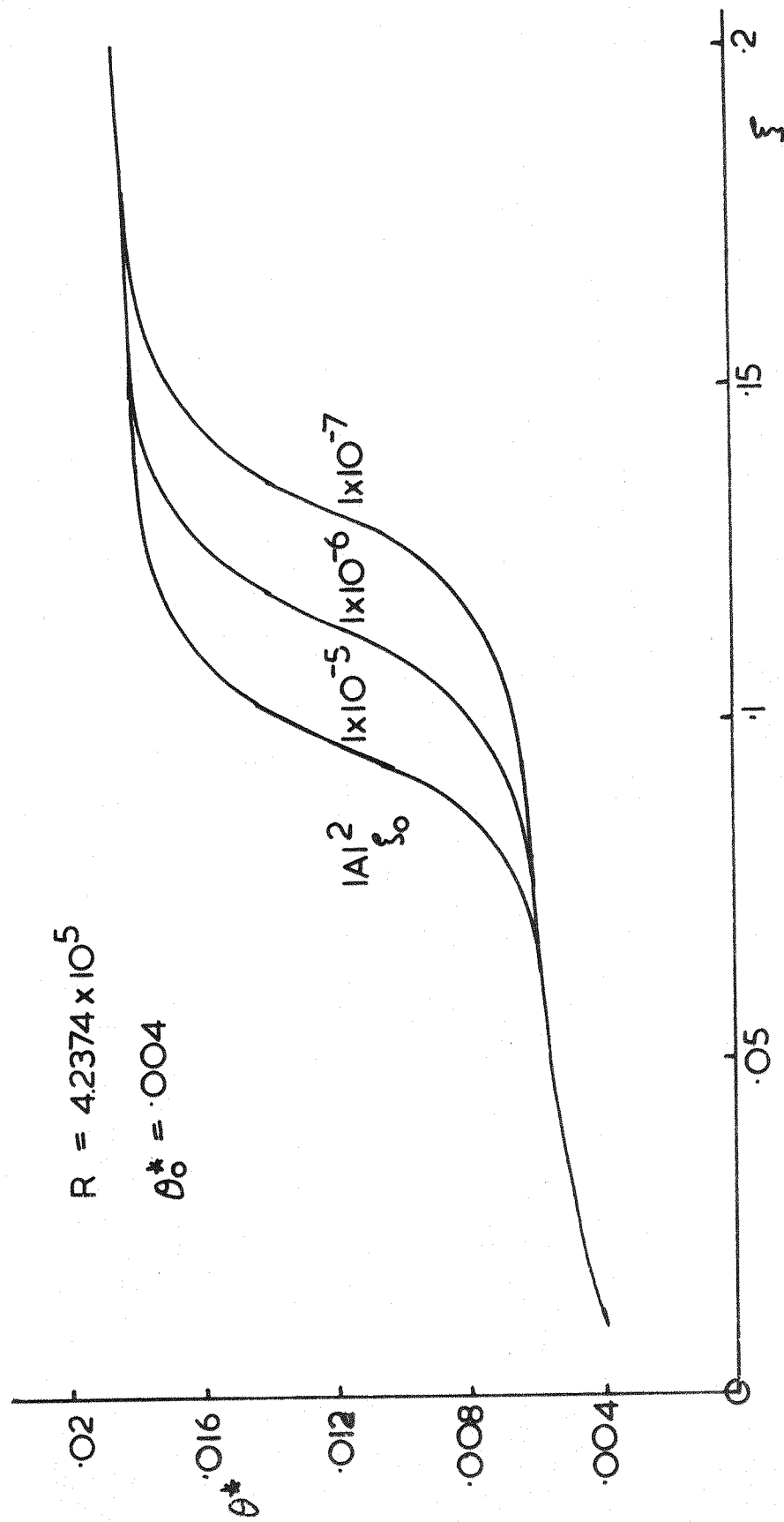
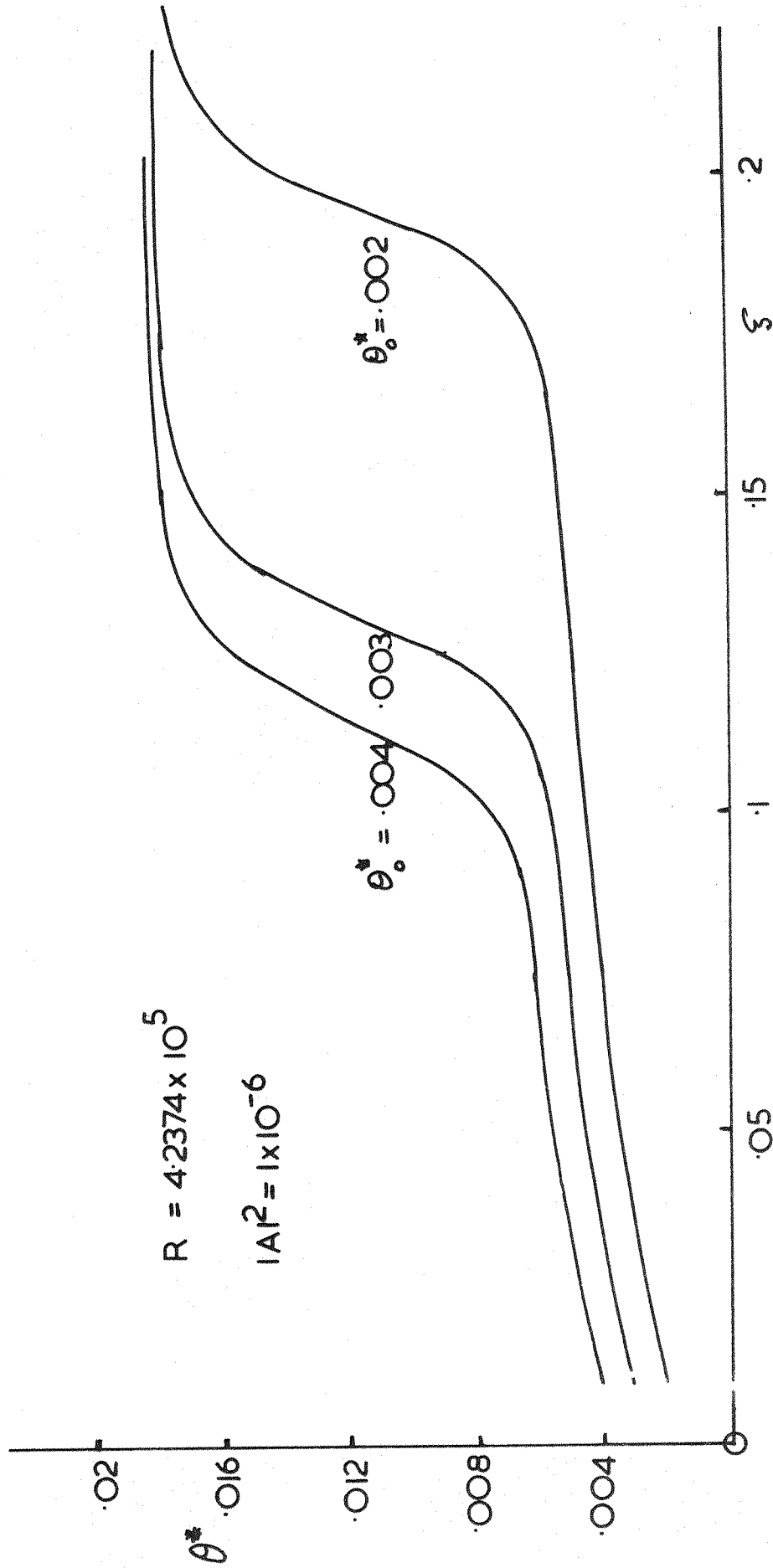Effect of Initial Value of $|A|^2$ on Growth of Momentum Thickness

Figure 46
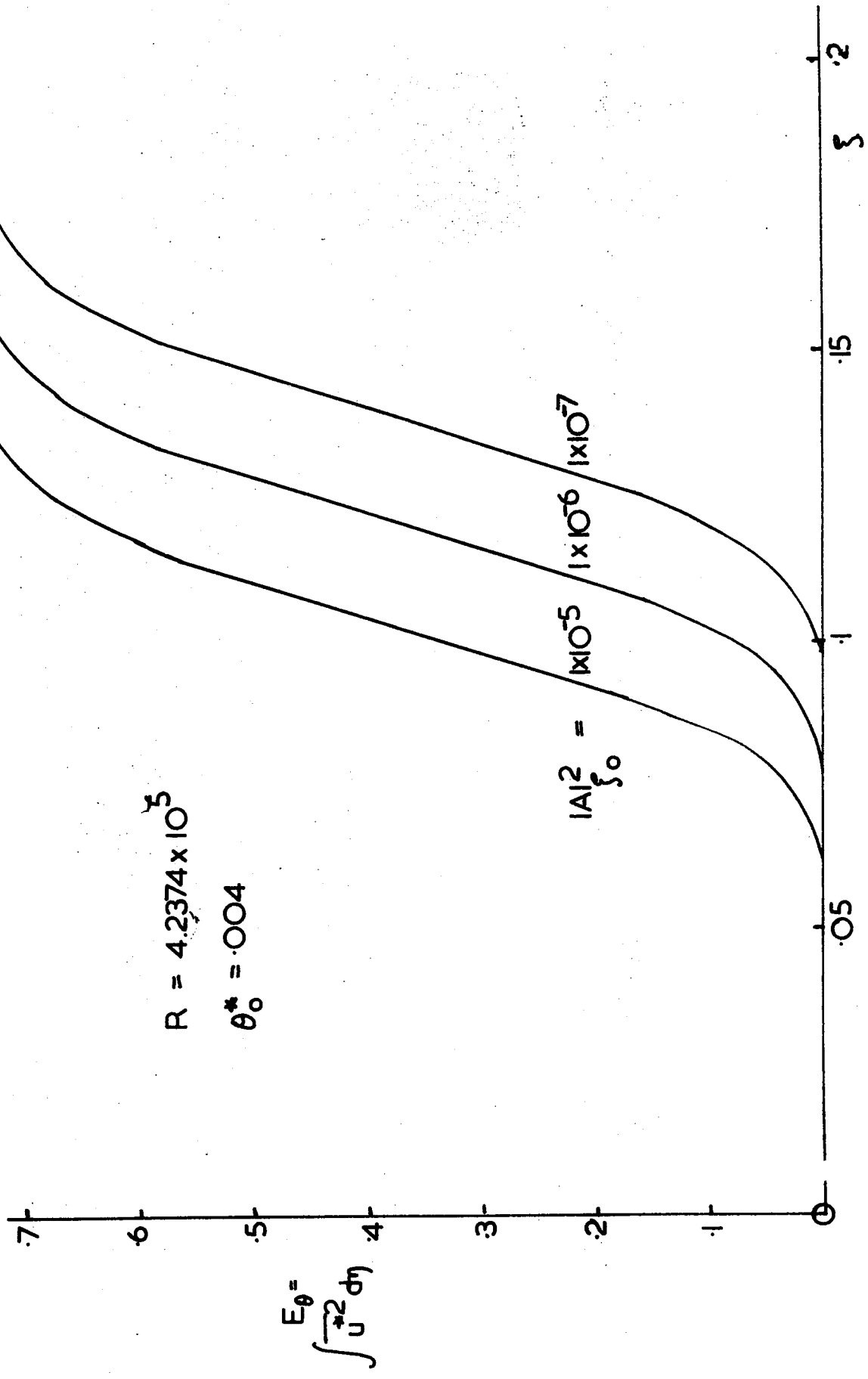
Effect of Initial Value of $|A|^2$ on Growth of Energy Density.   Figure 47

Effect of Reynolds Number on Growth of Energy Density   Figure 48

$$c_r = \frac{\omega_r}{\alpha_r}$$

$R = 4.2374 \times 10^5$

$|A|^2 = 1 \times 10^{-6}$

$\theta_o^* = .004$

Variation of Phase Velocity with ζ

Figure 49

Effect of Initial Value of θ^* on Growth of Momentum Thickness   Figure 50